PAGES 557–716

ISSN 0003–2654

The Analyst

A monthly international journal dealing with all branches of the theory and practice of analytical chemistry, including instrumentation and sensors, and physical, biochemical, clinical, pharmaceutical, biological, automatic and computer-based methods

Vol. 112 No. 5
May
1987

ROYAL SOCIETY OF CHEMISTRY

The Analyst

The Analytical Journal of The Royal Society of Chemistry

Editorial Office: The Royal Society of Chemistry, Burlington House, Piccadilly, London, W1V 0BN. Telephone 01-734 9864. Telex No. 268001

Advertisements: Advertisement Department, The Royal Society of Chemistry, Burlington House, Piccadilly, London, W1V 0BN. Telephone 01-437 8656. Telex No. 268001

The Analyst (ISSN 0003–2654) is published monthly by The Royal Society of Chemistry, Burlington House, London W1V 0BN, England. All orders accompanied with payment should be sent directly to The Royal Society of Chemistry, The Distribution Centre, Blackhorse Road, Letchworth, Herts. SG6 1HN, England. 1987 Annual subscription rate UK £160.00, Rest of World £179.00, USA $315.00. Purchased with *Analytical Abstracts* UK £364.00 Rest of World £403.00, USA $709.00. Purchased with *Analytical Abstracts* plus *Analytical Proceedings* UK £411.00, Rest of World £455.00, USA $801.00. Purchased with *Analytical Proceedings* UK £200.00, Rest of World £224.00, USA $394.00. Air freight and mailing in the USA by Publications Expediting Inc., 200 Meacham Avenue, Elmont, NY 11003.
USA Postmaster: Send address changes to *The Analyst* Publications Expediting Inc., 200 Meacham Avenue, Elmont, NY 11003. Second class postage paid at Jamaica, NY 11431. All other despatches outside the UK by Bulk Airmail within Europe, Accelerated Surface Post outside Europe. PRINTED IN THE UK.

Information for Authors

Full details of how to submit material for publication in *The Analyst* are given in the Instructions to Authors in the January issue. Separate copies are available on request.

The Analyst publishes papers on all aspects of the theory and practice of analytical chemistry, fundamental and applied, inorganic and organic, including chemical, physical, biochemical, clinical, pharmaceutical, biological, automatic and computer-based methods. Papers on new approaches to existing methods, new techniques and instrumentation, detectors and sensors, and new areas of application with due attention to overcoming limitations and to underlying principles are all equally welcome. There is no page charge.

The following types of papers will be considered:

Full papers, describing original work.

Short papers: the criteria regarding originality are the same as for full papers, but short papers generally report less extensive investigations or are of limited breadth of subject matter

Communications, which must be on an urgent matter and be of obvious scientific importance. Rapidity of publication is enhanced if diagrams are omitted, but tables and formulae can be included. Communications receive priority and are usually published within 5–8 weeks of receipt. They are intended for brief descriptions of work that has progressed to a stage at which it is likely to be valuable to workers faced with similar problems. A fuller paper may be offered subsequently, if justified by later work.

Reviews, which must be a critical evaluation of the existing state of knowledge on a particular facet of analytical chemistry.

Every paper (except Communications) will be submitted to at least two referees, by whose advice the Editorial Board of *The Analyst* will be guided as to its acceptance or rejection. Papers that are accepted must not be published elsewhere except by permission. Submission of a manuscript will be regarded as an undertaking that the same material is not being considered for publication by another journal.

Regional Advisory Editors. For the benefit of potential contributors outside the United Kingdom, a Panel of Regional Advisory Editors exists. Requests for help or advice on any matter related to the preparation of papers and their submission for publication in *The Analyst* can be sent to the nearest member of the Panel. Currently serving Regional Advisory Editors are listed in each issue of *The Analyst*

Manuscripts (three copies typed in double spacing) should be addressed to:
The Editor, *The Analyst,*
Royal Society of Chemistry,
Burlington House,
Piccadilly,
LONDON W1V 0BN, UK

Particular attention should be paid to the use of standard methods of literature citation, including the journal abbreviations defined in Chemical Abstracts Service Source Index. Wherever possible, the nomenclature employed should follow IUPAC recommendations, and units and symbols should be those associated with SI.

All queries relating to the presentation and submission of papers, and any correspondence regarding accepted papers and proofs, should be directed to the Editor, *The Analyst* (address as above). Members of the Analytical Editorial Board (who may be contacted directly or via the Editorial Office) would welcome comments, suggestions and advice on general policy matters concerning *The Analyst.*

Fifty reprints of each published contribution are supplied free of charge, and further copies can be purchased.

Modern Spectroscopy

by J. MICHAEL HOLLAS, University of Reading, UK

Introduces a wide range of spectroscopies, including the background theory and the applications to structure determination and chemical analysis.

CONTENTS INCLUDE: Some Important Results in Quantum Mechanics; Electromagnetic Radiation and its Interaction with Atoms and Molecules; Molecular Symmetry; Rotational Spectroscopy; Vibrational Spectroscopy; Electronic Spectroscopy; Photoelectron and Related Spectroscopies; Lasers and Laser Spectroscopy.

0471911216	408 pages	December 1986	(cl) £9.95/$16.95
0471911313	408 pages	December 1986	(pr) £9.95/$16.95

Quantitative Analysis using Chromatographic Techniques

by ELENA KATZ, Applied Research Department, Perkin Elmer Corp, Norwalk, Connecticut, USA

Covers the quantitative aspects of all the chromatographic methods and provides a unique single source of up-to-date information. Individual chapters are written by experts in the field, and special features include detailed treatment of the principles of quantitative detection and sources of error in data processing procedures.

Series: Separation Science.

CONTENTS INCLUDE: Detection in Quantitative Liquid Chromatography; Quantitative Analysis by Liquid Chromatography; Detection in Quantitative Gas Chromatography; Quantitative Analysis by Gas Chromatography; Quantitative Thin-Layer Chromatography; Chromatography as a Quantitative Tool in Pharmaceutical Analysis; Is Automation the Future of Quantitative Chromatography?; Physico-Chemical Information from Peak Shape and Width in Liquid Chromatography.

0471914061	446 pages	January 1987	£37.50/$63.95

Principles of Electrochemistry

by J. KORYTA, J. Heyrovski Institute of Physical Chemistry & Electrochemistry, Prague, Czechoslovakia and
J. DVORAK, Faculty of Science, Charles University, Prague, Czechoslovakia

Provides the basic theory and applications of electrochemistry, which is becoming increasingly important in a number of fields. Electron transfer theory and double layer theory are included in understandable terms and mathematics is kept to a basic minimum.

CONTENTS INCLUDE: Equilibrium Properties of Electrolytes; Transport Processes in Electrolyte Systems; The Electrical Double Layer; Process in Heterogeneous Electrochemical Systems; Membrane Electrochemistry and Bioelectrochemistry.

0471912115	460 pages	March 1987	£49.50/$84.40

Telephone your credit card order: (0243) 829121, Customer Service Dept. Freefone — Dial 100 and ask for Freefone 3477 (UK only)

We will refund your payment without question if you return any unwanted title to us in re-saleable condition within 30 days.

All books also available from your bookseller

John Wiley & Sons Ltd
Baffins Lane, Chichester, Sussex PO19 1UD, England

ANALYTICAL CHEMISTRY BY OPEN LEARNING

Gas Chromatography

by JOHN E. WILLETT, Wolverhampton Polytechnic, UK

CONTENTS INCLUDE: The Working Gas Chromatograph: The Carrier Gas, The Oven, The Column, The Injection System, Detectors; Columns; Materials, Liquid Stationary Phases, Solid Stationary Phases, The Support; Choosing the Other Parameters: Length of the Column, Temperature Programming, Sample Size, Attenuation, Flow Rate, Injection Heater Temperature; The Gas Chromatography of Less Volatile Samples; Qualitative Analysis by Gas Chromatography; Quantitative Analysis by Gas Chromatography.

0471913316	272 pages	March 1987	(cl) £28.00/$47.75
0471913324	272 pages	March 1987	(pr) £9.95/$16.95

Samples and Standards

by BRIAN W. WOODGET, Hatfield Polytechnic and
DEREK COOPER, North Staffordshire Polytechnic, UK

CONTENTS INCLUDE: The Analyst's Approach; Introduction to Sampling; Design of a Sampling Procedure; Methods of Taking Samples; Standardization and Calibration; Analytical Standards and Calibration Curves; Standard-addition Methods; Internal-standard Methods; Calibration by Computational Means; Comparison of Calibration Procedures; Monitoring the Performance of Analytical Procedures.

0471912891	318 pages	January 1987	(cl) £32.00/$54.60
0471912905	318 pages	January 1987	(pr) £11.50/$19.60

Principles of Electroanalytical Methods

by TOM RILEY and COLIN TOMLINSON, Brighton Polytechnic, UK

CONTENTS INCLUDE: Basic Principles of Solution Chemistry and Electrochemistry: Ions in Solution, Ion-ion Interactions, Ionic Migration in Electrolyte Solution, Electrodes and the Electrochemical Cell; Galvanic Cells: Electrode Types, The Nernst Equation, The Liquid Junction, EMF Measurements, PH and its Measurement, Potentiometry; Electrolysis; Review of Methods of Electroanalytical Chemistry: Classification and Relationships, Principles of the More Important Methods, Present Usage.

0471913294	272 pages	February 1987	(cl) £28.00/$47.75
0471913308	272 pages	February 1987	(pr) £9.95/$16.95

Radiochemical Methods

by WILLIAM J. GEARY, Department of Chemistry, Sheffield City Polytechnic,

CONTENTS INCLUDE: Introduction: Nuclear Properties and Radioactive Decay; Radio-Isotopes and Labelled Compounds: Preparation and Availability; Practical Aspects: Detection and Counting by Gas Ionization, Scintillation and Semi-Conductor Methods; Radio Analytical Methods: Direct Determination, Tracer Investigations, Activation Analysis; New Applications: Literature Examples, Potential Applications of Radiochemical Techniques.

0471911178	250 pages	October 1986	(cl) £28.00/$47.75
0471911186	250 pages	October 1986	(pr) £9.95/$16.95

Access the worlds analytical chemistry literature using...

Analytical Abstracts

Printed and Online

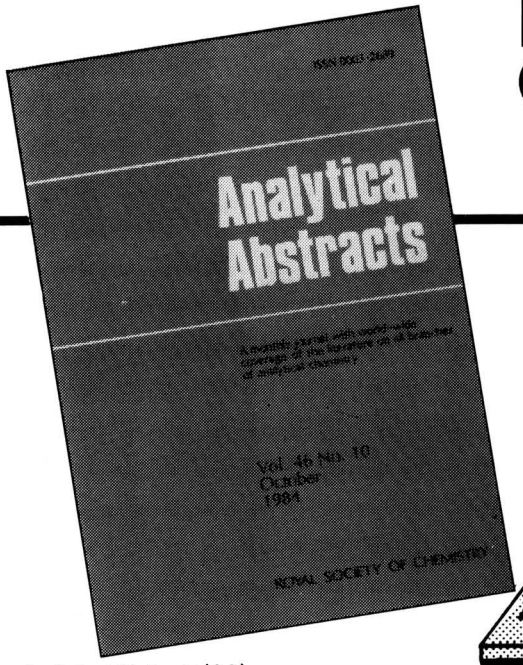

Analytical Abstracts (AA) ...
is the western world's most comprehensive abstracting journal dealing solely with analytical chemistry in all its aspects.

Analytical Abstracts (AA) ...
contains bibliographic information and detailed abstracts on general, inorganic, biochemical, pharmaceutical, food, agricultural and environmental aspects of analytical chemistry worldwide, including computer and instrumentational applications in analysis.

Analytical Abstracts Online ...

the online equivalent of printed AA, offering:

- Comprehensive coverage of analytical chemistry.
- Coverage 1980-to-date: over 85,000 items.
- Analytical methods in detail.
- Quality controlled-language indexes.

Price: UK £239.00 USA $463.00 Rest of World £263.00

Further details and a FREE sample issue available from:

The Royal Society of Chemistry,
University of Nottingham,
University Park,
Nottingham, NG7 2RD,
England.

Tel: 0602 507411
Telex: 37488

Orders should be sent to:

The Royal Society of Chemistry,
Distribution Centre,
Blackhorse Road,
Letchworth,
Herts., SG6 1HN,
England.

Tel: 0462 672555
Telex: 825372

Online information may be obtained from:

DATA-STAR
Data-Star, Plaza Suite, 114 Jermyn Street, London SW1Y 6HJ, England.
Radio-Suisse Ltd., Data-Star, PO Box 3000, Berne 14, Switzerland.

PERGAMON INFOLINE
Pergamon Infoline Ltd., 12 Vandy Street, London EC2A 2DE, England.
Pergamon Infoline Inc., 1340 Old Chain Bridge Road, McLean, Virginia 22101, USA.

DIALOG
DIALOG Information Retrieval Service, PO Box 8, Abingdon, Oxford OX13 6EG, England.
DIALOG Information Services Inc., 3460 Hillview Avenue, Palo Alto, CA 90406, USA.

ORBIT SEARCH SERVICE (SDC)
Bakers Court, Bakers Road, Uxbridge, Middx., UB8 1RG, England.
System Development Corporation, 2525 Colorado Avenue, Santa Monica, CA 90406, USA.

Systematic and Random Errors in Known Addition Potentiometry A Review

Derek Midgley
CEGB, Central Electricity Research Laboratories, Kelvin Avenue, Leatherhead, Surrey KT22 7SE, UK

Summary of Contents

Keywords: *Known addition potentiometry; systematic and random errors; review*

Introduction

Known addition potentiometry is a method that aims to eliminate the effect of the sample matrix and to remove the need for the calibration curves required in determinations by direct potentiometry. These aims are obviously desirable and the method has therefore been described in many texts on potentiometric analysis.[1–6] These descriptions list the ideal conditions necessary for the application of the method, but the analytical errors caused by failure to conform to these conditions are never quantified. Even the review by Mascini[7] does not elaborate these points. The ideal conditions for the use of the method are as follows:

(i) Activity coefficients should not vary.
(ii) The fraction of free, uncomplexed, determinand should not vary.
(iii) The slope factor of the electrode should not vary. This implies that (a) the temperature is constant and (b) the electrode calibration is linear throughout the range in question.
(iv) Liquid junction potentials are constant.

Conditions (i), (ii) and (iv) are difficult to achieve in principle, but in practice conditions can often be arranged so that the variations are negligible. By use of the known dilution method of obtaining the calibration slope, it is often possible to obtain accurate results even when the above conditions are not met.

This review aims to quantify the errors that arise from non-fulfillment of the above conditions and to show how far they can be avoided either by the use of the known dilution method of finding the slope factor or by adjusting the conditions of measurement. The multiple known addition method is not considered.

Theory

Basic Equations

The technique depends on measuring the change in potential of an A-selective electrode immersed in a known volume, V_0, of solution containing an unknown concentration of the determinand, A, when a known volume, V, of a standard solution of A (concentration C_s) is added.

The e.m.f. is related to the activity, {A}, of the determinand by equation (1)

$$E = E^0 + S\log\{A\} + E_j - E_{ref} \quad \ldots \quad (1)$$

where E^0 is the standard potential of the electrode, E_j is the liquid junction potential between the solution and the reference half-cell, E_{ref} is the reference half-cell potential, and S is the calibration slope of the electrode, nominally equal to the Nernst slope factor $RT\ln(10)/zF$.

The activity of A is related to its total concentration, C_A, by

$$\{A\} = f_A\,\alpha_A\,C_A \quad \ldots \quad (2)$$

where f_A is the activity coefficient for A and $\alpha_A = [A]/C_A$ is the ratio of free to total metal ion concentration. Hence, for the initial e.m.f. we obtain,

$$E_1 = E^0 + S\log f_A + S\log\alpha_A + S\log C_A + E_j - E_{ref} \quad \ldots \quad (3)$$

After the addition, the e.m.f. is

$$E_2 = E^0 + S'\log f'_A + S'\log\alpha'_A + S'\log C'_A + E'_j - E_{ref} \quad (4)$$

where the primed symbols represent the new values of S, f_A, α_A, C_A and E_j.

The successful application of the known addition method depends on the validity of the following approximations:

$$S \approx S' \quad \ldots \quad (5)$$

$$E_j \approx E'_j \quad \ldots \quad (6)$$

$$f_A \approx f'_A \quad \ldots \quad (7)$$

$$\alpha_A \approx \alpha'_A \quad \ldots \quad (8)$$

Approximations (5) and (6) are usually very good, but approximations (7) and (8) may fail, as will be discussed

below. Even so, it is usually possible either to treat the sample solution so as to make approximations (7) and (8) valid or to compensate for the inequalities by adjusting the slope factor.

Assuming that all the approximations are valid, therefore, we obtain from equations (3) and (4)

$$E_2 - E_1 = S \log C'_A - S \log C_A \quad .. \quad .. \quad (9)$$

Now

$$C'_A = (V_0 C_A + V C_s)/(V_0 + V) \quad .. \quad .. \quad (10)$$

Therefore,

$$E_2 - E_1 = S \log \left[\frac{V_0 C_A + V C_s}{C_A (V_0 + V)} \right] \quad .. \quad .. \quad (11)$$

which can be rearranged to give an expression for the total concentration of determinand

$$C_A = \left\{ \frac{V/V_0}{\left[\text{antilog} \left(\frac{E_2 - E_1}{S} \right) \right] \left[\frac{V}{V_0} + 1 \right] - 1} \right\} C_s \quad (12)$$

C_A may be obtained from equation (12) not only by arithmetical calculation but by the use of nomograms.[8,9] The calculation is often made simpler by the use of tabulated values of the term in braces in equation (12) at fixed values of V/V_0 and S, as in Orion electrode manuals.

If the analytical procedure requires the addition of reagents to adjust the pH of the sample, to maintain a constant ionic strength or to fix the degree of complexation of the determinand, let V_R be the total volume of all reagent solutions added prior to the measurement of e.m.f., E_1. Then, progressing as from equation (10) to equation (12), we obtain

$$C_A = \frac{V C_s}{V_0 \left\{ \left[\text{antilog} \left(\frac{E_2 - E_1}{S} \right) \right] \left(\frac{V}{V_0 + V_R} + 1 \right) - 1 \right\}} \quad ..(12a)$$

If $V \ll V_0$, equation (12) may be simplified to give the approximation (13)

$$C_A \approx \frac{V C_s}{V_0 \left[\text{antilog} \left(\frac{E_2 - E_1}{S} \right) - 1 \right]} \quad .. \quad .. \quad (13)$$

If $V \ll V_0$ and $V_R \ll V_0$, equation (12a) also reduces to equation (13). Tabulated values of the term in square brackets have been presented[5] for various values of $E_2 - E_1$ and S.

Volume error

The errors incurred by the use of the simplified equation (13) instead of equation (12) are shown in Table 1 for a range of volume additions. The concentration is always overestimated if the dilution of the sample by the standard addition is ignored and the errors increase with the volume of solution added. The errors, ΔC_A, also depend on the ratio, ϕ, of moles added to moles originally present and they can be approximately represented by

$$\frac{\Delta C_A}{C_A} \approx \frac{V}{V_0} \left(\frac{1 + \phi}{\phi} \right)$$

where $\phi = C_s V / C_A V_0$. The relative errors are independent of concentration. If equation (13) is to be used, it is desirable to keep $V/V_0 < 1\%$, but with the availability of programmable calculators and microcomputers equation (13) no longer gives a significant saving of time compared with the accurate equation (12): its use should, therefore, be discouraged.

Influence of the Calibration Slope on Accuracy

The calibration slope, S, is ideally equal to the Nernst slope factor $RT\ln(10)/zF$, where R is the gas constant, T the absolute temperature, F the Faraday constant and z the charge on the ion. In practice, S is determined empirically. The method used to find S must be related to the nature of the sample solution if the errors are to be minimised and the two procedures described below will be considered later in regard to the ionic strength of the sample solution and the presence of complexing agents.

Table 1. Relative errors (%) caused by neglecting the volume correction

	V/V_0, %			
ϕ	0.1	1	2	5
0.5	0.30	3.0	6.2	16.7
1	0.20	2.0	4.1	10.5
2	0.15	1.5	3.0	7.7

Calibration by known dilution

After the addition of the standard solution and the measurement of E_2 [equation (4)], a volume, V_D, of diluent is added and the new equilibrium e.m.f., E_3, is measured.

$$E_3 = E^0 + S'' \log f''_A + S'' \log \alpha''_A + S'' \log C''_A + E''_j - E_{ref} \quad (14)$$

Assuming a set of conditions equivalent to equations (5)–(8), *i.e.*, $S'' \approx S' \approx S$, $E''_j \approx E'_j$, $f''_A \approx f'_A$, $\alpha''_A = \alpha'_A$, we obtain

$$E_2 - E_3 = S \log C'_A - S \log C''_A \quad .. \quad .. \quad (15)$$

Now

$$C''_A = \frac{(V_0 + V) C'_A}{V_0 + V + V_D} \quad .. \quad .. \quad .. \quad (16)$$

Therefore,

$$E_2 - E_3 = S \log \left(\frac{V_0 + V + V_D}{V_0 + V} \right) \quad .. \quad .. \quad (17)$$

from which S can be calculated. If reagents are added prior to measurement, we have, corresponding to equation (17) as equation (12a) corresponds to equation (12),

$$E_2 - E_3 = S \log \left(\frac{V_0 + V_R + V + V_D}{V_0 + V_R + V_D} \right) \quad .. \quad ..(17a)$$

If S is to be determined with reasonable precision, the e.m.f. change, $E_2 - E_3$, should not be too small: conventionally the solution is diluted to twice its original volume, so that $E_2 - E_3$ is about 20 mV for a univalent determinand and 10 mV for a divalent determinand. With such a large dilution it is important that the diluent is at the same temperature (±1 °C) as the sample solution, otherwise it cannot be assumed that $S'' \approx S'$; Table 4 shows the errors arising from this source alone, but in the dilution procedure there are additional errors arising from changes in E^0 and E_{ref} with temperature. Moreover, where $\alpha_A \neq 1$, some change of α_A with temperature should also be expected.

The quantification of the errors associated with changes in E^0 and E_{ref} is possible through use of the isopotential concept familiar in pH measurements.[10] Isopotential data are almost completely lacking for ion-selective electrodes, although there is little experimental difficulty in determining them.

Over a limited range of temperature (± 10 °C) it is valid to express the e.m.f. by

$$E \approx E_I + S(\log C_A - \log C_I)$$

where E_I contains all the temperature-invariant terms and log C_I the temperature-dependent terms. Log C_I is the isopotential point.

Table 2. Effect of temperature variations during the known dilution procedure for an electrode with an isopotential point at log $C = -4$

Temperature change on dilution/°C	Parameter	Log C'_A 3	4	5	6
2	$\tilde{S}/S$	0.98	1.0	1.02	1.04
	Relative error in C_A, %	−2.7	0	2.7	4.4
1	$\tilde{S}/S$	0.99	1.0	1.01	1.02
	Relative error in C_A, %	−1.5	0	1.6	2.8
−1	$\tilde{S}/S$	1.01	1.0	0.99	0.98
	Relative error in C_A, %	1.6	0	−1.5	−3.2
−2	$\tilde{S}/S$	1.02	1.0	0.98	0.95
	Relative error in C_A, %	3.3	0	−3.3	−6.7

Table 3. Dilution factors required to restore solution to approximately its original concentration after known addition

$\lvert E_2 - E_1\rvert$/mV	V_D/V_0* for $\lvert z\rvert = 1$	V_D/V_0* for $\lvert z\rvert = 2$
4	0.2	0.4
6	0.3	0.6
8	0.4	0.9
10	0.5	1.2
12	0.6	1.6
14	0.8	2.1
16	0.9	2.6
18	1.0	3.2
20	1.2	3.9
22	1.4	†
24	1.6	†
26	1.8	†
28	2.1	†
30	2.3	†
32	2.6	†
34	2.9	†
36	3.2	†
38	3.5	†
40	3.9	†

* If reagents are added the ratio is $V_D/(V_0 + V_R)$.

† Use of such large e.m.f. differences is not recommended and the large dilutions are usually impracticable.

After the known dilution, therefore, we would have instead of equations (4) and (14)

$$E_2 = E_I + S' (\log C'_A - \log C_I) \quad .. \quad .. \quad (18)$$

$$E_3 = E_I + S'' (\log C''_A - \log C_I) \quad .. \quad .. \quad (19)$$

If no account is taken of the temperature variation, we obtain from equation (15) the apparent slope factor $\tilde{S}$.

$$\tilde{S} = (E_2 - E_3)/\log (C'_A/C''_A)$$

From the equations with isopotential corrections, (18) and (19),

$$S' = [E_2 - E_3 + (S'-S'') \log C_I]/(\log C'_A - \frac{S''}{S'} \log C''_A)$$

Hence

$$\frac{S'}{\tilde{S}} = \left(1 + \frac{\Delta S}{\Delta E} \log C_I\right) \Big/ \left[1 + \frac{\Delta S}{S'} \frac{\log C''_A}{\log (C'_A/C''_A)}\right] \quad .. \quad (20)$$

where $\Delta S = S' - S''$ and $\Delta E = E_2 - E_3$. In evaluating equation (20), if the temperature changes by 1 °C on dilution, $\Delta S = 0.2/z$ mV decade^{-1} and if the dilution, as usual, halves the concentration, then $\Delta E \approx S' \log(C'_A/C''_A) \approx 18/z$ mV. Substituting in equation (20) and taking, as an example, log $C_I = 4$, a 1 °C change in temperature would give the results shown in Table 2. At $C''_A = C_I$, no error is introduced, but the chances of this condition prevailing are very small. If log $(C''_A/C_I) = \pm 1$, the errors in concentration are about three times larger than the errors introduced by using a calibration slope obtained independently at temperatures 1 or 2 °C different from that at which the known addition was performed. If log $(C''_A/C_I) = \pm 2$, the errors are six times larger. It follows that temperature control may be very important if the known dilution procedure is used, especially as $\log(C''_A/C_I)$ increases. The value of log C_I chosen for the example was arbitrary and could vary by several units, depending on the nature of the electrode membrane's internal contact (electrolytic or solid state) and the choice of reference electrode.

In some instances (*e.g.*, to compensate for ionic strength effects, see below), it is advantageous to dilute the sample so that $E_3 \approx E_1$. The required degree of dilution can be obtained by taking a conveniently rounded figure close to antilog $[(E_2 - E_1)/(S/z)]$, S/z being a reasonable guess at the calibration slope. Dilution factors corresponding to values of $|E_2 - E_1|$ are given in Table 3, calculated with $S = 58$ mV decade^{-1}.

If the sample solution contains a background electrolyte or a strong complexing agent, the diluent should be matched to the sample, as described in the sections on ionic strength and complexing effects.

Calibration with standard solutions

As in direct potentiometry, S may be found as the slope of a plot of e.m.f. against the logarithm of the concentration of a series of standard solutions. It is generally desirable to keep the conditions of the calibration as identical as possible to those obtaining in the sample solution so that systematic errors may be minimised; in particular, reagents added to the sample should also be added to the standard solutions and the standard solutions should span the expected concentration range of the samples.

The temperature at which the calibration is carried out should be within 1 °C of the sample temperature but in practice, and especially in field work, this may be impracticable. In this event, the calibration slope at the sample temperature T_s °C may be approximated by

$$S = S_c (273 + T_s)/(273 + T_c) \quad .. \quad .. \quad (21)$$

where S_c is the slope determined at temperature T_c °C. Before such corrections are used generally, it is desirable to test the accuracy of equation (21) at a minimum of two temperatures different from the calibration temperature and preferably including the extremes of the sample temperature range.

The errors caused by calibrating at 25 °C and analysing at another temperature, T, without correcting by means of equation (21) are shown in Table 4. The errors caused by analysing at 25 °C after calibrating at temperature T are equal (to two significant figures) but opposite in sign.

It is important to note that the calibration plot is defined in terms of concentration and not thermodynamic activity. This means that in certain circumstances S will differ significantly from the thermodynamic slope factor, but as far as the known addition method is concerned this will compensate, to some extent, for deviations from the desired conditions represented by equations (6)–(8). This approximation will only be valid over a limited range of concentrations, particularly if $C_A > 10^{-3}$ mol l^{-1} and there is no background of indifferent electrolyte.

Ionic Strength Effects

In general, the known addition method involves a change in ionic strength and equation (7) is, therefore, only an approximation. The inaccuracy introduced by this inequality depends on the concentration of the determinand, the charge on the determinand, the presence of background electrolyte and the value adopted for the calibration slope. A consideration of these factors will show how errors may be reduced or even avoided.

The systematic errors caused by neglecting variations in activity coefficients were estimated by using equations (3), (4) and (14) to generate theoretical e.m.f.s for the three stages of the known addition procedure (with activity coefficients being calculated as below) and then using these e.m.f.s in equation (12), which assumes that the activity coefficients are constant, to give the apparent determinand concentration. Equation (12) was evaluated first with S equal to the Nernstian slope factor then with S derived from equation (17).

These calculations were carried out for many combinations of the parameters V_0, C_A, V, C_s and V_D for determinands with charge $z = 1$ and $z = 2$ and with background media of various ionic strengths μ in the sample solution, μ' in the standard solution and μ'' in the diluent solution. The total ionic strength, $I = 0.5\Sigma z_i^2 C_i$ was calculated at each stage from the above parameters. Thus if the determinand and its counterion have the same charge (in both the sample and standard solutions) the ionic strengths corresponding to equations (3), (4) and (14) are given by equations (22)–(24), respectively.

$$I = \mu + z^2 C_A \quad .. \quad .. \quad .. \quad (22)$$

$$I' = \frac{(\mu + z^2 C_A)V_0}{V_0 + V} + \frac{(\mu' + z^2 C_s)V}{V_0 + V} \quad .. \quad .. \quad (23)$$

$$I'' = \frac{(\mu + z^2 C_A)V_0}{V_0 + V + V_D} + \frac{(\mu' + z^2 C_s)V}{V_0 + V + V_D} + \frac{\mu'' V_D}{V_0 + V + V_D} \quad .. \quad (24)$$

Activity coefficients were calculated[11] from equation (25).

$$-\log f = Az^2 \left(\frac{\sqrt{I}}{1 + \sqrt{I}} - 0.3I \right) \quad .. \quad .. \quad (25)$$

where A here is the Debye - Hückel coefficient.

The e.m.f.s were calculated on the assumption that the electrodes had ideal Nernstian responses at 25 °C, *i.e.*, $S = 59.16/z$ mV decade^{-1}. Correspondingly, in equation (25) $A = 0.511$ at 25 °C. In all instances $V_D = V_0 + V$, C_A varied from 10^{-5} to 10^{-1} mol l^{-1}, V_0/V from 1000 to 20, VC_s/V_0C_A from 0.5 to 2.0 and μ varied from 0 to 10^{-1} mol l^{-1}, whereas $\mu' = 0$ or μ and $\mu'' = 0$ or μ.

Table 5 summarises the main conclusions of this, and Fig. 1 shows the error as a function of determinand concentration and background ionic strength for singly charged ions. Table 5 shows that the results obtained with the calibration slope calculated by known dilution are almost free from errors provided that the diluent has the same background ionic strength as the sample; this is so even if the ionic strength is not the same at all stages of the procedure, because the calibration slope so obtained compensates for the change in activity coefficients. Fig. 2 shows how the calibration slope varies with C_A, μ and μ''.

Good compensation is obtained by using the known dilution procedure in these examples, because $C'_A = 0.5C'_A \approx C_A$, but in practice it is not possible for the addition always to double the initial concentration and compensation then becomes less efficient for a fixed dilution. Taking the worst instance ($\mu = 0$), if $C'_A = 1.5C_A$, *i.e.*, $VC_s = 0.5\ V_0C_A$, the errors are three to ten times larger, but still <1%. If $C'_A = 3C_A$, *i.e.*, $VC_s = 2V_0C_A$, the errors are twice as large, but in the opposite direction. It is therefore better to arrange the addition so that $VC_s < V_0C_A$ as the initial concentration will then lie within the

Table 4. Errors caused by calibrating at 25 °C and analysing at T °C

T/°C	Error in C_A, %
15	4.7
16	4.2
17	3.8
18	3.3
19	2.8
20	2.3
21	1.8
22	1.4
23	0.9
24	0.5
25	0.0
26	−0.5
27	−0.9
28	−1.4
29	−1.8
30	−2.3

Table 5. Concentration errors caused by variations in activity coefficients. Errors are overestimates unless marked by an asterisk

Conditions†	Slope (S) from calibration graph	Slope (S) from known dilution‡
Singly charged ions:		
No background electrolyte	~1% at $C_A = 10^{-4}$	<0.1% if $VC_s = V_0C_A$
($\mu = \mu' = \mu'' = 0$)	~3% at $C_A = 10^{-3}$	<0.3% if $V_0C_A > VC_s \geq 0.5V_0C_A$
Dilute background electrolyte		
$\mu \approx C_A$ ($\leq 10^{-4}$)	<1%	<1% if $\mu'' = 0$; <*0.05% if $\mu'' = \mu$
$\mu \approx C_A$ (>10^{-4})	2–5%	2–5% if $\mu'' = 0$; <*0.05% if $\mu'' = \mu$
Concentrated background electrolyte		
$100C_A > \mu \geq 10C_A$	≤1% if $V_0/V \geq 100$ ≤0.05% if $20 \leq V_0/V < 100$	2–9% if $\mu'' = 0$; <*0.01% if $\mu'' = \mu$
$\mu \geq 100C_A$	<*0.1% if $V_0/V \geq 100$ <*0.7% if $20 \geq V_0/V < 100$	2–10% if $\mu'' = 0$; <*0.01% if $\mu'' = \mu$
Doubly charged ions:		
No background electrolyte	~2.5% at $C_A = 10^{-5}$	<0.1% at $C_A \leq 10^{-2}$ ($VC_s = V_0C_A$)
($\mu = \mu' = \mu'' = 0$)	~25% at $C_A = 10^{-3}$	≤1% at $C_A \leq 10^{-2}$ ($V_0C_A > VC_s \geq 0.5V_0C_A$)
Dilute background electrolyte		
$\mu \approx C_A$ ($\leq 10^{-4}$)	7%	<1% if $\mu'' = 0$; <*0.05% if $\mu'' = \mu$
$\mu \approx C_A$ (>10^{-4})	20–40%	3–8% if $\mu'' = 0$; <*0.05% if $\mu'' = \mu$
Concentrated background electrolyte		
$100C_A > \mu \geq 10C_A$	4–15%	*8–30% if $\mu'' = 0$; <*0.2% if $\mu'' = \mu$
$\mu \geq 100C_A$	<1%	*8–30% if $\mu'' = 0$; <*0.3% if $\mu'' = \mu$

† Variations of μ' between 0 and μ caused <0.1% error in any instance. Concentrations in mol l^{-1}.
‡ $V_D = V + V_0$. Errors increase as V_0/V decreases, but the difference is <0.1% in the range $20 \leq V_0/V \leq 1000$.

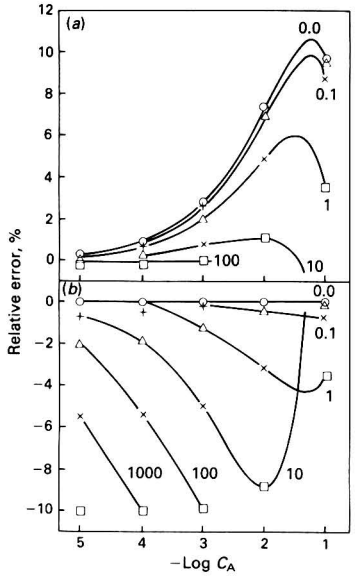

Fig. 1. Errors caused by ionic strength variations in determination of univalent species: (a) Nernstian calibration; (b) known dilution calibration with $V_D = V_0 + V$ and $\mu'' = 0$. Background ionic strength μ = 0 (○), 10^{-4} (+), 10^{-3} (Δ), 10^{-2} (×) and 10^{-1} mol l^{-1} (□). Lines are drawn through points of equal C_M/μ and labelled accordingly. $V = 0.01V_0$; $VC_s = V_0C_A$

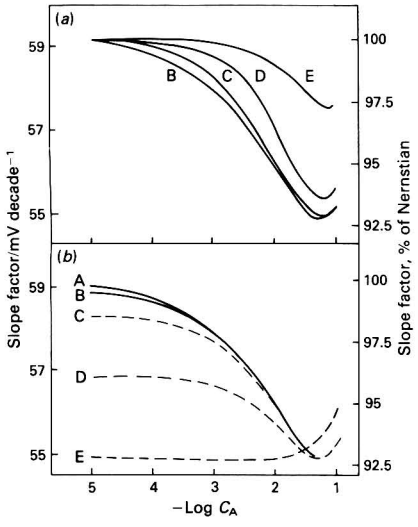

Fig. 2. Effect of ionic strength on slope factor by known dilution (univalent determinand) $V_D = V_0 + V$, $V = 0.01V_0$, $VC_s = V_0C_A$. (*a*) Same background in sample and diluent, $\mu'' = \mu$. (*b*) No background in diluent, $\mu'' = 0$. μ = 0.0 (A), 10^{-4} (B), 10^{-3} (C), 10^{-2} (D) and 10^{-1} mol l^{-1} (E). Solid lines join points with errors ≤1%, broken lines join points with errors >1%

range over which the calibration slope is determined. Alternatively, the correct dilution to ensure that $C'_A \approx C_A$ may be obtained from the e.m.f. change on addition (Table 3) and good compensation for ionic strength effects should ensue.

If a background electrolyte of sufficient concentration ($\mu \geq 100C_A$) is present in the sample (either naturally or by the addition of an ionic strength adjustment buffer), the use of the calibration slope obtained from standard solutions will give good results. The slope obtained by known dilution should not be used unless $\mu'' \simeq \mu$.

Provided that the total ionic strength is low ($\mu + z^2C_A < 5 \times 10^{-4}$) either type of calibration slope may be used with less than 1% error for univalent determinands, but for accurate work with divalent determinands at any ionic strength only the slope obtained by known dilution is recommended.

A background electrolyte is unnecessary in the standard solution added to the sample. Ideally,

$$\mu' + z^2C_s \approx \mu + z^2C_A \quad .. \quad .. \quad .. \quad (26)$$

as the activity coefficients would then be virtually constant. If a background electrolyte is added so that $\mu \gg C_A$, it is relatively simple to satisfy equation (26), but the improvement in accuracy is <0.1%. If the samples are known to have a moderate, but constant, background ionic strength, it may be more convenient to satisfy equation (26) than to add reagent to each sample solution to give a high ionic strength. If equation (26) is satisfied, the calibration slope obtained with separate standard solutions will give accurate results.

Effect of Complexing

So far it has been assumed in calculating C_A from equation (12) that $\alpha_A = \alpha'_A$. When this assumption breaks down, however, gross errors may arise, depending on the concentration of determinand, C_A, the concentration of ligand, C_L, and the stability constant, β, of the complex formed between them. In this context, ligand is defined as any substance that forms a complex with the determinand. With anion-selective electrodes, therefore, the ligand is usually a metal ion. The presence of complexing agents calls for great care in the use of the addition - dilution method, because even if $\alpha_A = \alpha'_A$, α''_A may be considerably different.

Let us consider a simple system containing a single type of ligand that does not participate in side reactions, *e.g.*, protonation, hydrolysis or complexing with other species in the sample solution. Assuming that the activity coefficients are constant, the stability constant is defined by equation (27)

$$\beta = [AL]/[A][L] \quad .. \quad .. \quad .. \quad (27)$$

The total determinand and ligand concentrations are given by equations (28) and (29)

$$C_A = [A] + [AL] = [A](1 + \beta[L]) \quad .. \quad .. \quad (28)$$

$$C_L = [L] + [AL] = [L](1 + \beta[A]) \quad .. \quad .. \quad (29)$$

Now,

$$\alpha_A = \frac{[A]}{C_A} = \frac{1}{1 + \beta[L]} \quad .. \quad .. \quad .. \quad (30)$$

From equation (30) it can be seen that any process changing the free ligand concentration, [L], will change α_A, *e.g.*, dilution or the addition of more determinand. Hence, when a sample solution contains a complexing agent, α'_A and α''_A will never be identical with α_A, but in practice there are wide ranges of conditions in which the differences are negligible.

Calculation with the Nernst slope factor

Fig. 3 shows as functions of β, C_A and C_L the theoretically calculated errors arising from the use of equation (12) with S equal to the electrode's Nernst slope factor; the conditions are $VC_s = V_0C_A$ and $V/V_0 = 0.01$. The errors are small (<2%) if $\beta C_A \leq 10^{-2}$, but increase with βC_A, becoming unacceptably large unless $C_L/C_A \geq 10^2$.

If α_A and α'_A in equations (3) and (4) cannot be equated, we obtain instead of equation (12)

$$C_A = \left\{ \frac{C_sV/V_0}{\left[\text{antilog}\left(\frac{E_2 - E_1}{S}\right)\right]\left(\frac{V}{V_0} + 1\right) - \frac{\alpha'_A}{\alpha_A}} \right\} \frac{\alpha'_A}{\alpha_A} \quad .. \quad (31)$$

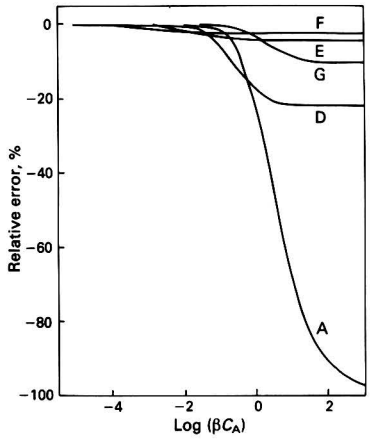

Fig. 3. Errors caused by complexing (Nernstian calibration). $V = 0.01V_0$, $VC_s = V_0C_A$, $C_L/C_A = 0.1$ (G), 1 (A), 10 (D), 100 (E) and 1000 (F)

If $\tilde{C}_A$ denotes the apparent concentration calculated from equation (12), we have

$$\tilde{C}_A \approx C_A\alpha_A/\alpha'_A \quad \ldots \quad \ldots \quad \ldots \quad (32)$$

Whereas the approximation (32) breaks down if α_A/α'_A deviates greatly from unity, especially if antilog $(E_2 - E_1)/S$ is less than about 1.5, it is useful as a basis for showing when the use of equation (12) cannot be justified. This is important because it may be inconvenient to do the extra calculation involved in equation (31) or the calculation may be impracticable unless a separate determination is made of the ligand concentration. In many instances the errors may be reduced by a simple modification to the analytical procedure (see below).

From equations (30) and (32) we have

$$\frac{\tilde{C}_A}{C_A} \approx \frac{\alpha_A}{\alpha'_A} = \frac{1 + \beta[L]'}{1 + \beta[L]} \quad \ldots \quad \ldots \quad \ldots \quad (33)$$

Now $[L]' < [L]$ because of dilution and complexing with the added determinand. Therefore, $\tilde{C}_A < C_A$, but equation (33) shows that there are two ranges of extreme conditions where $\alpha_A/\alpha'_A \simeq 1$ and $\tilde{C}_A$ is a good approximation to C_A. These favourable conditions occur when either $\beta[L] \ll 1$ and $\beta[L]' \ll 1$ or when $\beta[L] \simeq \beta[L]' \gg 1$, *i.e.*, when complexing is either very weak or very strong.

Weakly complexing conditions, $\beta[L] \ll 1$

With weak ligands ($\beta \leqslant 10^3$) in moderate to low concentrations, the degree of complexation is low and $[L] \approx C_L$. Equation (12) will give a <0.1% error if $\beta C_L < 10^{-2}$, and if $\beta C_L \leqslant 10^{-1}$ the error should not exceed 1%. If C_L is unknown, the answer given by equation (12), $\tilde{C}_A$, may be tested directly. It follows from equation (29) that if $[L] \approx C_L$, $\beta[A] \ll 1$. Assuming that with weakly complexing ligands, $[A] \approx \tilde{C}_A$, if $\beta\tilde{C}_A \leqslant 10^{-2}$ the errors will be small. For conditions in which $VC_s = V_0C_A$ and $V/V_0 \leqslant 0.01$, a maximum error of 2% may be expected (Fig. 3); even if $\beta\tilde{C}_A \approx 0.1$ the error should be no more than 5%.

The condition $\beta[L] \ll 1$ may also be satisfied at very low concentrations of strongly complexing ligands, such that $C_A > 100C_L$. With these ligands, if $C_A > C_L$, $[AL] \approx C_L$ and the error in $\tilde{C}_A$ is $-100(1 - C_L/C_A)\%$. Because $C_L \approx [AL] \gg [L]$, the test $\beta C_L \leqslant 10^{-2}$ used for weakly complexing ligands is very conservative, although still valid. The $\beta\tilde{C}_A$ test, however, is not valid with strong ligands.

Strongly complexing conditions, $\beta[L] \gg 1$

The condition $\beta[L] \simeq \beta[L]' \gg 1$ corresponds to the presence of either a strong ligand ($\beta > 10^4$) at moderate to high concentrations or a weak ligand at high concentrations. To obtain $[L] \simeq [L]'$, the addition step must involve no significant reduction in the free ligand concentration; keeping this reduction to acceptable levels depends on the ratio of ligand to determinand and on the degree of dilution.

(i) *Ligand - determinand ratio.* Assuming that dilution is negligible, $[L] \simeq [L]'$ only if the amount of complex formed is negligible compared with the free ligand concentration, *i.e.*, $[AL] \ll [L] \simeq C_L$ and $[AL]' \ll [L]' \simeq C'_L$. In these strongly complexing solutions, $[AL] \approx C_A$ and $[AL]' \approx C'_A$, hence we require the conditions $C_A \ll C_L$ and $C'_A \ll C'_L$.

If the analyst has no expected values for C_A and C_L, a test based on the initial e.m.f., E_1, can be applied, provided that a calibration graph has been prepared with solutions containing no complexing agent. The graph used to find the calibration slope should be adequate for this purpose, even if it has to be extrapolated.

From equation (27), $[AL] = \beta[A][L]$, but $[AL] \ll [L]$ and, therefore, $\beta[A] \ll 1$. The free determinand concentration, [A], is estimated from the calibration graph. If $\beta[A] \leqslant 10^{-3}$, the ligand - determinand ratio is high enough, provided that the addition step is of normal proportions, *i.e.*, $VC_s \approx V_0C_A$. A more conservative procedure is to make the addition and test $\beta[A]' \leqslant 10^{-3}$, where $[A]'$ is estimated from the e.m.f., E_2. The test $\beta\tilde{C}_A \leqslant 10^{-3}$ for weakly complexing systems is not appropriate here.

(ii) *Dilution.* In strongly complexing conditions with a large ratio of ligand to determinand, $[L] \simeq C_L$ and $[L]' \simeq C'_L$. From equation (30), if $\beta[L] \gg 1$ and $\beta[L]' \gg 1$,

$$\frac{\tilde{C}_A}{C_A} \simeq \frac{\alpha_A}{\alpha'_A} \simeq \frac{[L]'}{[L]} \simeq \frac{C'_L}{C_L} = \frac{V_0}{V_0 + V}$$

In equation (12), therefore, dilution will cause $\tilde{C}_A$ to be in error by $-100V/(V_0 + V)\%$ and it is desirable for V/V_0 not to exceed 0.01.

Complexing conditions such that $\alpha_A/\alpha'_A \neq 1$

When $10^{-2} < \beta[L] < 10^2$, equality of α_A and α'_A cannot be assumed and the approximate equation (32) becomes unreliable. Fig. 3 shows the large errors that occur as βC_A increases when $10^{-1} \leqslant C_L/C_A \leqslant 10$. Errors may be reduced by three procedures, depending on conditions.

(a) Diluting the sample so that $\beta C_A \leqslant 10^{-2}$ reduces the errors to less than 2% if $V/V_0 = 0.01$. This procedure is more likely to be useful with weak ligands than strong ligands because in the latter instance the ratio C_L/C_A also determines the size of the errors but is unaffected by dilution. If C_A is small, care should be taken that dilution does not reduce the determinand concentration to such an extent that the electrode is operating in its non-Nernstian response region.

(b) By adding more ligand, we can attain the conditions $C_L \gg C_A$ and $\beta[L] \gg 1$ required for the successful use of equation (12) in strongly complexing conditions. A 100-fold excess of ligand can be recommended (see Fig. 3). Instead of increasing the concentration of the ligand actually present in the sample solution, it is often permissible to add an excess of a second strongly complexing ligand, *e.g.*, EDTA for transition metal determinands. If the analyst has to deal with a wide variety of samples it may be convenient always to add the same ligand, hence avoiding having to prepare a range of different solutions. Mixtures of ligands are discussed below.

(c) As an alternative to dilution, the degree of complexing of the determinand may be reduced by adding a reagent that reacts preferentially with the ligand. This amounts to introducing a conditional stability constant, $\beta_C < \beta$ into the previous equations, so that $\beta_C C_A \leqslant 10^{-2}$. This effect will often be brought about by a change of pH. This subject is discussed below.

Compared with dilution, this procedure has the effect of increasing, rather than decreasing, the free determinand concentration, which may be advantageous near the electrode's limit of detection; on the other hand, interferences are more likely to be introduced.

Calibration by known dilution

No ligand in diluent. Fig. 4 shows as functions of β, C_A and C_L the theoretically calculated errors arising from the use of equation (12) with S determined from equation (17); the conditions are $VC_s/V_0C_A = 1$, $V/V_0 = 0.01$, $V_D = V_0 + V$ and no complexing agent in either the additive or diluent solutions. Unless conditions are such that complexing is scarcely significant, the errors are unacceptable for most purposes. If $C_L < C_A$, the maximum error possible is $100(C_A - C_L)/C_A$, but if $C_L \geqslant C_A$, errors of almost -100% can occur. The reason for the errors when $C_L \geqslant C_A$ is that the calibration slope obtained from equation (17) is inaccurate, because $\alpha'_A \neq \alpha''_A$; the deviation of the slope from the true Nernstian value is indicative of the size of the analytical error (see Fig. 5), except where $C_L \approx C_A$ (line A). In this instance the slope factor goes through a minimum as β increases and may approach Nernstian values at large values of β even though the error is large.

The errors shown in Fig. 4 are reduced if the ratio VC_s/V_0C_A is decreased or if V/V_0 is increased, but such reductions are too small to be of practical use. Fig. 5 shows that if the slope factor is less than 95% of its expected value (a deficiency of $3/z$ mV decade^{-1} for a determinand of charge z) the results should be regarded with caution: this rule of thumb will even catch most instances where $C_L \approx C_A$ (line A in Fig. 5).

Ligand in diluent. If the diluent contains the same concentration of ligand as the original solution, the errors in the use of known dilution to calculate S can be largely compensated. Fig. 6 shows that for $V_D = V_0 + V$ and $VC_s/V_0C_A = 1$ (the optimum conditions), the error is at most 1% when $V/V_0 = 0.01$ and $C_L \geqslant 10C_A$. For $C_L = 0.1C_A$ the error is very small. The errors are approximately proportional to V/V_0. Fig. 7 shows how the slope factor appears to be greater than Nernstian, the discrepancy being greatest at $C_L/C_A = 1$. The apparent deviation from Nernstian response increases as V/V_0 increases.

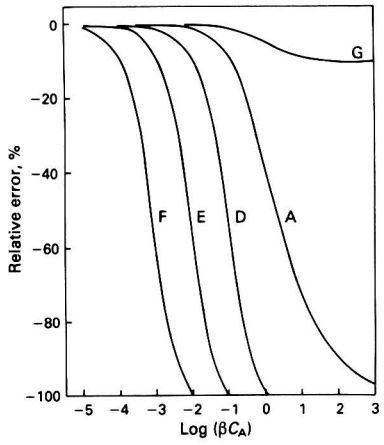

Fig. 4. Errors caused by complexing in addition - dilution method with no ligand in diluent. $V_D = V_0 + V$, $V = 0.01V_0$, $VC_s = V_0C_A$, $C_L/C_A = 0.1$ (G), 1 (A), 10 (D), 100 (E) and 1000 (F)

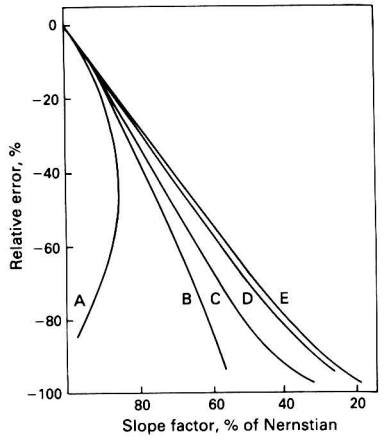

Fig. 5. Effect of complexing. Relationship between relative error and slope factor in addition - dilution method with no ligand in diluent. $V_D = V_0 + V$, $V = 0.01V_0$, $VC_s = V_0C_A$, $C_L/C_A = 1$ (A), 2 (B), 3 (C), 10 (D) and $\geqslant 100$ (E)

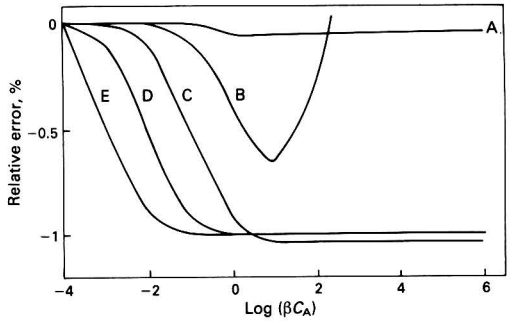

Fig. 6. Error caused by complexing (known dilution calibration with ligand in diluent: $V_D = V + V_0$; $V_0C_A = VC_s$). $C_L/C_A = 0.1$ (A), 1.0 (B), 10 (C), 100 (D) and 1000 (E)

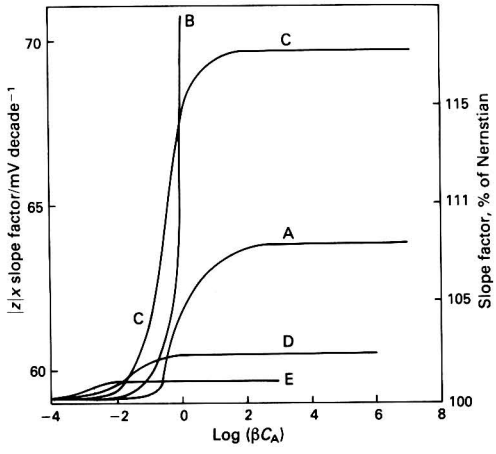

Fig. 7. Effect of complexing on slope by known dilution with ligand in diluent ($V_D = V + V_0$; $V_0C_A = VC_s$). $C_L/C_A = 0.1$ (A), 1.0 (B), 10 (C), 100 (D) and 1000 (E)

The method can sometimes even cope with the condition $C_L = C_A$. For $\beta C_A < 10^3$, the error is <1%. For $\beta C_A > 1$, the slope factor will be a multiple of the Nernstian value because the dilution step involves going from a state in which the determinand is in excess to one where it is almost completely complexed. If the slope factor is greater than $70/|z|$ mV decade^{-1}, the result should be treated with suspicion, as errors may be very large for $\beta C_A \geqslant 10^3$. If $C_L \approx C_A$ and $\beta C_A \geqslant 10^3$, it is desirable either to increase the ligand concentration so that $C_L \geqslant 10C_A$ or to dilute the sample so that $\beta C_A < 10^3$. The results are more diverse in less ideal conditions, where the dilution step does not restore the solution almost to its original state, *i.e.*, if, for $V_D = V_0 + V$, $VC_s \neq V_0C_A$. When $VC_s > V_0C_A$ the apparent slope factor exceeds the Nernstian value by even more than that shown in Fig. 7, and conversely for $VC_s < V_0C_A$. The effect on the analytical result can be seen in Table 6. A high value of C_L/C_A is needed to ensure that errors are no more than about 2%. If $C_L = C_A$ and $VC_s > V_0C_A$ the errors may approach −100% if $\beta C_A > 1$; this is, however, indicated by a slope factor that may be double the Nernstian value. If $C_L = C_A$ and $VC_s < V_0C_A$, the slope factor will again be greater than Nernstian if $\beta C_A > 1$, with errors varying from about −5% at $\beta C_A \approx 10$ to +15% at $\beta C_A > 10^4$. Using Table 3 to calculate the dilution necessary to restore the original concentration of the determinand would keep these errors to a minimum.

In view of the above results, whenever the slope factor is greater than $70/|z|$ mV decade^{-1} the conditions should be adjusted so that either there is a large excess of strong complexing agent at all times or the value of βC_A is reduced by dilution.

Multi-ligand systems

Real sample solutions, as opposed to the simple models discussed so far, are likely to contain more than one ligand. If the *i*th ligand, L_i, forms a complex with a stability constant β_i we would have instead of equations (28) and (30)

$$C_A = [A] + [AL_1] + [AL_2] + \ldots = [A](1 + \Sigma\beta_i[L_i]) \quad \ldots (34)$$

$$\alpha_A = \frac{[A]}{C_A} = \frac{1}{1 + \Sigma\beta_i[L_i]} \quad \ldots \quad \ldots (35)$$

The arguments developed from equations (27)–(33) for systems containing only one ligand are transferable to the multi-ligand example. Instead of equation (33), therefore, we have equation (36)

$$\frac{\tilde{C}}{C_A} \approx \frac{\alpha_A}{\alpha'_A} = \frac{1 + \Sigma\beta_i[L_i]'}{1 + \Sigma\beta_i[L_i]} \quad \ldots \quad \ldots (36)$$

and equation (12) will give good results if either (a) $\Sigma\beta_i[L_i] \ll 1$, $\Sigma\beta_i[L_i]' \ll 1$ or (b) $\Sigma\beta_i[L_i] \simeq \Sigma\beta_i[L_i]' \gg 1$. With weakly complexing ligands ($\beta < 10^3$), condition (a) is met if $\Sigma\beta_iC_{L_i} \leqslant 10^{-3}$ mol l^{-1} and for many purposes $\Sigma\beta_iC_{L_i} < 10^{-2}$ would give acceptable results (<1% low using the Nernst slope factor). If the total ligand concentrations, C_{L_i}, are unknown, $\tilde{C}_A$ may be tested directly. If $\beta_{max.}\tilde{C}_A \leqslant 10^{-2}$, where $\beta_{max.}$ is the largest of the β_i, errors will be <2%.

With strongly complexing ligands ($\beta > 10^4$), the simplest approach is to treat the system as if it contained only one ligand, that giving the largest value of the product $\beta_iC_{L_i}$. This is a good approximation if

$$(\beta_iC_{L_i})_{max.} \geqslant 10\sum_{i \neq i_{max.}} \beta_iC_{L_i} \quad \ldots \quad \ldots (37)$$

The treatment for systems containing one ligand then gives adequate guidance to the accuracy. In strongly complexing solutions the ligand for which $\beta_iC_{L_i}$ is maximal must be in a large excess over the determinand. If $(C_{L_i})_{max.} < 100C_A$ errors may be large even though other ligands are in large excess over the determinand.

If $\alpha_A \neq \alpha'_A$, the simplest remedy is to add a ligand in excess so as to satisfy condition (37). The ligand added need not be present naturally in the sample.

Table 6. Limiting error (%) under different experimental conditions for $V_D = V_0 + V$ and $V/V_0 = 0.01$

	C_L/C_M		
VC_s/V_0C_A	10	100	1000
0.5	−4.1	−2.3	−2.0
1.0	−1.1	−1.1	−2.0
2.0	6.4	0.2	−0.2

If the calibration slope is determined by known dilution, matching the composition of the diluent to the sample may be impracticable unless condition (37) is satisfied either naturally or by the deliberate addition of an excess of one ligand to the sample. Before this procedure is used with real samples thorough testing of model systems is recommended.

Effect of side reactions

Equations (28)–(37) were developed on the assumption that the ligands reacted only with the determinand. In practice, the ligands are likely to react with other species in solution and particularly with hydrogen ions. When such side reactions occur, the equations containing stability constants, β, can be re-written with conditional stability constants,[12] $\beta_C = \beta/\alpha_L$, where α_L includes terms for all the other interactions of the ligand L. For example, if L forms a complex with ion X having stability constant β_X, and participates in protonation equilibria having constants K_1, K_2, etc.,

$$\alpha_L = 1 + K_1[H] + K_2[H]^2 + \ldots + \beta_X[X]$$

As [H] and [X] will change on the addition of the standard and diluent solutions, α_L and, hence, β_C will also change. Values of α_L for the more common metal ions and ligands are available in tabular[12] and graphical[13] form.

The change in [H] depends not only on dilution but also on the buffer capacity of the system, making a general treatment of errors arising from this source too complicated to be of much use. If the ligand participates in protonation equilibria, the pH should be kept constant. Changes in pH are undesirable in any instance, because they are usually the biggest single influence on the liquid junction potential, which should always be kept as constant as possible.

Calculations with Nernstian slope. Errors arising from variations in [X] depend on the experimental conditions. If the determinand is weakly complexed ($\beta[L] \ll 1$), variations in [X] are of no significance; in so far as the formation of the XL complex reduces [L], errors will be smaller than in the absence of X.

If the determinand is strongly complexed, the accuracy of the known addition method depends on maintaining a high ratio of C_L to C_A. The formation of the XL complex is equivalent to reducing this ratio and a more conservative procedure is to keep a high ratio of $C_L - C_X$ to C_A, where C_X is the total concentration of X. The test $\beta[A] \leqslant 10^{-3}$ should be replaced by $\beta_C[A] \leqslant 10^{-3}$.

Calculations with slope from known dilution. If the determinand is weakly complexed, the presence of a competing substance reduces the errors compared with those discussed above. If the determinand is strongly complexed, the presence of a competing substance is equivalent to reducing the ratio C_L/C_A and it is desirable to have $C_L - C_X \geqslant 10C_A$ if the errors are to be within the limits described above.

Liquid Junction Potential

The liquid junction potential depends on the concentration and mobility of all ionic species in both the sample and reference junction solutions, and, therefore, even the qualitative effect of inconsistency of the liquid junction potential during known addition is very variable. In practice the factors

influencing the activity coefficients and complexing would simultaneously affect the liquid junction potential; however, the precautions necessary for controlling errors from these sources would also tend to keep the junction potential constant, *i.e.*, the maintenance of a high, constant, ionic strength, a constant pH and an effectively constant ratio of ligand to determinand.

As an example of the errors that could be caused by liquid junction potentials, calculations by means of the Henderson equation have been made for the most commonly used reference electrolyte (saturated potassium chloride) forming a junction with a sample solution containing only the salt of the determinand ion. The effect of variations in activity coefficients has been neglected. The size of the volume increment affected the error by <0.1% for $V/V_0 \leqslant 0.05$ and the results were valid throughout the range of concentration increments tested ($0.5 \leqslant VC_s/V_0C_A \leqslant 2$).

Calibration by known dilution [equation (17)] compensated for changes in the liquid junction potential so well that errors exceeded 0.1% only for high concentrations of determinand ($\geqslant 10^{-1}$ mol l^{-1}). The calibration slopes were sub-Nernstian (57–58 mV decade^{-1}) for cation determination and super-Nernstian (−60 to −61 mV decade^{-1}) for anion determination. The deviation from Nernstian response increased with increasing concentration when the anion in the sample was more mobile than the cation, but decreased when the cation was more mobile. These trends in the results for calibration slope are valid only for reference junctions in which the anion is more mobile than the cation, *e.g.*, potassium chloride. If the cation were the more mobile ion in the reference junction (*e.g.*, potassium nitrate) the trends would be reversed.

The use of the slope from a separate calibration graph should give accurate results if the conditions of the calibration match those of the analysis, otherwise errors of several per cent. may occur. Using the ideal Nernstian response with the data calculated above for a saturated potassium chloride junction produced errors of 2–5% (overestimates for cations, underestimates for anions). If the cation in the reference junction were more mobile than the anion, the procedure would underestimate cationic concentrations and overestimate anionic concentrations.

Measurements in the Non-Nernstian Response Region

At low concentrations, the responses of ion-selective electrodes cease to be Nernstian.[14] Two types of deviation will be considered here, that caused by the solubility of the electrode's material and that caused by the blank associated with the electrolyte added to the sample to maintain the ionic strength.

Deviations caused by solubility

This type of behaviour is usually associated with electrodes incorporating sparingly soluble isovalent salts, *e.g.*, AgCl, AgBr and AgI, and this will be the only instance considered. The non-Nernstian responses of many solid-state ion-selective electrodes are not governed by the solubility product mechanism alone and the following treatment would not apply, *e.g.*, Cu^{2+}, Cd^{2+}, Pb^{2+}, F^- and S^{2-} electrodes.

Consider an electrode, consisting of a sparingly soluble isovalent salt, immersed in a medium of constant ionic strength. Let the solubility product of the salt be K_s. The total concentration, C_t, of determinand at the surface of the electrode depends on the concentration in the sample solution, C_A, and the concentration that has dissolved from the electrode. It has been shown[14,15] that this concentration is given by equation (38)

$$C_t = \frac{C_A}{2} + \sqrt{\frac{C_A^2}{4} + K_s} \quad \ldots \ldots (38)$$

The systematic errors caused by solubility were estimated by using equations (3), (4) and (14) to generate theoretical e.m.f.s for the three stages of the known addition procedures, but C_A, C'_A and C''_A in these equations were replaced by C_t, C'_t and C''_t, calculated from equation (38). The e.m.f.s so calculated were used in equation (12) to give the apparent determinand concentration and in equation (17) to give the calibration slope. E_j, α_A and f_A were assumed to remain constant throughout. Errors calculated using the calibration slope obtained by known dilution are shown in Fig. 8 as a function of the ratio $C_A/K_s^{\frac{1}{2}}$ for the experimental conditions $V_0/V = 100$, $V_D = V + V_0$ and $VC_s/V_0C_A = 0.5$ (line X), 1.0 (line Y) and 2.0 (line Z). Errors calculated using the Nernst slope factor are shown as line Y′, corresponding to the conditions for line Y: the errors in conditions corresponding to lines X and Z are not shown but are slightly larger and slightly smaller, respectively, than those in line Y′. Using the Nernst slope factor, errors of less than about 2% can be expected only if $C_A > 10K_s^{\frac{1}{2}}$. Using the calibration slope obtained by the known dilution method, errors of less than 1% are achieved if the dilution step restores the determinand concentration to within 1% of its original value in the sample. This would rarely be achievable in practice and errors of less than 1% are obtained only if $C_A \geqslant 10K_s^{\frac{1}{2}}$ when the final determinand concentration is 75 or 150% of the initial concentration. In general, therefore, results indicating $C_A < 10K_s^{\frac{1}{2}}$ should be treated with caution. As a rule of thumb, the error, Δ, in the determination of $C_A \leqslant 2K_s^{\frac{1}{2}}$ is given by equation (39)

$$\Delta \approx i(E_3 - E_1)\, 5K_s^{\frac{1}{2}}/C_A\% \quad \ldots \ldots (39)$$

where $i = \pm 1$ and is positive when the e.m.f. becomes more positive with increasing concentration. For $C_A > 2K_s^{\frac{1}{2}}$ the error is smaller than that estimated from equation (39).

Equation (39) is valid for ratios of V/V_0 up to at least 5%: if $VC_s \leqslant V_0C_A$, the error is minimised by keeping V/V_0 small (~0.1%); but for $VC_s > V_0C_A$ values of $V/V_0 \approx 5\%$ would be preferred. The effect of the volume ratio V/V_0 is small (1–2%) compared with that of the ratio VC_s/V_0C_A (see Fig. 8). Only when $VC_s \approx V_0C_A$ does V/V_0 became significant in determining the total error; in such instances $V/V_0 = 1\%$ is a good compromise value.

In conclusion, at concentrations where the solubility of the salt in the electrode is significant, the addition - dilution method gives smaller errors than the addition method using

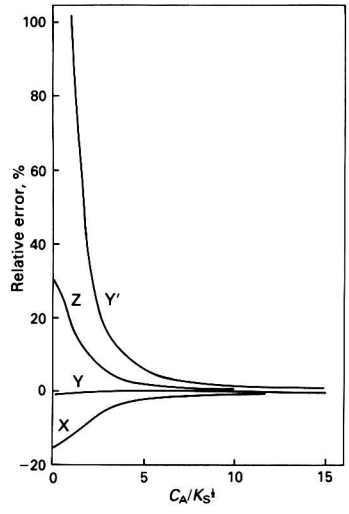

Fig. 8. Error caused by solubility product. Known dilution calibration ($V_D = V_0 + V$) with $VC_s/V_0C_A = 0.5$ (X), 1.0 (Y) and 2.0 (Z). Nernstian calibration (Y′) with $VC_s/V_0C_A = 1.0$

the Nernst slope factor and also indicates that results may be biased because the calibration slope so obtained deviates greatly from the Nernstian value (Fig. 9), although similar deviations are caused by reagent blanks (*cf.* Fig. 11).

Deviations caused by reagent blanks

Reagents added to the sample, *e.g.*, for maintaining the ionic strength, may contain material that would cause the calibration of the e.m.f. against the logarithm of the nominal concentration of determinand to deviate from linearity at low concentrations. This material may include interfering substances or determinand carried in the reagents as an impurity. Such interferences can often be the limiting factor in the response of glass and liquid ion-exchange electrodes, whereas determinand introduced as an impurity will affect all kinds of electrodes. Note that the effects described here are different from those caused by interferences present in the sample itself. When an electrode is influenced by reagent blanks the e.m.f. may be expressed by equation (40)

$$E = E^0 + S \log \alpha_A + S \log f_A + S \log (C_A + B) + E_j - E_{ref} \quad . . \quad (40)$$

where B represents the reagent blank and may be resolved into components as follows

$$B = b_0 + \Sigma K_i \frac{(b_i f_i \alpha_i)^{z_A/z_i}}{\alpha_A f_A} \quad . . \quad . . \quad (41)$$

where b_0 is the concentration of determinand introduced as an impurity and, for the ith interferent, z_i is the ionic charge, b_i is the concentration, f_i the activity coefficient, α_i the ratio of free to total concentration and K_i is the selectivity coefficient of the electrode for that interferent.

The systematic errors caused by reagent blanks were estimated by using equations (3), (4) and (14), with C_A, C'_A and C''_A replaced by $C_A + B$, $C'_A + B'$ and $C''_A + B''$, to generate theoretical e.m.f.s for the three stages of the known addition procedure. E_j, α_A and f_A were assumed to remain constant throughout. The e.m.f.s so calculated were used in equations (17) and (12) to give the calibration slope and the apparent determinand concentration. This was done for the instances where (a) only the sample, (b) sample and diluent and (c) sample, solution and diluent contained the reagents that gave rise to the blank.

Calibration slope obtained by known dilution. Errors calculated using the calibration slope obtained from equation (17) when the reagents are absent from the standard solution but present in the diluent are shown in Fig. 10 as a function of the ratio C_A/B for the experimental conditions $V_0/V = 100$, $V_D = V + V_0$ and $VC_s/V_0C_A = 0.5$ (line X), 1.0 (line Y) and 2.0 (line Z). When the reagents are present in the standard solution also, the errors are much the same, being slightly smaller when $VC_s/V_0C_A > 1$, slightly larger when $VC_s/V_0C_A < 1$ and equal but opposite in sign when $VC_s/V_0C_A = 1$. If the reagents are included in neither the standard solution nor the diluent, equation (17) gives a calibration slope equal to the Nernst slope factor for the electrode and equation (12) gives an apparent determinand concentration equal to $C_A + B$, *i.e.*, the blank appears as a positive bias. For the addition - dilution method to work successfully, therefore, the reagents must be added to the diluent, but there is no point in adding them to the standard solution. This conclusion broadly matches those reached for ionic strength effects, the control of which is one of the main reasons for adding reagents, but is much more important. An indication of the importance of the composition of the diluent is the large deviation of the calibration slope from the Nernst slope factor (Fig. 11).

If $VC_s \approx V_0C_A$, the error is roughly proportional to the volume addition ratio, V/V_0, but deviation of VC_s/V_0C_A from unity (which itself has a much greater effect on the errors than variations in V/V_0) obscures any simple relationship. $V/V_0 = 0.01$ gave the best results over a range of VC_s/V_0C_A.

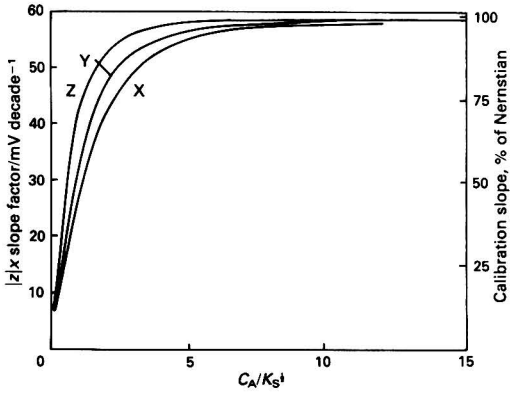

Fig. 9. Effect of solubility product on slope by known dilution ($V_D = V_0 + V$). $VC_s/V_0C_A = 0.5$ (X), 1.0 (Y) and 2.0 (Z)

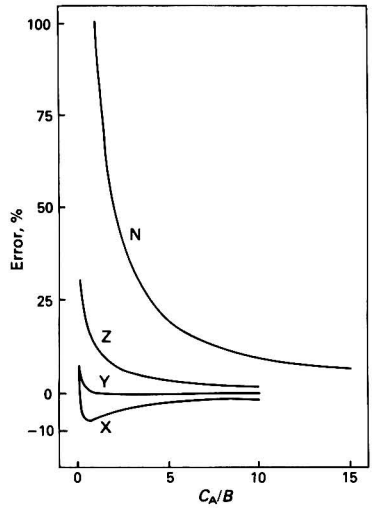

Fig. 10. Error caused by reagent blank with Nernstian (N) and known dilution (X, Y, Z) calibration. $VC_s/V_0C_A = 0.5$ (X), 1.0 (Y) and 2.0 (Z); $V_D = V_0 + V$

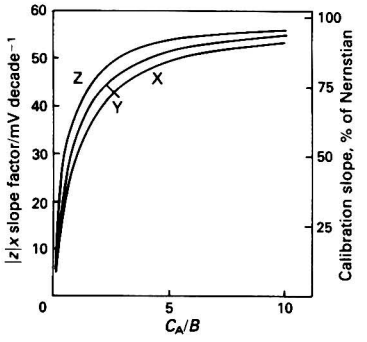

Fig. 11. Effects of reagent blank on slope by known dilution ($V_D = V_0 + V$). $VC_s/V_0C_A = 0.5$ (X), 1.0 (Y) and 2.0 (Z)

Because the calibration is not Nernstian, Table 3 cannot be used to predict the desired degree of dilution in the known dilution step. Within the range $2 \geqslant VC_s/V_0C_A \geqslant 0.5$, if the calibration slope is greater than 85% of the Nernstian value, errors will not exceed 5% for a fixed 2-fold dilution. At lower values of the calibration slope, large (>10%) errors should be expected unless $|E_3 - E_1| < 1/|z|$ mV.

Calibration with the Nernst slope factor. The use of the Nernst slope factor in equation (12) gives an apparent determinand concentration which is equal to $C_A + B$ when the reagents are not present in the standard solution (line N, Fig. 10) and only slightly smaller when the reagents are present in the standard solution. The Nernst slope factor should not be used unless an error of $100\ B/C_A\%$ is acceptable. The use of the Nernst slope factor also has the disadvantage that it does not indicate that bias is possible, whereas the calibration slope from equation (17) deviates considerably from the theoretical value when B is of the same order as C_A (or when there is a significant solubility effect). If a calibration graph is prepared properly, *i.e.*, using the same procedure as applied to the samples, the range over which the Nernstian response is valid becomes self-evident.

Source of the blank. Calculation of the apparent determinand concentration from equation (12), as above, corresponds to the reagents being present *in* the sample solution, *e.g.*, when a solid sample is dissolved or a gaseous one absorbed. When reagents are added *to* the sample solution, equation (12a) would be appropriate, but all the above arguments would still be valid. Figs. 10 and 11 would then represent the errors and calibration slopes obtained in conditions exactly corresponding to those above, *i.e.*, $(V_0 + V_R)/V = 100$, and $V_D = V_0 + V + V_R$, provided that B is regarded as the notional blank in the original volume of sample solution V_0. This is readily seen if the mixture of sample and reagent solutions is thought of as a volume, $\hat{V}_0 = V_0 + V_R$, of a new sample of concentration $\hat{C}_A = C_AV_0/\hat{V}_0$ with a blank $\hat{B} = BV_0/\hat{V}_0$, because $\hat{C}_A/\hat{B} = C_A/B$.

The accuracy with which the above treatment can predict the error caused by reagent blanks depends on the nature of the blank. If $B = b_0$, *i.e.*, no interferents are present, the predictions of the theory should be accurate. When interferents contribute to the blank, however, the outcome is less predictable because selectivity coefficients often vary with concentration.

Bias caused by interferences in the sample

Interfering substances present in the sample influence the e.m.f. of the electrode according to equation (42).

$$E = E^0 + \log \alpha_A + \log f_A + S \log (C_A + \theta_I) \quad .. \quad (42)$$

where $\theta_I = \Sigma \frac{K_i(C_if_i\alpha_i)z_A/z_i}{\alpha_A f_A}$, and K_i is the selectivity coefficient of the electrode for the ith interferent of concentration C_i and charge z_i with activity coefficient f_i, α_i being the ratio of free to total interferent.

Calibration with the Nernst slope factor. The determinand concentration calculated from equation (12) will be overestimated, so that

$$\tilde{C}_A - C_A = \theta_I \quad .. \quad .. \quad .. \quad (43)$$

Equation (43) is accurate for $z_A = z_i$, provided that K_i, f_i and α_i are constant at all stages of the procedure. In regard to f_i and α_i this requirement imposes no additional condition, as f_A and α_A must also be constant. K_i may change with concentration, but this is unlikely to be significant over the approximately 2-fold concentration range covered in the known addition procedure.

Even if $z_A \neq z_i$, equation (43) gives a good (±1%) estimate of the error in concentration provided $C_A \geqslant \theta_I$. As the interference term increases beyond C_A, equation (43) becomes less accurate. If $z_A < z_i$, $\tilde{C}_A$ is less than expected from equation (43) and conversely for $z_A > z_i$.

Calibration by known dilution. If $z_A = z_i$, equation (43) is valid, with the same provisos as before.

If $z_i = 2z_A$, use of the known dilution calibration reduces the interference effect, so that $\tilde{C}_A - C_A \approx 0.6\ \theta_I$. The slope factor becomes increasingly sub-Nernstian as θ_I increases relative to C_A.

If $z_A = 2z_i$, the interference effect is increased by the use of the known dilution calibration, which becomes increasingly super-Nernstian as θ_I increases, so that

$$\tilde{C}_A - C_A \approx 1.7\ \theta_I$$

If known interfering substances are systematically present in the sample solution at known concentrations, the error may be reduced in the known addition - dilution procedure by using a diluent that matches the sample solution in the concentrations of interfering substances present. The error will then be the same as that obtained when the interferents are introduced with the reagents.

Random Errors

The random errors in the calculation of the determinand concentration from equation (12) arise from uncertainties in measuring the e.m.f. of the electrode, in determining the calibration slope, in delivering the volumes V_0 and V and in the concentration, C_s, of the standard solutions. With ordinary laboratory techniques, the errors in V_0, V and C_s should be small, both in absolute terms (0.1–0.2%) and relative to the errors associated with the electrode.

Let equation (12) be rewritten as follows

$$C_A = p/s = p/(qr - 1) \quad .. \quad .. \quad .. \quad (44)$$

where $p = C_sV/V_0$, $q = 1 + V/V_0$ and $r = \text{antilog}\ \frac{(E_2 - E_1)}{S}$. Let the standard deviation of a single determination of a quantity, x, be denoted by $\sigma(x)$ and the corresponding relative variance be denoted by $R(x) = \sigma^2(x)/x^2$. Then from equation (44) and the rules for combination of errors, we have

$$R(C_A) = R(p) + R(s)$$

$$= R(p) + \frac{q^2r^2}{s^2}[R(q) + R(r)] \quad .. \quad .. \quad (45)$$

Now

$$R(p) = R(C_s) + R(V) + R(V_0) \quad .. \quad .. \quad (46)$$

$$R(q) = \left(\frac{V}{qV_0}\right)^2 [R(V) + R(V_0)] \quad .. \quad (47)$$

$$R(r) = (\ln 10)^2 \sigma^2 \left(\frac{E_2 - E_1}{S}\right) =$$

$$(\ln 10)^2 \left(\frac{E_2 - E_1}{S}\right)^2 [R(E_2 - E_1) + R(S)] \quad (48)$$

Progression from equations (45)–(48) requires some assumptions to be made about the source of the variability of $(E_2 - E_1)$. In all instances the error in $(E_2 - E_1)$ will be treated as being independent of the errors in V, V_0 and C_s, because these quantities are invariably known much more precisely than the e.m.f.s or slope factor and make a negligible contribution to $R(E_2 - E_1)$. The first treatment assumes that the variability of the e.m.f. is the dominant source of error. It would be applicable if the uncertainty in the e.m.f.s arose from the difficulty of actual measurement, *e.g.*, because of electrical noise caused by a bad liquid junction, a damaged sensing electrode or inadequate screening, or simply because a meter of inadequate sensitivity was used. If the e.m.f. can be measured with good precision but established with imperfect reproducibility, the first treatment becomes dubious, because the absolute value of E_1 is irrelevant to known addition potentiometry; this example may be typically envisaged as one where the liquid junction cannot be re-formed exactly as before or the temperature has changed. A different treatment is presented for this instance and then the two are compared with experimental data.

Error mainly caused by the imprecision of e.m.f.

It has been assumed[7,16] that $\sigma^2(E_2 - E_1) = \sigma^2(E_1) + \sigma^2(E_2)$ and in most instances it is reasonable to assume that $\sigma(E_1) = \sigma(E_2) = \sigma_E$ if the potentials are not too different, *e.g.*, the electrodes cited by Midgley.[17] Thus $R(E_2 - E_1) = 2\sigma_E^2/(E_2 - E_1)^2$, giving

$$R(r) = (\ln 10)^2 \left(\frac{E_2 - E_1}{S}\right)^2 \left[\frac{2\sigma_E^2}{(E_2 - E_1)^2} + R(S)\right] \quad (49)$$

Combining equations (45)–(47) and (49), we obtain

$$R(C_A) = R(C_s) + \left(1 + \frac{r^2V^2}{s^2V_0^2}\right)[R(V) + R(V_0)] + 2\left(\frac{qr\ln 10}{sS}\right)^2 \sigma_E^2 + \left[\frac{qr(E_2 - E_1)\ln 10}{sS}\right]^2 R(S) \quad (50)$$

In conditions typical of the known addition procedure, *i.e.*,

$$V \ll V_0 \text{ and } C_A \ll C_s, qr/s \simeq 1 + \frac{C_A V_0}{C_s V} \text{ and } r \simeq 1 + \frac{C_s V}{C_A V_0}$$

Substituting in equation (50),

$$R(C_A) = R(C_s) + \left(1 + \frac{r^2V^2}{s^2V_0}\right)[R(V) + R(V_0)] + 2\left[\left(1 + \frac{C_A V_0}{C_s V}\right)\ln 10\right]^2 \frac{\sigma_E^2}{S^2} + \left[\left(1 + \frac{C_A V_0}{C_s V}\right)\log\left(1 + \frac{C_s V}{C_A V_0}\right)\ln 10\right]^2 R(S) \quad (51)$$

With normal laboratory techniques it should be possible to obtain values of $R(C_s) \approx R(V) \approx R(V_0) \approx 10^{-6}$, *i.e.*, with a precision of ~0.1%, which is much better than can usually be obtained for potentiometric measurements. Neglecting terms in $R(C_s)$, $R(V)$ and $R(V_0)$, therefore, we obtain

$$R(C_A) \approx 2\left[\left(1 + \frac{C_A V_0}{C_s V}\right)\ln 10\right]^2 \frac{\sigma_E^2}{S^2} + \left[\left(1 + \frac{C_A V_0}{C_s V}\right)\log\left(1 + \frac{C_s V}{C_A V_0}\right)\ln 10\right]^2 R(S) \quad (52)$$

This equation may be compared with those derived by Ratzlaff[16] and Mascini,[7] who have overestimated the dependence of $R(C_A)$ on σ_E^2 by a factor of 2 and with that of Horvai and Pungor,[18] who assumed that $R(S) \approx 0$.

Equation (52) shows that the analytical error in C_A increases with $C_A V_0/C_s V$, *i.e.*, the precision is worse for a small increase in concentration leading to a small change in e.m.f. Increasing the amount of determinand added will improve the precision, but very large increases in concentration are more likely to cause bias by changing activity coefficients, liquid junction potentials, etc., as discussed above. The accepted best compromise is a doubling of concentration in the addition step, and for this instance equation (52) can be more closely evaluated, *i.e.*, for $C_A V_0/C_s V = 1$ and $S = 58/z_A$ where z_A is the charge on the determinand,

$$R(C_A) \approx 0.0126\, z_A^2 \sigma_E^2 + 5.7 \times 10^{-4} z_A^2 \sigma^2(S) \quad .. \quad (53)$$

$R(C_A)$ appears to depend more on σ_E than on $\sigma(S)$, which itself has a dependence on σ_E expressed by

$$\sigma(S) = \frac{\sigma_E}{\sigma_x\sqrt{n}} \quad .. \quad .. \quad .. \quad (54)$$

where σ_x is the standard deviation of the log (concentration) values of $n(>2)$ standard solutions used to calibrate the electrode (n may include replicates). If n is large and the solutions have a wide concentration range, $\sigma(S) \ll \sigma_E$, leading to a minimum possible value

$$R(C_A) = 0.0126\, z_A^2 \sigma_E^2 \quad .. \quad .. \quad .. \quad (55)$$

If only the simplest, two-point, calibration is used, equation (54) is invalid. Instead, we have

$$\sigma^2(S) = 2\sigma_E^2/(\log \psi)^2 \quad .. \quad .. \quad .. \quad (56)$$

where ψ is the ratio of the two concentrations. By experience and consensus, there should not be less than a 2-fold difference between the solutions and a practical maximum for $\sigma^2(S)$ can be established.

$$\sigma^2(S) = 2\sigma_E^2/(\log 2)^2 = 22\sigma_E^2 \quad .. \quad .. \quad (57)$$

In this instance, therefore, we have

$$R(C_A) \approx 0.0126 z_A^2 \sigma_E^2 + (22 \times 5.7 \times 10^{-4}) z_A^2 \sigma_E^2 = 0.025 z_A^2 \sigma_E^2 \quad (58)$$

The practical maximum errors predicted by equation (58) are twice the minimum possible errors predicted by equation (55). Errors calculated from equation (57) are given in Table 7 and show the need for precise readings of e.m.f. Meters reading to no better than ±1 mV are scarcely suitable.

Errors caused mainly by the imprecision of the slope factor

If it is assumed that $\sigma(E_2 - E_1)$ is directly dependent not on σ_E, but on $\sigma(S)$, we obtain from $E_2 - E_1 = S \log(C'_A/C_A)$

$$\sigma(E_2 - E_1) = \log \frac{C'_A}{C_A}\, \sigma(S) \quad .. \quad .. \quad (59)$$

which means that

$$R(E_2 - E_1) = R(S)$$

Substituting in equation (45) we obtain

$$R(C_A) \approx R(C_s) + \left(1 + \frac{r^2V^2}{s^2V_0^2}\right)[R(V) + R(V_0)] + 2\left[\frac{qr(\ln 10)}{s} \cdot \frac{(E_2 - E_1)}{S}\right]^2 R(S) \quad (60)$$

Neglecting $R(C_s)$, $R(V)$ and $R(V_0)$, and substituting for q, r and s as before [for equation (52)], we obtain

$$R(C_A) \approx 2\left[\left(1 + \frac{C_A V_0}{C_s V}\right)\log\left(1 + \frac{C_s V}{C_A V_0}\right)\ln 10\right]^2 R(S) \quad .. \quad (61)$$

For a typical example with $C_A V_0 = C_s V$ and $S = 58/z_A$ mV decade^{-1},

$$R(C_A) = 0.0011\, z_A^2 \sigma^2(S) \quad .. \quad .. \quad (62)$$

$\sigma(S)$ may be expressed in terms of σ_E as in equations (55)–(57). For the least precise (two-point) practical calibration, we obtain from equation (57)

$$R(C_A) = 0.024\, z_A^2 \sigma_E^2 \quad .. \quad .. \quad (63)$$

Columns 3 and 4 of Table 8 show the errors predicted by equation (62) at various values of $\sigma(S)$. As $\sigma(S)$ decreases below 0.2 mV decade^{-1}, the errors in C_s, V_0 and V are no longer negligible. The final column shows the effect of

Table 7. Maximum relative random errors in known addition potentiometry with $C_A V_0 = C_s V$, assuming σ_E is dominant source of error. Two-point calibration with solution concentrations differing by a factor of two. Minimum possible errors are half those in the table

	Relative error for charges, %	
σ_E/mV	$\lvert z_A\rvert = 1$	$\lvert z_A\rvert = 2$
0.1	1.6	3
0.2	3	6
0.5	8	16
1	16	32
2	32	63

including these terms in equation (60). For comparison, the value of σ_E that would produce each value of $\sigma(S)$ when calibrating with two solutions with a 2-fold difference in concentration is shown in column 2; in that instance the two treatments are equivalent [*cf.*, equations (58) and (63)]. In general, however, these calculations predict that the random errors can depend less on σ_E than the previous treatment implied.

Equation (61) may be compared with Ratzlaff's[16] equation (16). Apart from changes in notation, Ratzlaff's estimate of $R(C_A)$ is only half that given by equation (61) because he assumed that $\sigma(E_2 - E_1) = 0$. $E_2 - E_1$, however, depends on S and $\sigma(E_2 - E_1)$ is non-zero, as shown by equation (59). Ratzlaff's equation (17) which should differ from his equation (16) only in notation, contains either a typographical or algebraic error.

Errors caused by imprecision of both ($E_2 - E_1$) *and the slope factor*

Rice[19] assumed that the error in $E_2 - E_1$ could be independent of the error in the slope factor. The analytical error can be expressed by equation (64), assuming also that $R(V)$, $R(C_s)$ and $R(V_0)$ are negligible

$$R(C_A) \approx \left[\left(1 + \frac{C_A V_0}{C_s V}\right) \log \left(1 + \frac{C_s V}{C_A V_0}\right) \ln 10\right]^2 \times [R(E_2 - E_1) + R(S)] \quad (64)$$

In calculating $R(E_2 - E_1)$, $\sigma(E_2 - E_1)$ is measured directly and not assumed to be equal to $\sqrt{2}\sigma_E$ [in which instance equation (64) would be identical with equation (52)].

Table 8. Random errors in known addition potentiometry calculated assuming $\sigma(S)$ is dominant source of error

		Relative error for $C_A V_0 = C_s V$, %		
		Equation (62)		Equation (60)†
$\sigma(S)$/ mV decade^{-1}	σ_E*/ mV	$\lvert z_A \rvert = 1$	$\lvert z_A \rvert = 2$	$\lvert z_A \rvert = 1$
0.05	0.01	0.16	0.33	0.23
0.1	0.02	0.32	0.66	0.36
0.2	0.04	0.66	1.3	0.68
0.5	0.11	1.6	3.3	1.6
1.0	0.21	3.3	6.6	3.3

* Value of σ_E giving stated $\sigma(S)$ from calibration with two standard solutions differing in concentration by a factor of two.
† Evaluated with $R(C_s) = R(V) = R(V_0) = 10^{-6}$.

Rice showed that at a constant value of $\sigma(E_2 - E_1)$ and $\sigma(S) \approx 0.1$–0.5 mV decade^{-1}, the relative error in C_A had a minimum at values of $C_s V/C_A V_0$ around 1–2.

Comparison of observed and calculated errors

Table 9 shows published data for the precision of analysis by known addition potentiometry together with values of σ_E, $\sigma(E_2 - E_1)$ and $\sigma(S)$. The values of $\sigma(S)$ were obtained over at least one decade of concentration and usually from several repeat runs. Most types of ion-selective electrode are represented: solid-state (chloride, bromide, fluoride), liquid ion-exchange (nitrate, caffeine and phenothiazines), gas-sensing (ammonia) and redox - solid-state (chlorine). The errors predicted from σ_E by equations (58) and (53) are always too large, whereas those predicted from $\sigma(S)$ by equation (62) show good agreement with the observed values in a majority of instances. $\sigma(E_2 - E_1)$ is not only less than $\sqrt{2}\sigma_E$ but less than σ_E itself, showing that the first of the above treatments is not appropriate in any of the instances for which results have been reported.

If $\sigma(E_2 - E_1)$ is less than $\sqrt{2}\sigma_E$, so should be $\sigma(E_2 - E_3)$ in the known dilution procedure for finding the slope factor. The values of $\sigma(S)$ for this procedure would then be much less than those predicted by equations (56) and (57) and in consequence equations (58) and (63) would overestimate the random error in the determinand concentration. This could not be confirmed as no data on known dilution were found in the literature.

In two of the three instances for which known addition data were available (chloride and chlorine), equation (64) predicted the error very well. As the same data were used to calculate $\sigma(E_2 - E_1)$ and C_A, however, the agreement may be better than would be expected for the prediction of future results. In the third instance (fluoride), equation (62) gave a better approximation. It is likely that with a good electrode, constant conditions and a stable solution the assumption that the variance in $E_2 - E_1$ depends directly on the variance in S is a valid one. Equation (62) would give a good prediction in such instances, *e.g.*, Midgley's fluoride data.[20] With the chlorine data,[27] however, the solution was far less stable, because the determinand was both reactive and volatile. Additional sources of variance in $E_2 - E_1$ were possible, therefore, and equation (64) was the more appropriate.

Even with one type of electrode, the relevance of equations (62) and (64) may depend on circumstances, *e.g.*, sample matrices can vary over many decades of concentration of concomitant substances and require various chemical treatments before measurement and even an abnormally wide range of ambient temperature during the measurements may invalidate equation (62). Table 9 shows, however, that

Table 9. Observed and calculated precision in known addition potentiometry

					Relative standard deviation in concentration, %				
Determinand	Sample	σ_E/ mV	$\sigma(E_2 - E_1)$/ mV	$\sigma(S)$/ mV decade^{-1}	Observed	Eqn. (62)	Eqn. (53)	Eqn. (58)	Eqn. (64)
Fluoride[20]	Boric acid solution	0.44	0.08	0.24	0.7	0.8	5.0	6.8	1.5
Fluoride[19]	Sodium hydroxide solution	—	—	0.08	0.3–0.8	0.3	—	—	—
Chloride[21]	Paper machine water	0.39	0.32	0.24	2.1	0.8	4.4	6.1	2.5
Chloride[22]	Water	0.39	—	0.49	2.3	1.8	4.5	6.2	—
Nitrate[23]	Drinking water	0.5	—	—	2.3	—	—	7.9	—
Nitrate[24]	Pickling baths	—	—	0.26	0.6	0.9	—	—	—
Ammonia[25]	Water	—	—	0.20	1.0	0.7	—	—	—
Ammonia[26]	Kjeldahl digests	0.53	0.10	—	1.1	—	—	8.4	—
Residual chlorine[27]	Sea water	0.75	0.29	0.17	5.3	1.2	8.4	12	5.3
Bromide[28]	Peach extract	—	—	1	3	3.3	—	—	—
Chlorpromazine[29]	Solutions and tablets	—	—	0.32	1.4–2.6	1.1	—	—	—
Promethazine[29]	Solutions and tablets	—	—	0.43	1.1–1.9	1.4	—	—	—
Perphenazine[29]	Solutions and tablets	—	—	0.65	2.1	2.1	—	—	—
Caffeine[30]	Analgesic tablets	—	—	0.7	1.2–2.6	2.5	—	—	—

equation (62) is a generally good predictive tool and its relative simplicity makes it attractive for this purpose.

Discussion

A number of general rules for the successful application of the known addition method may be extracted from the preceding detail.

In discussing electrode performance, sub- and super-Nernstian refer to empirical slope factors that are, respectively, below and above the theoretical value, although the linear relationship between the e.m.f. and the logarithm of the concentration or activity may still be valid. A non-Nernstian response is one where this relationship has been established as having broken down.

Use of Nernstian Calibrations

Applying a fixed value of the slope factor is liable to cause errors of several per cent. except in fairly restricted circumstances. The temperature of analysis should be within 1 °C of the calibration temperature. The sample should contain, or have added to it, a background electrolyte about 100 times the concentration of the determinand if activity coefficient effects are to be avoided; this same step will also reduce the effects of liquid junction potentials. If the determinand is strongly complexed there should be a 100-fold molar excess of ligand over determinand.

The method will not in any way avoid the errors caused by the presence of interferences in the sample or by the introduction of interferences or additional determinand in reagents added to the sample. Use of the Nernst slope factor at concentrations where the electrode response deviates from ideality will cause errors: the determinand concentration should be ten times the solubility of the electroactive component in the membrane.

Use of Known Dilution Calibration

If the slope factor is obtained by this means, many of the errors associated with potentiometric analysis can be minimised. This can only be achieved if the diluent is appropriately matched to the sample (including any reagents added). The temperature should not differ by more than 1 °C. The diluent should contain the same background ionic strength as the sample and the same concentration of ligand. The errors caused by reagent blanks can be much reduced, but the effects of interfering substances present in the original sample are not. Even if the electrode is operating in its non-Nernstian response region, errors are much smaller than those obtained with a fixed value for the calibration slope: note, however, that direct potentiometry would generally be preferred in such circumstances.

A feature of the known dilution calibration is that it alerts the analyst to the reliability of the result.

(a) If the slope factor agrees with the electrode's Nernst slope factor, systematic errors in concentration should be small, unless there are interferents in the sample. Even if the slope factor differs from the Nernstian value, the concentrations should be accurate provided that the e.m.f. after dilution (E_3) is approximately the same (±1 mV) as in the original sample (E_1) and the diluent has been matched to the sample as above. Interferents present in the original sample, however, will always bias the result.

(b) If $E_3 \neq E_1 \pm 1$ mV, and the slope factor is non-Nernstian, the result should be regarded with suspicion. Except near the electrode's limit of detection, the degree of dilution needed to make $E_3 \approx E_1$ can be obtained from Table 3 (provided that the diluent and sample are matched with respect to background ionic strength, ligand concentration and temperature).

If ionic strength effects are significant, the known dilution calibration is sub-Nernstian even if the ionic strength in the diluent is at the correct level for effective compensation. Having less ligand in the diluent than in the sample causes the slope factor to be low when complexing is a significant factor. Reagent blanks and solubility product effects always produce sub-Nernstian responses.

The known dilution calibration is super-Nernstian if the diluent contains too much ligand, or even the correct (non-zero) concentration, or if the ionic strength in the diluent is too high. The ligand concentration is the more significant factor in producing super-Nernstian responses.

Random Errors

The analytical precision is more dependent on the precision of the slope factor than on the precision of the standard potential. Equations (62) and (64) for the prediction of errors are more appropriate than equation (58), unless the measurement of e.m.f. is imprecise because of some deficiency in the equipment. Equation (58) and its related formulae are applicable to analysis by separate measurements of e.m.f. in a sample and a spiked sample, in which the mathematics of calculating the concentration are the same as for known addition. Known addition should be the more precise technique because of its lower dependence on σ_E, the standard deviation of the e.m.f.

Activity Coefficients

If the Nernst slope factor is used, errors caused by variations in the activity coefficients are small (<1%) if the sample contains a background electrolyte that is about 100 times the determinand concentration [Fig. 1(*a*) and Table 5]. If the background is not present naturally, it can be added, as is usual in direct potentiometry.

If the known dilution calibration is used, the errors are small (<0.5%) if the concentration of the background electrolyte is the same in the sample and the diluent, but in other instances it may be large, especially for divalent ions (Table 5).

Effect of Complexing

The presence of complexing agents with stability constants, β, such that $\beta C_A > 10^2$ will cause errors, which may be very large, except in certain circumstances (Figs. 3 and 4).

If a strong ligand ($\beta > 10^4$) is in large molar excess (~ 100-fold) the errors are less than 5% with a Nernstian slope factor (Fig. 3) and less than 2% with a slope factor obtained by known dilution (Fig. 6), but the diluent must contain the same concentration of ligand as the sample.

If the ligand is weak ($\beta < 10^3$) and its concentration, C_L, is not too high ($\beta C_l \leqslant 10^{-1}$), the error obtained with the Nernst slope factor is <1% (Fig. 3). The slope obtained by known dilution gives errors of <1% if the diluent contains the same concentration of ligand (Fig. 6), but if the diluent contains no ligand the errors are <5% only if $\beta C_L < 10^{-1.5}$ (Fig. 4).

The prediction of errors for intermediate cases is difficult and it may be best to modify the sample so that it conforms to one of the two instances above. Solutions containing fairly high concentrations of weak ligands can be diluted as long as the determinand concentration is not taken below the limit of Nernstian response of the electrode. More of the strong ligand can be added to bring its concentration up to the required excess.

If the sample solution is inadequately characterised, the results can be tested for the likeliness of errors. For calculation with the Nernstian slope, $\beta C_L < 10^{-2}$ or $\beta C_L \leqslant 10^{-2}$ with weak ligands and $\beta[A] \leqslant 10^{-3}$ with strong ligands indicate that errors should be small. With the known dilution calibration a slope factor exceeding $70/|z|$ mV decade^{-1} is a sign that the sample requires some treatment.

Allowance can be made for systems containing more than one ligand and for ligands that complex species other than the determinand.

Table 10. Sources of systematic error for ion-selective electrodes

Type of electrode	Species sensed	Ionic strength effect	Principal complexing species	Principal interferences	Causes of non-Nernstian response	Limit of Nerstian response,‡ −log (concentration/mol l^{-1})
Solid state	F^-	Small	H^+,* Al^{3+},* Fe^{3+},* H_3BO_3	OH^-	Kinetic	>5
	Cl^-	Small	Hg^{2+}, Cd^{2+}, Tl^{3+}	SO_3^{2-}, CN^-, Br^-,† I^-,† S^{2-}†		4(AgCl), 5(Hg_2Cl_2)
	Br^-	Small	Hg^{2+}, Tl^{3+}, Cd^{2+}	SO_3^{2-}, CN^-, I^-,† S^{2-}†		5(AgBr), 6(Hg_2Br_2)
	I^-	Small	Hg^{2+}, Cd^{2+}, Pb^{2+}	CN^-, S^{2-}†	Solubility	6
	CN^-	Small	Transition metals	I^-, S^{2-}†		6
	SCN^-	Small	Fe^{3+}, Hg^{2+}	Br^-, I^-,† S^{2-}†		5
	S^{2-}	Significant*	H^+*	-SH groups	Oxidation of S^{2-}	>5.5
	Residual chlorine	Nil	Cl^-, Br^-	Oxidants	Trace organics	7
	Cu^{2+}	Significant	Many	Hg^{2+},† Ag^+†		6
	Pb^{2+}, Cd^{2+}	Significant	organic and inorganic	Hg^{2+},† Ag^+,† Cu^{2+}†	Oxidation of membrane	4–5
	Ag^+	Small	compounds	Hg^{2+}†	Adsorption?	6(Ag_2S)
Glass and liquid ion exchange	Na^+	Small		H^+, Li^+, Ag^+		4(ix), >6 (glass)
	Li^+	Small		H^+, Na^+, Ag^+		4(ix), 5 (glass)
	K^+	Small		H^+, NH_4^+, Ag^+	Mainly reagent blanks but solubility effects are possible	5–6
	NH_4^+	Significant		K^+, Na^+		4–5(ix)
	Ca^{2+}	Significant	Carboxylic acids, EDTA	Transition metals		≤5
	Ba^{2+}	Significant				4
	NO_3^-	Small		Large anions		>4
	ClO_4^-, BF_4^-	Small				4
Gas sensing	NH_3	Nil	H^+,* transition metals	Alkylamines	Kinetic? or blank	<6
	CO_2	Significant*	H^+*	SO_2	Blank	4–5
	NO_x	Significant*	H^+*	CO_2, SO_2	Atmospheric CO_2 blank	>5
	SO_2	Significant*	H^+,* HCHO		Blank (SO_2)	5

* In these instances it is very unusual to omit sample treatment that nullifies the effect.
† These have catastrophic interferences and must be absent.
‡ These are limits in optimum conditions at about 25 °C.

Non-Nernstian Calibrations

Factors causing the electrode to have a non-Nernstian response will produce large errors if the Nernst slope factor is used, but will be smaller if the known dilution calibration is used and this will at least indicate that the interpretation of the results may be problematic (Figs. 8 and 9). If the e.m.f. after dilution is returned to the original value in the sample, the errors may be kept within reasonable limits (5%). The factors responsible are usually the solubility of the membrane material or the presence of a reagent blank.

The known dilution calibration may also give a non-Nernstian value because it is compensating for variations in complexing, activity coefficients or liquid junction potentials.

In this region of the electrode's response, direct potentiometry with a carefully prepared calibration graph will usually give the best results.

Interferences and Reagent Blanks

Interfering substances present in the original sample will interfere in known addition potentiometry as in direct potentiometry. A good example is given by Hassan *et al.*[31] for measurements on calcium - magnesium mixtures with a variety of liquid ion-exchange electrodes. One possible exception occurs if the concentration of the interfering substance is known: it can then be added to the diluent for the known dilution calibration and treated as if it were a reagent blank. Errors caused by a reagent blank (interferents or additional determinand in reagents added to the sample and diluent) can be minimised by the correct use of the known dilution calibration, but not when the Nernst slope factor is used (Fig. 10).

There may also be an option of removing the interference by processes such as precipitation, oxidation, complexation and volatilisation, as appropriate to the interfering substance and the electrode.

Conclusions

The systematic errors ensuing from the use of an ideal (Nernstian) slope factor in non-ideal conditions have been demonstrated for the following instances: (a) variations in activity coefficients; (b) the effect of complexing; (c) the solubility of the electrode membrane; (d) the presence of a reagent blank; and (e) the presence of interferences.

Table 10 gives a qualitative classification of the sources of error affecting the known range of commercially available electrodes. The errors would arise in both direct potentiometry and known addition potentiometry, although not necessarily to the same extent. In many instances the errors can be eliminated by suitable treatment of the sample solution. The lists of complexing and interfering substances are indicative rather than exhaustive, as the effects depend on the concentration and many other substances could be significant in appropriate circumstances.

The known dilution method of obtaining the calibration slope has been shown to be capable of largely compensating for errors otherwise expected in the examples (a)–(d) above. The conditions necessary to achieve compensation have been determined.

Errors arising from procedural variations have been investigated for temperature and volume addition.

The precision of the slope factor is of paramount importance in the over-all precision if analysis is carried out by this method.

The known addition method is not, as is sometimes implied, a cure-all for difficult potentiometric analyses, but its intelligent application can often yield results inaccessible to direct potentiometry.

Published by the permission of the Central Electricity Generating Board.

References

1. Moody, G. J., and Thomas, J. D. R., "Selective Ion Sensitive Electrodes," Merrow, Watford, 1971.
2. Camman, K., "Das Arbeiten mit ionenselektiven Elektroden," Springer, Berlin, 1973.
3. Koryta, J., "Ion-selective Electrodes," Cambridge University Press, Cambridge, 1973.
4. Bailey, P. L., "Analysis with Ion-Selective Electrodes," Heyden, London, 1976.
5. Midgley, D., and Torrance, K., "Potentiometric Water Analysis," Wiley, Chichester, 1978.
6. Veselý, J., Weiss, D., and Štulík, K., "Analysis with Ion-Selective Electrodes," Ellis Horwood,Chichester, 1978.
7. Mascini, M., *Ion-Sel. Electrode Rev.*, 1980, **2**, 17.
8. Karlberg, B., *Anal. Chem.*, 1971, **43**, 1911.
9. Ip, S. Y., and Pilkington, N. H., *J. Water Pollut. Contr. Fed.*, 1978, **50**, 2778.
10. Mattock, G., "pH Measurement and Titration," Heywood, London, 1961, p. 190.
11. Davies, C. W., "Ion Association," Butterworths, London, 1962.
12. Ringbom, A., "Complexation in Analytical Chemistry," Interscience, New York, 1963, p. 35.
13. Kragten, J., "Atlas of Metal - Ligand Equilibria in Aqueous Solution," Ellis Horwood, Chichester, 1978.
14. Midgley, D., *Ion-Sel. Electrode Rev.*, 1981, **3**, 43.
15. Bardin, V. V., *Zavod. Lab.*, 1962, **28**, 910.
16. Ratzlaff, K. L., *Anal. Chem.*, 1979, **51**, 232.
17. Midgley, D., *Analyst*, 1979, **104**, 248.
18. Horvai, G., and Pungor, E., *Anal. Chim. Acta*, 1980, **113**, 287.
19. Rice, T. D., *Anal. Chim. Acta*, 1983, **151**, 383.
20. Midgley, D., *Analyst*, 1985, **110**, 841.
21. Korhonen, J., and Lumme, P.O., *Pap. Puu*, 1977, **59**, 558.
22. Neupert, L., *Acta Hydrochim. Hydrobiol.*, 1982, **10**, 557.
23. Hulanicki, A., Lewandowski, R., and Maj, M., *Anal. Chim. Acta*, 1974, **69**, 409.
24. Burman, J. O., and Johansson, G., *Anal. Chim. Acta*, 1975, **80**, 215.
25. Vandevenne, L., and Oudewater, J., *Trib. CEBEDEAU*, 1973, **26**, 127.
26. Nubé, M., Van den Aarsen, C. P. M., Giliams, J. P., and Hekkens, W. T. J. M., *Clin. Chim. Acta*, 1980, **100**, 239.
27. Dimmock, N. A., and Midgley, D., *Talanta*, 1982, **29**, 557.
28. Austin, R. K., and Phillips, D. J., *J. Agric. Food Chem.*, 1985, **33**, 1165.
29. Cosofret, V. V., and Buck, R. P., *Analyst*, 1984, **109**, 1321.
30. Hassan, S. S. M., Ahmed, M. A., and Saoudi, M. M., *Anal. Chem.*, 1985, **57**, 1126.
31. Hassan, S. K. A. G., Moody, G. J., and Thomas, J. D. R., *Analyst*, 1980, **105**, 147.

Paper A6/451
Received November 26th, 1986
Accepted December 1st, 1986

Temperature Compensation in Potentiometry: Isopotentials of pH Glass Electrodes and Reference Electrodes
Part I. Theory

Derek Midgley
CEGB, Central Electricity Research Laboratories, Kelvin Avenue, Leatherhead, Surrey KT22 7SE, UK

The reasons for the non-linearity of the temperature response of glass pH electrodes are explored theoretically and the relationship between pH_{iso}, the isopotential pH (at which the e.m.f. is invariant with temperature), and the different components of the potentiometric cell is demonstrated. In particular, the temperature coefficient of pH of the glass electrode's filling solution is shown to be paramount in designing electrodes with characteristics convenient for instrumental temperature compensation. The pH of most filling solutions varies parabolically with temperature and the linear correction applied by the temperature compensation circuits of pH meters will have a limited useful range. Filling solutions with linear temperature characteristics are proposed, but the resultant electrodes would be incompatible with the many pH meters having a fixed isopotential setting of 7. Liquid junction potentials are shown to make a small and essentially linear contribution to the temperature dependence of the cell.

Keywords: *pH; glass electrode; reference electrode; temperature compensation; isopotential*

Although the most accurate measurements of pH require sample and standard solutions to be at the same temperature, some applications have to cope with varying temperatures. Temperature compensation is, therefore, a normal feature of pH meters and is also found on some process analysers for use with ion-selective electrodes. Modern instruments may incorporate digital thermometers reading to 0.1 °C and those incorporating microprocessors may have settings for the slope factor and isopotential pH (enabling corrections to be made for the temperature variation of the standard potential) as precise as 0.01 mV pH^{-1} and 0.001 pH, respectively. Instrumentally, therefore, it should be possible to compensate for temperature more accurately than before, provided that the thermal characteristics of sensing and reference electrodes can be defined with adequate precision and the theory implicit in the design of the temperature compensation circuitry is correct. In this paper, the temperature dependence of pH cells is examined theoretically and in Part II the performance of commercially available glass pH and reference electrodes will be considered.

All pH meters incorporate some form of temperature compensation, although its exact nature is not always made explicit by the controls on the meter or the operating manual. In the equation relating e.m.f. to pH,

$$E = E^{\circ}_{cell} - k\,pH \quad . . \quad . . \quad . . \quad (1)$$

both "constants" (the standard potential, E°_{cell}, and the slope factor, k) vary with temperature. The temperature coefficient of the slope factor should be constant and predictable for all electrodes and compensation for this is a feature of almost all pH meters, under either manual or automatic control.

The temperature coefficient of the standard potential is the source of various approximations, errors and misapprehensions. In principle, it can be calculated for known reference elements in known solutions inside the glass and reference electrodes; in practice, the analyst does not know the composition of the solution inside the glass electrode. An indication of this temperature coefficient is sometimes supplied by the manufacturer in the form of the isopotential pH, but unfortunately this is often quoted with insufficient rigour (not being defined with respect to a named reference electrode) and may even be confused with the zero-point pH (at which the e.m.f. = 0 mV). For temperature compensation with most pH meters it is desirable that these points should coincide in practice, but they are theoretically distinct and may differ considerably.

Even with electrodes whose temperature characteristics are well defined, errors may arise from the limitations of pH meters. Many pH meters lack an isopotential pH adjustment and work on the basis (often unstated in the instruction manual) that the isopotential pH is 7; errors are unavoidable if the electrodes have different characteristics. Commercially available pH meters invariably apply a correction that assumes that the standard potential varies linearly with temperature, but the non-linearity of the temperature variation of the standard potential has long been known.[1]

Isopotential pH values are usually determined experimentally and applied as if they were linear temperature coefficients. Theoretical treatments have expressed isopotentials only in empirical coefficients.[1-3] This paper relates the isopotential pH to the internal reference electrode and filling solution of the glass pH electrode and to the external reference electrode and its liquid junction with the test solution. The sources of non-linearity in temperature compensation are considered. Factors analogous to isopotential pH can also be derived for ion-selective electrodes[3,4] and in these instances better linearity may be obtained.

Theory

The conventional potentiometric cell with a glass electrode for measuring pH may be represented as below.

$$\underbrace{M\,|\,MX\,|\,\begin{matrix}\text{solution containing}\\ X^-\text{ ions, } a_X\end{matrix}\,||\,\begin{matrix}\text{test solution}\\ \text{pH}\end{matrix}}$$

$$\underbrace{|\,\begin{matrix}\text{glass}\\ \text{membrane}\end{matrix}\,|\,\begin{matrix}\text{inner solution}\\ a'_X, \text{pH}'\end{matrix}\,|\,M'X\,|\,M'}$$

In practice, X^- is the chloride ion and M and M′ are either silver or mercury or, more rarely, thallium. If the membrane responds to hydrogen ions with perfect selectivity, the e.m.f. of the above cell may be represented as in equation (2).

$$E = (E^{\circ\prime} - k\log a'_X + k\text{pH}')_{glass} - k\text{pH} + E_j - (E^{\circ} - k\log a_X)_{ref} \quad . . \quad (2)$$

where $E^{\circ\prime}$ and E° are the standard potentials of the two reference elements M′| M′X and M|MX, E_j is the liquid junction potential and k is the Nernst slope factor, equal to $RT\ln 10/F$ where R is the gas constant, T K is the temperature and F is Faraday's constant. The terms in brackets are constant at a given temperature and E_j is assumed to be so for

the sake of calibrating the pH meter (the reference electrode is chosen so that this is a reasonable assumption). Equation (2) can be re-expressed as equation (1), where E°_{cell} contains all the constant terms. pH meter temperature compensation circuits[2,5] assume that E°_{cell} and k vary linearly with temperature. For k it may be seen that this is correct because

$$\frac{\partial k}{\partial T} = \frac{R\ln 10}{F} = \text{constant} \quad \ldots \quad \ldots \quad \ldots \quad (3)$$

In the case of E°_{cell}, however, this assumption is an approximation.

Subtracting equation (1) from equation (2) and differentiating, we obtain

$$\frac{\partial E^\circ_{cell}}{\partial T} = \left(\frac{\partial E^{\circ\prime}}{\partial T} - \frac{k\,\partial \log a'_X}{\partial T} - \log a'_X \frac{\partial k}{\partial T} + \frac{k\,\partial \mathrm{pH}'}{\partial T} + \mathrm{pH}' \frac{\partial k}{\partial T}\right)_{glass} + \frac{\partial E_j}{\partial T} - \left(\frac{\partial E^\circ}{\partial T} - \frac{k\,\partial \log a_X}{\partial T} - \log a_X \frac{\partial k}{\partial T}\right)_{ref} \quad \ldots \quad (4)$$

Rearranging equation (4) gives

$$\frac{\partial E^\circ_{cell}}{\partial T} = (-\log a'_X + \mathrm{pH}' + \log a_X)\frac{\partial k}{\partial T} + \left(\frac{\partial E^{\circ\prime}}{\partial T} - \frac{\partial E^\circ}{\partial T}\right) + k\left(\frac{\partial \log a_X}{\partial T} - \frac{\partial \log a'_X}{\partial T}\right) + \frac{\partial E_j}{\partial T} + \frac{k\,\partial \mathrm{pH}'}{\partial T} \quad (5)$$

Examination of the terms in equation (5) shows the conditions necessary for obtaining an E°_{cell} that varies linearly with temperature.

(i) The terms grouped as $(-\log a'_X + \mathrm{pH}' + \log a_X)\,\partial k/\partial T$ will vary linearly because of equation (3).

(ii) The standard potential terms dE°/dT and $dE^{\circ\prime}/dT$ are not necessarily linear, but the curvature is negligible over a range of ±15 °C for calomel and silver - silver chloride electrodes. With matching reference elements in the glass and reference electrodes, however, these terms cancel provided that the cell is isothermal.

(iii) On a molal scale, the terms $k\partial \log a'_X/\partial T$ and $k\partial \log a_X/\partial T$ are approximately zero, provided that the solutions are not saturated. With saturated solutions, the introduction of a temperature-dependent solubility makes the terms non-zero and, generally, non-linear, *e.g.*, with saturated potassium chloride solutions $\partial a_{Cl}/\partial T$ is approximately linear, making $\partial \log a_{Cl}/\partial T$ curved.

(iv) The liquid junction term $\partial E_j/\partial T$ should be small for any junction likely to be used in a pH cell and it will be shown below that any variation should be almost linear over a range of 30 °C for concentrated, but not saturated, potassium chloride bridge solutions. If the junction contains a saturated reference solution, additional non-linear terms may arise.

(v) The term $k\partial \mathrm{pH}'/\partial T$ depends on the nature of the solution inside the glass electrode. With a solution of strong acid (pH ≤4), $\partial \mathrm{pH}'/\partial T \approx 0$ and this approximation is still fairly good for many weak acid buffers over a moderate range of temperature, *e.g.*, acetate buffers. However, because the circuitry of some pH meters restricts the choice of pH_{iso}, glass electrodes generally contain buffers closer to neutrality and for such solutions $\partial \mathrm{pH}'/\partial T$ is both non-zero and non-linear. This will be discussed after the consideration of isopotentials.

It can be seen that careful consideration needs to be given to points (ii)–(v) if a linear variation of E°_{cell} with temperature is to be achieved. Points (ii)–(iv) come readily within the control of the analyst, but point (v) does not.

Isopotential Correction

The temperature coefficient of the standard potential is usually expressed in pH methodology as the isopotential pH, *i.e.*, the pH at which the e.m.f. of the electrode pair is invariant with temperature.

From equation (1), the e.m.f. at the isopotential point, E_{iso}, is given by

$$E_{iso} = E^\circ_{cell} - k\mathrm{pH}_{iso} \quad \ldots \quad \ldots \quad \ldots \quad (6)$$

By the definition of pH_{iso}, $\partial E_{iso}/\partial T = 0$. Hence,

$$\partial E^\circ_{cell}/\partial T = \mathrm{pH}_{iso}\partial k/\partial T \quad \ldots \quad \ldots \quad (7)$$

Substituting from equation (3),

$$\partial E^\circ_{cell}/\partial T = \mathrm{pH}_{iso}R\ln 10/F \quad \ldots \quad \ldots \quad (8)$$

Equation (8) and the definition of pH_{iso} imply that E°_{cell} varies linearly with temperature, hence E°_{cell} may be expressed as

$$E^\circ_{cell} = E_s + (T - T_s)\frac{R\ln 10}{F}\mathrm{pH}_{iso}$$

where E_s is the value of E°_{cell} at reference temperature, T_s. Hence

$$E^\circ_{cell} = E_s - \frac{RT_s\ln 10}{F}\mathrm{pH}_{iso} + \frac{RT\ln 10}{F}\mathrm{pH}_{iso} \quad \ldots \quad (9)$$

Comparison of equations (6) and (9) shows that

$$E_{iso} = E_s - \frac{RT_s\ln 10}{F}\mathrm{pH}_{iso}$$

Substituting in equation (1) gives an expression that relates the experimental variables (E, pH) at (ideally) all temperatures by means of two temperature-independent constants (E_{iso}, pH_{iso}) and the theoretically predictable slope factor (k) with its simple linear dependence on absolute temperature.

$$E = E_{iso} - k(\mathrm{pH} - \mathrm{pH}_{iso}) \quad \ldots \quad \ldots \quad (10)$$

Equation (10) forms the basis of temperature compensation in pH meters. Once E_{iso}, k and pH_{iso} have been set at one temperature, through the "buffer," "slope factor" and "isopotential" controls, respectively, the meter thereafter requires adjustment only of the temperature setting for it to be used to measure pH at other temperatures.

The analysis of the temperature-dependent components of the cell potential [equation (5)] indicated that, in general, $\partial E^\circ_{cell}/\partial T$ is not constant, and it follows that, in terms of the idealised pH_{iso} defined above, equation (8) can only be an approximation. pH_{iso} may be obtained graphically by plotting e.m.f. against pH for a number of solutions at a series of temperatures. If $\partial E^\circ_{cell}/\partial T$ were a constant, all the isotherms would intersect at pH_{iso}. In practice, non-linearity of the temperature dependence means that the intersecting isotherms form a zone covering a range of pH_{iso}.

The minimum data for calculating pH_{iso} are e.m.f.s in two standard buffer solutions at two temperatures, enabling intersecting isotherms to be drawn or solution by simultaneous equations of the form of equation (10). Hence,

$$\mathrm{pH}_{iso} = \frac{E - E' + k\mathrm{pH} - k'\mathrm{pH}'}{k - k'} \quad \ldots \quad \ldots \quad (11)$$

where k and k' are obtained from $\Delta E/\Delta \mathrm{pH}$ at temperatures T and T', pH and pH′ are known and E and E' are measured.

The precision of pH_{iso} calculated in this way can be estimated from the standard deviation of the e.m.f. by the usual rules for combination of random errors. Neglecting random errors in the pH values of standard buffer solutions we obtain from equation (11)

$$\frac{\sigma^2(\mathrm{pH}_{iso})}{(\mathrm{pH}_{iso})^2} = \frac{\sigma^2(E - E') + (\mathrm{pH})^2\sigma^2(k) + (\mathrm{pH}')^2\sigma^2(k')}{(E - E' + k\mathrm{pH} - k'\mathrm{pH})^2} + \frac{\sigma^2(k) + \sigma^2(k')}{(k - k')^2} \quad \ldots \quad \ldots \quad \ldots \quad (12)$$

where $\sigma(x)$ is the standard deviation in quantity x.

Evaluating equation (12) for an ideal case with $\mathrm{pH}_{iso} = 7.0$,

determined from measurements with potassium hydrogen phthalate buffer (pH 4) at 15 and 25 °C and with the standard deviation of all e.m.f. measurements assumed to be 0.1 mV, we obtain $\sigma (E - E') = 0.14$ mV, $\sigma(k) = 0.05$ mV decade^{-1} (for determination over a 3 pH span) and $E - E' = -5.4$ mV. Substituting in equation (12),

$$\frac{\sigma^2(\mathrm{pH_{iso}})}{49} = 5.2 \times 10^{-4} + 2.47 \times 10^{-3}$$

Hence $\sigma(\mathrm{pH_{iso}}) = 0.38$ and is dominated by the error in $k - k'$ [the second term on the right-hand side of equation (12)].

Alternatively, equation (10) can be transformed into

$$E + k\mathrm{pH} = E_{\mathrm{iso}} + k\mathrm{pH_{iso}} \quad .. \quad .. \quad (13)$$

If e.m.f.s are recorded in a buffer solution over a range of temperatures, the left-hand side of equation (13) can be plotted against k. Ideally the graph should be linear, with a slope equal to $\mathrm{pH_{iso}}$, but it will generally be curved in practice. This method has the advantage that the curvature gives a qualitative indication of the range of usefulness of $\mathrm{pH_{iso}}$.

$\mathrm{pH_{iso}}$ as an Electrode Characteristic

$\mathrm{pH_{iso}}$ is a characteristic of the electrode pair in the potentiometric cell, but if the body of the reference electrode is separated from the junction by a long tube and held at a constant temperature, the cell $\mathrm{pH_{iso}}$ can be equated with the glass electrode's $\mathrm{pH_{iso}}$. Such an assumption neglects the contribution to $\mathrm{pH_{iso}}$ from the temperature coefficient of the liquid junction potential (discussed below). Provided that a remote junction reference electrode of the above sort is used, the same $\mathrm{pH_{iso}}$ should be found for the glass electrode, regardless of the nature of the reference electrode or its temperature (provided that it is constant). With a non-isothermal cell of this kind, therefore, $\mathrm{pH_{iso}}$ can be regarded as a characteristic of the glass electrode.

If the glass electrode in the non-isothermal cell is replaced by a second reference electrode and the temperature of the test solution is varied, the change in e.m.f. can be attributed to the second reference electrode alone and its temperature coefficient calculated. This temperature coefficient can be expressed as an isopotential factor characteristic of the reference electrode; in a pH cell this factor would be formally equivalent to a $\mathrm{pH_{iso}}$ value, although it is unrelated to any real solution pH. This terminology is adopted below: a graph of E against k gives $\mathrm{pH_{iso}}$ for the reference electrode as the slope of the line represented by equation (14).

$$E = E_{\mathrm{iso}} + k\mathrm{pH_{iso}} \quad .. \quad .. \quad .. \quad (14)$$

$\mathrm{pH_{iso}}$ for an isothermal cell consisting of glass and reference electrodes may now be calculated as the difference of individual $\mathrm{pH_{iso}}$ values obtained as above.

$$\mathrm{pH_{iso}(cell)} = \mathrm{pH_{iso}(glass)} - \mathrm{pH_{iso}(reference)}$$

Relationship between the Isopotential and Zero Points

Glass electrodes should[6] be marked with their zero point, denoted by $E°X$, with respect to a stated reference electrode at 25 °C, *i.e.*, X is the pH at which the glass - reference electrode pair gives 0 mV. Almost all commercial electrodes are nominally $E°7$. Manufacturers rarely quote $\mathrm{pH_{iso}}$ and it is often assumed that $\mathrm{pH_{iso}} = 7$ also. However, these quantities are not identical. Hence $\mathrm{pH_{iso}}$ for a non-isothermal cell with a remote junction exceeds that for the corresponding isothermal cell by pH 2.2 or 0.4 for reference electrodes with calomel or Ag - AgCl elements in 3 mol l^{-1} potassium chloride solution, respectively. With the remote junction electrode at 25 °C, the zero-point pH is the same for both configurations of cell.

From equation (2), at $E = 0$ mV the zero-point pH is given by equation (15), where $\Delta E° = E°' - E°$.

$$\mathrm{pH°} = \frac{\Delta E° + E_j}{k} - \log\frac{a'_X}{a_X} + \mathrm{pH'} \quad .. \quad .. \quad (15)$$

From equations (4) and (7),

$$\mathrm{pH_{iso}} = \frac{\frac{\partial \Delta E°}{\partial T} + \frac{\partial E_j}{\partial T} + \frac{k\partial \mathrm{pH'}}{\partial T} + \frac{k\partial \log a_X}{\partial T} - \frac{k\partial \log a'_X}{\partial T}}{\partial k/\partial T} - \log\frac{a_X'}{a_X} + \mathrm{pH'} \quad .. \quad .. \quad .. \quad (16)$$

The relationship between pH° and $\mathrm{pH_{iso}}$ will be considered for a range of electrode types.

Isothermal cells with non-saturated inner and reference solutions

In this instance,

$$\frac{\partial \log a_X}{\partial T} = \frac{\partial \log[X]}{\partial T} + \frac{\partial \log f_X}{\partial T} \approx 0$$

where f_X is the activity coefficient. Concentrations defined as molality are independent of temperature and activity coefficients[7] are observed to vary by about 0.01% K^{-1}, which is equivalent to 0.0025 mV K^{-1} and less than can be detected with a pH meter reading to 0.1 mV. Similarly, $\partial \log a'_X/\partial T \approx 0$. Further, any small non-zero components of the two terms tend to cancel. On a molar scale $\partial \log a_X/\partial T \neq 0$, and this would involve additional terms in the density of the solutions and different $\partial E°/\partial T$ terms from those which follow. The temperature coefficient of the e.m.f. is itself independent of the concentration scale and use of the molal scale gives simpler expressions. The NBS standard buffers are defined on a molal scale.

Combining equations (15) and (16) and eliminating $\partial \log a_X/\partial T$ terms,

$$\mathrm{pH_{iso}} = \mathrm{pH°} - \frac{\Delta E° + E_j}{k} + \frac{\frac{\partial \Delta E°}{\partial T} + \frac{\partial E_j}{\partial T} + \frac{k\partial \mathrm{pH'}}{\partial T}}{\partial k/\partial T} \quad (17)$$

If the two reference elements are of the same type, $\Delta E° = 0$ and $\partial \Delta E°/\partial T = 0$.
Hence

$$\mathrm{pH_{iso}} = \mathrm{pH°} - \frac{E_j}{k} + \frac{\frac{\partial E_j}{\partial T} + \frac{k\partial \mathrm{pH'}}{\partial T}}{\partial k/\partial T}$$

$$= \mathrm{pH°} + \frac{T\partial \mathrm{pH'}}{\partial T} - \left(\frac{E_j}{k} - \frac{F}{R\ln 10}\frac{\partial E_j}{\partial T}\right) \quad .. \quad (18)$$

In practical pH cells, E_j is arranged to be small and its variation with temperature will make only a small contribution (see below). As an approximation, therefore,

$$\mathrm{pH_{iso}} \approx \mathrm{pH°} + T\frac{\partial \mathrm{pH'}}{\partial T} \quad .. \quad .. \quad (19a)$$

or

$$\mathrm{pH_{iso}} \approx \mathrm{pH°} + \frac{1}{\ln 10}\frac{\partial \mathrm{pH'}}{\partial \log T} \quad .. \quad .. \quad (19b)$$

Equation (19a) shows that even with identical inner and external reference electrodes and favourable assumptions about liquid junction potentials, $\mathrm{pH_{iso}}$ will not coincide with pH° unless $\partial \mathrm{pH'}/\partial T = 0$. The latter condition could only be expected from a solution of a strong mineral acid. From equation (15), with a 3 mol l^{-1} KCl reference electrolyte, $\Delta E = 0$ and $E_j = 0$, it follows that for $\mathrm{pH°(= pH_{iso})} = 7.0$ as desired, the internal filling solution of the glass electrode would have to be 4×10^{-4} mol l^{-1} hydrochloric acid (or a solution having the same activity of hydrochloric acid).

With non-identical reference elements, equation (18) shows that $pH_{iso} = pH^\circ$ only if (again setting $E_j = 0$ and $\partial E_j/\partial T = 0$)

$$\frac{\Delta E^\circ}{k} = \frac{\frac{\partial \Delta E^\circ}{\partial T} + \frac{k\partial pH'}{\partial T}}{\partial k/\partial T} \quad \ldots \quad (20)$$

Equation (19b) shows that pH_{iso} is a constant only if pH′ changes linearly with the logarithm of the absolute temperature. However, this is not a property of real solutions (see below), except in the trivial case $\partial pH'/\partial \log T = 0$. The present state of pH meter technology treats pH_{iso} as a constant and hence meters have a limited range in which temperature compensation can be applied with a given accuracy. The next stage of sophistication (which would require a microprocessor-based pH meter only slightly more complicated than present models) would be to apply a linear correction to pH_{iso} by equation (19a): a prerequisite for this would be a glass electrode whose internal pH changed linearly with temperature. There are probably no such electrodes available at present, although suitable solutions could be devised.

With present pH meters, requiring $pH^\circ = pH_{iso} = 7$, ideal conditions inside the glass electrode can be calculated from equations (15) and (20). This has been done in columns (3) and (4) of Table 1 for calibration at 25 °C *versus* reference electrodes with 3 mol l^{-1} KCl reference electrolyte (neglecting liquid junction potentials). Microprocessor-based meters should be able to cope with a much wider range of electrodes, because the equalities $pH^\circ = pH_{iso} = 7$ are unnecessary, although some microprocessor meters imitate the limitations of older meters.

Table 1 gives mathematical solutions, but it does not follow that real chemical compounds exist to fulfil them, particularly when $\partial pH'/\partial T$ is required to be constant over the desired range of temperature. Even when the reference elements are identical and $\partial pH'/\partial T = 0$, the concentration of hydrochloric acid required may be considered too low for chemical stability inside the electrode.

Isothermal cells with at least one saturated solution

Because the solubility of potassium chloride varies by about 0.04 mol kg^{-1} K^{-1}, we have $\partial \log a_{Cl}/\partial T \approx 0.005$ (equivalent to an increase of 0.14 in pH_{iso}).

Reference solution saturated with potassium chloride

Derivations can be carried out exactly as before, except that the term $\partial pH'/\partial T$ in equations (17) and (18) is replaced by $(\partial pH'/\partial T + \partial \log a_{Cl}/\partial T)$. The conditions required for $pH_{iso} = pH^\circ = 7.0$ with a saturated potassium chloride reference solution can be obtained from Table 1 by (i) subtracting 0.17 from the $pH' - \log a'_{Cl}$ column and (ii) subtracting 5×10^{-3} from the isothermal $\partial pH'/\partial T$ column.

Inner solution saturated with potassium chloride

The derivation proceeds as before except that in equations (16) and (17) $\partial pH'/\partial T$ is replaced by $(\partial pH'/\partial T - \partial \log a'_{Cl}/\partial T)$. The conditions required for $pH_{iso} = pH^\circ = 7.0$ are obtained from Table 1 by (i) adding 0.40 to the $pH' - \log a'_{Cl}$ column to obtain pH′ at 25 °C and (ii) adding 5×10^{-3} to the isothermal $\partial pH'/\partial T$ column.

Both inner and reference solutions saturated with potassium chloride

In this instance $\partial \log a_{Cl}/\partial T = \partial \log a'_{Cl}/\partial T$ and equations (16) and (17) are still valid. Conditions for $pH_{iso} = pH^\circ = 7.0$ are obtained from Table 1 by (i) adding 0.23 to the $pH' - \log a'_{Cl}$ column to give pH′ at 25 °C and (ii) retaining the isothermal $\partial pH'/\partial T$ values.

Non-isothermal cells

The reference electrode is kept at a constant temperature as that of the rest of the cell is varied. The temperature coefficient of the e.m.f. is obtained by differentiating equation (2), omitting the terms in the $(\ )_{ref}$ parentheses.

$$\frac{\partial E}{\partial T} = \left(\frac{\partial E^{\circ\prime}}{\partial T} - \frac{k\partial \log a'_X}{\partial T} - \log a'_X \frac{\partial k}{\partial T} + \frac{k\partial pH'}{\partial T} + pH' \frac{\partial k}{\partial T}\right)_{glass} - pH \frac{\partial k}{\partial T} - k \frac{\partial pH}{\partial T} + \frac{\partial E_j}{\partial T} \quad \ldots \quad (21)$$

Non-saturated inner and reference solutions

As before, $\partial \log a'_X/\partial T = 0$. At $pH = pH_{iso}$ we have, by definition, $\partial E/\partial T = 0$ at constant pH, hence

$$\frac{\partial E^{\circ\prime}}{\partial T} + \frac{\partial E_j}{\partial T} - \frac{\partial k}{\partial T}(\log a'_X - pH') + k \frac{\partial pH'}{\partial T} - pH_{iso} \frac{\partial k}{\partial T} = 0 \quad (22)$$

Therefore,

$$pH_{iso} = pH' - \log a'_X + \frac{\frac{\partial E^{\circ\prime}}{\partial T} + \frac{\partial E_j}{\partial T} + \frac{k\partial pH'}{\partial T}}{\partial k/\partial T} \quad (23)$$

At $E = 0$, equation (16) is still valid for the non-isothermal cell, hence substituting in equation (23) gives

$$pH_{iso} = pH^\circ - \log a_X - \frac{\Delta E^\circ + E_j}{k} + \frac{T\partial pH'}{\partial T} + \frac{\partial E^{\circ\prime}}{\partial T} \cdot \frac{\partial T}{\partial k} + \frac{\partial E_j}{\partial T} \cdot \frac{\partial T}{\partial k} \quad (24)$$

Evaluating equations (16) and (24) for electrodes calibrated at 25 °C and with neglect of liquid junction potentials gives the results in columns 3 and 5 of Table 1.

Inner solution saturated with potassium chloride

For $\partial \log a'_{Cl}/\partial T \approx 0.005$ and wherever $\partial pH'/\partial T$ appears in equations (22)–(24) it should be replaced by $(\partial pH'/\partial T - \partial \log a'_{Cl}/\partial T)$. The conditions for $pH_{iso} = pH^\circ = 7.0$ are obtained from Table 1 by (i) adding 0.40 to the $pH' - \log a'_{Cl}$ column to obtain pH′ at 25 °C and (ii) adding 5×10^{-3} to the non-isothermal $\partial pH'/\partial T$ column.

Table 1. Conditions required inside glass electrodes to give $pH_{iso} = pH^\circ = 7.0$. (Calibrated at 25 °C *versus* reference electrodes with 3 mol l^{-1} KCl reference solutions)

Reference element		$pH' - \log a'_{Cl}$	$\partial pH'/\partial T$ required for isothermal cell	$\partial pH'/\partial T$ required for non-isothermal cell
Glass electrode	Reference half-cell			
AgCl	AgCl	6.77	0	-2.7×10^{-3}
AgCl	Hg_2Cl_2	7.54	3.5×10^{-3}	-5.3×10^{-3}
Hg_2Cl_2	Hg_2Cl_2	6.77	0	-8.8×10^{-3}
Hg_2Cl_2	AgCl	5.99	-3.5×10^{-3}	-6.2×10^{-3}

Reference solution saturated with potassium chloride

As the temperature of the reference electrode is constant, pH_{iso} is unaffected, but 0.17 is subtracted from column 3 to give $pH' - \log a'_{Cl}$ (non-saturated inner solution) or 0.23 added to give pH′ at 25 °C (saturated inner solution).

Influence of the Liquid Junction Potential on the Isopotential Point

The contribution of the liquid junction potential, evident in equations (18) and (24), has so far been neglected, mainly because it was expected to be small for practical liquid junctions, but also because the liquid junction potential of an unknown sample is not directly calculable. However, evaluation of the liquid junction contribution in some instances is instructive.

Equations (18) and (24) for expressing the isopotential pH each contain the terms $-E_j/k$ and $(\partial E_j/\partial T)\,(\partial T/\partial k)$. Calculations by Picknett[8] show that for a reference electrode with a concentrated potassium chloride electrolyte, E_j is likely to vary within the range −3 to −7 mV for a wide range of sample electrolytes in the concentration range 10^{-2}–10^{-6} mol l^{-1}. (Although the basis of these calculations is not strictly rigorous,[9] experimental e.m.f.s in dilute solutions were predicted to within ±0.5 mV.) The approximate maximum effect on pH_{iso}, therefore, is $7/k \approx 0.12$, but as only the variation of E_j with respect to the calibrating solution can be discerned, the effect is unlikely to exceed 0.06 units of pH_{iso}. If pH_{iso} is determined from measurements in the same buffers as are used for calibration, the contribution to pH_{iso} from this term should be even smaller. However, at the worst the E_j/k term is a fraction of the experimental variation in determining pH_{iso}.

An estimate of $\partial E_j/\partial T$ may be obtained by differentiating the Henderson equation for the liquid junction potential, which is conveniently simple but involves assumptions that do not always apply to real junctions in pH measurements.[10]

$$E_j = -k\frac{\Sigma\lambda_i(C_i^R - C_i^L)/z_i}{\Sigma\lambda_i(C_i^R - C_i^L)}\log\frac{\Sigma\lambda_i C_i^R}{\Sigma\lambda_i C_i^L}$$

where λ_i, C_i and z_i are the molar conductivity, concentration and charge (with sign) of the ith ion, respectively, and the superscripts R and L denote the right- and left-hand sides of the liquid junction. Letting P, Q, X and Y equal the sums in the numerators and denominators of the pre-logarithmic and logarithmic terms, we obtain

$$E_j = -k\frac{P}{Q}\log\frac{X}{Y}$$

Hence

$$\frac{\partial E_j}{\partial T} = -\frac{\partial k}{\partial T}\cdot\frac{P}{Q}\log\frac{X}{Y} - k\left[\log\frac{X}{Y}\cdot\frac{\partial}{\partial T}\left(\frac{P}{Q}\right) + \frac{P}{Q}\cdot\frac{\partial}{\partial T}\left(\log\frac{X}{Y}\right)\right] \quad (25)$$

$$= -\frac{\partial k}{\partial T}\cdot\frac{P}{Q}\log\frac{X}{Y} - k\left(\log\frac{X}{Y}\cdot\frac{Q\frac{\partial P}{\partial T} - P\frac{\partial Q}{\partial T}}{Q^2} + \frac{P}{Q}\cdot\frac{Y}{X}\ln 10\cdot\frac{Y\frac{\partial Y}{\partial T} - X\frac{\partial Y}{\partial T}}{Y^2}\right)$$

The only temperature-dependent variables in P, Q, X and Y are the molar conductivities. Hence

$$\frac{\partial E_j}{\partial T} = \frac{\partial k}{\partial T}\cdot\frac{E_j}{k} - k\left[\frac{\log\left(\frac{X}{Y}\right)Q\frac{\Sigma(C_i^R - C_i^L)}{z_i}\frac{\partial\lambda_i}{\partial T} - P\Sigma(C_i^R - C_i^L)\frac{\partial\lambda_i}{\partial T}}{Q^2} + \frac{PY\ln 10}{QX}\frac{\left(Y\Sigma C_i^R\frac{\partial\lambda_i}{\partial T} - X\Sigma C_i^L\frac{\partial\lambda_i}{\partial T}\right)}{Y^2}\right] \quad (26)$$

Equation (26) can be evaluated by replacing $\partial\lambda_i/\partial T$ by $\Delta\lambda_i/\Delta T$ from tabulations by Robinson and Stokes[7] which show that conductivities vary approximately linearly with temperature over a range of about 30 °C. With concentrated (but not saturated) potassium chloride electrolyte in the reference electrode, both E_j/k and the variation in $\log X/Y$ are negligible and with dilute test solutions $C_i^L \gg C_i^R$, so that the terms P and Q are influenced only by C_K^L and C_{Cl}^L. Hence

$$\frac{\partial E_j}{\partial T} \approx -k\log\frac{\Sigma\lambda_i C_i^R}{\Sigma\lambda_i C_i^L}\cdot\frac{C_K{}^L\frac{\partial\lambda_K}{\partial T} - C_{Cl}{}^L\frac{\partial\lambda_{Cl}}{\partial T}}{C_K{}^L\lambda_K + C_{Cl}{}^L\lambda_{Cl}}$$

With a 3 mol l^{-1} potassium chloride reference solution at 25 °C,

$$\frac{\partial E_j}{\partial T}(\text{mV K}^{-1}) \approx 0.04\log\Sigma\lambda_i C_i^R - 0.10$$

Table 2 shows the terms in equation (25) for two different test solutions. The dominance of the middle term is obvious. From equations (18) or (24) the variation of junction potential with temperature contributes about −0.5 unit to pH_{iso} for 10^{-4} mol l^{-1} hydrochloric acid solutions or −0.2 for 0.1 mol l^{-1} acetic acid - acetate buffer. In the empirical determination of pH_{iso} these contributions would only be apparent if pH_{iso} were determined in solutions different from the calibration solutions. The results in Table 2 show that pH_{iso} determined in a buffer solution is likely to be about 0.3 unit too high for application to dilute sample solutions.

From equation (26) and the known conductivities we may also infer that $\partial E_j/\partial T$ makes an almost linear contribution to the over-all temperature coefficient provided that the temperature range does not exceed about 30 °C. The first term on the right-hand side of equation (26) is truly linear, but is dominated by the others in $\partial\lambda_i/\partial T$.

The calculations show that liquid junction potentials make a small contribution to the temperature coefficient of the e.m.f. of a cell. However, empirically determined values of isopotential pH should largely compensate for this effect and the likely error in pH is small compared with that from other sources.

Temperature Variation of pH of Electrode Filling Solutions

The appearance of the term $\partial pH'/\partial T$ in equations (18)–(24) shows that the internal filling solution has a significant effect on the thermal characteristics of an electrode. Restricting consideration to the conditions required to produce Table 1, it can be seen from column 3 of that table that $pH' = 7 + \log a'_{Cl} \pm 1$. The practical limits for a'_{Cl} are about 10^{-3}–10^{0} mol l^{-1}, hence the limits of pH′ are 3–8.

Inspection of the properties of standard buffer solutions[11] shows that most carboxylate and phosphate buffers go through a minimum in pH somewhere in the range 0–50 °C, *i.e.*, neither pH′ nor $\partial pH'/\partial T$ is constant. Over a wide range of temperature (0–60 °C), a 0.1 mol l^{-1} acetic acid + 0.1 mol l^{-1} sodium acetate buffer comes nearest to constancy, with a

Table 2. Components of temperature coefficient of liquid junction potential and contribution to isopotential pH

Test solution	$\left\|\frac{\partial k}{\partial T}\cdot\frac{E_j}{k}\right\|$ mV K^{-1}	$\left\|-k\log\frac{X}{Y}\frac{\partial}{\partial T}\left(\frac{P}{Q}\right)^{\dagger}\right\|$ mV K^{-1}	$\left\|-k\frac{P}{Q}\frac{\partial}{\partial T}\log\frac{X}{Y}^{\dagger}\right\|$ mV K^{-1}	$\left\|\frac{\partial E_j}{\partial T}\right\|$ mV K^{-1}	Contribution to pH$_{iso}$
10^{-4} mol l^{-1} hydrochloric acid	−0.015	−0.086	−0.002	−0.10	−0.5
0.1 mol l^{-1} sodium acetate + 0.1 mol l^{-1} acetic acid	−0.006	−0.037	+0.001	−0.043	−0.2

* Reference solution 3 mol l^{-1} potassium chloride.
† Symbols refer to equation (25).

maximum spread of 0.05 pH, but in the ambient and sub-ambient range (0–30 °C) 0.05 mol l^{-1} potassium hydrogen phthalate has a spread of only 0.012 pH.

Buffers in which $\partial pH'/\partial T$ is more nearly constant are those with amino groups of suitable strength, *e.g.*, *N*-tris(hydroxymethyl)methyl-2-aminoethanesulphonic acid (TES) and *N*-2-hydroxyethylpiperazine-*N*′-2-ethanesulphonic acid (HEPES) buffers[12] (pH ≈ 7.5). 3-(*N*-Morpholino)propanesulphonic acid (MOPS) would seem to be a good candidate for a pH 7.1 buffer.[13] However, these buffers generally would give too negative a value of $\partial pH'/\partial T$ in Table 1 for $pH_{iso} = pH^{\circ} = 7$ to be achieved. Other buffers of this type are known[11] but they have not been studied at different temperatures. The more acidic buffers might be especially worthy of study in relation to glass electrode filling solutions. Amine buffers in aqueous glycerol have also been suggested for this purpose.[14]

Calculation of $\partial pH/\partial T$

The only instance considered is that of a solution of a single monobasic acid, HA, partially neutralised by sodium hydroxide. The system is defined by the mass and charge balance equations, the protonation constant, $K = [HA]/[A][H]$, and the autoprotolysis constant, K_w. For convenience, charges have been omitted and activity coefficients neglected.

Total acid = $T_A = [HA] + [A] = [A](1 + K[H])$
Total base = $T_B = [Na]$
Charge balance: $[H] + [Na] = [OH] + [A]$

i.e.,

$$[H] + T_B = \frac{K_w}{[H]} + \frac{T_A}{1 + K[H]}$$

Rearrangement followed by differentiation with respect to temperature gives

$$\frac{\partial[H]}{\partial T}\left\{3K[H]^2 + 2[H](1 + KT_B) + T_B - T_A - KK_w\right\} = -\frac{\partial K}{\partial T}([H]^3 + [H]^2 T_B - [H]K_w) + \frac{\partial K_w}{\partial T}(1 + K[H])$$

Expressing the temperature differentials in logarithmic form gives

$$\frac{\partial pH}{\partial T} = \frac{\frac{\partial \log K}{\partial T}([H]^2 + [H]T_B - K_w) - \frac{\partial \log K_w}{\partial T}K_w(1 + K^{-1}[H]^{-1})}{3[H]^2 + 2[H](K^{-1} + T_B) + (T_B - T_A)K^{-1} - K_w} \quad (27)$$

Equation (27) shows that the variation of pH with temperature is fairly complicated, as $\partial \log K_w/\partial T$ is almost linear whereas $\partial \log K/\partial T$ may be parabolic. In certain circumstances, the above general equation can be greatly simplified. For moderately concentrated solutions of moderately weak acids (such that $K^2K_w \leqslant 1$ and $KT_A \gg 1$) $[H] \approx K^{-1}$ at half-neutralisation and then $\partial pH/\partial T \approx \partial \log K/\partial T$.

Discussion

The relationship between the zero point and the isopotential point, and the conditions necessary to make them coincide, have been demonstrated. The non-linearity of an electrode's temperature coefficient is shown to depend mainly on the temperature coefficient of the pH of the solution inside the glass electrode, but the use of saturated solutions in the glass or reference electrodes is another cause. The contribution of the liquid junction potential (and its temperature coefficient) to the isopotential correction has been shown to be small for the usual concentrated potassium chloride bridging solutions. In an alternative approach (the Ross electrode), the non-linearity of the pH buffer's temperature response is compensated by an oppositely-responding reference electrode based on a redox couple.[15]

With the factors listed above, the approximate nature of the linear temperature corrections applied by pH meters becomes apparent. For linear characteristics to be achieved, new filling solutions need to be devised for glass electrodes, but such solutions are unlikely to give $pH_{iso} = 7$ and a meter with an adjustable isopotential control would be necessary. Over a limited temperature range, certain weak acid filling solutions have attractive properties for electrodes intended for use in the environmental range (0–30 °C) and could give $pH_{iso} \approx 7$.

Non-ideal Electrodes

Midgley and Torrance[16] observed with symmetrical pH cells, in which the glass electrode was filled with a more concentrated potassium chloride solution than usual, that the temperature-dependent terms did not cancel as expected unless the test solution also contained concentrated potassium chloride. As the anomaly was observed only with very dissimilar solutions on each side of the membrane, it is inferred that differences in hydration, ion exchange or adsorption between the inner and outer surfaces of the membrane could be induced by the nature of the two bathing solutions and give rise to an additional source of temperature dependence which has not been considered in this paper or elsewhere.

This work was carried out at the Central Electricity Research Laboratories and is published by permission of the Central Electricity Generating Board.

References

1. Jackson, J., *Chem. Ind.* (*London*), 1948, 7.
2. Mattock, G., "pH Measurement and Titration," Heywood, London, 1961.
3. Covington, A. K., *CRC Crit. Rev. Anal. Chem.*, 1974, **3**, 355.
4. Negus, L. E., and Light, T. S., *Instrum. Technol.*, 1972, **19** (Dec.), 23.
5. Westcott, C. C., "pH Measurements," Academic Press, New York, 1978.
6. British Standard BS 2586, "Glass and Reference Electrodes for the Measurement of pH," British Standards Institution, London, 1979.

7. Robinson, R. A., and Stokes, R. J., "Electrolyte Solutions," Second Edition (Revised), Butterworths, London, 1965.
8. Picknett, R. G., *Trans. Faraday Soc.*, 1968, **64**, 1059.
9. Covington, A. K., "Specialist Periodical Report, Electrochemistry," Volume 1, Chemical Society, London, 1970, p. 72.
10. MacInnes, D. A., "The Principles of Electrochemistry," Reinhold, New York, 1939, p. 231.
11. Perrin, D. D., and Dempsey, B., "Buffers for pH and Metal Ion Control," Chapman and Hall, London, 1974.
12. Bates, R. G., Vega, C. A., and White, D. R., *Anal. Chem.*, 1978, **50**, 1922.
13. Sankar, M., and Bates, R. G., *Anal. Chem.*, 1978, **50**, 1922.
14. Simon, W., and Wegmann, D., *US Pat.*, 3445363, 1969.
15. Ross, J. W., *US Pat.* 4495050, 1985.
16. Midgley, D., and Torrance, K., *Analyst*, 1982, **108**, 1297.

Paper A6/281
Received August 14th, 1986
Accepted December 10th, 1986

Temperature Compensation in Potentiometry: Isopotentials of pH Glass Electrodes and Reference Electrodes

Part II.* Performance of Commercial Electrodes

Derek Midgley
CEGB, Central Electricity Research Laboratories, Kelvin Avenue, Leatherhead, Surrey KT22 7SE, UK

Commercial glass electrodes were shown to have non-linear temperature characteristics with isopotential pH values up to 2 pH below the expected pH_{iso} = 7.0. The use of calomel rather than silver - silver chloride reference electrodes causes a reduction of about 2 pH in the pH_{iso} of an isothermal cell. Each unit by which pH_{iso} is lower than the value assumed by the meter causes an error of −0.0035 pH K^{-1}. The design of some reference electrodes makes it almost impossible for them to achieve rapid thermal equilibrium with the test solution and, hence, for proper temperature compensation to be applied. Cells containing such electrodes are not isothermal and may approach the character of cells with remote junction reference electrodes. Such cells may suffer from drifting e.m.f.s and give different temperature errors in solutions above and below the standardisation temperature. The liquid junction potential is shown to make a small contribution to the cell's temperature coefficient, so that the value of pH_{iso} obtained for electrodes calibrated in standard buffers is 0.3 pH too high for use with dilute acid solutions.

Keywords: *pH; glass electrode; reference electrode; temperature compensation; isopotential*

In Part I[1] the components of pH cells incorporating glass electrodes were examined theoretically with respect to temperature dependence and compensation. In this paper the performance of some commercial glass and reference electrodes is assessed in regard to their suitability for pH measurements in samples of various temperatures.

Theory

The theory has been given in Part I[1] and will be repeated only in summary. pH_{iso} (notionally the pH at which the cell e.m.f. is invariant with temperature) is used as a linear compensation factor for the variation of the standard potential with temperature. Hence [equation (10) of Part I]

$$E = E_{iso} - k\,(pH - pH_{iso}) \quad .. \quad .. \quad (1)$$

where k is the Nernst slope factor. With E_{iso} and pH_{iso} known, the temperature dependence of the E − pH relationship can be calculated from the regularly varying coefficient of k [equation (3) of Part I].

$$\partial k/\partial T = R\ln 10/F = \text{constant} \quad .. \quad .. \quad (2)$$

pH_{iso} can be calculated from measurements in two solutions at two temperatures, T and T', by equation (3).

$$pH_{iso} = (E - E' + k\text{pH} - k'\text{pH}')/(k - k'). \quad (3)$$

The precision of pH_{iso} is then obtained from equation (4).

$$\frac{\sigma^2(pH_{iso})}{(pH_{iso})^2} = \frac{\sigma^2(E - E') + (\text{pH})^2\sigma^2(k) + (\text{pH}')^2\sigma^2(k')}{(E - E' + k\text{pH} - k'\text{pH})^2} + \frac{\sigma(k) + \sigma^2(k')}{(k - k')^2} \quad (4)$$

where $\sigma(x)$ is the standard deviation in quantity x.

Alternatively, pH_{iso} can be obtained by plotting the left-hand side of equation (5) against k over a range of temperature.

$$E + k\text{pH} = E_{iso} + k\text{pH}_{iso} \quad .. \quad .. \quad (5)$$

Similarly, the reference electrode's contribution to the overall pH_{iso} is obtained by plotting the e.m.f. of a non-isothermal cell containing two reference electrodes against k [equation (6)].

$$E = E_{iso} + k\text{pH}_{iso} \quad .. \quad .. \quad .. \quad (6)$$

In this instance pH_{iso} is a formal coefficient unrelated to any real solution pH. Equations (3)–(6) correspond to equations (11)–(14) of Part I.

It is necessary to distinguish between pH_{iso} and the zero-point pH (at which E = 0 mV).

Experimental

Apparatus

Electrodes were purchased from leading manufacturers. The glass electrodes (Table 1) were all nominally $E^{\circ}7$. The reference electrodes were of the usual calomel and silver - silver chloride type (Table 2). E.m.f.s were measured with a

Table 1. Glass electrodes under test

Type*	Internal element	pH at E = 0 mV: Quoted	Found†
XIVB	Ag - AgCl	7 ± 0.5	6.58
XVC	Ag - AgCl	7.0	5.75
XVIC	Calomel	7.0	6.46
XVIID	Ag - AgCl	—	6.02

* Letters indicate different manufacturers.
† *vs.* 3 mol l^{-1} KCl calomel electrode at 25 °C.

Table 2. Reference electrodes under test

Type*	Internal element	Filling solution concentration/ mol l^{-1} KCl	Junction
IA	Ag - AgCl	3	Frit
VIA	Calomel	3	Frit
VIIB	Calomel	4	Frit
VIIIE	Calomel	3	Remote frit
XVIIIE	Calomel	3.8	Glass sleeve
XIXE	Calomel	3.8	Glass sleeve

* Letters indicate different manufacturers.

* For Part I of this series, see page 573.

Corning 110 digital pH meter reading to 0.1 mV. Techne C-100 thermocirculators were used to control the temperature of the water-jacketed glass test cell.

Reagents

NBS standard phosphate and phthalate buffer solutions (pH 6.865 and 4.008, respectively, at 25 °C) were used as test solutions. With the reference electrodes, 3 mol l^{-1} potassium chloride solutions were also used.

Procedure

Measurements were first made with the electrodes in solution at 25 °C. The temperature was then changed in 5 °C steps within the range 5–50 °C and the e.m.f. was recorded when it was steady.

Results

Glass Electrodes

A graph corresponding to equation (5) is shown in Fig. 1 for data obtained with electrode XVIID between 5 and 50 °C. It is evident that the graph is non-linear, and this was so for all the glass electrodes tested, although the curvature was less obvious in the other instances. The data were fitted empirically by least-squares regression to first-, second- and third-order graphs. For all electrodes the best fit was obtained with the second-order graph. Isopotentials were calculated at a series of temperatures by differentiating the empirical second-order equations of the graphs with the results shown in Table 3. The slope of the linear least-squares fit is shown for comparison.

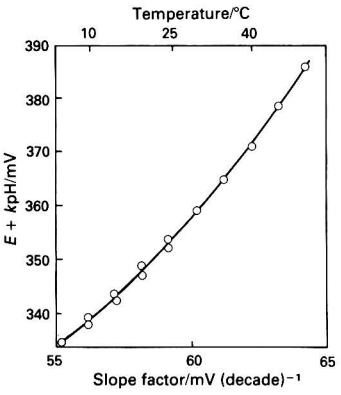

Fig. 1. Graph for determining pH_{iso} of glass electrode XVIID in potassium hydrogen phthalate buffer (pH 4.008 at 25 °C)

The spread of the pH_{iso} values indicates the degree of curvature of the graph and it is evident that the electrodes differ considerably in this respect. Even at the standard temperature of 25 °C, some of the pH_{iso} values differ considerably from the expected value of pH 7. These values were obtained with respect to a remote reference electrode and are larger than would be expected in isothermal cells with commonly used reference electrodes.

These were new electrodes and the results were checked (at only two temperatures) after an interval of 4 months to see if any significant change had occurred. Whereas the results for electrodes XIVB and XVC increased by about 0.3 pH, those for the others had changed by less than 0.05 pH.

A total of 10 determinations of pH_{iso} for electrode XIVB over a period of 2 months by three different operators gave a mean of 7.8 with a standard deviation for a single result of 0.35, which is very close to the value of 0.38 calculated[1] from equation (4) with $\sigma(E) = 0.1$ mV. In each instance pH_{iso} was calculated from equation (3) using two temperatures. It is obvious that pH_{iso} is not a very precise characteristic, even of an individual electrode. Variations in manufacture must add to the uncertainty of pH_{iso} for a particular type of electrode.

Reference Electrodes

Temperature coefficients expressed as pH_{iso}

The data were plotted in accordance with equation (6). The graphs (Fig. 2) were non-linear and the data were fitted empirically by least-squares regression to first- and second-order curves. Isopotential pH values were obtained at round temperatures by differentiating the empirical second-order equations of the graphs, with the results shown in Table 4. The value of pH_{iso} obtained from the linear fit is shown for comparison. Measurements were made in the range 5–50 °C but e.m.f. values of the calomel electrodes at the extremes of the range were suspect and the 5 and 50 °C readings were disregarded. The reasons for this probably lay in the temperature hysteresis of the calomel electrode, which caused errors

Table 3. Isopotential pH values for glass electrodes with respect to a remote junction reference electrode. pH_{iso} values from second-order fit refer to the temperatures indicated

Electrode	pH_{iso} from linear graph	Temperature of second-order fit of pH_{iso}/°C									
		5	10	15	20	25	30	35	40	45	50
XIVB	7.31	6.90	6.97	7.05	7.14	7.22	7.37	7.44	7.54	7.62	7.76
XVC	4.98	4.09	4.31	4.49	4.65	4.84	5.11	5.28	5.49	5.67	5.85
XVIC	6.17	5.38	5.55	5.71	5.87	6.04	6.34	6.50	6.64	6.74	6.99
XVIID	5.55	3.67	4.18	4.48	4.85	5.27	6.04	6.35	6.64	6.96	7.40

Table 4. Formal isopotential pH values for reference electrodes (with respect to a remote junction reference electrode)

Electrode	Solution*	pH_{iso} from linear graph	Temperature of second-order fit of pH_{iso}/°C									
			5	10	15	20	25	30	35	40	45	50
VIA calomel (3 mol l^{-1} KCl) ..	A	2.23	—	1.83	1.98	2.12	2.27	2.41	2.58	2.70	2.85	—
	B	2.16	—	—	—	2.20	2.19	2.17	2.16	2.15	2.14	—
VIIB calomel (4 mol l^{-1} KCl) ..	A	2.04	—	1.76	1.85	1.94	2.04	2.13	2.22	2.31	2.41	—
	B	2.02	—	—	—	1.58	1.72	1.87	2.02	2.16	2.31	—
IA Ag - AgCl (3 mol l^{-1} KCl) ..	A	0.42	0.49	0.47	0.46	0.45	0.43	0.42	0.41	0.40	0.38	0.37
	B	0.44	—	—	—	0.57	0.53	0.48	0.44	0.39	0.34	0.30

* A, 3 mol l^{-1} potassium chloride solution; and B, in phosphate buffer solution (pH 6.685 at 25 °C).

that would be most evident at the extremes. No such problem was observed with the silver - silver chloride reference electrode.

Two series of tests were carried out. The first, over the full temperature range, used 3 mol l^{-1} potassium chloride solution but a second series was carried out over a limited range of temperature (20–50 °C) in phosphate buffer solution to check that the solution and, therefore, the liquid junction were not significant factors in determining pH_{iso}. In both series of tests the electrodes were more fully immersed and given longer to equilibrate than might be usual for pH measurements.

Internal temperatures of reference electrodes

In the preceding sections, care was taken to see that the reference electrodes took up a definite temperature. Electrodes were either fully immersed, so that the element was at the same temperature as the test solution, or the elements were kept at a constant temperature and joined to the test solution by a long "remote junction" tube. However, in common practice the reference electrode temperature will often be indeterminate if the solution differs markedly from air temperature because (a) manufacturers give no instructions as to the immersion depth, unless it is to recommend that there is a sufficient head of reference electrolyte solution, and (b) the design of the electrode may allow more or less convection to occur within the body and involve considerable variation in the position of the reference element.

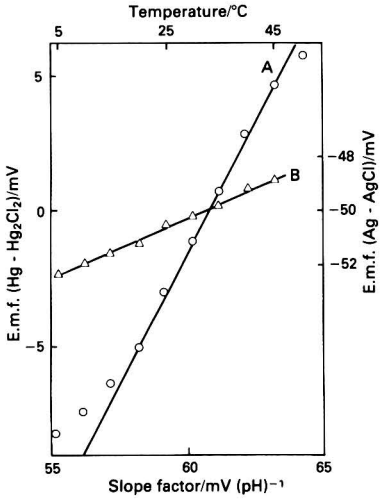

Fig. 2. Effect of temperature on calomel (A) and silver - silver chloride (B) reference electrodes in 3 mol l^{-1} KCl solution *versus* a remote 3 mol l^{-1} KCl calomel electrode at 25 °C

The temperature inside a variety of reference electrodes subjected to different temperature gradients was measured with a 0.6 mm diameter thermistor which could be manoevered into various positions within the body. Initially, two types of electrode were studied, representing extremes of design for "standard" commercially available laboratory electrodes, *i.e.*, having bodies about 12 mm in diameter and 10 cm long and excluding remote junction electrodes and electrodes designed to withstand high temperatures or pressures. Electrode IA (similar in construction to calomel electrode VIA) had the reference element set low in the body with a baffle immediately above it to restrict convection. A 4-cm immersion covered the element completely. Electrode XVIIIE (now discontinued) had no constraints on convection, with the element placed mid-way down the body with wide clearances all round.

The results in Table 5 show that electrode IA's baffle, by limiting convection, shortened the response time in the immersed part of the electrode and enabled this part of the electrode, including the element, to approach closely the temperature of the solution outside. Provided that the electrode was immersed up to the level of the baffle, the element inside attained the temperature of the solution outside. The temperature above the baffle changed only slowly.

In electrode XVIIIE convection caused the temperature inside the electrode to become almost uniform in a warm solution, but in a cold solution the temperature gradient was almost the same as in electrode IA. When the temperature was uniform, it was lower than that of the warm test solution (and pH electrode). A reference element in such a body could not be guaranteed to form part of an isothermal cell, but neither would it resemble a remote junction electrode in its thermal characteristics. Thermal equilibrium in such electrodes could also contribute to long response times or drifting e.m.f.s.

Other examples of reference electrodes between the above extremes were tested, but only in warm solutions, as it was

Table 5. Temperature variations inside reference electrodes

Electrode	External solution temperature/ °C	Electrode immersion depth/ cm	Thermometer height*/ cm	Internal temperature/ °C	Time to equilibrium/ min
IA, baffle 4 cm from end (air temperature 24 °C)	34.3	1	1	34.3	3
	34.3	1	8	27.7	25
	34.3	2	3†	32.7	15
	16.5	2	3†	20.2	15
	16.5	3.5	1	16.8	4
	16.5	3.5	8	24.1	20
XVIIIE (air temperature 24 °C)	34.3	3	2†	33.3	6
	34.3	3	8	33.1	18
	16.5	3	1.5	16.8	8
	16.5	3	8	23.7	25
XIXE, spacer 6 cm from end (air temperature 22 °C)	35.1	1.5	3.5†	29.3	10
	35.1	5	3.5†	34.5	2
VIIB (air temperature 22 °C)	35.1	<0.5	3†	25.9	25
	35.1	4.5	3†	34.9	3
IVC, spacer 3.5 cm from tip (air temperature 22 °C)	35.1	3.5	3†	35.1	5
	35.1	3.5	4.5†	32.4	10

* Height above the tip of reference electrode.
† At these heights the thermistor was alongside the reference element.

evident from the earlier tests that in a cold solution the temperature gradients were much the same in all electrodes. A current model (electrode XIXE) from the same manufacturer was tested; this had a perforated spacer 6 cm from the tip and above the reference element. Table 5 shows that this electrode was intermediate in performance between electrodes IA and XVIIIE. It appears that the spacer was not as effective a barrier as the baffle in electrode IA, as the element remained below the temperature of the exterior solution, even when fully immersed.

Electrode VIIB had no baffle, but the element was set in a glass tube that narrowly cleared the walls of the electrode body. This seemed to restrict convection sufficiently for the element to reach the external solution temperature in a fairly short time, provided that the electrode was immersed to a depth of 4.5 cm so as to cover the element. When only the glass tip carrying the ceramic frit junction was immersed, the temperature inside the electrode rose only slowly and its performance then approached that of a remote junction electrode.

Electrode IVC had a perforated spacer mid-way up the reference element. Provided that the electrode was immersed up to the level of the spacer (3.5 cm), the solution around the lower part of the element was at the same temperature as the external solution but that around the upper part was 2–3 °C lower. As the spacer was half-way up the element, it was likely to worsen the temperature gradients in the element, which was so long that it could not be adequately immersed in the thermostated vessel.

Apparent pH_{iso} values in non-ideal conditions

The above results show that thermal equilibrium between a reference electrode and a sample solution cannot be readily assumed without more care being taken than is implied in standard analytical procedures. Most reference electrodes are of a design likely to produce the indeterminate type of thermal characteristics found above and in such circumstances the pH_{iso} values obtained in Table 4 may not be reproduced.

Electrode VIA was tested at various depths of immersion. This calomel electrode has a baffle above the element so that isothermal behaviour can be expected if the electrode is immersed sufficiently (*cf.* electrode IA in Table 5). The results in Table 6 show that partial immersion results in values of pH_{iso} considerably below those obtained with a fully immersed electrode. Different values were also obtained for increases and decreases in temperature, which may be attributed to hysteresis of the calomel electrode. Although all the e.m.f.s were apparently steady values, even in the most favourable circumstances (full immersion, temperature increase) pH_{iso} differed from that obtained after careful equilibration (Table 4). In the worst instance, pH_{iso} differs by 2 pH from the equilibrium value, which is equivalent to a reading error of 0.07 pH over a 10 °C range.

The discrepancies in pH_{iso} are much worse for the calomel electrode than for the silver - silver chloride electrode, which shows a difference of only 0.4 in pH_{iso} between fully immersed and completely remote positions and is far less prone to hysteresis. This further strengthens the preference for silver - silver chloride reference electrodes when measurements are made at different temperatures.

Temperature coefficient of the slope factor

Equation (2) expresses the theoretical variation of the slope factor with temperature. However, the slope factor itself often deviates from the ideal value and the possibility that its temperature coefficient might differ from that given by equation (2) was tested. Four glass electrodes were tested over a period of 6 months with a variety of reference electrodes (remote junction and immersion types), all of which had 3 mol l^{-1} potassium chloride reference solutions. The slope factors were determined from measurements in pH 4 and pH 7 buffer solutions at temperatures between 5 and 35 °C. The slope factors showed small (≤1%) negative deviations from the ideal values but the temperature coefficients of the slope factors agreed with equation (2) within 0.2%, as shown in Table 7. The deviations from ideality are small compared with the uncertainty in the isopotential pH, or even with the precision of setting the temperature on many pH meters. No problems are expected with the temperature coefficient of the slope factor, at least for electrodes with acceptable slope factors (≥98% of Nernstian). No predictions can be made about seriously non-Nernstian electrodes.

Table 6. Effect of immersion depth on isopotential pH of calomel reference electrode VIA

Temperature change/°C	Isopotential pH: Immersed up to baffle	Isopotential pH: Immersed half-way to baffle
25–35	1.6	0.6
35–25	0.8	0.5
25–15	0.4	0.15

Table 7. Temperature coefficient of the slope factor

Electrode	$(\partial k/\partial T)_{obs}$ / $R\ln 10/F$	Standard deviation (single result)	No. of results
XIVB	1.001	0.007	11
XVC	1.000	0.002	6
XVIC	0.998	0.004	8
XVIID	1.001	0.001	4

Effect of the liquid junction potential

pH_{iso} was determined from measurements at 25 and 35 °C for electrode XIVB *vs.* a remote calomel reference electrode. Potassium hydrogen phthalate buffer solutions (pH 4.01, 0.05 mol kg^{-1}) gave pH_{iso} = 7.3 whereas 5 × 10^{-5} mol kg^{-1} sulphuric acid solution (pH 4.00) gave pH_{iso} = 7.0. This difference is similar to that predicted in Table 2 of Part I for dilute acid and buffer solutions, and would cause a reading error of 0.01 pH over a 10 °C range. However, the difference is within one standard deviation for the empirical determination of pH_{iso} and so the contribution of the liquid junction potential to the over-all pH_{iso} may reasonably be neglected.

Discussion

Glass Electrodes

The results for glass electrodes confirm the theoretical prediction[1] that the temperature dependence of their e.m.f.s is non-linear, *i.e.*, the isopotential pH is not a true constant. The significance of errors caused by applying a linear correction to a curved function can only be judged in relation to a specific requirement for accuracy over a given temperature range. The error in pH measured at T °C with an electrode calibrated at T_s °C with an incorrect isopotential setting is given by equation (7).

$$\Delta pH \approx \frac{T - T_s}{273 + T}[pH_{iso}(set) - pH_{iso}(true)] \quad .. \quad (7)$$

For the worst electrode in Table 3, the error caused by non-linear temperature characteristics is about 0.03 pH over a 10 °C range, but for most electrodes the error is only *ca.* 0.01 pH.

A further source of error is the deviation from the expected value of pH_{iso} = 7.0. Some pH meters can correct for such deviations, but in general electrodes are supplied without acknowledgement that their pH_{iso} may be other than 7.0.

Treating the electrodes in Table 3 as having pH_{iso} = 7 would cause errors of up to 0.07 pH over a 10 °C range in temperature in the worst case. The reference electrode can also contribute to this error, *e.g.*, changing from a remote to an isothermal calomel reference electrode without adjusting the meter would cause an error of 0.07 pH over a 10 °C range.

Reference Electrodes

Both calomel and silver - silver chloride reference electrodes behaved regularly, provided that the inner reference element could readily reach thermal equilibrium with the test solution. Three factors impede the attainment of this condition.

(a) The element is of such a size or so positioned that the electrode cannot easily be immersed to a depth sufficient for good thermal contact. Most of the electrodes tested required more than 4 cm immersion, which is attainable in about 75 ml of solution in a 100-ml beaker or 150 ml in a 250-ml beaker. A small reference element positioned near the tip of the electrode is an advantage.

(b) Convection within the body of the electrode prevents equilibrium being attained. This is best controlled by means of a baffle placed above the electroactive part of the reference element. Few proprietary electrodes are well designed in this respect.

(c) The calomel element is subject to temperature hysteresis. If temperature changes are large or rapid, silver - silver chloride reference electrodes are preferable.

A way of avoiding these three problems is to remove the reference element completely from the influence of the test solution by using a remote junction arrangement. Calomel and silver - silver chloride elements are both suitable. This type of electrode is at least as convenient as other types for laboratory work, but may be less so for field measurements.

Many proprietary reference electrodes have characteristics intermediate between those of isothermal and remote electrodes, indicating that they are poorly designed with respect to factors (a) and (b). For silver - silver chloride electrodes the difference in pH_{iso} between the two extremes is fairly small, which is a further reason for preferring them to calomel electrodes for use at various temperatures. In most laboratory measurements the solutions and electrodes are close to air temperature and errors from the above sources are probably negligible.

The liquid junction potential makes a small contribution to pH_{iso} and can be the cause of small errors in temperature compensation if the ionic strength of the test solution differs substantially from that of the buffers used for calibration. Many liquid junctions, especially if they do not permit a free outflow of electrolyte solution, behave anomalously even at constant temperature[2-6] and limited studies of the thermal properties of such junctions[2,6] indicate that they could affect the temperature compensation more than has been observed in this work.

Avoiding Errors in Temperature Compensation

The best practice is to eliminate temperature compensation by bringing calibrating and test solutions to the same temperature. In the laboratory this is easily done in a water-bath, with little effect on the over-all time of analysis. For field measurements it is usually more convenient to immerse the buffer solutions in the lake or stream for 10–15 min, preferably in portions of no more than about 100 ml.

However, in some circumstances, temperature compensation is unavoidable. A remote junction reference electrode has many advantages, but, if convenience of handling demands an immersion type of electrode, a silver - silver chloride element would be preferred because it does not suffer from hysteresis and its pH_{iso} varies in only a small range, even if ideal conditions of thermal equilibrium are unattainable because of the electrode's design. The labelling on glass electrodes is sometimes misleading and pH_{iso} should be determined empirically (for a glass - reference electrode pair). Many pH meters can only accommodate a pH_{iso} of 7 (±0.5) and so restrict the choice of electrodes.

The most stringent requirement for temperature compensation in on-line pH equipment in power stations is for an error not exceeding 0.05 pH over a +30 °C range from 20 °C. This implies, by equation (7), a pH_{iso} set to within 0.5 pH of its true value. The results show that many commercial glass and reference electrodes would not enable the specification to be met if the meter had a fixed isopotential setting of 7.0. Considering the fairly low precision with which pH_{iso} could be determined, the requirement may be hard to fulfil. However, the more general requirement is only half as stringent (with a ±15 °C range), and with improved sample conditioning in modern power stations the actual range of temperature should be even narrower. The temperature of environmental samples is, in field work, usually outside the analyst's control, yet the author is unaware of any agency's requirements for the accuracy of temperature compensation in this application.

I thank Mr. C. Gatford for performing most of the practical work. This work was carried out at the Central Electricity Research Laboratories and is published by permission of the Central Electricity Generating Board.

References

1. Midgley, D., *Analyst*, 1987, **112**, 573.
2. Midgley, D., and Torrance, K., *Analyst*, 1976, **101**, 833.
3. Midgley, D., *Atmos. Environ.*, 1987, **21**, 173.
4. Davison, W., and Woof, C., *Anal. Chem.*, 1985, **57**, 2567.
5. Brezinski, D. P., *Analyst*, 1983, **108**, 425.
6. Brezinski, D. P., *Anal. Chim. Acta*, 1982, **134**, 247.

NOTE—Reference 1 is to Part I of this series.

Paper A6/282
Received August 14th, 1986
Accepted December 10th, 1986

Use of Lipophilic Additives for the Improvement of the Characteristics of PVC Membrane Lithium-selective Electrodes Based on Non-cyclic Neutral Carriers

Tatsuhiro Okada, Kazuhisa Hiratani and Hideki Sugihara
Industrial Products Research Institute, Ministry of International Trade and Industry, Yatabe, Tsukuba, Ibaraki 305, Japan

Favourable effects were found for poly(vinyl chloride) (PVC) membrane lithium-selective electrodes based on synthesised non-cyclic neutral carriers to which a lipophilic salt in combination with organophosphorus compounds had been added. Tetrabutylammonium tetraphenylborate as a lipophilic salt appreciably increased the selectivity for lithium over alkali metal ions when used in combination with trioctylphosphine oxide in the ion-sensitive membrane. The selectivity coefficient $-\log k^{pot}_{Li,M}$ increased from 1.5 to 2.2 for Li^+ over Na^+ and from 2.0 to 3.0 for Li^+ over K^+ by the addition of these compounds. The results obtained here are of practical use in developing lithium-selective electrodes, as the proposed additives have been shown to exert positive effects on several kinds of non-cyclic lithium-selective carriers in PVC matrix ion-selective electrodes.

Keywords: *Lithium determination; ion-selective electrode; poly(vinyl chloride) membrane; lipophilic additives; tetrabutylammonium tetraphenylborate*

Considerable attention has recently been focused on the development of ion-selective electrodes for the determination of lithium ion activities. The monitoring of Li^+ in biological systems is very important as lithium is used in the treatment of maniacal psychosis,[1-3] and a sensitive Li^+-selective electrode is required for this purpose. The electrode should exhibit at least a 10^3-fold selectivity for Li^+ over Na^+ and a detection limit for Li^+ of 10^{-4} mol dm^{-3}.[4] Unfortunately, it is very difficult to obtain Li^+-selective electrodes that satisfy these requirements commercially.

A great deal of research has been directed towards polymer matrix ion-selective electrodes that use electrically neutral carriers as sensors.[5] There are very few naturally occurring antibiotics that have a marked selectivity towards small ions such as Li^+, and therefore efforts have been devoted to the synthesis of cyclic[6-9] and non-cyclic[4,10,11] neutral carriers with sufficient ability to complex Li^+. Recently, a novel type of Li^+-selective carrier was synthesised and was found to exhibit excellent properties in ion-selective transport[12] and in lithium-selective electrodes.[13]

In developing polymer matrix ion-selective electrodes, efforts have been focused so far on the design of carriers that have satisfactory complexing ability.[5,14] It is evident that the change in conformation that occurs during the complexation of carriers with ions, and hence the change in the solvent atmosphere, could greatly affect the thermodynamic and kinetic properties of ion-extraction and complex-formation processes.[15] Hence it can be assumed[16-18] that the choice of solvent atmosphere could stabilise the primary complex formation or destabilise the complexation of interfering ions, and that it should greatly affect the ion selectivity of liquid membrane electrodes. Such effects could be enhanced in non-cyclic carriers as these have more freedom in their molecular structure than cyclic carriers.

In the work reported here, attempts were made to examine the solvent effects of poly(vinyl chloride) matrix lithium-selective electrodes based on synthesised non-cyclic neutral carriers by the addition of solvent mediators (plasticisers) and several lipophilic additives to the ion-sensitive membranes. The selectivity for lithium and other electrode characteristics were improved when lipophilic salts were used in the membrane in combination with organophosphorus additives.

Experimental

Materials

3,3-Bis(8-quinolyloxymethyl)oxcetane (**I**) was utilised as a netural carrier for Li^+-selective PVC membrane electrodes. It was synthesised as reported recently[12,13] and used after purification by column chromatography (alumina - chloroform) followed by recrystallisation from cyclohexane.

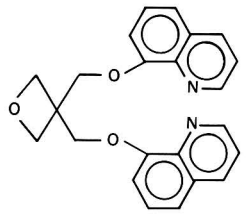

I

The plasticisers used were *o*-nitrophenyl octyl ether (NPOE), dioctyl phenylphosphonate (DOPP), dioctyl phthalate (DOP), bis(2-ethylhexyl) sebacate (DOS), tris(2-ethylhexyl) phosphate (TOP), trioctyl phosphite (TOPi), 2,3-dimethylnitrobenzene, dibutyl sebacate (DBS), decan-1-ol, 2-ethylnitrobenzene, acetophenone, nitrobenzene (NB) and 2-nitro-*p*-cymene. These were available commercially and were used without further purification.

Poly(vinyl chloride) (PVC, average degree of polymerisation 1100), which was also commercially available from Wako Pure Chemical Industries, was purified by precipitation from tetrahydrofuran (THF) in methanol.

The lipophilic additives used were potassium tetrakis(*p*-chlorophenyl) borate (KTCPB) (anionic sites) and trioctylphosphine oxide (TOPO), TOP, DOPP and TOPi as organophosphorus additives, which were used as received. Series of tetraalkylammonium tetraphenylborate compounds were also used as lipophilic salts. Table 1 shows these compounds, together with their abbreviations. Tetraalkylammonium chloride or bromide was mixed with an equimolar amount of sodium tetraphenylborate in dichloromethane at room tem-

Table 1. Lipophilic additives used in the experiments

Lipophilic additive	Abbreviation
Organophosphorus compounds:	
$(C_8H_{17})_3P=O$	TOPO
$(C_8H_{17}O)_3P=O$	TOP
$(C_8H_{17}O)_2C_6H_5P=O$	DOPP
$(C_8H_{17}O)_3P$	TOPi
Lipophilic salts:	
$R^1R^2R^3R^4N^+(C_6H_5)_4B^-$	
$R^1=R^2=R^3=R^4=CH_3$	$(4C_1NTPB)$
$R^1=R^2=R^3=R^4=C_2H_5$	$(4C_2NTPB)$
$R^1=R^2=R^3=R^4=C_3H_7$	$(4C_3NTPB)$
$R^1=R^2=R^3=R^4=C_4H_9$	$(4C_4NTPB)$
$R^1=R^2=R^3=R^4=C_5H_{11}$	$(4C_5NTPB)$
$R^1=R^2=R^3=R^4=i\text{-}C_5H_{11}$	$(4i\text{-}C_5NTPB)$
$R^1=R^2=R^3=R^4=C_6H_{13}$	$(4C_6NTPB)$
$R^1=C_{12}H_{25}, R^2=R^3=R^4=CH_3$	$(C_{12}3C_1NTPB)$
$R^1=C_{14}H_{29}, R^2=R^3=R^4=CH_3$	$(C_{14}3C_1NTPB)$
$R^1=R^2=C_{14}H_{29}, R^3=R^4=CH_3$	$(2C_{14}2C_1NTPB)$
$R^1=R^2=C_{18}H_{37}, R^3=R^4=CH_3$	$(2C_{18}2C_1NTPB)$
Anionic site $(p\text{-}ClC_6H_4)_4B^-K^+$	KTCPB

perature and the reaction was completed overnight. The product was filtered and the solvent removed from the filtrate by evaporation. The residue was recrystallised from ethyl acetate. For the tetramethyl- and tetraethylammonium chloride, which were not soluble in dichloromethane, the solid reaction product obtained after filtration was washed with pure water and then dichloromethane and the residual solid was dried and used.

Membrane Preparation

The carrier (5 mg), plasticiser (250 mg), PVC (100 mg), KTCPB (3 mg), organophosphorus compounds and/or lipophilic salts (3–10 mg) were dissolved in 4 ml of THF. The mixture was then poured into a petri dish (42 mm diameter), which was kept horizontally on a mercury pool, and the THF was allowed to evaporate slowly at room temperature. A polymeric membrane of *ca.* 0.2 mm thickness was obtained. A disc (5 mm diameter) was cut from the PVC membrane and was incorporated into a Teflon electrode body (13 mm in diameter, 120 mm in length) for e.m.f. measurements.

E.m.f. Measurements

The e.m.f. measurements were carried out using the following electrochemical cell: Ag - AgCl|10^{-2} mol dm^{-3} LiCl‖membrane‖sample solution|10^{-1} mol dm^{-3} NH_4NO_3|saturated KCl - AgCl - Ag. The sample solutions were prepared from analytical-reagent grade chlorides of alkali and alkaline earth metals and de-ionised water (specific conductivity $<5 \times 10^{-7}$ Ω^{-1} cm^{-1}).

A computer-aided automatic testing apparatus for the measurement of the e.m.f. response of the electrode and for data processing based on separate solutions methods[19] was prepared and utilised in this experiment. Fig. 1 depicts the apparatus. The test-tube (120 ml volume) containing sample solutions with different concentrations of metal ions was placed in position by a fraction collector. A unit composed of the ion-selective electrode, the reference electrode and a stirrer was introduced into or pulled out of the sample solution by means of a pulse motor. The e.m.f. of the solution was measured with a Keithley Model 614 electrometer (input impedance $>5 \times 10^{13}$) and was input into an NEC PC8801 microcomputer through an analogue - digital converter.

A flow chart showing the sequence of measurements made is given in Fig. 2. After the initial set-up period, the cationic species I was settled and the test-tubes were programmed to be placed so that the concentration, J, of the relevant cationic

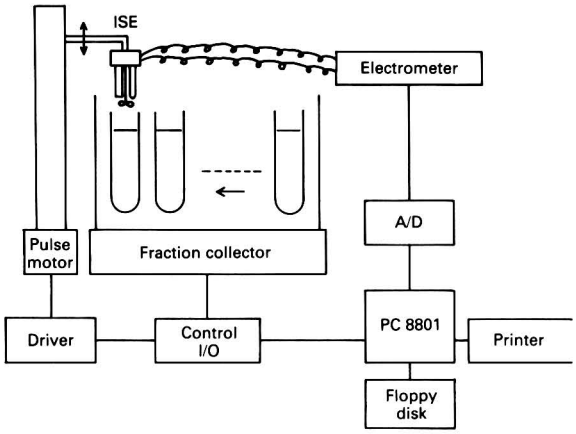

Fig. 1. Illustration of the automated testing apparatus for ion-selective electrodes

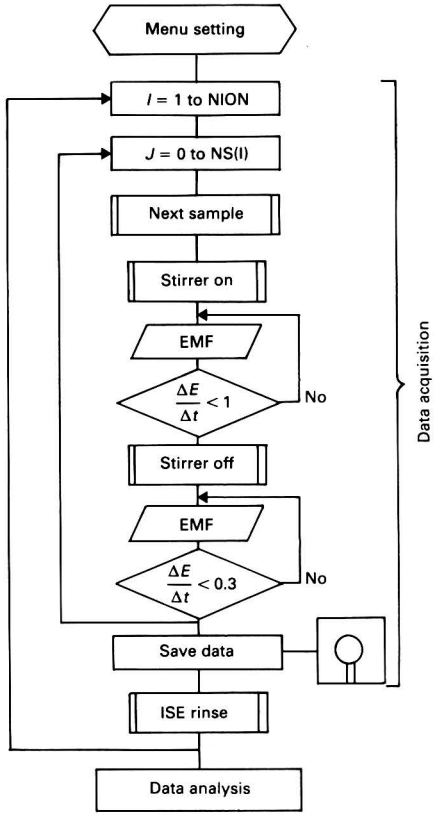

Fig. 2. Flow chart of the measuring and data processing program for testing ion-selective electrodes

species fell in a 10-fold ascending order. The test-tube containing the sample solution to be measured was put into place by the "NEXT SAMPLE" routine, the electrode was placed in the solution, the stirrer was turned on and an e.m.f. value was input into the computer every 10 s until a steady-state value was attained. The stirrer was then turned off and the e.m.f. was measured. This procedure was repeated for each concentration of solution. After a series of measure-

ments for a cationic species the electrode was rinsed with pure water and the process was repeated for all the cationic species. All experiments were performed at 25 °C, and all the measurements were controlled by the microcomputer, the data were saved on a floppy disk and the results were printed out. The potentiometric selectivity coefficients were calculated from the calibration graphs obtained.

Results and Discussion

The solvent medium of the PVC membrane exerted an appreciable effect on the characteristics of the electrode. In Fig. 3, the logarithm of the selectivity coefficient of Li^+ relative to the ion M (log $k^{pot}_{Li,M}$) for membranes consisting of various plasticisers is plotted against the dielectric constants of the plasticisers. The electrode responded fairly rapidly to changes in Li^+ activity; the response time ranged from 30 to 50 s, depending on the plasticiser used. Very poor Nernstian responses were obtained for the membrane with DBS, decan-1-ol, *o*-nitroethylbenzene, acetophenone and NB plasticisers.

According to the electrostatic model[5,14] in which the ion - ligand complex is treated as a sphere, the smallest differences in ion selectivity among monovalent cations are expected to be caused by the change in polarity of the membrane. The observed change in Li^+ - alkali metal ion selectivity in Fig. 3 appears to be due to the slight change in the size of the coordination sphere of the non-cyclic carrier caused by a change in the membrane solvent. For divalent cations, no specific change in the selectivity was observed. Among the plasticisers tested, NPOE gave the best membrane characteristics and was utilised in the following experiments.

The e.m.f. response of the membrane containing the carrier and the lipophilic salt $4C_4NTPB$ with the plasticiser NPOE are shown in Fig. 4(*a*)–(*c*). Fig. 4(*a*) shows the calibration graph for the PVC membrane containing 1.4% *m/m* carrier, 70% *m/m* NPOE and 0.8% *m/m* KTCPB, for which a good Nernstian response of 59 mV decade^{-1} and a detection limit of 5×10^{-5} mol dm^{-3} for Li^+ were observed. The membrane with the addition of 1.1% *m/m* $4C_4NTPB$ and no KTCPB had a low e.m.f. and a poor electrode behaviour, as seen in Fig. 4(*b*). However, if KTCPB and the lipophilic salt $4C_4NTPB$ were incorporated in the membrane, the electrode characteristics were significantly improved and the interference from divalent cations was suppressed.

The selectivity coefficients of the membrane containing various amounts of additives are shown in Fig. 5. KTCPB improved the Nernstian response of the electrode, but an excess amount of it increased the K^+ interference. $4C_4NTPB$ together with 0.8% *m/m* KTCPB improved the Li^+ selectivity, especially against divalent cations. In this instance an optimum concentration was shown to exist for the appearance of

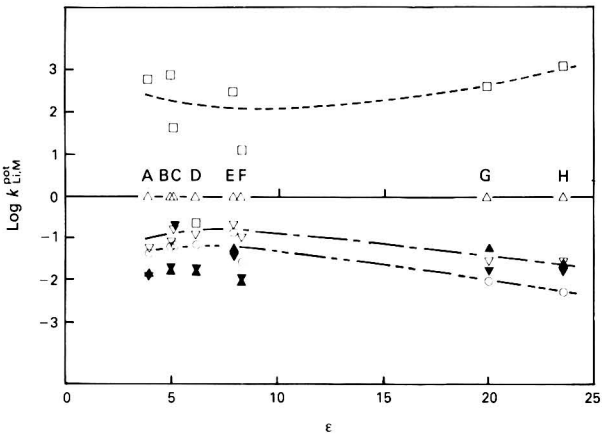

Fig. 3. Selectivity coefficients of PVC membranes plotted against dielectric constants of plasticisers composing the membranes. Membrane composition: 1.4% *m/m* carrier (**I**), 70% *m/m* plasticiser, 0.8% *m/m* KTCPB. Plasticisers: (A) DOS; (B) DOP; (C) TOPi; (D) DOPP; (E) decan-1-ol; (F) TOP; (G) 2-nitro-*p*-cymene; and (H) NPOE. □, H^+; △, Li^+; ▽, Na^+; ○, K^+; ▲, Mg^{2+}; and ▼, Ca^{2+}

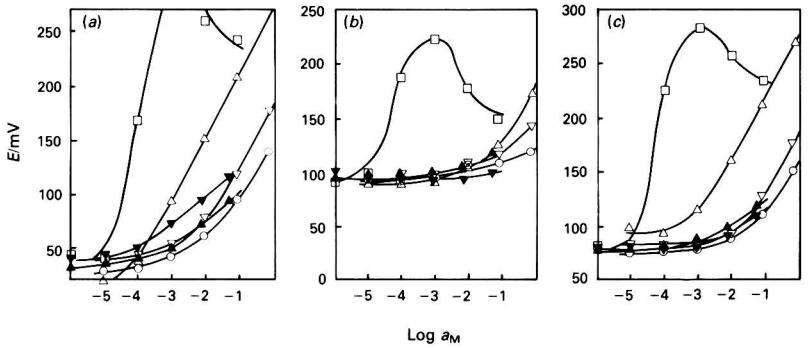

Fig. 4. Calibration graphs for electrodes with PVC membranes containing carrier (**I**) and lipophilic additives. Membrane composition: (*a*) 1.4% *m/m* carrier, 70% *m/m* NPOE, 0.8% *m/m* KTCPB; (*b*) 1.4% *m/m* carrier, 70% *m/m* NPOE, 1.1% *m/m* $4C_4NTPB$; and (*c*) 1.4% *m/m* carrier, 69% *m/m* NPOE, 1.1% *m/m* $4C_4NTPB$, 0.8% *m/m* KTCPB. □, H^+; △, Li^+; ▽, Na^+; ○, K^+; ▲, Mg^{2+}; and ▼, Ca^{2+}

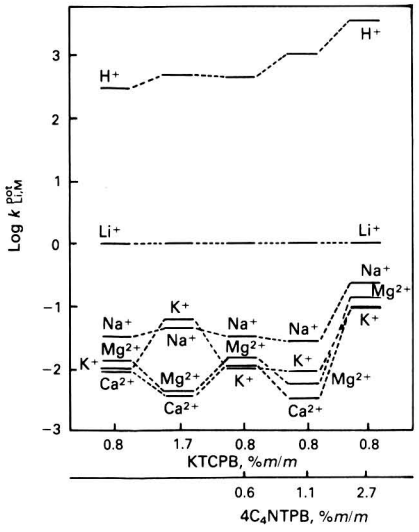

Fig. 5. Selectivity coefficients of PVC membranes containing various amounts of lipophilic additives. Membrane composition: 1.4% *m/m* carrier (**I**), 68–70% *m/m* NPOE

good electrode characteristics. In Fig. 6, the Li^+ selectivity is shown for various kinds of lipophilic additives. The presence of the butyl group as the alkyl moiety of tetraalkylammonium tetraphenylborate proved to be the best for improving the Li^+ selectivity of the electrode. Ethylene glycol, which is a polar, non-ionic additive was tested in comparison with lipophilic salts and did not have any effect on the Li^+ selectivity.

The e.m.f. response of the membrane incorporating organophosphorus additives is shown in Fig. 7(*a*)–(*c*). TOPO has been reported to enhance the Li^+ selectivity of neutral carrier based ion-selective electrodes.[16] Our results also indicated that TOPO improved the selectivity for Li^+ over other alkali metal ions, especially over Na^+, which is essential for the use of the electrode in biological applications [Fig. 7(*a*)]. However, too much TOPO caused a detrimental interference from divalent cations [Fig. 7(*b*)]. TOPi proved to be better than TOPO, as the interference from divalent cations was much less for the TOPi [Fig 7(*c*)]. The selectivities obtained with various kinds of organophosphorus additives are shown in Fig. 8. Some organophosphorus compounds were shown to exert positive effects on the Li^+ selectivity of the electrode, especially TOPi. However, all the compounds had optimum concentrations in the membrane, above which the electrode characteristics deteriorated.

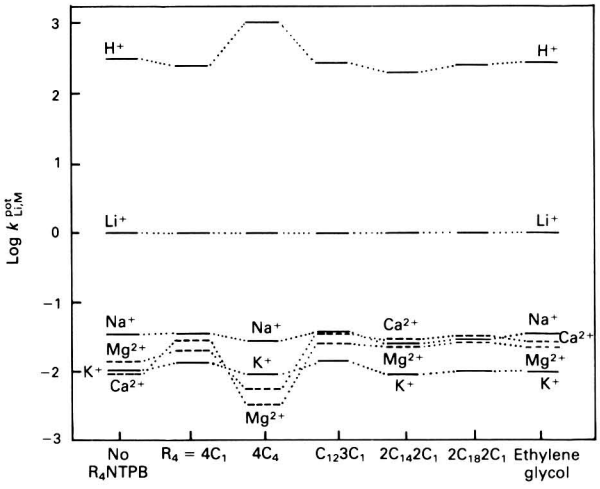

Fig. 6. Selectivity coefficients of PVC membranes containing various kinds of tetraalkylammonium tetraphenylborate as lipophilic salts. Membrane composition: 1.4% *m/m* carrier (**I**), 69–70% *m/m* NPOE, 0.8% *m/m* KTCPB, 1.1% *m/m* R_4NTPB

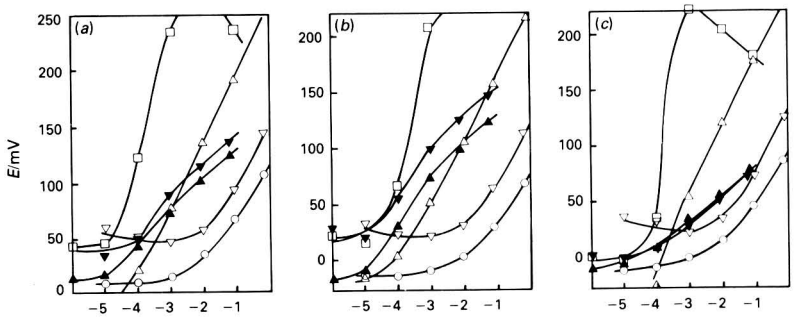

Fig. 7. Calibration graphs for electrodes with PVC membranes containing carrier (**I**) and organophosphorus additives. Membrane composition: (*a*) 1.4% *m/m* carrier, 69% *m/m* NPOE, 0.8% *m/m* TOPO, 0.8% *m/m* KTCPB; (*b*) 1.4% *m/m* carrier, 69% *m/m* NPOE, 1.6% *m/m* TOPO, 0.8% *m/m* KTCPB; and (*c*) 1.4% *m/m* carrier, 69% *m/m* NPOE, 1.6% *m/m* TOPi, 0.8% *m/m* KTCPB. □, H^+; △, Li^+; ▽, Na^+; ○, K^+; ▲, Mg^{2+} and ▼, Ca^{2+}

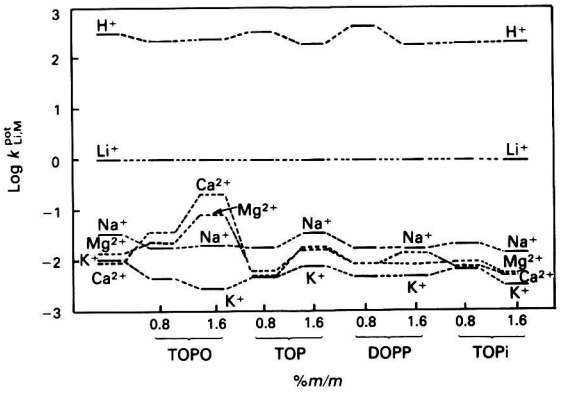

Fig. 8. Selectivity coefficients of PVC membranes containing various kinds of organophosphorus compounds as lipophilic additives. Membrane composition: 1.4% *m/m* carrier (**I**), 68–70% *m/m* NPOE, 0.8% *m/m* KTCPB

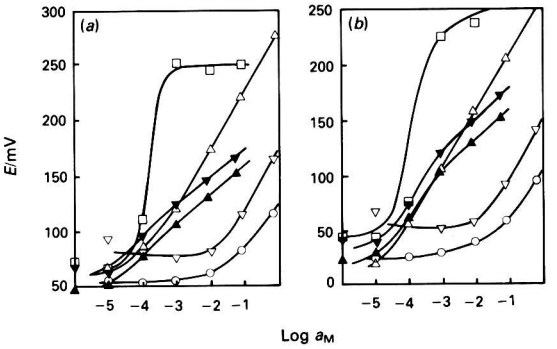

Fig. 9. Calibrations graphs for electrodes with PVC membranes containing carrier (**I**) and lipophilic additives. Membrane composition: (*a*) 1.4% *m/m* carrier, 68% *m/m* NPOE, 0.8% *m/m* TOPO, 1.1% *m/m* $4C_4NTPB$, 0.8% *m/m* KTCPB; and (*b*) 1.4% *m/m* carrier, 67% NPOE, 1.6% *m/m* TOPO, 2.2% *m/m* $4C_4NTPB$, 0.8% *m/m* KTCPB. □, H^+; △, Li^+; ▽, Na^+; ○, K^+; ▲, Mg^{2+}; and ▼, Ca^{2+}

Table 2. Effect of various additives on the selectivity of the electrode for lithium

Additive, % *m/m*			Log $k_{Li,M}^{pot}$				
Carrier	TOPO	$4C_4NTPB$	KTCPB	H^+	Na^+	K^+	Mg^{2+}	Ca^{2+}
II			0.8		−1.8	−1.6	−4.0	−3.8
		0.8	0.8	−2.6	−1.9	−1.2	−3.6	−3.4
III			0.8	1.8	−1.9	−1.6	−2.7	−0.80
		0.8	0.8	0.38	−2.3	−2.4	−3.5	−1.7
	0.8	0.8	0.8	1.2	−2.0	−2.3	−2.3	−1.3

The e.m.f. response of the membrane when both TOPO and $4C_4NTPB$ were present as additives is shown in Fig. 9(*a*) and (*b*). In this instance favourable effects were observed, and the Li^+ selectivity was enhanced whereas the interference from divalent cations remained suppressed. Fig. 10 shows the selectivity of the membrane when various kinds of organophosphorus compounds are incorporated together with $4C_4NTPB$. The coexistence of TOPO and the lipophilic salt appreciably increased the Li^+ selectivity of the electrode and optimum ratios of the additives were shown to exist. Combinations of TOPO with tetraalkylammonium tetraphenylborates of various aliphatic chain lengths were tested (Fig. 11) and the best electrode characteristics were obtained with the butyl group as the alkyl moiety.

In order to investigate the effects of lipophilic additives, the change in ionic selectivity of the carrier-free membrane containing various kinds of lipophilic additives was examined. The results are shown in Fig. 12. The plasticiser NPOE is known to show K^+ selectivity in itself, as seen in the figure. At higher concentrations of TOPO the electrode responded to Li^+ and to divalent cations to a greater extent than either Na^+ or K^+. This trend corresponds to the change in ion selectivity of the carrier-containing membranes.

Other organophosphorus compounds incorporated in the carrier-free membranes gave similar trends in ion selectivities to those seen in carrier-containing membranes, although the effects were less distinct than those obtained with TOPO. These results could be explained if organophosphorus compounds could be shown to stabilise the lithium - carrier complex, perhaps owing to their interaction with the complexed cation as a monodentate ligand, or by acting as Li^+ carriers in the membrane.

The lipophilic salt $4C_4NTPB$, incorporated in a carrier-free membrane, brought about little change in ion selectivity, except for changes in the H^+ response. $4C_4NTPB$ appears to act differently to the organophosphorus compounds, at least no ligating interaction with the primary cation. $4C_4NTPB$ was applied as the additive to the membrane based on the reported cyclic (**II**)[9] and non-cyclic (**III**)[11] Li^+-selective neutral carriers (membrane composition: 1.4% *m/m* carrier, 68–69% *m/m* NPOE, 0.8–2.4% *m/m* additives). The effectiveness of $4C_4NTPB$ was again observed in the non-cyclic carrier **III**,

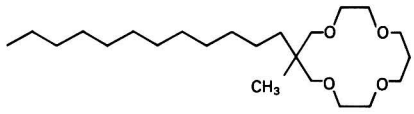

II

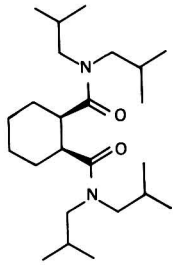

III

where Li^+ selectivity over other alkali or alkaline earth metal ions was improved significantly with the addition of as little as 0.8% *m/m* $4C_4NTPB$. These results are shown in Table 2. One possible mechanism for its interaction might be the reduction of the electrical resistance of the membrane owing to the presence of lipophilic salts,[18] although it might also be considered that $4C_4NTPB$ as a lipophilic salt in the organic phase could prevent the uptake of cations into the membrane and hence the complexation of interfering ions that were not well suited to coordination by the carriers.

Non-cyclic carriers have in general much more freedom in the conformation of their structures than cyclic carriers which have coordination sites in a fixed cavity size. The steric interaction between the cation and the coordinants could vary with these non-cyclic carriers, depending on the atmosphere of the solvent, and thus favourable effects caused by the lipophilic additives were observed in this experiment. Further studies are required for clarification of the reaction mechanisms.

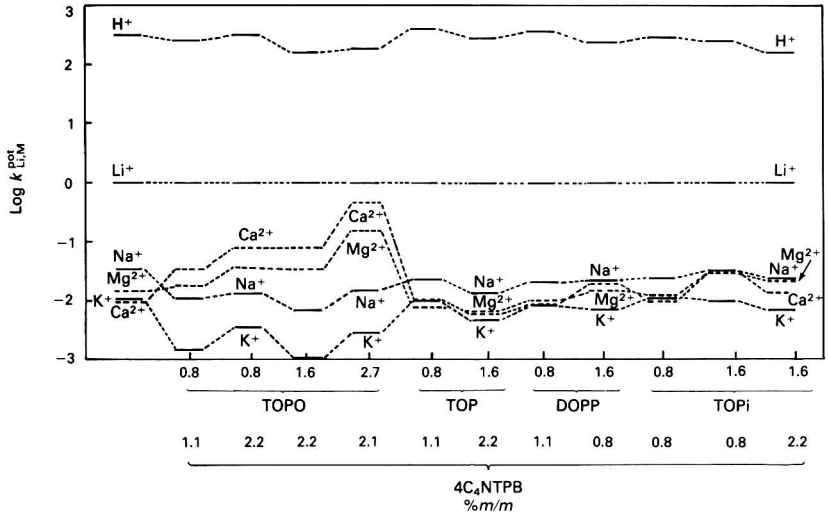

Fig. 10. Selectivity coefficient of PVC membranes containing various kinds of organophosphorus compounds in combination with $4C_4NTPB$. Membrane composition: 1.4% *m/m* carrier, 66–68% *m/m* NPOE, 0.8% *m/m* KTCPB

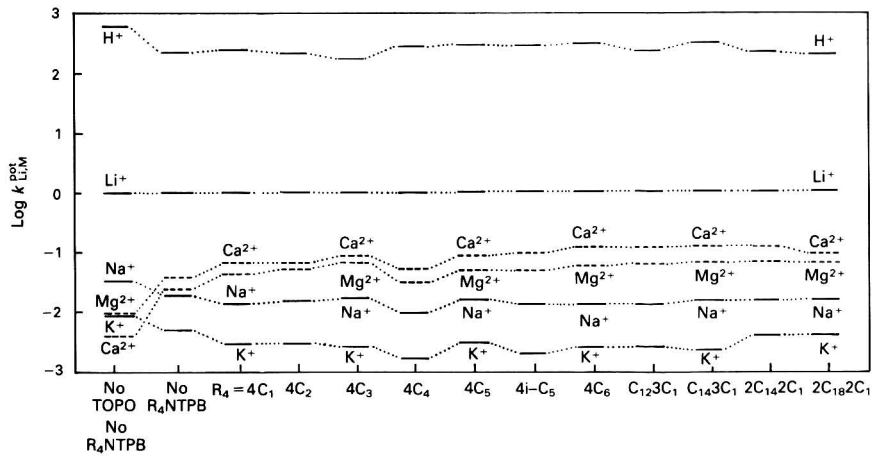

Fig. 11. Selectivity coefficients of PVC membranes containing various kinds of tetraalkylammonium tetraphenylborate in combination with TOPO. Membrane composition: 1.4% *m/m* carrier, 69% *m/m* NPOE, 0.8% *m/m* TOPO, 1.1% *m/m* R_4NTPB, 0.8% *m/m* KTCPB

Table 3. Comparison of selectivity coefficients for the PVC matrix Li^+-selective electrodes based on neutral carriers

Membrane components		Log $k^{pot}_{Li,M}$							
Carrier	Plasticiser	H^+	Na^+	K^+	NH_4^+	Mg^{2+}	Ca^{2+}	Reference	(Year)
ETH 149	TEHP	−0.1	−1.3	−2.1	−1.3	−3.7	−3.3	10	(1975)
ETH 1644	NPOE	0.7	−2.1	−2.2	−2.1	−3.2	−3.0	11	(1981)
Crown ether	NPOE	−3.5	−1.0	−0.84	−2.0	−3.7	−4.0	7	(1982)
Crown ether	TEHP	0.67	−1.0	−1.7	−0.47	−2.8	−2.9	8	(1982)
Crown ether	NPOE	−3.4	−2.2	−2.0	−3.0	−4.6	−4.3	9	(1984)
ETH 1810	NPOE	0.95	−2.45	−2.6	−2.5	−4.0	−2.7	20	(1984)
This work	NPOE	2.5	−1.5	−2.0	—	−1.9	−2.0	13	
With TOPO and $4C_4NTPB$	NPOE	2.2	−2.2	−3.0	—	−1.5	−1.1	—	
Required value		2.1	−4.3	−2.8	—	−3.4	−3.6	4	(1986)

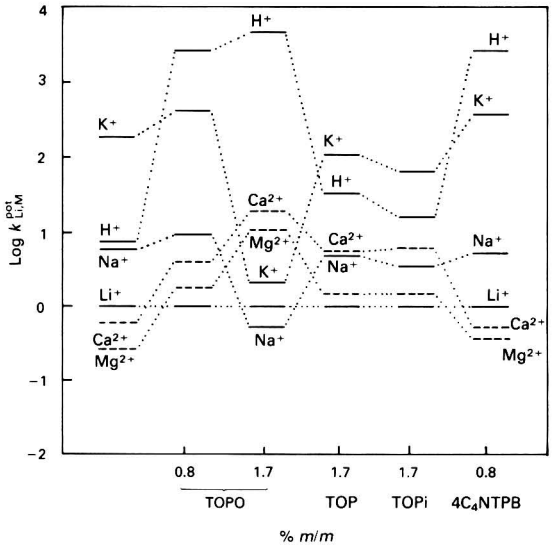

Fig. 12. Selectivity coefficients of carrier-free membranes containing various lipophilic additives. Membrane composition: 70–71% *m/m* NPOE, 0.8% *m/m* KTCPB

Conclusion

The use of tetrabutylammonium tetraphenylborate as a lipophilic additive gave a remarkable increase in the Li^+ selectivity of PVC membrane electrodes based on non-cyclic carriers, especially when it was incorporated in the membrane in combination with organophosphorus additives such as TOPO. The optimum composition of the membrane is 1.4% *m/m* carrier, 67% *m/m* NPOE, 1.6% *m/m* TOPO, 2.2% *m/m* $4C_4NTPB$ and 0.8% *m/m* KTCPB.

In Table 3 comparisons are made between selectivity coefficients for the reported PVC matrix Li^+-selective electrodes based on neutral carriers. In this work, Li^+ selectivity over Na^+ and K^+ was enhanced 5- and 10-fold, respectively, by the use of lipophilic additives in the membrane. This could compare with the synthesis of a novel Li^+ carrier.

The results obtained are an indication that the characteristics of ion-selective electrodes based on non-cyclic carriers would be considerably improved by using a solvent atmosphere in which the carriers are incorporated. Although there are still difficulties in the application of sensor systems to real samples to be overcome,[21] the effect of the solvent atmosphere should be of practical aid in developing lithium-selective electrodes.

The authors are indebted to Professor Toshiyuki Shono and Dr. Keiichi Kimura of Osaka University for supplying compound **II** and for helpful discussions. This work was supported in part by grants from the Science and Technology Agency.

References

1. Amidsen, A., *Dan. Med. Bull.*, 1975, **22**, 277.
2. Canessa, M., Adragna, N., Salomon, H. S., Connolly, T. M., and Tosteson, D. C., *N. Engl. J. Med.*, 1980, **302**, 772.
3. Tosteson, D. C., *Sci. Am.*, 1981, **244**, 164.
4. Metzger, E., Ammann, D., Asper, R., and Simon, W., *Anal. Chem.*, 1986, **58**, 132.
5. Freiser, H., *Editor*, "Ion-Selective Electrodes in Analytical Chemistry," Volume 1, Plenum Press, New York, 1978, Chapters 3 and 4.
6. Schindler, J. G., Stork, G., Strüh, H.-J., and Schäl, W., *Fresenius Z. Anal. Chem.*, 1978, **290**, 45.
7. Olsher, U., *J. Am. Chem. Soc.*, 1982, **104**, 4006.
8. Aalmo, K. M., and Krane, J., *Acta Chem. Scand., Ser. A*, 1982, **36**, 227.
9. Kitazawa, S., Kimura, K., Yano, H., and Shono, T., *J. Am. Chem. Soc.*, 1984, **106**, 6978.
10. Güggi, M., Fiedler, U., Pretsch, E., and Simon, W., *Anal. Lett.*, 1975, **8**, 857.
11. Zhukov, A. F., Erne, D., Ammann, D., Güggi, M., Pretsch, E., and Simon, W., *Anal. Chim. Acta*, 1981, **131**, 117.
12. Hiratani, K., Taguchi, K., Sugihara, H., and Okada, T., *Chem. Lett.*, 1986, 197.
13. Hiratani, K., Okada, T., and Sugihara, H., *Anal. Chem.*, in the press.
14. Ammann, D., Morf, W. E., Anker, P., Meier, P. C., Pretsch, E., and Simon, W., *Ion-Sel. Electrode Rev.*, 1983, **5**, 3.
15. Dunitz, J. D., *Editor*, "Structure and Bonding," Volume 16, Springer-Verlag, Berlin, 1973.
16. Imato, T., Katahira, M., and Ishibashi, N., *Anal. Chim. Acta*, 1984, **165**, 285.
17. Hara, H., Okazaki, S., and Fujinaga, T., *Bull. Chem. Soc. Jpn.*, 1980, **53**, 3610.
18. Pretsch, E., Wegmann, D., Ammann, D., Bezegh, A., Dinten, O., Läubli, M. W., Morf, W. E., Oesch, U., Sugahara, K., Weiss, H., and Simon, W., *in* Kessler, M., Harrison, D. K., and Höper, J., *Editors*, "Ion Measurements in Physiology and Medicine," Springer-Verlag, Berlin, 1985, p. 11.
19. Srinivasan, K., and Rechnitz, G. A., *Anal. Chem.*, 1969, **41**, 1203.
20. Metzger, E., Ammann, D., Schefer, U., Pretsch, E., and Simon, W., *Chimia*, 1984, **38**, 440.
21. Gadzekpo, V. P. Y., Moody, G. J., and Thomas, J. D. R., *Analyst*, 1986, **111**, 567.

Paper A6/19
Received January 20th, 1986
Accepted October 21st, 1986

Flow Injection Determination of Inorganic Bromide in Soils with a Coated Tubular Solid-state Bromide-selective Electrode

Jacobus F. van Staden
Department of Chemistry, University of Pretoria, Pretoria 0002, South Africa

Inorganic bromide can be determined in soil extracts by flow injection potentiometry at a rate of 80 samples per hour with a standard deviation of 1.6%. Soil-extracted samples (30 μl) are injected into a 1 mol dm^{-3} potassium nitrate carrier solution containing 100 mg dm^{-3} chloride as an ionic strength adjustment buffer. The sample - buffer zone formed is transported through a laboratory-made coated tubular solid-state bromide-selective electrode on to the reference electrode. The method is suitable for the determination of bromide in the range 1–5000 mg dm^{-3}.

Keywords: *Soil; bromide determination; flow injection analysis; ion-selective electrodes; flow-through electrodes*

The use of brominated pesticides for the fumigation of soils has greatly increased in the past few years. Organically bound bromine is normally not taken up by plants from fumigated soil. However, these compounds are readily degraded to liberate inorganic bromide to the soil. The latter is easily taken up by plants. From both toxicological and control viewpoints, a knowledge of inorganic bromide concentrations in soil is therefore required. There are several methods available for the determination of inorganic bromide in soils, plants and foodstuffs following fumigation with brominated pesticides.[1–3] However, these methods are all tedious and require extensive analytical facilities. The development and use of halide ion-selective electrodes is more attractive than other detection techniques and offers the possibility of simpler and faster methods for the determination of halide ion concentration.[4–6] Bromide ion-selective electrodes have been used for the determination of brominated vegetable oil concentrations in soft drinks,[7] of bromide ion in wine[8] and of bromide in soils.[9] However, these are all manual methods and the batchwise mode involved is time consuming for laboratories where bromide levels are to be monitored continuously.

Since its introduction in 1974–75, flow injection analysis (FIA) has established itself as an analytical technique that is suitable for increasing sample output in most analytical laboratories.[10,11] There are several considerations in the design of flow-through electrochemical detectors that can be interfaced with FIA. Potentiometric and amperometric detectors have included wall-coated (or open) tubular, packed-bed (or porous) tubular, wire, cascade, wall-jet and thin-layer designs. Slanina *et al.*[12] used the cascade configuration for the flow injection determination of bromide. However, some novel flow-through tubular arrangements for ion-selective electrodes have also been used as sensors[13–17] in flow injection systems. In this geometric mode the sample solution is channelled through the tubular configuration across the sensing membrane in a kind of open path. The incorporation of a tubular ion-selective electrode into the conduits of a flow injection system seems an ideal design as the hydrodynamic flow conditions can be kept constant throughout the flow system. This approach opens new dimensions and was recently extended to the concept of coated tubular solid-state ion-selective electrodes[18–21] incorporated into the conduits of flow injection systems. In the work described here, the combination of FIA with a coated tubular solid-state bromide-selective electrode forms the basis of a study of the determination of inorganic bromide in soils.

Experimental

Reagents and Solutions

All reagents were prepared from analytical-reagent grade chemicals unless specified otherwise. Doubly distilled, de-ionised water was used throughout. The water was tested beforehand for traces of chloride and bromide. All solutions were de-gassed before measurements by use of a water vacuum pump. The main solutions were prepared as follows.

Ionic-strength adjustment reagent (ISA)

Dissolve 202.22 g of potassium nitrate and 0.4206 g of potassium chloride in 1500 cm^3 of distilled water in a 2-dm^3 calibrated flask. Dilute this solution to 2 dm^3 with distilled water. This gives a 1 mol dm^{-3} potassium nitrate solution containing 100 mg dm^{-3} chloride. (For a 0.1 mol dm^{-3} potassium nitrate solution, 20.222 g of potassium nitrate is used.)

Standard bromide solutions

Dissolve 29.7860 g of dried potassium bromide in 2 dm^3 of distilled water to give a stock solution with a bromide concentration of 10 000 mg dm^{-3}. Standard working solutions are prepared by dilution of appropriate aliquots of the stock solution with the ISA solution (containing 0.1 mol dm^{-3} potassium nitrate and 100 mg dm^{-3} chloride) to cover the range 5–5000 mg dm^{-3}.

Apparatus

Coated tubular flow-through electrode construction

The basic design of the coated tubular flow-through solid-state bromide-selective membrane electrode was the same as that used for the construction of a chloride-selective electrode previously described.[18] The unit consisted of 0.025 mm thick silver metal foil wound around two pieces of Tygon tubing at both ends. An inner wire of a shielded cable was wound around the outside body of the silver metal cylinder to ensure electrical contact between the electrode and the Ionalyzer instrument. The whole unit was isolated with Araldite epoxy resin. The silver - silver bromide electrode was activated by anodic deposition of silver bromide as a fine membrane on the inner wall of the tubular silver cylinder. The coating was carried out at a current density of about 20 mA cm^{-2} and 0.1 mol dm^{-3} potassium bromide solution was circulated at a rate of 1.6 cm^3 min^{-1} through the tubular cylinder.

Flow injection system

A schematic diagram of the flow injection system used is illustrated in Fig. 1. A Carle microvolume two-position sampling valve (Carle No. 2014) containing two identical sample loops was used. Each loop has a volume of 30 μl. A Cenco sampler unit was used to supply a series of samples to the sampling valve system. The timing of the sampler unit was 45 s for sampling with zero wash time and valve actuation at 43 s. A Cenco peristaltic pump operating at 10 rev. min^{-1} supplied the carrier and reagent streams to the manifold system; the sampling valve system was synchronised with a Cenco sampler unit. Tygon tubing (0.51 mm i.d.) was used to construct the manifold; coils were wound round suitable lengths of glass tubing (15 mm o.d.).

The tubular flow-through bromide-selective electrode was incorporated into the conduits of the flow injection system as shown in Fig. 1. The potentials were measured at room temperature with an Orion Research (Model 901) microprocessor Ionalyzer. The detector output was recorded with a two-channel Cenco recorder (Model 34195-041). The constructed flow-through tubular indicator electrodes were used in conjunction with an Orion 90-02 double-junction reference electrode with 10% *m/V* potassium nitrate as the outer chamber filling solution.

Procedure

The carrier stream (1 mol dm^{-3} potassium nitrate) is pumped at a constant flow-rate of 3.90 cm^3 min^{-1} (Fig. 1). A pulse suppressor coil (200 cm × 0.51 mm i.d.) is incorporated between the peristaltic pump and the sampling valve. Samples taken from the turntable of an automatic sampler are injected automatically from a 30-μl sampling loop into the carrier stream by means of a two-position valve. Whereas one loop serves the carrier stream, the other draws the sample through at a constant flow-rate of 2.00 cm^3 min^{-1}. Injected samples are mixed with the carrier stream in a 105-cm mixing coil. Potassium nitrate (1 mol dm^{-3}) is added at a flow-rate of 1.40 cm^3 min^{-1} further downstream for improvement of hydrodynamic flow and mixed in a second mixing coil (160 cm) before the potential is measured in the coated tubular indicator electrode. To eliminate chloride interference in the determination of inorganic bromide in soils, 100 mg dm^{-3} chloride is included in the 1 mol dm^{-3} potassium nitrate solutions. A 45-s cycle sampling time is used, giving a capacity of 80 samples per hour. The valve system is actuated on a time basis that is correlated with the sampler unit; the sampling valve is actuated every 43 s.

Preparation of Soil Samples

Extraction efficiency studies were conducted as follows. Sandy soil (92% sand, 5.5% silt, 2.5% clay, carbon content 0.19%), loamy sand soil (84% sand, 10% silt, 6% clay, carbon content 0.31%), sandy loam soil (66% sand, 27% silt, 7% clay, carbon content 0.39%) and loam soil samples (53% sand, 35% silt, 12% clay, carbon content 0.42%) were pre-treated and tested for traces of bromide to ensure that the amount of bromide initially present was negligible further on. Bromide was added as potassium bromide solutions to 25-g portions of the above-mentioned soil samples to give a bromide concentration range of 3, 5, 10, 20, 60, 100, 250 and 1000 μg of bromide per gram of oven-dried soil. Portions (25-g) of the soil samples with no bromide added were used as blank samples. The samples were dried overnight at 105 °C and ground to pass through a 2-mm sieve. The samples were transferred into screw-capped glass jars. ISA solution (25 cm^3), containing 0.1 mol dm^{-3} potassium nitrate and 100 mg dm^{-3} chloride, was added to each sample. The jars were shaken vigorously on a reciprocating shaker for 30 min. The suspensions were centrifuged, the supernatant liquid filtered (Whatman No. 41 filter-paper) and bromide was determined in the filtrate.

Results and Discussion

The preparation procedure for laboratory-made tubular electrodes is simple and easy to conduct. However, experimental results revealed that greater care had to be taken in the preparation of suitable homogeneous coated tubular bromide-selective electrodes from AgBr alone compared with the preparation of a suitable chloride-selective electrode previously described.[18] Maximum contact area is obtained by using a tubular electrode that is well coated. The maximum sensitivity was obtained when the electrode was coated, tested, left in *ca.* 500 mg dm^{-3} bromide solution, re-coated, etc., until maximum response was obtained, and then conditioned overnight in 20 mg dm^{-3} bromide solution. It was also necessary to carry out an actual test run of about 10 min every

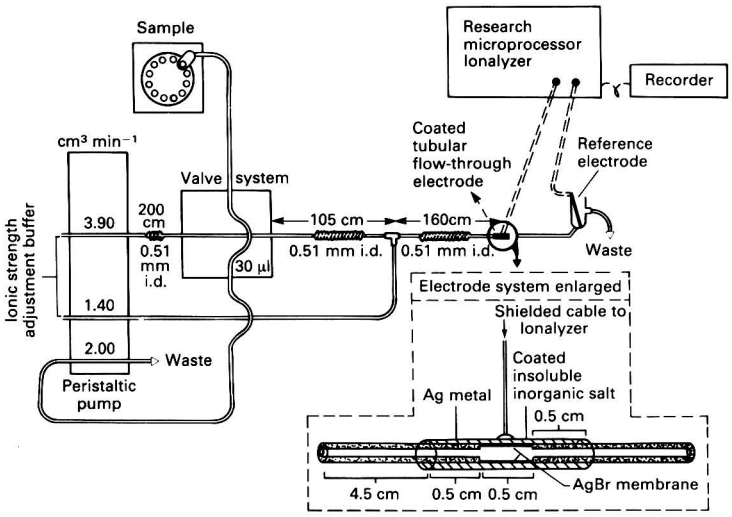

Fig. 1. Manifold and flow diagram of the FIA system. Valve loop size, 30 μl; sampling time, 45 s; wash time, 0 s; valve actuation at 43 s; sampling rate, 80 h^{-1}

morning under the same conditions as would be used for FIA, before actual work could be started for the rest of the day.

A series of preliminary tests were conducted to optimise the flow injection system parameters and the performance of the electrode itself. These experiments revealed the same results as obtained for the chloride-selective electrode[18] concerning the design, contact area and volume of the tubular assembly and the FIA parameters. The only difference was an increase to 1.40 cm^3 min^{-1} during the addition of the reagent solution further downstream in order to maintain a reasonable sample throughput. An electrode (volume 15.7 μl) with an inside diameter of *ca.* 2 mm and a length of 5 mm gave the best results for the type of flow system shown in Fig. 1.

Typical calibration graphs, illustrating the linear response of the electrode, are presented in Fig. 2. The linear response range of the electrode was measured by using the following flow system parameters. Aspiration of standard working bromide solutions in 1.0 mol dm^{-3} KNO_3 via a 3.90 cm^3 min^{-1} carrier stream into a single-line manifold system to the detector was carried out until a steady state was just obtained. The electrode showed a linear response between about 5 and 5000 mg dm^{-3}. The calculated Nernstian response of the tested electrode is 57 ± 1 mV $decade^{-1}$ [Fig. 2(A)] with a correlation coefficient of 0.9996. The linear range and slope also depend on the pre-treatment of the electrode and care should be taken during the preparation of each new coated tubular electrode. The dynamic linear response range was less [Fig. 2(B)] than that shown in Fig. 2(A) when a sample volume of 30 μl was injected into a single-line flow injection system with a carrier stream of 3.90 cm^3 min^{-1}. However, the deviation of the graph at low concentrations is the opposite of the deviation obtained for chloride-selective[18] and iodide-selective[20] electrodes.

Real sample throughput of bromide samples and carryover and reproducibility of results are dependent on the FIA system (Fig. 1), the main contribution arising from the practical response time of the coated tubular bromide-selective electrode. The results indicated that the practical response time of the bromide-selective electrode is slower than that of the chloride-selective electrode[18] with KNO_3 as the ionic strength adjustment buffer. However, the practical response time is fast enough to give the flow system used (Fig. 1) a sample throughput of about 80 samples per hour.

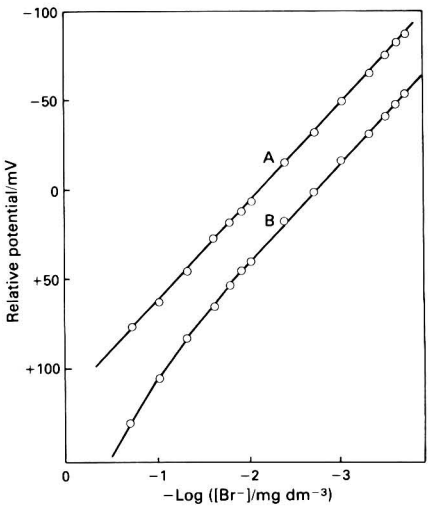

Fig. 2. Experimental calibration graphs giving the electrode response range. (A) Aspiration of standard working bromide solutions in 1.0 mol dm^{-3} KNO_3 into a single-line manifold system via a 3.9 cm^3 min^{-1} carrier stream. Aspiration was continued until a steady-state reading was just obtained on the detector. (B) Single-line manifold FIA system with 3.9 cm^3 min^{-1} carrier stream of 1.0 mol dm^{-3} KNO_3 and a sample volume of 30 μl

The pH of soil samples can vary considerably and various contaminants that may interfere are usually found in soil. The coated tubular bromide-selective electrode was also subjected to these interferences. Interferences were evaluated by conducting a series of experiments using flow systems. However, it was clear from the experimental results that the FIA system was much less affected than the continuous sample-flow method. High levels of ammonia (>1000 mg dm^{-3}) in soil samples destroyed the electrode response rapidly, owing to the formation of soluble diammine silver complexes. It is therefore not advisable to use the electrode for the determination of bromide in freshly fertilised soil. However, the electrode performance was not influenced when the pH in the samples was changed from 2 to 12. Iodide, cyanide, sulphide and arsenate, which form silver salts more insoluble than silver bromide, interfere. However, the concentration of these interferents in soil is negligible and there was no noticeable effect on the electrode system. Chloride levels in soils varied considerably. The interference of chloride with the tubular bromide-selective electrode increased linearly with increasing chloride concentrations, in solutions containing no bromide, which confirmed the results obtained by Onken *et al.*[9] The results obtained with mixed standard solutions containing bromide and chloride are summarised in Table 1. It is clear that interference from chloride became noticeable in solutions containing less than 100 mg dm^{-3} bromide, which again confirmed the results of Onken *et al.*[9] However, applying the *t*-test to the two sets of data (Table 1) obtained from mixtures of 20–250 mg dm^{-3} bromide with 0 and 1000 mg dm^{-3} chloride showed no statistical difference between them (95% probability). This implies that only bromide concentrations lower than 20 mg dm^{-3} are affected by chloride present at up to 1000 mg dm^{-3}. A series of experiments were therefore performed to try to eliminate chloride interference. The results revealed that the incorporation of 100 mg dm^{-3} chloride in an ionic strength adjustment

Table 1. Interference studies of standard solutions containing combinations of bromide and chloride. Studies conducted with the FIA system in Fig. 1 with 1.0 mol dm^{-3} potassium nitrate as the ionic strength adjustment solution. Values given are peak heights measured in mm

Bromide concentration/ mg dm^{-3}	Chloride concentration in mixture/mg dm^{-3}					
	0	1000	500	300	150	80
250	110	110	110	110	110	110
100	95	95	94	95	94	95
60	86	88	88	88	87	87
40	76	80	80	79	80	79
20	62	68	67	68	67	66
10	45	59	55	54	54	54

Table 2. Performance and electrode response stability over a period of time. All results are the mean of triplicate determinations

	Period			
	Day 1*	Day 2	Day 7	Day 14
Concentration of injected bromide solutions/mg dm^{-3}	10	9	8	8
	40	39	38	37
	100	98	96	93
	250	248	245	241
	500	498	495	490
	1000	995	986	979
	5000	4991	4979	4968

* Calibrations standards started. Days 2, 7 and 14 refer to the response obtained on day 1 as calibration.

Table 3. Recovery of inorganic bromide in soil samples fortified with potassium bromide

	Bromide recovered							
	Sandy soil		Loamy sand soil		Sandy loam soil		Loam soil	
Bromide added/ μg g^{-1}	Mass*/ μg g^{-1}	Mass*, %	Mass*/ μg g^{-1}	Mass*, %	Mass*/ μg g^{-1}	Mass*, %	Mass*/ μg g^{-1}	Mass*, %
0	<1	—	<1	—	<1	—	<1	—
3	3.1 ± 0.05	103	3.1 ± 0.05	103	2.9 ± 0.05	97	2.8 ± 0.04	93
5	5.2 ± 0.08	104	5.1 ± 0.08	102	4.9 ± 0.07	98	4.8 ± 0.09	96
10	9.6 ± 0.13	96	9.5 ± 0.14	95	9.5 ± 0.14	95	9.4 ± 0.15	94
20	19 ± 0.25	95	19 ± 0.27	95	19 ± 0.26	95	18 ± 0.26	90
60	59 ± 0.70	98	58 ± 0.74	97	57 ± 0.72	95	56 ± 0.74	93
100	96 ± 1.2	96	97 ± 1.1	97	94 ± 1.2	94	92 ± 1.4	92
250	246 ± 2.1	98	247 ± 2.0	99	246 ± 2.0	98	244 ± 2.0	98
1000	988 ± 4.6	99	989 ± 4.4	99	979 ± 4.6	98	974 ± 4.5	97

* Average of five soil replicate samples ± standard error.

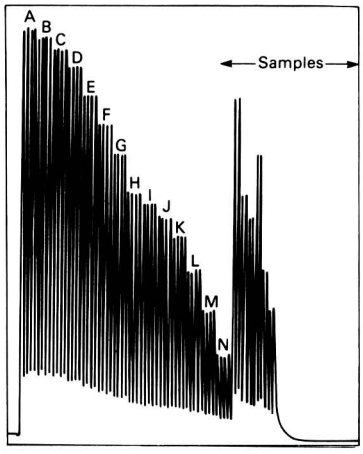

Fig. 3. Typical strip-chart recording for the determination of bromide with the FIA system of Fig. 1 and 1.0 mol dm^{-3} KNO_3 as ionic strength adjustment solution. From left to right: 5000–5 mg dm^{-3} standard bromide solutions followed by samples. Standard solutions were injected four times each; samples in duplicate. Recorder paper speed = 2 mm min^{-1}. Recorder range = 20 mV. Bromide concentrations: (A) 5000; (B) 4000; (C) 3000; (D) 2000; (E) 1000; (F) 500; (G) 250; (H) 100; (I) 80; (J) 60; (K) 40; (L) 20; (M) 10; and (N) 5 mg dm^{-3} (p.p.m.)

Table 4. Performance and reproducibility of the proposed flow injection method (FIA) for the determination of bromide in soil. Comparison of inorganic bromide concentrations (μg g^{-1}) recovered from soils using the proposed FIA method against a standard iodimetric titration method

	Bromide concentration/μg g^{-1}		
Soil sample	Titration	FIA	Coefficient of variation,* %
Sandy soil:			
1	3.0	3.1	1.59
2	9.5	9.6	1.48
3	58	59	1.27
4	247	246	0.82
5	987	988	0.43
Loamy sand soil:			
1	5.2	5.1	1.56
2	19	19	1.40
3	96	97	1.28
4	248	247	0.81
5	990	989	0.44
Sandy loam soil:			
1	2.9	2.9	1.58
2	19	19	1.41
3	56	57	1.28
4	95	94	1.09
5	247	246	0.81
Loam soil:			
1	4.7	4.8	1.57
2	9.5	9.4	1.48
3	57	56	1.28
4	245	244	0.81
5	977	974	0.44

* Mean result of 15 tests in each instance with relative standard deviation for the flow injection method.

buffer containing 1.0 mol dm^{-3} potassium nitrate gave the best results for the proposed FIA system (Fig. 1). Thus interference of chloride in bromide solutions is reduced to a level of less than 20 mg dm^{-3} bromide, where the interference of 1000 mg dm^{-3} chloride became noticeable. Inclusion of 100 mg dm^{-3} chloride in the ionic strength adjustment buffer also gave a faster response time for solutions containing 1000–5000 mg dm^{-3} of bromide.

A typical representative recorder output for the determination of bromide with a FIA system (Fig. 1) at a sampling rate of 80 determinations per hour is illustrated in Fig. 3. Determinations performed in a random order shows that carryover from one sample to another is negligible with no base-line drift experienced. It can be seen from the typical recorder output (Fig. 3) that the coated tubular solid-state bromide-selective electrode gave a very stable base line.

The performance and stability of electrode response were evaluated over a period of time (Table 2). It is clear that the response was very stable. Due to oscillations of about 1 mV per day in electrode potentials, calibration on a daily basis was necessary. An electrode stored for 10 months maintained a slope of 57–55 mV, which indicated a relatively long lifetime.

The flow injection system (Fig. 1) with an incorporated coated tubular bromide-selective electrode was also applied to the determination of bromide in soils. KNO_3 (1.0 mol dm^{-3}) containing 100 mg dm^{-3} chloride was used as the ionic strength adjustment buffer. Soil samples were fortified with potassium bromide solutions. The extracted bromide was then determined using the flow injection system. The extraction and measurement procedure gave satisfactory results for inorganic bromide determination in soil. The flow injection tubular electrode system measured over 90% of the bromide added (Table 3). The lower limit of detection was 1 mg dm^{-3}. The performance and reproducibility of the proposed flow injection potentiometric method are shown in Table 4. In addition to a high sample throughput (80 h^{-1}) over a wide

concentration range, the procedure is characterised by good reproducibility (<1.6%). Direct flow injection potentiometric measurement of bromide ion in soil gave results fairly similar to those obtained by a standard iodimetric titration method (Table 4) with thiosulphate.[22,23]

Conclusion

A coated tubular bromide-selective flow injection electrode system is suitable for the determination of extracted inorganic bromide in soils at a rate of about 80 samples per hour with a coefficient of variation of better than 1.6%. The system offers certain advantages over conventional sensor endcaps and manual methods with the elimination of chloride interference.

The author thanks the Council for Scientific and Industrial Research, Pretoria, and the University of Pretoria for financial support. He also thanks Mr. C. C. P. Wagener and Miss M. L. Aveling for assistance in performing some of the experiments.

References

1. Turner, A., *J. Sci. Food. Agric.*, 1964, **15**, 265.
2. Beckman, H., Allen, P. T., Crosby, D. G., Gauer, W. O., and Mourer, C., *J. Food. Sci.*, 1967, **32**, 595.
3. Getzendaner, M. E., Doty, A. E., McLaughlin, E. L., and Lindgren, D. L., *J. Agric. Food. Chem.*, 1968, **16**, 265.
4. LaCroix, R. L., Keeney, D. R., and Walsh, L. M., *Soil Sci. Plant Anal.*, 1970, **1**, 1.
5. Hipp, B. W., and Langdale, G. W., *Soil Sci. Plant Anal.*, 1971, **2**, 237.
6. Smart, R. St. C., Thomas, A. D., and Drover, D. P., *Soil Sci. Plant Anal.*, 1974, **5**, 1.
7. Turner, D. L., *J. Food Sci.*, 1972, **37**, 791.
8. Graf, J. E., Vaughn, T. E., and Kipp, W. H., *J. Assoc. Off. Anal. Chem.*, 1976, **59**, 53.
9. Onken, A. B., Hargrove, R. S., Wendt, C. W., and Wilke, O. C., *Soil Sci. Soc. Am. Proc.*, 1975, **39**, 1223.
10. Růžička, J., and Hansen, E. H., "Flow Injection Analysis," Wiley, Chichester, 1981.
11. "Flow Injection Analysis Bibliography," Tecator, Höganäs, Sweden, 1985.
12. Slanina, J., Lingerak, W. A., and Bakker, F., *Anal. Chim. Acta*, 1980, **117**, 91.
13. van der Linden, W. E., and Oostervink, R., *Anal. Chim. Acta*, 1978, **101**, 419.
14. Meyerhoff, M. E., and Kovach, P. M., *J. Chem. Educ.*, 1983, **60**, 766.
15. Frend, A. J., Moody, G. J., Thomas, J. D. R., and Birch, B. J., *Analyst*, 1983, **108**, 1357.
16. Mascini, M., and Palleschi, G., *Anal. Chim. Acta*, 1978, **100**, 215.
17. Alegret, S., Alonso, J., Bartroli, J., Paulis, J. M., Lima, J. L. F. C., and Machado, A. A. S. C., *Anal. Chim. Acta*, 1984, **164**, 147.
18. van Staden, J. F., *Anal. Chim. Acta*, 1986, **179**, 407.
19. van Staden, J. F., *Anal. Lett.*, 1986, **19**, 1407.
20. van Staden, J. F., *Fresenius Z. Anal. Chem.*, 1986, **325**, 247.
21. van Staden, J. F., *Analyst*, 1986, **111**, 1231.
22. Kolthoff, I. M., and Belcher, R., "Volumetric Analysis, Volume 3, Titration Methods," Interscience, New York, 1957, pp. 256.
23. Kempton, R. J., and Maw, G. A., *Ann. Appl. Biol.*, 1972, **72**, 71.

Paper A6/356
Received September 22nd, 1986
Accepted November 24th, 1986

Voltammetric Study of Copper(II) Dialkyldithiophosphates Formed by the Interaction of Dialkyldithiophosphates with Copper Salts

Miles J. Hutchings, G. J. Moody and J. D. R. Thomas*
Department of Applied Chemistry, Redwood Building, UWIST, P.O. Box 13, Cardiff CF1 3XF, UK

The *in situ* formation in organic media of copper(II) *O,O'*-dialkylphosphorodithioates [dialkyldithiophosphates (DDPs), where alkyl = 2-methylethyl (isobutyl) or 1-methylethyl (isopropyl)] can be detected voltammetrically at the mercury electrode. The results show that the electrode reactions involve irreversible, diffusion-controlled processes with adsorption phenomena featuring significantly in studies involving DDP (alkyl = isopropyl) species. From a quantitative analytical perspective, the measurement of the Cu^{II} reduction peak height may prove useful for the determination of CuDDP complexes. Voltammetric wave assignments and a scheme for the processes occurring are presented. Finally, the log(stability constant) of copper(II) - DDP (alkyl = isobutyl) is calculated to be 17.3.

Keywords: *Dialkyldithiophosphates; O,O'-dialkylphosphorodithioates; voltammetry; copper(II) dialkyldithiophosphates*

Metal dialkyldithiophosphate (*O,O'*-dialkylphosphorodithioates)(MDDPs) are added to lubricating oils to serve as antioxidants. In addition, owing to the formation of protective films on metal surfaces, they prevent the corrosive attack of oxidation products and also exhibit very useful load-carrying properties.[1] Zinc dialkyldithiophosphates (ZDDPs) have been used as lubricating oil antioxidants for many years and their inhibition of hydrocarbon autoxidation was first investigated by Kennerly and Patterson[2] in 1956. A wealth of information has since been accumulated on the mechanism of action[2-6] and on the analysis of ZDDPs.[7-21]

Other metal DDPs in addition to zinc have received attention although their performance as antioxidants is not so well documented. Copper dialkyldithiophosphates (CuDDPs) have been reported to exhibit chain-breaking, antioxidant activity in the radical initiated oxidation of a hydrocarbon such as cumene,[3] and it is proposed that this may arise owing to the participation of a copper(I) species in the inhibitory action. Recently, findings involving the antioxidant behaviour[22] and electron spin resonance spectra[23] of CuDDPs have been published, but they appear to present conflicting information with the oxidation state of the copper species in solution being a contentious issue. A voltammetric investigation of the speciation of CuDDP systems was therefore undertaken.

CuDDP formation was achieved by the following interactions:

(i) Copper(II) 9-octadecanoate (copper oleate) and zinc di(1,1-dimethylethyl)dithiophosphate (ZDDP, alkyl = isobutyl).
(ii) Copper(II) perchlorate and ZDDP (alkyl = isobutyl).
(iii) Copper(II) oleate and zinc di(1-methylethyl)dithiophosphate (ZDDP, alkyl = isopropyl).
(iv) Copper(II) perchlorate and ZDDP (alkyl = isopropyl).
(v) Copper perchlorate and NH_4DDP (alkyl = isopropyl).

Experimental

Reagents and Solutions

Either copper(II) perchlorate hexahydrate (BDH Chemicals, laboratory-reagent grade) or copper(II) oleate (a gift from Esso Chemicals, Abingdon) was used as a source of copper for the *in situ* formation of CuDDP in solution. Solvent media used were heptane (BDH Chemicals, laboratory-reagent grade), absolute ethanol (James Burrough, analytical-reagent grade) or an American Society for Testing and Materials (ASTM) solvent. The ASTM solvent consisted of propan-2-ol, toluene and water (50 + 49.5 + 0.5 *V/V*).

Solutions of ZDDP (alkyl = isobutyl), ZDDP (alkyl = isopropyl) and NH_4DDP (alkyl = isopropyl) (gifts from Esso Chemicals) were prepared in absolute ethanol. Supporting electrolyte solutions were 0.1 M sodium perchlorate (BDH Chemicals, analytical-reagent grade) in absolute ethanol.

Instrumentation

All voltammetric experiments were carried out with a PAR 174A polarographic analyser coupled to a PAR 303A static mercury dropping electrode (SMDE) assembly. Voltammograms were recorded using either a Hewlett-Packard 7040A or a Bausch and Lomb Omnigraphic 2000 *x* - *y* recorder.

Procedure

Voltammetric determinations were conducted under quiescent conditions at ambient temperature. Supporting electrolyte solutions (0.1 M; 8 cm^3) contained within the polarographic cell were purged for 8 min with oxygen-free nitrogen. Small volumes (5–50 mm^3) of concentrated analyte were then spiked into the cell using a Finnpipette and the measurements made.

For differential-pulse and d.c. polarographic experiments, a drop-time of 0.5 s and modulation amplitude of 50 mV were used throughout. Linear sweep and cyclic voltammetric experiments were carried out at a hanging mercury drop electrode (HMDE) with an area of 0.020 cm^2. Scan rates and scan ranges are indicated on the voltammograms presented. All potentials were recorded *versus* a silver - silver chloride reference system with an internal filling solution of 1 M lithium chloride dissolved in ethanol - water (1 + 1 *V/V*).

Results and Discussion

Copper(II) Oleate - ZDDP (Alkyl = Isobutyl)

This interaction was studied by differential-pulse polarography, direct-current polarography, linear sweep voltammetry and cyclic voltammetry in various solvents.

Differential-pulse polarography

Heptane solvent. Copper(II) oleate in heptane in the presence of ZDDP (alkyl = isobutyl) results in the formation of a CuDDP complex. This is apparent on examination of the

* To whom correspondence should be addressed.

Table 1. Polarographic waves arising from the interaction of copper(II) oleate and ZDDP (alkyl = isobutyl)

		Wave I		Wave II		Wave III		Wave IV	
Copper(II) oleate*/mM	ZDDP/ mM	E_p/ V	I_p/ μA	$-E_p$/ V	I_p/ μA	$-E_p$/ V	I_p/ μA	$-E_p$/ V	I_p/ μA
0.41	0.16	+0.180	0.10	0.125	0.37	0.435	0.48	0.915	0.22
0.41	0.32	+0.165	0.34	0.145	1.01	0.465	0.72	0.925	0.52

* Copper(II) oleate (0.41 mM) has a peak potential (E_p) of +0.255 V and a peak current (I_p) of 0.29 μA.

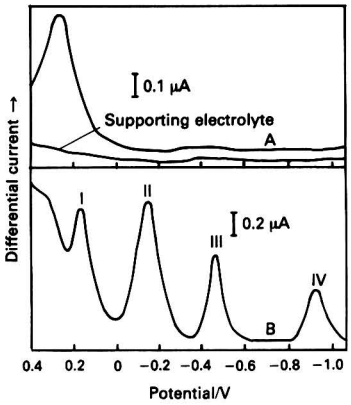

Fig. 1. Differential-pulse polarogram at the SMDE of 0.41 mM copper(II) oleate (in heptane) (A) and of 0.41 mM copper(II) oleate (in heptane) with added 0.32 mM zinc diisobutyldithiophosphate (B). Scan rate: 10 mV s^{-1}

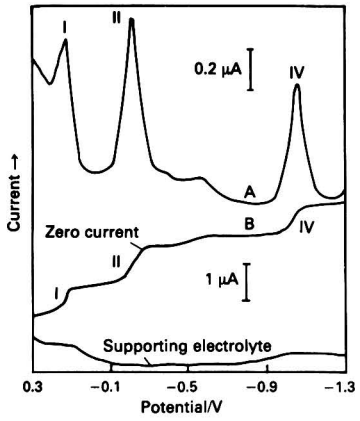

Fig. 2. (A) Differential-pulse and (B) sampled d.c. polarograms of 0.21 mM zinc diisobutyldithiophosphate (in ethanol) at the SMDE. Scan rate: 10 mV s^{-1}

polarographic profile of copper(II) oleate in both the absence and presence of ZDDP (alkyl = isobutyl) (Fig. 1). The broad peak in Fig. 1 arises from the reduction of copper(II) in copper(II) oleate to copper metal at the SMDE. On adding ZDDP (alkyl = isobutyl), a CuDDP reduction wave appears (Fig. 1, B, wave III) together with three other waves (Fig. 1, B, waves I, II and IV). The peak potentials (E_p) and peak currents (I_p) of these waves are given in Table 1.

Waves I and II may be attributed to the formation of mercury(II) complexes from interaction of the SMDE with the DDP anion. Bond *et al.*[24] have characterised these waves for

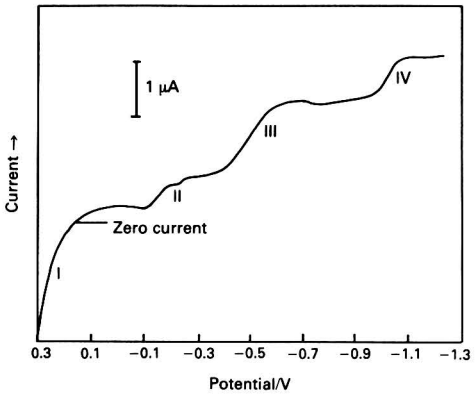

Fig. 3. Sampled d.c. polarogram of 0.79 mM copper(II) oleate (in heptane) in the presence of 0.2 mM zinc diisobutyldithiophosphate. Scan rate: 10 mV s^{-1}

studies involving NH_4DDP in acetone and proposed the following electrode processes:

$$2Hg^0 + 6DDP^- \rightleftharpoons 2Hg^{II}DDP_3^- + 4e^- \quad .. \quad (1)$$
$$2Hg^{II}DDP_3^- + Hg^0 \rightleftharpoons 3Hg^{II}DDP_2 + 2e^- \quad .. \quad (2)$$

Indeed, the sampled d.c. polarogram of ZDDP (alkyl = isobutyl) (2.1×10^{-4} M in ethanol) shows three distinct processes (Fig. 2). Waves I and II may be assigned to the oxidation processes (2) and (1), respectively. The third process (wave IV) corresponds to the reduction of Zn^{2+} to Zn^0 at the mercury electrode and the peak potential of −1.05 V *versus* silver - silver chloride for ZDDP (alkyl = isobutyl) observed here in an ethanolic medium agrees with the observations of Shafiqul Alam *et al.*[21] who noted a peak potential of −0.900 V *versus* silver - silver chloride for the differential-pulse polarographic determination of ZDDP (alkyl = isopropyl) in a medium containing 0.1 M tetraethylammonium perchlorate in dimethylformamide.

On adding copper(II) oleate to a solution of ZDDP (alkyl = isobutyl), there is interaction and wave III appears (see Fig. 1, B). After interaction, the sample d.c. polarographic trace of wave II appears as a cathodic process (Fig. 3); in the absence of copper(II) oleate it is an anodic electrode reaction. As a reversal in the electrode reaction can be explained by considering reaction (1), if DDP^- is removed by complexation with copper(II), then a cathodic process is required to redress the equilibrium. Likewise, a cathodic process would also be expected for process (2) (wave I) but this is not observed as wave I still appears anodic (Fig. 3). Bond *et al.*[24] observed a reversal in both electrode processes when $Hg^{II}DDP_2$ was added to a solution of DDP^- at the DME, and this is consistent with processes (1) and (2). The half-wave potentials of waves I and II cited[24] are +0.14 and −0.121 V *versus* silver - silver chloride for 5×10^{-4} M NH_4DDP (alkyl = ethyl). Peak potentials of waves I and II for ZDDP (alkyl = isobutyl) (2×10^{-4} M) in this study occurred at +0.16 and −0.14 V, respectively, *versus* silver - silver chloride. These

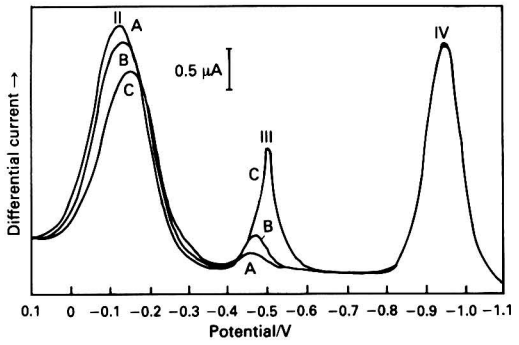

Fig. 4. Differential-pulse polarograms of copper(II) oleate (in heptane) (A = 0.14, B = 0.28 and C = 0.75 mM) in the presence of 0.79 mM zinc diisobutyldithiophosphate at the SMDE. Scan rate: 10 mV s^{-1}

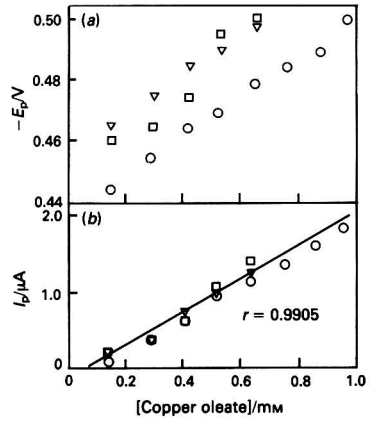

Fig. 5. Graph of (*a*) peak potential and (*b*) peak current *versus* concentration of copper(II) oleate (in heptane) at constant concentration of zinc diisobutyldithiophosphate (0.79 mM) for wave III in differential-pulse polarography. Scan rate: 10 mV s^{-1}. ○, □ and ▽ represent separate experiments

Table 2. Parameters for waves II and III for different concentrations of copper(II) oleate in the presence of 0.79 mM ZDDP (alkyl = isobutyl

	Wave II			Wave III		
Copper(II) oleate/mM	$-E_p$/ V	I_p/ μA	$W_{\frac{1}{2}}$/ mV	$-E_p$/ V	I_p/ μA	$W_{\frac{1}{2}}$/ mV
0.14	0.090	2.20	172	0.445	0.175	72
0.28	0.102	2.05	176	0.555	0.425	72
0.41	0.112	1.93	179	0.465	0.675	70
0.52	0.119	1.82	182	0.470	1.000	64
0.64	0.125	1.63	180	0.480	1.200	62
0.75	0.130	1.59	182	0.485	1.350	64
0.86	0.133	1.55	176	0.490	1.600	60
0.95	0.138	1.52	176	0.500	1.800	58
—	0.092	2.85	156	—	—	—
0.14	0.105	2.75	160	0.460	0.200	76
0.28	0.120	2.62	156	0.465	0.425	72
0.41	0.128	2.35	165	0.475	0.675	69
0.52	0.135	2.31	160	0.495	1.050	60
0.64	0.142	2.20	158	0.500	1.400	59
—	0.132	2.33	128	—	—	—
0.14	0.140	2.30	136	0.465	0.200	72
0.28	0.145	2.15	152	0.475	0.425	70
0.41	0.148	1.97	140	0.485	0.775	66
0.52	0.151	1.82	144	0.490	1.030	64
0.64	0.155	1.62	160	0.499	1.250	60

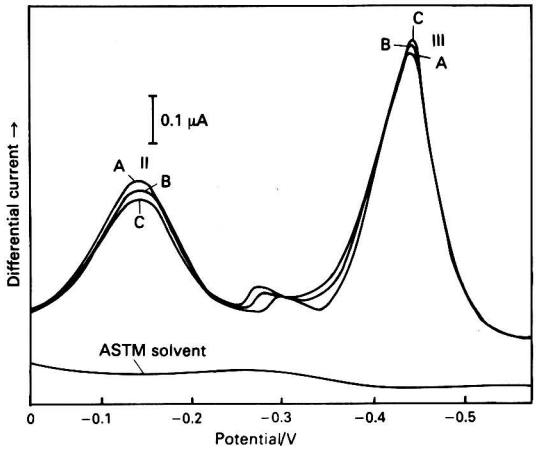

Fig. 6. Time-dependent differential-pulse polarograms of 0.69 mM copper(II) oleate (in ASTM solvent) in the presence of 0.14 mM zinc diisobutyldithiophosphate. A, B and C were run at 7-min intervals. Scan rate: 10 mV s^{-1}

observations are in good agreement considering the different supporting media employed, namely acetone and ethanol.

It is wave III that is ascribed to the formation of the CuDDP complex and is of importance in this work. Fig. 4 shows the differential-pulse polarographic profiles corresponding to increasing concentrations of copper(II) oleate (dissolved in heptane) interacting with ZDDP (alkyl = isobutyl) (0.79 mM) in an ethanolic medium. Table 2 lists the values of peak potentials (E_p), peak currents (I_p) and peak widths at half-peak height ($W_{\frac{1}{2}}$) obtained from the mean of three experiments involving copper(II) oleate (dissolved in heptane) and ZDDP (alkyl = isobutyl) (0.79 mM). The variations of E_p and I_p with the concentration of copper(II) oleate are represented graphically in Fig. 5(*a*) and (*b*), respectively. It is obvious from these graphs that the peak height of wave III is more reproducible than the peak potential for the copper(II) oleate - ZDDP (alkyl = isobutyl) system. It follows, therefore, that whereas the measurement of peak heights may have analytical implications, peak potentials cannot be used for quantification.

ASTM solvent. Experiments were also conducted with copper(II) oleate dissolved in ASTM solvent. The results differ in one major respect from those involving heptane in so far as a time dependence of waves II and III is encountered (Fig. 6). With successive scanning, the peak height of wave II decreases whereas that of wave III shows a definite increase. The visible absorption band, attributed to $Cu^{II}DDP$,[25] centred at 418 nm for this interaction also shows a time dependence and increases with time suggesting that wave III is due to the reduction of a copper(II) species and the concentration of this species increases with time. It is not until after *ca.* 150 min that equilibrium is reached, giving a constant absorbance (λ = 418 nm) of $Cu^{II}DDP$ (Fig. 7).

Direct-current polarography

The d.c. polarographic behaviour of 0.69 mM copper(II) oleate (dissolved in heptane) in the presence of ZDDP (alkyl = isobutyl) (0.14 mM) is illustrated in Fig. 8 together with the differential-pulse polarogram for comparison. From an analysis of the d.c. polarograms, it is possible to ascertain values of

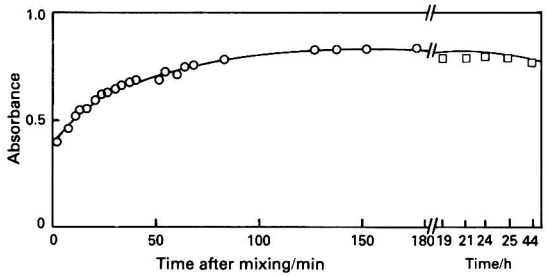

Fig. 7. Variation of spectral absorbance ($\lambda_{max.}$ at 418 nm) with time for copper(II) oleate (in ASTM solvent) in the presence of zinc diisobutyldithiophosphate

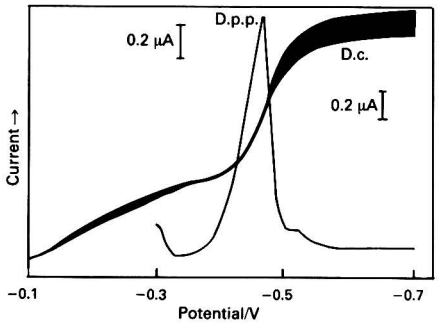

Fig. 8. Differential-pulse and d.c. polarograms of 0.69 mM copper(II) oleate (in heptane) in the presence of 0.14 mM zinc diisobutyldithiophosphate. Scan rate: 10 mV s^{-1}

Table 3. D.c. polarographic data for copper(II) oleate (0.69 mM) in the presence of ZDDP (alkyl = isobutyl) (0.14 mM)

Solvent	Half-wave potential/ V (= $E_{\frac{1}{4}}$)	Limiting current/ μA (= I_L)	αn_a*	αn_a†
Heptane ..	−0.464	0.88	0.86	0.88
ASTM ..	−0.477	0.93	0.94	0.98

* αn_a determined from graphs of log $(I_d - I)/I$.
† αn_a determined from $|E_{\frac{3}{4}} - E_{\frac{1}{4}}| = 51.7/\alpha n_a$ mV.

the half-wave potential ($E_{\frac{1}{4}}$) and the product (αn_a) of the transfer coefficient (α) and the rate-determining number of electrons (n_a). The results for copper(II) oleate (0.69 mM) dissolved in heptane and ASTM solvent in the presence of ZDDP (alkyl = isobutyl) (0.14 mM) are shown in Table 3.

Heptane solvent studies

Linear sweep voltammetry. Linear sweep voltammograms of 0.69 mM copper(II) oleate (dissolved in heptane) in the presence of ZDDP (alkyl = isobutyl) (0.14 mM) are illustrated in Fig. 9 at three different scan rates. Table 4 lists the peak potentials (E_p) and peak current (I_p) values for these experiments together with values of αn_a.

$I_p/V^{\frac{1}{2}}$ exhibits a certain degree of constancy, whereas I_p/V values vary considerably over the scan ranges used (Table 4). It is therefore possible to infer that the reduction process giving rise to wave III is diffusion controlled and a negative shift of E_p with scan rate is diagnostic of an irreversible process.[26] Consequently, the electrode process can be explained by the equation for an irreversible electrode reaction at a HMDE.[27]

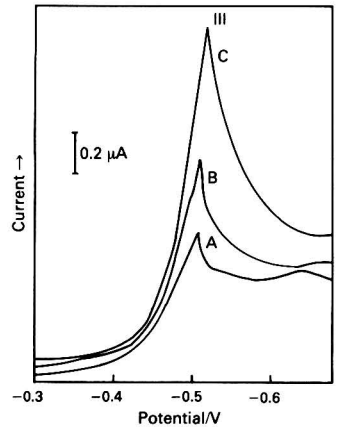

Fig. 9. Linear sweep voltammogram of 0.69 mM copper(II) oleate (in heptane) in the presence of 0.14 mM zinc diisobutyldithiophosphate at the HMDE (area 0.020 cm^2) at scan rates of 10, 20 and 50 mV s^{-1} for A, B and C, respectively

Table 4. Linear sweep voltammetric data for copper(II) oleate (0.69 mM) in the presence of ZDDP (alkyl = isobutyl) (0.14 mM)

Scan rate/ mV s^{-1}	$-E_p$/V	I_p/μA	$\lvert E_p - E_{p/2}\rvert$/ mV	αn_a*	$I_p/V^{\frac{1}{2}}$†/ μA $V^{-\frac{1}{2}} s^{\frac{1}{2}}$	I_p/V/ μA V^{-1} s
10	0.504	0.55	37	1.29	5.5	55.0
20	0.513	0.91	53	0.90	6.4	45.5
50	0.518	1.54	39	1.22	6.4	30.8
100	0.525	1.65	40	1.19	5.2	16.5

* αn_a determined from $|E_p - E_{p/2}| = 47.7/\alpha n_a$ mV.
† Mean $I_p/V^{\frac{1}{2}} = 6.0$; $s = 0.78$; CV = 13.1%.

Cyclic voltammetry. The cyclic voltammetric profile of 0.69 mM copper(II) oleate (dissolved in heptane) in the presence of ZDDP (alkyl = isobutyl) (0.14 mM) is shown in Fig. 10. The forward scan involves the electrochemical reduction of the CuDDP complex and the reverse scan is the oxidation profile where the oxidation of Cu^0 to Cu^{2+} occurs. The difference between the anodic and cathodic peak potentials ($E_{pa} - E_{pc}$) is 53 mV and the ratio of the cathodic and anodic peak currents (I_{pc}/I_{pa}) is 1.4. These values confirm the linear sweep observations that the electrode process is irreversible.

ASTM solvent studies

The stationary electrode behaviour of copper(II) oleate dissolved in ASTM solvent differs from that for heptane as solvent in so far as an additional reduction wave is observed at potentials more negative than the main CuDDP reduction profile [Fig. 11(A–C)]. From Fig. 11 (A–C), it is evident that the postwave IIIa becomes more pronounced with increasing scan rate. Also, if the linear sweep voltammetric experiment is delayed, wave IIIa intensifies and becomes larger than the CuDDP reduction wave III [Fig. 11 (a–c)]. These observations are consistent with a process involving adsorption of an electroactive species, as at larger scan rates adsorption waves develop more than the associated diffusion controlled waves.[28] Increasing the delay time (t_d) before carrying out the voltammetric scan has the effect of enabling more of the electroactive substance to become adsorbed at the mercury surface and therefore produce a large peak current.[29] The cyclic voltammogram of the above system (Fig. 12) possesses a similar oxidation profile to that already discussed for studies involving copper(II) oleate dissolved in heptane. Also, as encountered with the linear sweep experiments, the presence of an adsorption peak is obvious (Fig. 12, wave IIIa).

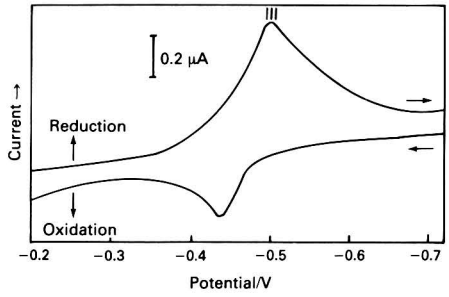

Fig. 10. Cyclic voltammogram of 0.69 mM copper(II) oleate (in heptane) in the presence of 0.14 mM zinc diisobutyldithiophosphate at the HMDE (area 0.020 cm^2). Scan rate: 10 mV s^{-1}

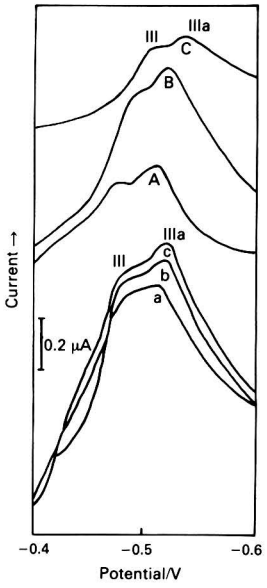

Fig. 11. Linear sweep voltammograms of 0.69 mM copper(II) oleate (in ASTM solvent) in the presence of 0.14 mM zinc diisobutyldithiophosphate. Scan rates of 20, 50 and 100 mV s^{-1} for A, B and C, respectively; scan rate of 100 mV s^{-1} for delay times of 5, 20 and 35 s for a, b and c, respectively

Copper(II) Perchlorate - ZDDP (Alkyl = Isobutyl)

The polarographic and stationary electrode behaviour pattern of copper(II) perchlorate complexing with ZDDP (alkyl = isobutyl) is, as expected, very similar to the interaction discussed above for copper(II) oleate. The characteristics of the CuDDP reduction wave for both studies are in good agreement and comparisons of peak potential (E_p), peak current (I_p) and peak width at half-peak height ($W_{\frac{1}{2}}$) for (*i*) 0.14 mM copper(II) perchlorate - 0.78 mM ZDDP (alkyl = isobutyl) and (*ii*) 0.14 mM copper(II) oleate (heptane) - 0.79 mM ZDDP (alkyl = isobutyl) are as follows: (*i*) copper(II) perchlorate: $E_p = -0.452$ V; $I_p = 0.15$ μA; $W_{\frac{1}{2}} = 62$ mV; (*ii*) copper(II) oleate: $E_p = -0.460$ V; $I_p = 0.20$ μA; $W_{\frac{1}{2}} = 72$ mV.

Copper(II) Oleate - ZDDP (Alkyl = Isopropyl)

Polarography

The major difference between the voltammetric response of interaction between copper(II) oleate and ZDDP (alkyl = isopropyl) as opposed to interaction with ZDDP (alkyl = isobutyl) is the presence of adsorbed species. Both ZDDP (alkyl = isopropyl) and the CuDDP complex formed from the interaction possess adsorption post-peaks (Fig. 13) and these have been designated waves IIa and IIIa. Bond *et al.*[24] also observed such an adsorption - desorption process for NH_4DDP (alkyl = ethyl) at the DME and attributed the adsorption wave to a Hg^{II}DDP species.

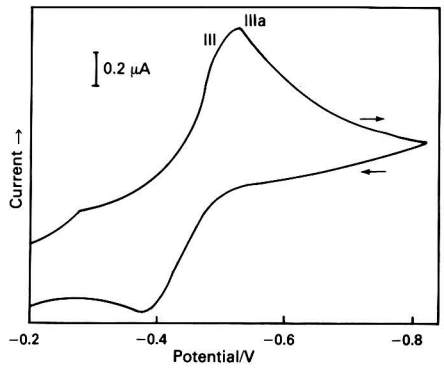

Fig. 12. Cyclic voltammogram of 0.69 mM copper(II) oleate (in ASTM solvent) in the presence of 0.14 mM diisobutyldithiophosphate at the HMDE (area 0.020 cm^2). Scan rate: 50 mV s^{-1}

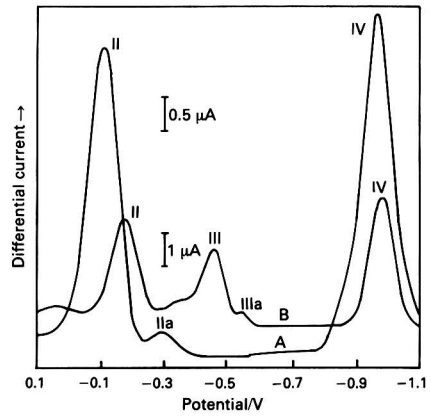

Fig. 13. Differential-pulse polarograms of 0.50 mM zinc diisopropyldithiophosphate (A) and 0.42 mM copper(II) oleate (in heptane) in the presence of 0.33 mM zinc diisopropyldithiophosphate (B) at the SMDE. Scan rate: 10 mV s^{-1}

Linear sweep voltammetry

Linear sweep profiles of the copper(II) oleate - ZDDP (alkyl = isopropyl) interaction clearly show the adsorption phenomena mentioned above. With reference to Fig. 14, for 0.14 mM copper(II) oleate, two principal reduction waves are observed (waves IIa and IIIa). These can be ascribed to the adsorption of Hg^{II}DDP (IIa) and CuDDP (IIIa) complexes. The fact that the peaks are symmetrical about the peak potential (E_p) suggests that they are adsorption waves[30] and a time dependence is also characteristic of adsorption.[29] At this low concentration of copper(II) oleate, an increase in the delay time results in an increase in the adsorption wave IIa and a decrease in the adsorption profile of wave IIIa. These observations can be explained in terms of the adsorbed Hg^{II}DDP species displacing the adsorbed CuDDP complex from the surface of the mercury electrode.

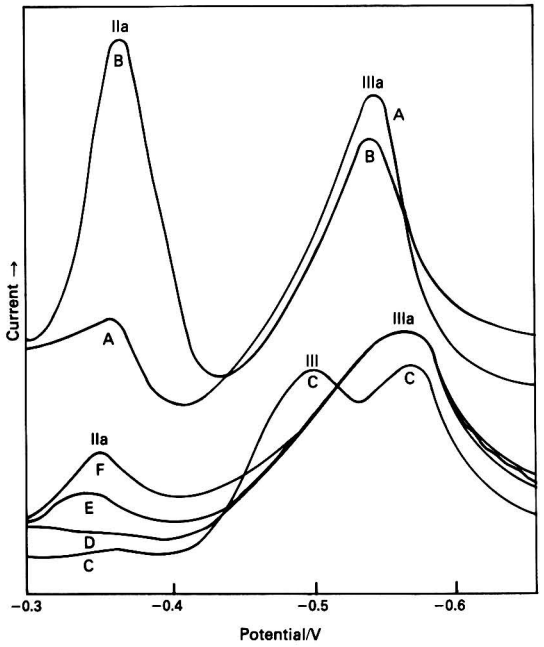

Fig. 14. Linear sweep voltammograms of copper(II) oleate (in heptane) in the presence of zinc diisopropyldithiophosphate at the HMDE (area 0.020 cm^2) at different delay times. Upper traces: [Cu^{II} oleate] = 0.14 mM, [ZDDP] = 0.44 mM, delay times of 14 and 16 s, respectively, for A and B. Lower traces: [Cu^{II} oleate] = 0.42 mM, [ZDDP] = 0.33 mM, delay times of 10, 31, 60 and 92 s, respectively, for C, D, E and F. Scan rate: 100 mV s^{-1}

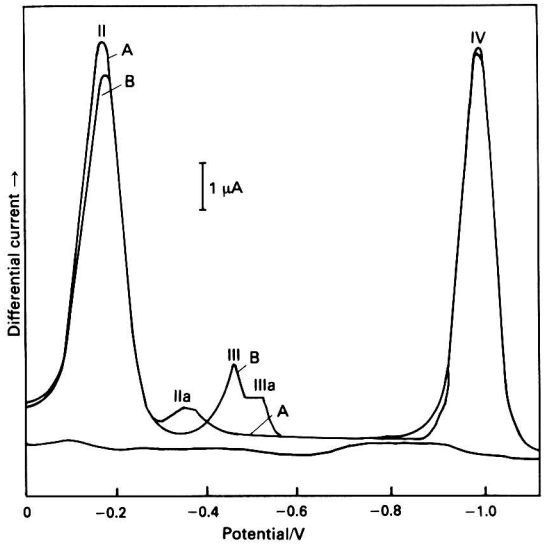

Fig. 15. Differential-pulse polarograms of 0.79 mM zinc diisopropyldithiophosphate (A) and 0.14 mM copper(II) perchlorate (in ethanol) in the presence of 0.79 mM zinc diisopropyldithiophosphate (B) at the SMDE. Scan rate: 10 mV s^{-1}

An increase in copper(II) oleate concentration to 0.42 mM yields the unadsorbed CuDDP reduction wave III (Fig. 14). Both adsorption waves IIa ($E_p \approx -0.35$ V) and IIIa ($E_p \approx -0.53$ V) occur at more negative potentials than the waves attributed to the reduction of their bulk species, II ($E_p \approx 0.25$ V) and III ($E_p \approx 0.48$ V). This is indicative of the reactant, and not the product, being involved in the adsorption electrode reaction in both instances.[28]

The peak potential separation between the adsorbed wave IIIa and the main unadsorbed profile (wave III) for the CuDDP complex is *ca.* 65 mV. For the studies involving ZDDP (alkyl = isobutyl) and copper(II) oleate dissolved in ASTM solvent, this difference is only *ca.* 35 mV [Fig. 11(A–C)]. The peak separation is related to the free energy of adsorption of the complex, that is, the greater the free energy of adsorption, the stronger the adsorption of the reactant at the mercury surface. More energy is required in the form of electrical energy to effect reduction, resulting in a peak potential separation that increases with increasing extent of adsorption.[28] It therefore follows from this study that the adsorption of CuDDP (alkyl = isopropyl) is stronger than that of CuDDP (alkyl = isobutyl) at the mercury electrode.

Copper(II) Perchlorate - ZDDP (Alkyl = Isopropyl)

This interaction is predictably similar to that of copper(II) oleate and ZDDP (alkyl = isopropyl) with the same type of differential-pulse polarographic and linear sweep voltammetric waves being evident in both instances (Figs. 15 and 16). Notably, it is again apparent that the use of ZDDP (alkyl = isopropyl) as a complexing agent results in adsorbed species contributing significantly to the electrode processes taking place in solution.

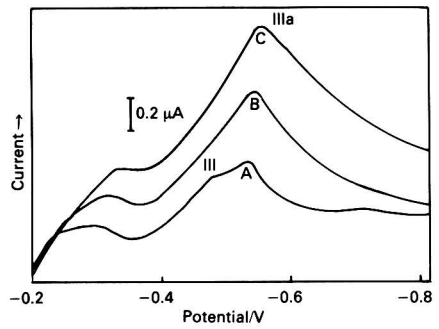

Fig. 16. Linear sweep voltammograms of 0.14 mM copper(II) perchlorate (in ethanol) in the presence of 0.79 mM zinc diisopropyldithiophosphate at the HMDE (area = 0.020 cm^2) at scan rates of 20, 50 and 100 mV s^{-1}, respectively, for A, B and C

Copper(II) Perchlorate - NH_4DDP (Alkyl = Isopropyl)

The addition of copper(II) perchlorate (0.1 mM) to NH_4DDP (alkyl = isopropyl) (0.42 mM) results in the formation of a CuDDP complex and this yields a differential-pulse polarographic wave III in the range previously encountered for the formation of CuDDP involving ZDDP, namely, between −0.45 and −0.50 V (Fig. 17). Again, adsorption post-peaks manifest themselves when the stationary electrode voltammetric behaviour of the interaction is investigated (Fig. 18).

Oxidation State of Copper

With regard to the oxidation state of copper following the various interactions and undergoing reduction, the electron spin resonance signals for the *in situ* formation of CuDDP (Fig. 19) closely resembles that reported by Shopov and Yordanov[31] who studied a range of Cu^{II}DDPs.

The formation of a Cu^{I}DDP complex would be expected to produce a "splitting" of the polarographic waves reminiscent of the polarographic studies[32,33] where stabilisation of the

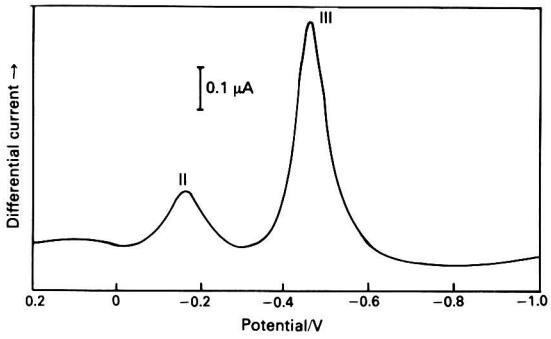

Fig. 17. Differential-pulse polarogram of 0.10 mM copper(II) perchlorate (in ethanol) in the presence of 0.42 mM ammonium diisopropyldithiophosphate at the SMDE. Scan rate: 10 mV s^{-1}

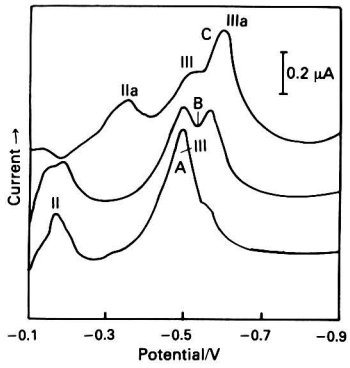

Fig. 18. Linear sweep voltammograms of 0.1 mM copper(II) perchlorate (in ethanol) in the presence of 0.42 mM ammonium diisopropyldithiophosphate at the HMDE (area 0.020 cm^2) at delay times of 30, 180 and 1200 s, respectively, for A, B and C. Scan rate: 50 mV s^{-1}

copper(I) oxidation state occurs. No corresponding behaviour has been encountered in the CuDDP interactions reported here, suggesting that under the conditions imposed the existence of $Cu^{I}DDP$ in quantifiable amounts is unlikely.

Conclusion

Electrode Processes and Wave Assignments

The voltammetry of $Cu^{II}DDP$ complexes formed *in situ* can be represented by the following scheme:

$$Cu^{2+} \rightleftharpoons Cu^{II}DDP_2 + 2e \rightleftharpoons Cu^0 + 2DDP^- \quad \text{(wave III)}$$
$$+$$
$$2Hg^0 + 6DDP^- \rightleftharpoons 2Hg^{II}DDP_3^- + 4e^- \quad \text{(wave II)}$$
$$2Hg^{II}DDP_3^- + Hg^0 \rightleftharpoons 3Hg^{II}DDP_2 + 2e^- \quad \text{(wave I)}$$

In addition to the above three waves, there is a further reduction process when ZDDP is present, due to the reduction of zinc to zinc metal (wave IV). Adsorption waves for $Cu^{II}DDP$ and $Hg^{II}DDP$ are also observed when either ZDDP (alkyl = isopropyl) or NH_4DDP (alkyl = isopropyl) are present and these waves have been designated IIIa and IIa, respectively. The CuDDP (alkyl = isobutyl) complexes do not exhibit adsorption characteristics except when ASTM solvent is used.

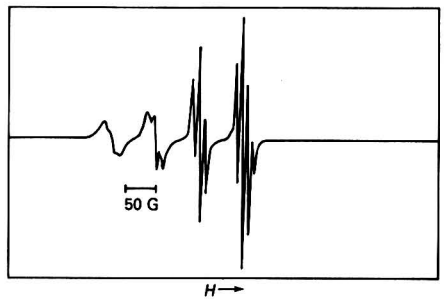

Fig. 19. Electron spin resonance spectrum of 0.98 mM copper(II) perchlorate (in ethanol) in the presence of 1.2 mM zinc diisopropyldithiophosphate

Table 5. Differential-pulse polarographic peak potentials for $Cu^{II}DDP$ complex formed *in situ*

	Wave assignment					
	I	II	IIa	III	IIIa	IV
E_p/V	+0.16	−0.14	−0.30	−0.45	−0.50	−1.00

The observed differential-pulse peak potentials (E_p) for the interactions discussed are summarised in Table 5 for convenience.

Stability Constant Determination

The data contained in Table 3 and Subrahmanya's[34] equation enable the stability constant of $Cu^{II}DDP$ to be determined This approach yields a value of 17.3 for log(stability constant), which agrees with the literature[35] value of 17.4. However, Subrahmanya's equation is rigorously applicable only when αn_a remains constant for the irreversible reduction of the complexed metal ion. A decrease in αn_a with increasing concentration of the CuDDP complex has been encountered in these studies; hence, the value of 17.3 should be seen in this light.

The Science and Engineering Research Council is thanked for a research studentship (to M. J. H.) within its CASE scheme in association with Esso Chemicals, Abingdon, Oxon. Dr. Lynne Griffiths, Dr. T. Colclough and Dr. J. Marsh of Esso Chemicals are thanked for their enthusiastic encouragement and many helpful suggestions. Also, Professor J. E. Simao of the Univeridade do Minho, Portugal, is thanked for discussions on voltammetric assignments made possible by NATO Grant No. 84/0069.

References

1. Ford, J. F., *J. Inst. Petrol., London*, 1968, **54**, 535.
2. Kennerly, G. W., and Patterson, W. L., *Ind. Eng. Chem.*, 1956, **48**, 1917.
3. Burn, A. J., *Tetrahedron*, 1966, **22**, 2153.
4. Burn, A. J., *in* Mayor, F. R., *Editor*, "Oxidation of Organic Compounds," Volume I, American Chemical Society, Washington, DC, 1968, p. 323.
5. Colclough, T., and Cunneen, J. I., *J. Chem. Soc.*, 1964, 4799.
6. Bridgewater, A. J., Dever, J. R., and Sexton, M. D., *J. Chem. Soc., Perkin Trans. 2*, 1980, 1006.
7. Kendall, P. F., and Rimmer, A., *Chem. Ind. (London)*, 1962, **43**, 1864.
8. Lewkowitsch, P. R. E., *Chem. Ind. (London)*, 1962, **27**, 1214.
9. Jenkins, G. I., and Humphreys, C. M. A., *J. Inst. Petrol., London*, 1965, **51**, 493.

10. Fodor, G. E., and Newman, F. M., *ASLE Trans.*, 1977, **22**, 389.
11. Perry, S. G., *J. Gas Chromatogr.*, 1964, **2**, 93.
12. Legate, C. E., and Burnham, H. D., *Anal. Chem.*, 1960, **32**, 1042.
13. Butlin, A. G., and Lynes, A., *in* Hodges, D. R., *Editor*, "Recent Analytical Developments in the Petroleum Industry," Applied Science, Barking, 1974, p. 283.
14. Coates, J. P., *J. Inst. Petrol., London*, 1971, **57**, 209.
15. Killer, F. C. A., and Amos, R., *J. Inst. Petrol., London*, 1966, **52**, 515.
16. Brook, A. J. W., Davies, J. E., and King, B. M. J., *in* Hodges, D. R., *Editor*, "Recent Analytical Developments in the Petroleum Industry," Applied Science, Barking, 1974, p. 97.
17. Lamotte, A., and Auvray, J., *J. Chromatogr.*, 1974, **97**, 213.
18. Leighton, D., Moody, G. J., and Thomas, J. D. R., *Analyst*, 1974, **99**, 442.
19. Jamson, B., and Hillman, D. E., *J. Chromatogr.*, 1978, **150**, 499.
20. Płaza, S., *Analyst*, 1984, **109**, 1313.
21. Shafiqul Alam, A. M., Martin, J. M., and Kapsa, Ph., *Anal. Chim. Acta*, 1979, **107**, 391.
22. Sexton, M. D., *J. Chem. Soc., Perkin Trans. 2*, 1984, 1771.
23. Yordanov, N. D., Alexiev, V., Macicek, J., Glowiak, T., and Russell, D. R., *Transition Met. Chem.*, 1983, **8**, 257.
24. Bond, A. M., Casey, A. T., and Thackeray, J. R., *J. Electrochem. Soc.*, 1973, **120**, 1502.
25. Rudzinski, W., and Fernando, Q., *Anal. Chem.*, 1978, **50**, 472.
26. Bard, A. J., and Faulkner, L. R., "Electrochemical Methods," Wiley, New York, 1980, p. 219.
27. Nicholson, R. S., and Shain, I., *Anal. Chem.*, 1964, **36**, 706.
28. Wopschall, R., and Shain, I., *Anal. Chem.*, 1967, **39**, 1515.
29. Webber, A., Shah, M., and Osteryoung, J., *Anal. Chim. Acta*, 1984, **154**, 105.
30. Bond, A. M., "Modern Polarographic Methods in Analytical Chemistry," Marcel Dekker, New York, 1980, p. 193.
31. Shopov, D., and Yordanov, N. D., *Inorg. Chem.*, 1970, **9**, 1943.
32. von Stackelberg, M., and von Freyhold, H., *Z. Electrochem.*, 1940, **46**, 120.
33. Clark, G. C. F., Moody, G. J., and Thomas, J. D. R., *Anal. Chim. Acta*, 1978, **98**, 215.
34. Subrahmanya, R. S., "Advances in Polarography," Pergamon Press, Oxford, 1960, p. 674.
35. Toropova, V. F., Cherkasov, R. A., Savel'eva, N. I., Gorshkova, V. N., and Pudovik, A. N., *Zh. Obshch. Khim.*, 1971, **41**, 1469.

Paper A6/400
Received October 22nd, 1986
Accepted November 26th, 1986

Voltammetry of Copper(I) *O,O'*-Di(1-methylethyl)phosphorodithioate

Miles J. Hutchings, G. J. Moody and J. D. R. Thomas*
Department of Applied Chemistry, Redwood Building, UWIST, P.O. Box 13, Cardiff CF1 3XF, UK

The reduction of copper(I) - diisopropyldithiophosphate [dialkyldithiophosphate (DDP), alkyl = isopropyl] in an ethanolic medium gives rise to well defined polarographic waves. In the differential mode the polarographic wave divides when the concentration of Cu^{I}DDP (alkyl = isopropyl) is between 0.3 and 0.4 mM. Limiting current data obtained in the d.c. polarographic mode suggest that the oxidation state of the copper species undergoing reduction is common before and after the division occurs and ESR studies confirm that it is a copper(II) species that is present in solution. Stationary electrode voltammetric observations show that the electrode process occurring is electrochemically irreversible and diffusion controlled. In addition, at long delay times (>60 s), an adsorbed species manifests itself and this can be attributed to the adsorption of a mercury(II) - DDP complex formed from the interaction of mercury metal with the dialkyldithiophosphate ligand.

From an analytical standpoint, the differential polarographic currents are linearly related to the Cu^{I}DDP (alkyl = isopropyl) concentration between 0.07 and 1.0 mM with an inflection to higher slope occurring at 0.4 mM.

Keywords: *Voltammetry; diisopropyldithiophosphate; copper(I) dialkyldithiophosphates;* O,O'*-dialkylphosphorodithioates*

The use of metal *O,O'*-dialkylphosphorodithioates, commonly known as dialkyldithiophosphates (MDDPs), as antioxidants and the reasons for adopting an investigative voltammetric approach have been discussed in a project[1] detailing the *in situ* formation of copper dialkyldithiophosphate complexes. The aim of this paper is to present and discuss voltammetric observations for the direct analysis of copper *O,O'*-di(1-methylethyl)phosphorodithioate, that is, copper(I) diisopropyldithiophosphate [Cu^{I}DDP, alkyl = isopropyl] in an ethanolic medium.

Experimental

Reagents and Solutions

Solutions of copper(I) di(1-methylethyl)dithiophosphate [Cu^{I}DDP, alkyl = isopropyl] (a gift from Esso Chemicals, Abingdon) were prepared using absolute ethanol (James Burrough analytical-reagent grade) as were supporting electrolyte solutions of either lithium nitrate (Fluka, purum) or sodium perchlorate (BDH Chemicals, AnalaR grade).

The PAR 174A polarographic and associated instrumentation and procedures used are as described previously[1] with a drop time of 0.5 s and a modulation amplitude of 50 mV.

Results and Discussion

Differential-pulse polarography, d.c. polarography and cyclic voltammetry were used to investigate Cu^{I}DDP (alkyl = isopropyl) in solution at the mercury electrode. From an electrochemical and speciation perspective, it is the reduction of copper in the complex to copper metal that is of interest, and it is this process that is featured in the following discussion. The electrochemistry of the DDP ligand is briefly mentioned but this has been discussed more extensively elsewhere[1] in studies involving interactions between DDPs and copper salts.

Differential-pulse Polarography

Fig. 1 shows differential-pulse polarograms of Cu^{I}DDP (alkyl = isopropyl) in a supporting electrolyte medium of 0.1 M

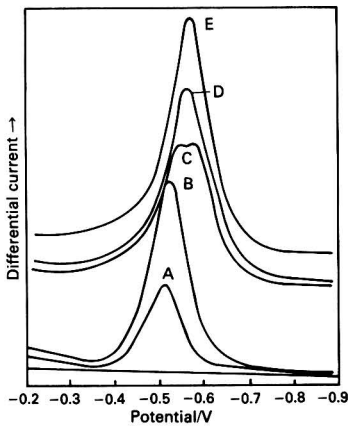

Fig. 1. Differential-pulse polarograms of copper(I) diisopropyldithiophosphate at the static mercury drop electrode (SMDE), showing effect of concentration. [Cu^{I}DDP] = 0.054, 0.11, 0.38, 0.54 and 0.65 mM, respectively, for A, B, C, D and E. Scan rate, 10 mV s^{-1}; supporting electrolyte, 0.1 M lithium nitrate in ethanol

Table 1. Differential-pulse polarographic data for Cu^{I}DDP (alkyl = isopropyl) in ethanol at the SMDE

Concentration of Cu^{I}DDP/mM	$-E_p$*/V	I_p†/μA	$-E_p$†/V	I_p†/μA	$W_{\frac{1}{2}}$/mV
0.054	0.512	0.175			92
0.110	0.526	0.385			96
0.160	0.540	0.635			106
0.220	0.555	0.780	—	S‡	—
0.270	0.565	0.950	—	S‡	—
0.380	0.585	1.130	0.525	1.110	—
0.430	0.575	1.410	0.545	1.430	—
0.540	—	S‡	0.560	1.930	—
0.650			0.575	2.400	108
0.750			0.592	3.130	108
0.860			0.599	3.680	105
0.970			0.608	4.550	104

* Profiles observed at low concentrations (original).
† Profiles observed at high concentrations (new).
‡ S = shoulder.

* To whom correspondence should be addressed.

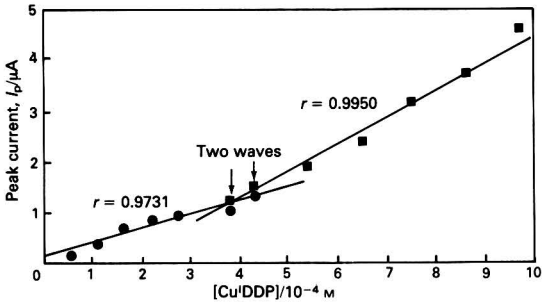

Fig. 2. Plot of differential-pulse polarographic peak current *versus* concentration of copper(I) diisopropyldithiophosphate. Scan rate, 10 mV s^{-1}; supporting electrolyte, 0.1 M lithium nitrate in ethanol. ●, Before splitting; ■, after splitting

Table 2. D.c. polarographic data for Cu^{I}DDP (alkyl = isopropyl) in ethanol at the SMDE

[Cu^{I}DDP]/ mM (= C)	$-E_p$/V	I_L/μA	$\lvert E_{\frac{1}{4}} - E_{\frac{3}{4}}\rvert$/ mV	α_a*	α_a†	I_L/C‡/μA l mmol^{-1}
0.054	0.532	0.37	98	0.56	0.53	6.9
0.110	0.546	0.68	74	0.65	0.70	6.2
0.160	0.558	1.35	76	0.70	0.68	8.4
0.220	0.563	1.70	74	0.68	0.70	7.7
0.650	0.591	4.05	90	0.66	0.57	6.2
0.750	0.593	4.65	72	0.70	0.72	6.2
0.860	0.607	5.75	70	0.72	0.74	6.7
0.970	0.617	7.20	70	0.77	0.74	7.4

* αn_a, determined from log $(I_d - I)/I$ *vs.* E data of Fig. 3.
† αn_a, determined from $\lvert E_{\frac{3}{4}} - E_{\frac{1}{4}}\rvert = 51.7/\alpha n_a$ mV.
‡ I_L/C: $\bar{x} = 7.0$; $s = 0.81$; CV = 11.6%.

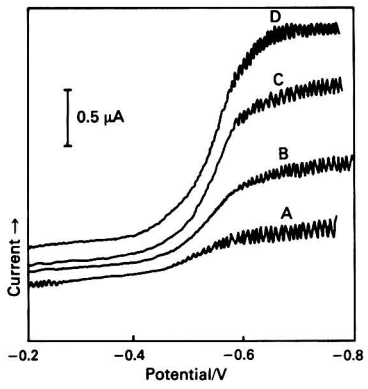

Fig. 3. D.c. polarograms of copper(I) diisopropyldithiophosphate of concentrations 0.05, 0.11, 0.16 and 0.22 mM, respectively, for A, B, C and D. Scan rate, 10 mV s^{-1}; supporting electrolyte, 0.1 M sodium perchlorate in ethanol

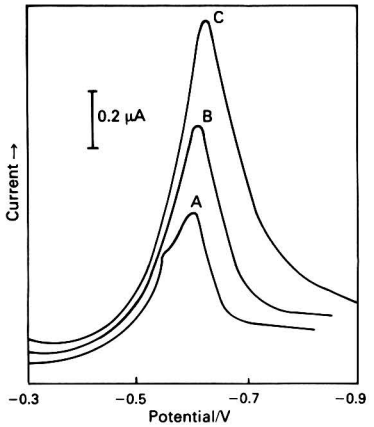

Fig. 4. Linear sweep voltammograms of 0.11 mM copper(I) diisopropyldithiophosphate at the HMDE (area 0.020 cm^2) at scan rates of 50, 100 and 200 mV s^{-1} for A, B and C, respectively. Supporting electrolyte: 0.1 M sodium perchlorate in ethanol

lithium nitrate dissolved in absolute ethanol. At low concentrations only a single reduction process is observed. However, on increasing the concentration of the complex, a second reduction process becomes evident and the original reduction wave disappears. These results are tabulated in Table 1 and a graph of peak height (I_p) *versus* concentration is shown in Fig. 2. It can be seen from Fig. 2 that the polarographic waves give different concentration - current slopes with the change in the wave profile occurring when the Cu^{I}DDP (alkyl = isopropyl) concentration is between 0.3 and 0.4 mM. Where possible, values of peak widths at half-peak height ($W_{\frac{1}{2}}$) have been included in Table 1.

D.c. Polarography

The d.c. polarograms of the Cu^{I}DDP (alkyl = isopropyl) system show a characteristic increase in limiting currents (I_L) with increasing concentration (C) of analyte (Fig. 3 and Table 2). Values of I_L/C are essentially constant (Table 2), suggesting that the electroactive species undergoing reduction exists in a single oxidation state throughout the concentration range investigated (0.05–0.97 mM). This range includes the region where a change in the differential-pulse polarographic profile was observed (0.3–0.4 mM) leading to the conclusion that copper possesses a common oxidation state before and after the change. The inference that a single oxidation state participates in the reduction process is supported by the observation that $W_{\frac{1}{2}}$ values are not significantly different before and after the change (Table 1), as $W_{\frac{1}{2}}$ depends on the oxidation state of the electroactive species.[2] Possible explanations for the difference in peak current - concentration profiles at low and high concentrations of Cu^{I}DDP (alkyl = isopropyl) (Fig. 2) are a change in electrochemical reversibility of the reaction in the differential mode, or differing diffusion coefficients of the electroactive species at the low and high concentrations.

Stationary Electrode Voltammetry

Typical linear sweep voltammograms for solutions of Cu^{I}DDP (alkyl = isopropyl) undergoing reduction at the hanging mercury drop electrode (HMDE) are shown in Fig. 4. A shift of the peak potential to more negative values with increasing scan rate is indicative of an electrochemically irreversible electrode process[3] (Table 3). The irreversibility of the process is also borne out in cyclic voltammetric observations where values for the difference between anodic and cathodic peak potentials ($E_{pa} - E_{pc}$) are significantly larger than those expected for a reversible process[4] (Fig. 5 and Table 4).

Also, ratios of anodic to cathodic peak currents (I_{pa}/I_{pc}) differ from unity, again suggesting that the electrode process being investigated is irreversible.[3] Values of $I_p/V^{\frac{1}{2}}$ are essentially constant at concentrations of 0.11 and 0.55 mM Cu^{I}DDP (alkyl = isopropyl) (Table 3), suggesting that the reduction processes are diffusion controlled. In contrast, large variations in the values of I_p/V preclude adsorption processes

Table 3. Linear sweep voltammetric data for 0.11 and 0.55 mM $Cu^{I}DDP$ (alkyl = isopropyl) at the SMDE

[$Cu^{I}DDP$]/ mM	Scan rate/ mV s^{-1} (= V)	$-E_p$/V	I_p/μA	$\lvert E_p - E_{p/2}\rvert$/ mV	αn_a*	$I_p/V^{\frac{1}{2}}$†/ μA $V^{-\frac{1}{2}}$ $s^{\frac{1}{2}}$	I_p/V/ μA V^{-1} s
0.11	50	0.603	0.50	70	0.68	2.24	10.00
	100	0.616	0.77	68	0.70	2.44	7.70
	200	0.630	1.09	65	0.73	2.44	5.45
	500	0.655	1.45	67	0.71	2.05	2.90
0.55	50	0.622	1.40	50	0.95	6.26	28.00
	100	0.652	2.00	65	0.73	6.32	20.00
	200	0.665	2.65	66	0.72	5.93	13.25
	500	0.690	3.05	72	0.66	4.31	6.10

* αn_a, determined from $\lvert E_p - E_{p/2}\rvert = 47.7/\alpha n_a$.
† $I_p/V^{\frac{1}{2}}$ (0.11 mM): $\bar{x} = 2.29$; $s = 0.187$; CV = 8.16%. $I_p/V^{\frac{1}{2}}$ (0.55 mM): $\bar{x} = 5.71$; $s = 0.946$; CV = 16.60%.

Table 4. Cyclic voltammetric data for 0.11 and 0.55 mM $Cu^{I}DDP$ (alkyl = isopropyl) at the SMDE

[$Cu^{I}DPP$]/ mM	Scan rate/ mV s^{-1} (= V)	$-E_{pa}$/V	$-E_{pc}$/V	I_{pa}/μA	I_{pc}/μA	I_{pa}/I_{pc}	$\lvert E_{pa} - E_{pc}\rvert$/ mV
0.11	50	0.520	0.603	0.22	0.50	0.44	83
	100	0.505	0.616	0.32	0.77	0.41	111
	200	0.470	0.630	0.44	1.09	0.40	160
	500*	—	0.655	—	1.45	—	—
0.55	50	0.605	0.622	0.60	1.40	0.43	17
	100	0.585	0.652	0.90	2.00	0.45	67
	200	0.515	0.665	1.10	2.65	0.42	150
	500	0.532	0.690	1.45	3.05	0.47	158

* Anodic data difficult to interpret owing to broad profile.

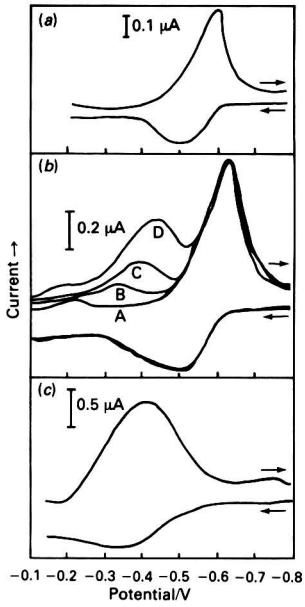

Fig. 5. Cyclic voltammograms at the HMDE (area = 0.020 cm^2) of (*a*) 0.11 mM copper(I) diisopropyldithiophosphate; (*b*) 0.11 mM copper(I) diisopropyldithiophosphate at delay times of 8, 60, 167 and 227 s for A, B, C and D, respectively; and (*c*) 0.04 mM ammonium diisopropyldithiophosphate. Scan rates, 100 mV s^{-1}; supporting electrolyte, 0.1 M sodium perchlorate in ethanol

as major contributors to the electrochemistry of $Cu^{I}DDP$ (alkyl = isopropyl) at the HMDE.

The cyclic voltammogram shows an interesting development in the form of a pre-peak when the delay time is increased [Fig. 5(*b*), A]. (The delay time is the time interval between the formation of the mercury drop and the commencement of the voltammetric scan.) For comparison, the cyclic voltammogram of ammonium DDP (alkyl = isopropyl) is shown in Fig. 5(*c*). This time-dependent pre-wave may be attributed to the formation of an adsorbed mercury(II) - DDP species as characterised by Bond *et al.*[5] Also, Hutchings *et al.*[1] have discussed a pre-wave of this type encountered in studies of CuDDP where the interaction of mercury metal with DDP produced a pre-wave.

Table 5. Determination of n from linear sweep voltammetric data at the SMDE

[$Cu^{I}DPP$]/ mM	Scan rate/ mV s^{-1} (= V)	αn_a	I_p/μA	n*
0.11	50	0.68	0.50	1.91
	100	0.70	0.77	2.05
	200	0.73	1.09	2.01
	500	0.71	1.45	1.70
0.55	50	0.95	1.40	0.90
	100	0.73	2.00	1.04
	200	0.72	2.65	1.02
	500	0.66	3.05	0.75

* n determined from $I_p = 2.99 \times 10^5 n (\alpha n_a)^{\frac{1}{2}} A C_o D_o^{\frac{1}{2}} V^{\frac{1}{2}}$.

Determination of the Number of Electrons (n) Involved in the Reduction of $Cu^{I}DDP$ (Alkyl = Isopropyl) in Solution

The reduction of CuDDP (alkyl = isopropyl) at the mercury electrode can be represented as follows:

$$Cu(DDP)_n + ne + Hg \rightleftharpoons Cu(Hg) + nDDP^- \quad (1)$$

Voltammetry

Application of electrochemical theory for the determination of n from an analysis of the polarographic - voltammetric waveform is based on a knowledge of diffusion coefficients for the participating electroactive species. The average value of I_L/C from d.c. polarographic data is 7.0×10^{-3} μA l mol^{-1} (Table 2). Applying a modified form of the Cottrell equation,[6] which takes into account electrode sphericity, enables diffusion coefficients to be evaluated with the premise that either a one- or two-electron change is taking place. The respective diffusion coefficients are 3.7×10^{-5} and 1.1×10^{-5} cm^2 s^{-1}.

Table 6. Coulometric results obtained with copper(II) perchlorate, Cu^{I}DDP and ZDDP (alkyl = isopropyl). Background current ≈ 200 μA

Standard	Mass taken/ mg	Oxidation - reduction potential/V	n	Expected charge/C	Observed charge/C	Final current/μA
Copper(II) perchlorate ..	1.0022	+0.2/−0.3	2	3.0426	4.6729	300
Cu^{I}DDP	0.3415	−0.8*	1	0.5185	1.0820	976
			2	1.0370		
ZDDP	0.3655	+0.1/−1.1	2	1.0787	3.8470	2476

* Reduction only.

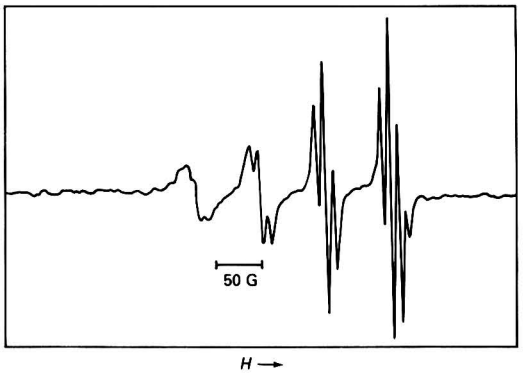

Fig. 6. Electron spin resonance spectrum of copper(I) diisopropyldithiophosphate in ethanol after de-gassing

An estimate of the diffusion coefficient (D_o) by application of the Stokes - Einstein relation is possible[7]:

$$D_o\,(\mathrm{cm^2\,s^{-1}}) = \frac{2.96 \times 10^{-7}}{\eta}\left(\frac{d}{M}\right)^{\frac{1}{3}}$$

at 25 °C, where η is the viscosity of the solvent, d is the density of the pure substance and M is its relative molecular mass. Using the Stokes - Einstein approach yields a value of 4.27×10^{-6} cm^2 s^{-1} for D_o. On comparing this with the values calculated from the limiting currents, it is clear that the experimental value of 1.1×10^{-5} cm^2 s^{-1} is large for a two-electron change, and the even larger value of 3.7×10^{-5} cm^2 s^{-1} for $n = 1$ is unlikely to describe the reduction observed here for what started out as a copper(I) species.

Earlier discussions have indicated that the electrode process occurring at the HMDE is irreversible and diffusion controlled. By applying the relevant equation for such a process[8] and using the value of 1.1×10^{-5} cm^2 s^{-1} as the diffusion coefficient enables a value for n to be determined under linear sweep voltammetric conditions. Table 5 lists the calculated n values at 0.11 and 0.55 mM of Cu^{I}DDP (alkyl = isopropyl) in solution. It can be seen from these results that the experimentally determined diffusion coefficient adequately describes a two-electron process at a concentration of 0.11 mM, but it does not account for the relatively low peak currents, and hence small n values, obtained at 0.55 mM of Cu^{I}DDP (alkyl = isopropyl). At this higher concentration a value of *ca.* 3×10^{-6} cm^2 s^{-1} for the diffusion coefficient would be required to describe a two-electron reduction process.

Controlled Potential Coulometry (CPC)

It is clear from the above discussion that a technique that does not rely on the determination of diffusion data is desirable for providing information that is unambiguous in respect to the number of electrons involved in a particular process.

CPC is a useful method for studying electrode reactions and for determining the n value of a process without prior knowledge of electrode area of diffusion coefficient. In all the experiments conducted in ethanolic media, the final current was greater than the background current attributable to the supporting electrolyte alone (Table 6). In each instance, this had the effect of indicating a greater charge than that expected for complete electrolysis. Hence, a credible value for n could not be obtained. This type of behaviour is encountered when a reaction of the electrolysis product regenerates starting material or another electroactive substance. However, with copper(II) perchlorate as a primary standard it is difficult to ascribe the observations to the above explanation. Blankespoor[9] noticed this type of behaviour when looking at the oxidation of zinc (DDP) (alkyl = isopropyl) in a non-aqueous medium.

Electron Spin Resonance (ESR)

Although elemental analyses and magnetic moment studies irrefutably show that Cu^{I}DDP (alkyl = isopropyl) is present in the solid state, dissolution in ethanol produces a strong copper(II) ESR signal indicating transformation to Cu^{II}DDP (alkyl = isopropyl) (Fig. 6). This is accordance with observations of Yordanov *et al.*,[10] who stated that Cu^{I}DDP (alkyl = isopropyl) produces Cu^{II}DDP (alkyl = isopropyl) in solution via an inner self-redox reaction.

Conclusion

The voltammetric behaviour of copper(I) diisopropyldithiophosphate in an ethanolic medium is complex. Reduction processes observed at high and low concentrations of the complex are diffusion controlled and involve a common oxidation number for the copper species undergoing reduction at a mercury electrode, but the reduction process is complicated by adsorption of an electroreducible species on to the surface of the mercury drop. Nevertheless, graphs of differential-pulse polarographic currents *versus* concentration of the Cu^{I}DDP (alkyl = isopropyl) are linear from 0.07 to 1 mM, with an inflection to higher slope occurring at 0.4 mM. However, with regard to determination in specific systems, it can be envisaged that interactions with other components will call for preliminary treament to assure analytical usefulness of voltammetry for this type of compound.

The Science and Engineering Research Council is thanked for a research studentship (to M. J. H.) within its CASE scheme in association with Esso Chemicals, Abingdon, Oxon. Dr. Lynne Griffiths, Dr. T. Colclough and Dr. J. Marsh of Esso Chemicals are thanked for their inspiring encouragement and many helpful suggestions. Also, Professor J. E. Simao, Universidade do Minho, Portugal is thanked for discussions made possible by NATO Grant No. 84/0069.

References

1. Hutchings, M. J., Moody, G. J., and Thomas, J. D. R., *Analyst*, 1987, **112**, 601.
2. Baird, A. J., and Faulkner, L. R., "Electrochemical Methods," Wiley, New York, 1980, p. 195.
3. Baird, A. J., and Faulkner, L. R., "Electrochemical Methods," Wiley, New York, 1980, p. 219.

4. Matsuda, H., and Ayabe, Y., *Z. Elektrochem.*, 1955, **59**, 494.
5. Bond, A. M., Casey, A. T., and Thackeray, J. R., *J. Electrochem. Soc.*, 1973, **120**, 1502.
6. Baird, A. J., and Faulkner, L. R., "Electrochemical Methods," Wiley, New York, 1980, p. 145.
7. Meites, L., "Polarographic Techniques," Wiley, New York, 1965, p. 144.
8. Nicholson, R. S., and Shain, I., *Anal. Chem.*, 1964, **36**, 706.
9. Blankespoor, R. L., *Inorg. Chem.*, 1985, **24**, 1126.
10. Yordanov, N. D., Alexiev, V., Macicek, J., Glowiak, T., and Russell, D. R., *Transition Met. Chem.*, 1983, **8**, 257.

Paper A6/399
Received October 22nd, 1986
Accepted November 26th, 1986

On-line Determination of Ethanol During Fermentation Processes Using a Fuel Cell Sensor

W. James Criddle* and Keith W. Parry
Department of Applied Chemistry, UWIST, P.O. Box 13, Cardiff CF1 3XF, UK

and Thomas P. Jones
Lion Laboratories Ltd., Barry, South Glamorgan, UK

A procedure is described for the determination of ethanol formed during alcoholic fermentation which involves a novel technique combining a flow dilution system with dynamic headspace analysis. An electrochemical fuel cell sensor is used as the detector. The procedure is both simple and rapid and is comparable in precision to gas chromatography.

Keywords: *Ethanol determination; fermentation; on-line analysis; fuel cell sensor*

In recent years, extensive research has been undertaken to develop techniques for the continuous monitoring of ethanol produced during fermentation processes. Comberbach and Bu'lock[1,2] have utilised a headspace gas chromatograph for this purpose, Mütze[3] has studied the continuous measurement of the ethanol concentration in fermenters by means of an infrared gas analyser, and work has been undertaken, primarily in Japan,[4] on microbial sensors. However, close scrutiny of the literature reveals surprisingly little concerning the use of electrochemical sensors for this purpose.

Worsfold *et al.*[5] combined flow injection analysis (FIA) with an enzyme-based detection procedure for the determination of ethanol in alcoholic beverages and from their results it was thought that a system based loosely on the principles of FIA or continuous flow analysis coupled with an electrochemical sensor (*i.e.*, the fuel cell) could provide a basis for the on-line monitoring of ethanol.

In this paper we describe a procedure that can be used in conjunction with the prototype version of a now commercially available instrument (DA-1, Lion Laboratories, Barry, South Glamorgan, UK), the development of which has been recently described by the authors,[6] to monitor the production of ethanol during a fermentation process.

Experimental and Results

The electronic component of the instrument used in all the experimental procedures for the determination of ethanol was the prototype Lion Laboratories AE-D3 ethanol analyser, which has been described in an earlier paper.[6] The associated headspace generation vessels were a modified form (see below) of those described in the same paper.[6]

Modification of Headspace Generation Vessels

The headspace generation vessels employed were modified to incorporate a lower liquid inlet and a liquid overflow to enable a constant head of liquid to be maintained in the vessel (Fig. 1). The working capacity was about 100 cm^3, although the vessels were usually flushed with about 200 cm^3 of solution between samples.

On-line Ethanol Analysis

The ethanol produced during fermentation was monitored using the apparatus depicted in Fig. 2.

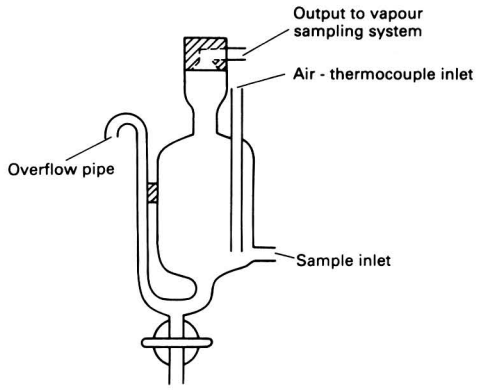

Fig. 1. Modified headspace generation vessel

The precision of the dilution system was initially tested using appropriate ethanol standards and diluent streams rather than fermenting liquids; the results of these initial experiments are given in Table 1.

In order to follow actual fermentations, the on-line apparatus (Fig. 2) was utilised in the following manner. An appropriate ethanol standard (*e.g.*, 0.2% *V/V*) was transported using precision peristaltic pumping (Masterflex pump, C.D. Instrument, Bishops Stortford, Herts., UK) through a mixing system (Vigreaux tube, 6 mm i.d., length 10 cm) to the standard headspace generation vessel. On completion of this procedure, the fermenting beverage was made to flow via a coarse filter (cotton-wool plug), to a small three-necked flask (100 cm^3) where most of the de-gassing occurred, and thence back to the fermentation vessel. Using the precision pump, samples from the bottom of the three-necked vessel were then pumped via a fine de-bubbler (Jones Chromatography, Llanbradach, Mid-Glamorgan, UK), along the same path as that followed by the standard ethanol solution into the sample headspace generation vessel where the ethanol content of the beverage was determined. Both solutions were then drained from the vessels via the tap.

This procedure was repeated until the ethanol content of the beverage was equal to that of the ethanol standard. From this point onwards the beverage and appropriate standard were diluted before any subsequent determinations were undertaken. These latter determinations were carried out as described below.

* To whom correspondence should be addressed.

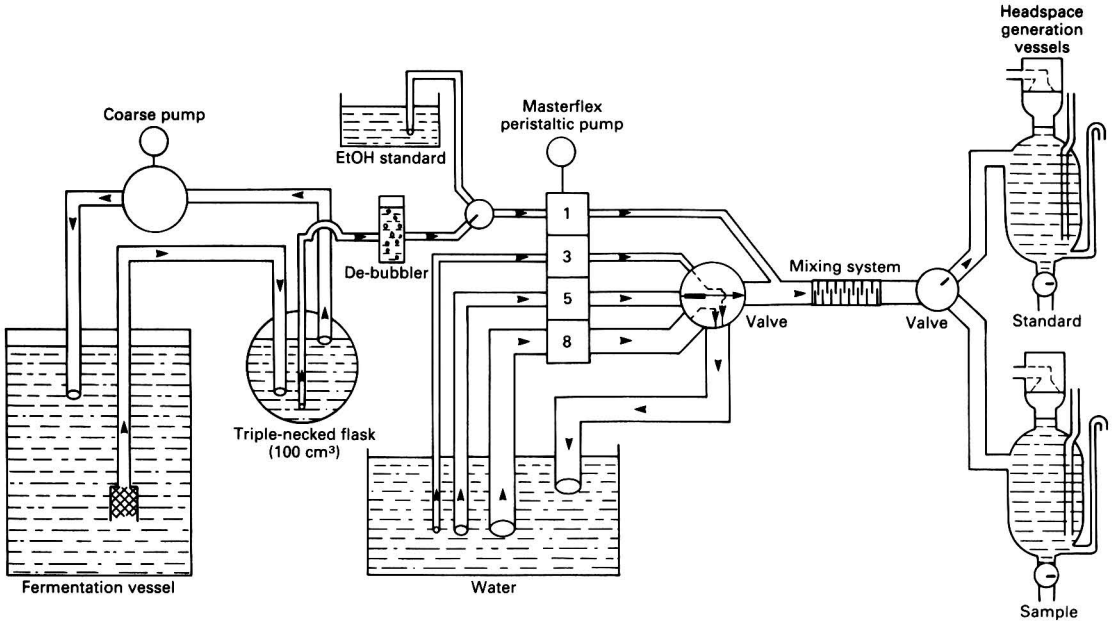

Fig. 2. Schematic diagram of working on-line monitor

Table 1. Calibration of on-line system using standard ethanol solutions

Ethanol standard, % *V/V*	Diluent tube internal diameter*/mm	Dilution factor (*F*)	Ethanol content, % *V/V*
0.20	—	—	0.19
			0.20
			0.22
			$\bar{x} = 0.21$
2.00	3	10	2.06
			2.02
			2.00
			$\bar{x} = 2.03$
5.00	5	26	5.06
			5.01
			5.03
			$\bar{x} = 5.03$
10.00	8	65	9.9†
			9.9†
			10.0†
			$\bar{x} = 9.9$

* Sample tube internal diameter 1 mm. See Fig. 2.
† Instrument display to one decimal place only.

The diluent tubes carrying water were manually activated using a specially designed valve which allowed water to flow through the appropriate diluent tube. An ethanol standard (2% *V/V*) was allowed to flow along the standard - beverage line via the mixing chamber (where it was thoroughly mixed with water flowing in the 3 mm i.d. diluent line) into the standard headspace generation vessel. Similarly, after thorough flushing of the identical line with the fermenting liquid, the beverage was diluted in the same manner, the flowing stream being diverted to the sample headspace generation vessel where the analysis of the solution was undertaken. This procedure was repeated until the ethanol content of the beverage again reached that of the ethanol standard.

The position of the valve was adjusted to allow the water flowing in the 5 mm i.d. diluent tube to flow into the mixing chamber and a 5% *V/V* ethanol standard was employed in a fashion identical with that described for the 2% standard. When the fermentation exceeded 5% *V/V*, instrument calibration was initiated by the use of a suitably diluted (8-mm diluent tube) 10% *V/V* ethanol standard.

Headspace Ethanol Analysis

When both the standard and sample vessels had been filled, an air supply (*ca.* 200 cm³ min⁻¹) was generated using a small air pump and was passed through the standard vessel, thus creating a dynamic ethanol-containing headspace. The air emerging from the vessel was passed through a short polypropylene T-piece pierced by a Microlance hypodermic needle fitted to a standard Lion Laboratories fuel cell sensor head.[6] Sampling of the flowing air - ethanol stream was achieved by pressing the RESET button and then the READ button. This resulted in a standard volume of ethanol - water vapour being drawn into the fuel cell, where an electrical potential was developed. This potential was amplified and used as a measure of the ethanol concentration in the vapour. The procedure was repeated using the sample vessel and the ethanol content was determined in the sample as described previously with appropriate correction for temperature variations in the standard and sample solutions.[6]

Gas Chromatographic Analysis of the Fermentaion Liquor

The ethanol content of the fermenting beverage (sampled directly from the fermentation vessel) was determined at several stages in the fermentation process by gas chromatography (Figs. 3–5) using a Perkin-Elmer 8310 gas chromatograph fitted with a 3 m × 3 mm internal diameter stainless-steel column (containing 10% Carbowax 20M in 60–80 mesh Celite) and a flame-ionisation detector (FID). The column was isothermally heated at 100 °C using helium as carrier gas (20 cm³ min⁻¹). Propan-1-ol was used as an internal standard.

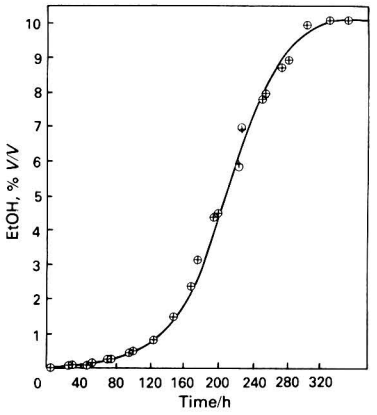

Fig. 3. Ethanol - time profile of a typical dry red wine fermentation. ○, GC determination; +, on-line determination

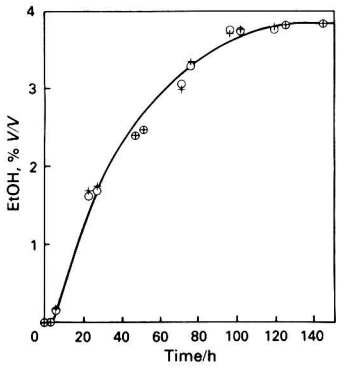

Fig. 4. Ethanol - time profile of a typical beer fermentation. ○, GC determination; +, on-line determination

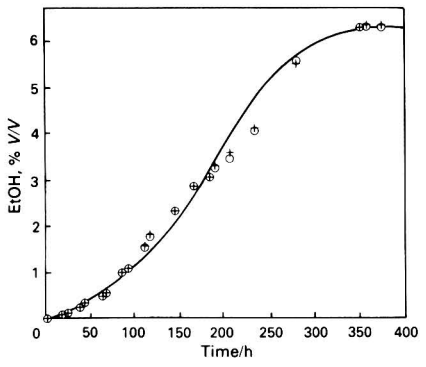

Fig. 5. Ethanol - time profile of a typical cider fermentation. ○, GC determination; +, on-line determination

Discussion

As headspace analysis using a fuel cell sensor[6] is limited by the response of the cell, which is linear only to ethanol concentrations (at 20 °C) of up to about 0.4% *V/V*, alcoholic beverages derived from fermentation must be diluted from an early stage. In addition, it follows that the level of dilution necessary course of the fermentation, as ethanol concentrations of 0–14% *V/V* are not uncommon. Hence when using the Lion Laboratories standard fuel cells, the usage of the cell was restricted to solutions (at 20 °C) not exceeding 0.2% *V/V*, in order to guarantee a linear response in the working range.

It is possible to dilute the ethanol solution using a series of tubes of various internal diameters carrying water transported by peristaltic pumping. This diluting water may be mixed with sample solutions using the same peristaltic pump. It is possible to estimate the level of dilution achieved from the internal diameter (cross-sectional area) of the tubes used. The dilution factor (F) is therefore a function of the total volumetric flow and the volumetric flow of the ethanol solution.

$$F = \frac{\text{Total volumetric flow}}{\text{Volumetric flow of ethanol solution}} \quad \ldots \quad (1)$$

Hence, if D_1 = i.d. of standard or sample tube and D_2 = i.d. of diluent (water) tube, then

$$F = \frac{D_1^2 + D_2^2}{D_1^2} \quad \ldots \quad (2)$$

Provided that the calibration ethanol solutions and the sample solution are passed through the same tube (Fig. 2, tube 1), the level of dilution can be predicted with reasonable accuracy from equation (2), which, although not very precise, gives an adequate approximation for the purposes of our procedure. Precise dilution, in absolute terms, is not required as long as the standard and sample solutions are diluted to the same degree.

Prior to the study of actual fermentation systems, the equipment was calibrated using identical standard and sample solutions. Table 1 shows the internal diameter and dilution factors at various ethanol concentrations such that the 0.2% *V/V* ethanol barrier was not exceeded. It also shows the high degree of accuracy that can be achieved under ideal conditions using the system described.

In order to apply the system to actual fermentation conditions, additional features were incorporated to give the complete system shown in Fig. 2. The final unit therefore consisted of three main sections, the sampling system for obtaining a solid and bubble-free sample from the fermenter, the dilution system and the analytical system for the determination of ethanol in the final solutions.

It was found to be necessary to incorporate a filter in the sample line of the sampling system in order to remove suspended solids that could lead to a blockage of the subsequent small bore tubes, and it was also necessary to feed the filtered sample to a secondary 50-cm^3 vessel. Using a reasonably rapid (1 dm^3 min^{-1}) flow-rate generated by a peristalic pump (coarse pump, Fig. 2) in a closed system resulted in the de-gassing of the solution in the 50-cm^3 vessel, most of the froth being returned with the fermenting liquor to the main fermentation vessel.

It is important that the liquor sample in the vessel is representative of the main bulk of the liquor in the fermenter. It is therefore important that a fast throughput of liquor is achieved, particularly if the on-line analyser is some distance from the fermenter. On a laboratory scale, however, we found that the above flow-rate was adequate. The closed circulating system has the advantage of preventing an ingress of air and thus bacterial contamination of the main fermentation liquor.

Samples for analysis were drawn from the bottom of the 50-cm^3 vessel and were passed through a commercial de-bubbler prior to transport to the small bore tubing used in the final sampling and dilution system. No problems of blockage or deterioration of the associated tubing was experienced over a 6-month working period.

The mixing system, which consisted of a simple Vigreaux tube, was an essential component in the system. Without

obtained were erratic and generally meaningless, particularly when the fermenting liquor was of high viscosity, as is often so in the early stages of most fermentations.

The vessels used in the final ethanol determination are shown in Fig. 1. These are a modified form of those previously described for direct ethanol determination.[6] However, calibration of the vessels used in the on-line equipment is not necessary as the dilution of the sample to the appropriate concentration is achieved directly and a reasonably constant depth is all that is required, this being achieved by using the overflow system shown in Fig. 1. It should be noted that when an air bubble passes through an ethanol solution, equilibration is rapidly achieved and only a few centimetres passage through the solution is required.[7] In the vessels used, this passage depth is approximately 7–8 cm, which is more than adequate for equilibration.

The analysis of the final solutions was carried out as outlined in this paper and described in detail previously,[6] the results being shown as ethanol - time profiles in Figs. 3–5. The results show a high degree of correlation between the results obtained by the on-line system and ethanol determinations carried out by simultaneous gas chromatographic analysis. Little difference was experienced in the analytical capability of the procedures described in this paper when they were applied to different kinds of alcoholic fermentation, *e.g.*, beer, cider and various wines. It would therefore appear that the procedure offers the analyst the capability of establishing ethanol - time profiles for most alcoholic fermentations, and it is hoped that if suitably automated it will provide the basis of a commercial on-line instrument for the brewing and wine-making industries.

References

1. Comberbach, D. M., and Bu'lock, J. D., *Chromatogr. Newsl.*, 1982, **10**, 19.
2. Comberbach, D. M., and Bu'lock J. D., *Biotechnol. Bioeng.*, 1983, **25**, 2503.
3. Mütze, B., *Biotechnol. Bioeng.*, 1984, **26**, 390.
4. Karube, I., and Suzuki, S., *Ion-Sel. Electrode Rev.*, 1984, **6**, 15.
5. Worsfold, P. J., Růžička, J., and Hansen, E. H., *Analyst*, 1981, **106**, 1309.
6. Criddle, W. J., Jones, T. P., and Parry, K. W., *Analyst*, 1986, **111**, 507.
7. Jones, A. W., *PhD Thesis*, University of Wales, 1974.

Paper A6/409
Received October 29th, 1986
Accepted November 24th, 1986

Application of a Photodiode Array Detector to Multi-component Determination by Flow Injection Analysis

Marcelo Blanco,* Jordi Gené, Hortensia Iturriaga and Santiago Maspoch
Departament de Química, Divisió de Química Analítica, Universitat Autonoma de Barcelona, Bellaterra, Barcelona, Spain

The capabilities of a photodiode array detector in flow injection analysis for multi-component determination with normal and derivative spectra is outlined. Mixtures of two, three and four components with completely overlapping spectra have been accurately resolved. The effect of wavelength range and mode of spectral selection has also been studied. The proposed analytical method has been successfully applied to the determination of the four active components of a commercial pharmaceutical formulation.

Keywords: *Photodiode array detector; multi-component analysis; flow injection analysis; derivative spectra; pharmaceutical preparations*

The development of quantitative methods for the simultaneous determination of different components in the same sample, multi-component analysis, is a matter of great practical importance in environmental, clinical and pharmaceutical analysis.

Flow injection analysis (FIA) has attracted increasing interest in recent years owing to its simplicity, versatility, low cost, precision, high sampling rate and ease of automation. In view of the general characteristics of FIA it would not appear to be very difficult to design devices adapted to the determination of several species in the same sample, and consequently it can be envisaged that FIA offers possibilities in the field of multi-component analysis. However, few simultaneous FIA determinations have so far been described, such methods accounting for less than 10% of the papers published on FIA.[1,2]

The problem of multi-component analysis using FIA, in both conventional methodology and in methods based on differential kinetics, has been solved either with the use of several detectors or with a single detector and several different injection systems. FIA systems for simultaneous determinations which use a single detector and single injections use a pH gradient or ion-exchange process for species separation before their detection.[1]

The introduction of photodiode array multi-wavelength detectors enables UV - visible spectra to be recorded at short time intervals and has opened the way for new trends in detection methods in HPLC and FIA systems.[3,4] However, although photodiode array detectors have already been applied to unresolved peak analysis in HPLC,[5-8] their use has just begun in multi-component determination by FIA.[9]

A review of papers published on the spectrophotometric analysis of multi-component mixtures shows that the quantification of compounds continues to be a difficult problem when there is high spectral overlap and components of unequal concentration, and the application of derivative spectroscopy offers a powerful approach to the problem of resolution of mixtures.[10-12] The two factors with the greatest influence on the accuracy of the results are the wavelength range and derivative spectra selection. To date, the selection of both factors has been made empirically, in spite of the development of some theoretical methods to define relationships quantitatively.[13-15]

We are involved with a research programme on multi-component analysis by FIA and this paper reports the simultaneous determination of compounds in mixtures by a spectrophotometric diode array detection system. Mixtures of two, three and four components with completely overlapped spectra and different concentrations have been studied. The proposed analytical method has been successfully applied to the determination of four active components in a commercial pharmaceutical formulation.

Experimental

Reagents

Etafedrine (2-methylethylamino-1-phenylpropan-1-ol) hydrochloride, phenylephrine (3-hydroxyphenyl-2-methylaminoethanol) hydrochloride, doxylamine (2-dimethylaminoethoxyphenylmethyl-2-picoline) succinate and theophylline were of analytical-reagent grade.

All stock solutions were prepared by dissolving 200–400 mg in 100 ml of 0.1 M hydrochloric acid. This solvent was also used for preparing more dilute solutions.

Apparatus

The manifold used was a single-channel system consisting of a Gilson Minipuls 2 peristaltic pump, a Tekator V-200 variable-volume electric injection valve and an HP8541A diode array spectrophotometer equipped with a Hellma 178.712QS flow cell (inner volume 18 μl and path length 1 cm). A HP82940A GPIO interface was used for the activation of the injection valve. All the coils and sample loops were made of PTFE tubing (i.d. 0.5 mm). The carrier was 0.1 M hydrochloric acid pumped at a flow-rate of 1.6 ml min^{-1}, and 100 μl of a sample solution were injected.

All the absorption spectra were measured on an HP8451A diode-array spectrophotometer (Hewlett-Packard), equipped with a floppy disk drive for bulk data storage (Hewlett-Packard Model HP9121) and a digital plotter for the graphical representation of data (Hewlett-Packard Model HP7470A).

The derivative spectra and multi-component resolution of mixtures were obtained by the use of software programs supplied with the spectrophotometer.

Procedure

The greatest reproducibility of results is obtained when the spectrum is recorded at the peak maximum. The elapsed time between the injection of the sample and the appearance of the maximum signal in the detector is the residence time, t_R, and

* To whom correspondence should be addressed.

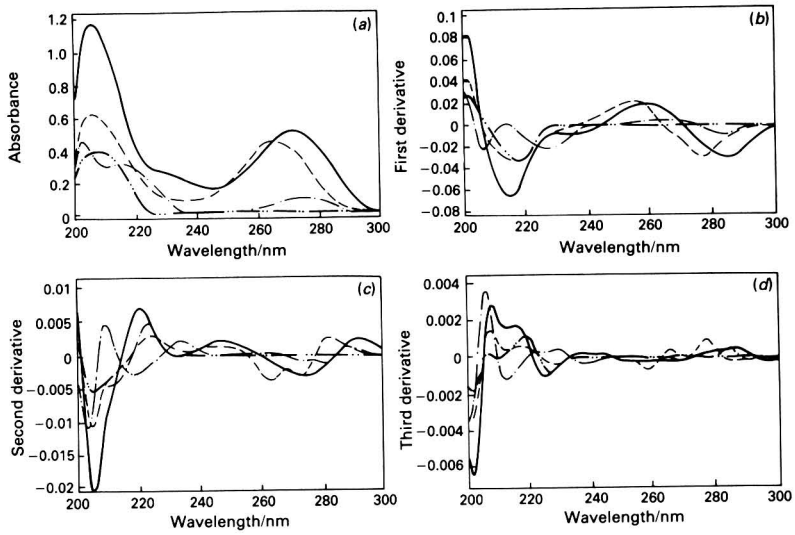

Fig. 1. Normalised absorbance and derivative spectra of each component in a mixture (normalised to 1.00×10^{-4} mol l^{-1}). ——, Theophylline; – – – –, doxylamine succinate; – · – · –, phenylephrine hydrochloride; and — ·· — ·· —, etafedrine hydrochloride. (*a*) Absorption, (*b*) first-derivative, (*c*) second-derivative and (*d*) third-derivative spectra

Table 1. Relative errors (%) in multi-component analysis of two-component mixtures from normal and derivative spectra in different wavelength ranges

Mixture and concentration*/ 10^{-5} mol l^{-1}		Wavelength range†/nm											
		200–240				240–290				214–290			
		A	1D	2D	3D	A	1D	2D	3D	A	1D	2D	3D
E	13.890	−2.5	−3.2	−3.0	−3.3	14.2	−1.0	−3.0	−4.7	−2.7	−2.0	−1.8	−1.6
F	6.319	2.8	5.2	9.9	10.6	1.2	−1.1	−1.4	−2.0	1.3	−1.3	−1.6	−0.1
E	12.150	−2.1	−2.4	−2.2	−2.4	0.8	−7.9	−5.9	3.8	−0.3	−0.4	−0.8	−0.8
D	6.059	5.9	7.3	8.3	11.3	3.5	3.0	2.9	3.2	3.6	2.9	2.9	3.0
F	9.874	2.5	5.2	9.9	11.4	−0.9	−0.4	−0.3	−0.9	−0.6	−1.0	−1.4	0.0
D	6.059	−2.4	−7.5	10.5	15.6	−1.7	−2.0	−2.0	−1.8	−1.8	−1.6	−1.6	−1.3
E	4.166	0.6	1.8	1.0	−1.7	−11.8	−6.5	−4.2	4.9	−0.2	−0.3	−0.7	0.1
T	6.200	0.6	0.1	0.6	0.9	0.9	0.9	0.9	1.0	0.8	0.9	0.8	0.3
F	5.277	0.5	−1.4	−1.4	−1.8	−0.4	−0.7	−2.8	−3.0	−0.9	−2.0	−2.2	−0.9
T	4.332	−3.3	−5.7	−7.0	−9.0	−3.4	−3.6	−3.1	−3.0	−3.3	−2.7	−2.4	−0.8
D	4.922	−2.4	−6.9	6.5	23.6	−0.8	−0.5	−0.8	0.1	1.2	−0.1	−1.1	0.7
T	4.332	−1.0	1.8	−4.1	−10.7	−1.1	−1.0	−1.3	−1.9	−3.6	−3.2	−3.2	−5.1

* E, Etafedrine hydrochloride; F, phenylephrine hydrochloride; D, doxylamine succinate; and T, theophylline.
† A, Absorbance; 1D, first-derivative; 2D, second-derivative; and 3D, third derivative spectra.

this was determined at the beginning of the investigation. In successive injections the spectra were recorded at this time during a pre-determined integration time, t_I. The integration time is the time interval of spectrophotometric measurement required to obtain the average spectrum.

In a diode-array detector the minimum integration time can be as low as 0.1 s, but this does not necessarily give spectral reproducibility in successive injections. Increasing the integration time generally increases the reproducibility, but in dynamic systems such as FIA the integration time should be as short as possible. For this reason it is necessary to find the optimum balance between reproducibility and integration time. A relative deviation of $\leqslant 1\%$ was obtained for $t_I \geqslant 0.3$ s. Under our experimental conditions the absorbance spectra of each solution were recorded at 10.7 s after sample injection for an integration time of 0.4 s.

In order to obtain a standard spectrum of pure components, three replicate solutions were prepared for each component. Each replicate was injected three times into the FIA system and an average was obtained from nine spectra. The averaged spectra of three solutions of different concentration were used to obtain a normalised spectrum (1.0×10^{-4} mol l^{-1}) for each component by regression (the absorbance of each solution was less than 1.0). Fig. 1 shows the normalised absorbance and derivative spectra obtained in the range 200–300 nm.

Mixtures of two, three and four components, with two replicates per composition, were prepared from the stock solutions. Each replicate solution was injected into the FIA system three times and an average spectrum was obtained.

Quantitation of the components of the mixture was achieved, in both absorbance and derivative modes, by the multi-component analysis program supplied by Hewlett-Packard. This program fits, by means of the least-squares method, a combination of standard spectra to the spectrum of the mixture. Normalised spectra of the pure component and its derivatives were used as standard spectra by the program.

Results and Discussion

Six two-component mixtures, four three-component mixtures and three four-component mixtures of etafedrine, phenylephrine, doxylamine and theophylline were studied. The completely overlapping spectra of the four compounds are shown in Fig. 1.

The accuracy of results obtained in the multi-component analysis of overlapping spectra depends on the wavelength range and the spectral mode considered. The optimum conditions are selected empirically.[11] Three wavelength ranges were initially selected, a broad range at 200–290 nm (full absorption range) and two narrower ranges at 200–240 nm and 240–290 nm, each corresponding to an absorption band.

In this study, the multi-component analysis program was applied to the quantitation of mixtures using absorbance, first-, second- and third-derivative spectra in the above ranges and in narrower ranges selected in each, *i.e.*, 206–290, 210–290, 214–290, 214–280, 210–240, 210–230 and 240–270 nm.

The results from the multi-component analysis were good for all of the mixtures studied.

Two-component Mixtures

The analysis of six two-component mixtures over the ten wavelength ranges studied showed three ranges which had more spectral significance for the determination of the components considered.

Table 1 includes the results obtained from absorbance and derivative spectra in these more significant ranges (200–240, 240–290 and 214–290 nm). The selection of 214–290 nm as a broader range to be studied is a consequence of the better results obtained with the suppression of the first 13-nm interval. The other ranges studied yielded similar results, but none gave better results and the small differences found have no apparent significance.

Table 2. Relative errors (%) in multi-component analysis of three- and four-component mixtures from normal and derivative spectra in the range 214–290 nm. Abbreviations as in Table 1

Mixture and concentration/ 10^{-5} mol l^{-1}		A	1D	2D	3D
E	12.500	−1.6	−0.9	−1.1	−1.0
F	5.529	1.9	0.3	−0.5	1.3
D	2.555	2.0	0.3	0.1	−0.9
E	5.208	−0.8	−0.4	−0.2	1.9
F	5.134	−1.3	−1.4	−1.2	4.1
T	2.894	−1.5	−2.0	−1.9	−4.9
E	5.208	−1.0	−0.9	0.7	2.7
D	4.040	−0.2	−1.3	−1.5	−1.5
T	2.894	−5.1	−2.2	−3.4	−8.1
F	5.134	2.6	1.9	1.1	2.2
D	4.040	2.8	2.8	2.8	3.0
T	2.894	2.5	2.8	2.6	1.7
E	1.042	−3.3	−3.0	−3.1	−3.1
F	3.950	0.7	0.7	0.9	2.6
D	2.020	−0.1	−0.1	−0.9	−1.3
T	2.067	1.8	0.9	1.5	1.8
E	2.083	−1.3	−0.6	0.8	−0.2
F	1.185	−1.8	3.1	4.8	1.4
D	0.606	−5.8	−4.9	−5.6	−1.8
T	6.200	−0.4	−0.9	−1.0	−1.3
E	2.430	−1.4	−0.4	0.3	0.0
F	1.185	0.2	4.0	5.0	3.8
D	0.444	−7.7	−5.8	−6.2	−0.9
T	6.200	1.0	0.5	0.3	−0.1

Normal absorbance spectra

The overlapping of bands does not seem to affect the determination of compounds in the studied mixtures and the results obtained are satisfactory in the three wavelength ranges mentioned. The almost null absorption of etafedrine in the range 240–290 nm seems to account for the large errors obtained (14.2 and −11.8%) for two of the mixtures; nevertheless the mixture etafedrine - doxylamine is correctly resolved.

It can be concluded that, although in some instances the imprecision is small (depending on the spectral range), the systematic errors are generally improved by the use of the broader spectral range 214–290 nm.

Derivative spectra

First and second-derivative spectra give poor resolution for the doxylamine and phenylephrine mixture in the range 200–240 nm. However, the results are very good in the range 240–290 nm, except for etafedrine because of its small absorbance in this range.

The third-derivative spectra resolve mixtures with important errors in the range 200–240 nm in samples containing phenylephrine, doxylamine or theophylline, except for the mixture theophylline - etafedrine. In third-derivative spectra, the determination is also very satisfactory in the range 240–290 nm, with similar considerations to those mentioned for the first- and second-derivative spectra of etafedrine.

In determinations using derivative spectra, it therefore can also be concluded that the systematic errors are reduced when the broader spectral range is used.

Three-component Mixtures

Four three-component mixtures of the four cited substances have been studied. Multi-component analysis with normal and derivative spectra over the mentioned wavelength ranges has been carried out. Table 2 shows the results obtained with the broader spectral range (214–290 nm), which in this instance also enhances the quality of data obtained from other wavelength ranges. The multi-component analysis of three-component mixtures yields high-quality results from each of the four spectral modes (normal, first-, second- and third-derivative) in spite of overlapping spectra.

There are only two instances with theophylline mixtures where the systematic errors are as high (4.9 and 8.1%) with the third-derivative spectra. However, with the normal, first- and second-derivative spectra, the maximum errors are always less than 3%, except for the mixture with theophylline in normal spectra, which has an error of 5.1%.

Four-component Mixtures

Table 2 also shows the results for the multi-component analysis of three four-component mixtures in the range 214–290 nm for each of the four spectral modes.

Again, a good resolution is obtained which is relatively independent of the spectral mode used and of the number of components in the mixture.

It should be noted that if one of the mixture components has smaller concentrations than the others, such as doxylamine in the two mixtures studied last, the error in its determination is between 4.9 and 7.7% in the normal, first- and second-derivative spectral modes. However, in this example of multi-component analysis, the third-derivative spectra yields substantially better results.

It can be concluded that the best results are obtained in the analysis of complex mixtures by using the third-derivative spectra in the range 214–290 nm.

Determination of Active Components in Nethaprin Tablets

The analytical method developed for the simultaneous spectrophotometric analysis of two-, three- and four-component mixtures by FIA has been applied to the determination of the four active components in Nethaprin tablets. The active components are etafedrine hydrochloride, phenylephrine hydrochloride, doxylamine succinate and ambuphylline (theophylline aminoisobutanol).

For the determination of the four active components in Nethaprin tablets, weigh and powder ten tablets. Shake an aliquot of about 140 mg with 70 ml of 0.1 M hydrochloric acid for 30 min. Dilute to 100 ml with the same solvent and then filter the suspension, discarding the first 10–15 ml of filtrate. Dilute 5 ml of this filtered solution to 100 ml with 0.1 M HCl and inject into the flow injection system.

Table 3 shows the results obtained from three aliquots with three injections each, using third-derivative spectra multicomponent analysis in the range 214–290 nm.

The variation in concentration between tablets of the active components has been also studied. For this, the following process was applied to each of ten different tablets. Weigh and powder each tablet and shake with about 70 ml of 0.1 M HCl for 30 min. Dilute to 250 ml with the same solvent and filter the suspension, discarding the first 10–15 ml. Dilute 2.5 ml of this filtered solution to 100 ml with 0.1 M HCl and inject three aliquots into the flow injection system.

The results of determination of each of the four active components in ten different tablets have good precision and were within the boundary fixed by the British and US Pharmacopoeias.

Table 3. Results of the determination of active components in Nethaprin tablets using third-derivative spectra in the range 214–290 nm

Component	Label claim/ mg per tablet	Amount found/ mg per tablet	Standard deviation/mg
Etafedrine hydrochloride . .	50	53.9	0.7
Phenylephrine hydrochloride	25	25.9	0.9
Doxylamine succinate . .	25	24.3	0.4
Ambuphylline	180	169.2	1.2

Conclusions

It can be concluded that a photodiode array multi-wavelength detector, together with multi-component analysis, is a very efficient tool for the analysis of multi-component samples using flow injection analysis. The overlapping of spectra is not an insoluble problem in the simultaneous determination of substances. The resolution is affected by the absorbance and concentration of components in the mixture.

The accuracy of the results depends on the wavelength ranges used and the order of derivative spectra selected. If the substances have well defined absorption ranges, better results are obtained. As the complexity of the mixtures increases, third-derivative spectra generally give better results.

We acknowledge the financial support given by CAICYT (Project 821/84) and the Fundación Roviralta to this research project.

References

1. Luque de Castro, M. D., and Valcárcel Cases, M., *Analyst*, 1984, **109**, 413.
2. Luque de Castro, M. D., *Talanta*, 1986, **33**, 45.
3. Fell, A. F., *Anal. Proc.*, 1980, **17**, 266.
4. Borman, S. A., *Anal. Chem.*, 1983, **55**, 836A.
5. Fell, A. F., Clark, B. J., and Scott, H. P., *J. Pharm. Biomed. Anal.*, 1983, **1**, 557.
6. Hoshino, T., Senda, M., Hondo, T., Saito, M., and Thohei, S., *J. Chromatogr.*, 1984, **316**, 473.
7. Osten, D. W., and Kowalski, R., *Anal. Chem.*, 1984, **56**, 991.
8. Vandengiste, B., Essers, R., Bosman, T., Reijnen, J., and Kateman, G., *Anal. Chem.*, 1985, **57**, 971.
9. Lázaro, F., Ríos, A., Luque de Castro, M. D., and Valcárcel, M., *Anal. Chim. Acta*, 1986, **179**, 279.
10. Davidson, A. G., and Elsheikh, H., *Analyst*, 1982, **107**, 879.
11. Rossi, D. T. and Pardue, H. L., *Anal. Chim. Acta*, 1985, **175**, 153.
12. Ueda, H., Pereira-Rosario, R., Riley, C. M., and Perrin, J. H., *Drug. Dev. Ind. Pharm.*, 1985, **11**, 833.
13. Frans, S. D., and Harris, J. M., *Anal. Chem.*, 1985, **57**, 2680.
14. Ditusa, M. R., and Schilt, A., *J. Chem. Educ.*, 1985, **62**, 541.
15. Pilipenko, A. T., Savranskii, L. I., and Mas'ko, A. N., *Zh. Anal. Khim.*, 1985, **40**, 232.

Paper A6/214
Received July 2nd, 1986
Accepted October 10th, 1986

A New Way of Organising Spectral Line Intensity Ratio Fluctuations of Different Elements

Bo Thelin
Kiruna Geophysical Institute, P.O. Box 812, S-981 28 Kiruna, Sweden

A new method of organising spectral line intensity ratio fluctuations for different elements has been developed in order to establish which line pair of analysis is more or less stable for repeated measurements. A linear graph was obtained for spectral lines from different elements when the spectral line intensity ratio fluctuations were plotted *versus* the photon energies and the ionisation energies of these lines. When these fluctuations were plotted *versus* the upper level energies instead, no linear structure relationship was obtained.

The light sources used were an inductively coupled plasma with a slot-type nebuliser system and a hollow-cathode lamp for flat metal samples. The analyses were carried out by using a computerised image dissector échelle spectrometer system.

Keywords: *Inductively coupled plasma; intensity equation; line intensity ratio fluctuations; échelle spectrometry*

The basis of modern analytical atomic spectrometry was introduced in 1925 by Gerlach,[1] who introduced the internal standard technique. The principle of the internal standard technique is based on relating the intensity ratio of selected spectral lines of the analytical and internal standard elements to concentration ratios.

In many papers following Gerlach's innovation there has been a tendency to exclude some "bad" line pairs from the analysis without explanation. No satisfactory explanation of such observed discrepancies in this method of analysis appears to have been presented so far.

In a theoretical paper by Barnett *et al.*,[2] the principles that affect the choice of analysis and internal standard lines in analytical atomic spectrometry were investigated using an ICP. The effects of excitation energy, ionisation energy, partition functions and electron density on the analytical line pair intensity ratio were studied.

Suckewer[3] described the essential sources of spectroanalytical errors connected with the determination of the density ratios of atoms in plasmas. Together with a powerful pulsed discharge system the effect of the distribution function of the atom density for different plasma radii and of deviations from local thermal equilibrium (LTE) in the plasma was studied. These authors and others assumed that the line intensity from an atomic transition $E_m \rightarrow E_n$ is proportional to the Boltzmann factor, $\exp(-E_m/\mathrm{kT})$, where E_m is here the energy of the upper energy level, and $h\nu_{mn} = E_m - E_n$ is the energy of the emitted photon. Thus the conventional intensity equation is written as

$$I^{a}_{mn} = C^{a}_{mn}\left[\sum_i g_i \exp(-E^{a}_i/kT)\right]^{-1} \exp(-E^{a}_m/kT) \quad (1)$$

where I^{a}_{mn} is the intensity of light with the photon energy $h\nu_{mn}$ from sample constituent a; C^{a}_{mn} is a combination of factors that are derived from transition probability, electron and atomic density, quenching, absorption effects, sample geometry and apparatus constants; $\sum_i g_i \exp(-E_i/kT)$ is the partition sum over all energy levels of an atom; and g_i is the statistical weight of an energy level.

In this paper the new method of analysing spectral line ratio fluctuations[4–6] has been used for different elements. The result of this analysis is that the data fit equation (1) badly but fit very well an equation with a new exponential factor instead of the exponential in equation (1).

Experimental

The experimental part of the work concerning the spectral line ratio fluctuations was carried out at the Swedish Institute for Metals Research in Stockholm, where a "side-on" mounted inductively coupled plasma (ICP) light source was used in combination with an image dissector échelle spectrometer (IDES) system. The same type of experimental work was also carried out with a flat sample lamp[7,8] using the same spectrometer system at the same Institute.

A Plasma Therm (2.5 kW) ICP unit with an automatic tuning system was used. The optimised experimental parameters of this ICP in combination with a new kind of slot-type nebuliser and a cyclone spray chamber,[9,10] are given in Table 1. A dissolved steel sample (NBS 363) at concentrations of 1 and 5 g per 100 ml was used.

A new excitation source for the spectrochemical determination of trace elements in steel, a flat metal sample hollow-cathode lamp (FSHC), was also used. The experimental parameters are given in Table 1.

Table 1. Optimised experimental parameters

ICP light source—	
Type	Slot-type nebuliser with cyclone spray chamber
Power	1.2 kW
Henry frequency	27.12 MHz
Argon cooling gas flow-rate	12 l min^{-1}
Nebuliser flow-rate of argon	7 l min^{-1}
Nebuliser pressure	131 Pa
Sample uptake rate	3 ml min^{-1}
Observation height	15 mm
FSHC lamp—	
Flush time	60 s
Pre-burn time	60 s
Pressure (Ne)	0.4 Torr
Current	0.03 A
Power	120 W
Sample	Flat
Spectrometer—	
Type	Échelle (IDES)
Wavelength region	200–800 nm
Linear dispersion	0.16 nm mm^{-1} at 200 nm; 0.32 nm mm^{-1} at 400 nm
Entrance and exit slits	35 μm
Integration time	60 s
Integration time per line	1.5 s
Integration time per measured point	0.1 s

An IDES system was used as a registration system.[11] This system, which works with photon counting, is very versatile and consists of an échelle spectrograph with high resolution, an image dissector tube and a minicomputer system.

In the measurements and analyses using the IDES system, a computer program for peak measurements was used. In this program every spectral line is measured for 0.1 s on the top at each integration. By integrating 15 times, each spectral line is measured for 1.5 s, which is sufficient to obtain accurate results with this spectrometer system.

Results and Discussion

In a previous paper[6] a new method of analysis was presented in which fluctuations of ratios between the intensities of two simultaneously measured spectral lines were studied, using ICP light sources ("end-on" and "side-on") and IDES spectrometer systems. By forming the ratio between the intensities of two simultaneously measured lines from sample constituents a and b and by using logarithmic differentiation of equation (1), one obtains

$$\frac{\mathrm{d}(I^{\mathrm{a}}_{mn}/I^{\mathrm{b}}_{m'n'})}{(I^{\mathrm{a}}_{mn}/I^{\mathrm{b}}_{m'n'})} = \frac{\mathrm{d}(C^{\mathrm{a}}_{mn}/C^{\mathrm{b}}_{m'n'})}{(C^{\mathrm{a}}_{mn}/C^{\mathrm{b}}_{m'n'})} + \frac{1}{kT}\cdot\frac{\mathrm{d}T}{T}(E^{\mathrm{a}}_{m} - E^{\mathrm{b}}_{m'} - \bar{E}^{\mathrm{a}} + \bar{E}^{\mathrm{b}}) \quad \ldots \quad (2)$$

where $\bar{E}^{\mathrm{a}}$ is the Boltzmann mean value and is equal to

$$\sum_i g_i E_i \exp(-E_i/kT) / \sum_i g_i \exp(-E_i/kT)$$

and is estimated from the term-scheme for each element.[12]

The absolute values of the logarithmic derivatives have been identified as maximum relative deviations observed in the set of data obtained in a series of repeated simultaneous measurements of line intensities. By forming ratios of pairs of simultaneously measured line intensities, the average value of each line pair ratio is determined. The maximum relative deviation from the average value of a line pair ratio will be identified with the absolute value of the left-hand side of equation (2). Using "R-value" as an abbreviation for the maximum relative deviation and by substituting

$$D(E) = |E^{\mathrm{a}}_{m} - E^{\mathrm{b}}_{m'} - \bar{E}^{\mathrm{a}} + \bar{E}^{\mathrm{b}}| \quad \ldots \quad (3)$$

we can write equation (2) in the form

$$R(I^{\mathrm{a}}_{mn}/I^{\mathrm{b}}_{m'n'}) = D(E)\,R(T)/kT + R(C^{\mathrm{a}}_{mn}/C^{\mathrm{b}}_{m'n'}) \quad \ldots \quad (4)$$

According to equation (4) it should be mathematically possible to obtain a straight line with the direction coefficient $(1/kT)R(T)$ when $R(I^{\mathrm{a}}_{mn}/I^{\mathrm{b}}_{m'n'})$ is plotted *versus* $D(E)$ for all studied line pairs of the elements a and b. In equation (4) $R(C^{\mathrm{a}}_{mn}/C^{\mathrm{b}}_{m'n'})$ is independent of $R(T)$, the maximum relative temperature fluctuation, and is assumed to be constant. Large fluctuations coming from "bulk" effects due to changes in the instrumental parameters or sample densities will not affect the $R(C^{\mathrm{a}}_{mn}/C^{\mathrm{b}}_{m'n'})$ values very much. The concept of maximum relative fluctuation and its statistical implications are discussed in greater detail in reference 6.

By using a very stable ICP light source when making repeated intensity measurements of different iron lines with the IDES system, it was discovered that no linear structure was obtained with $D(E) = |E_m - E_{m'}|$ in equation (4). An example of this lack of linearity is shown by the circular points in the R - D graph in Fig. 1 of a "side-on" ICP. These points form a cloud with no linear structure. It was then discovered that when the R values of the intensity ratios were plotted *versus* $D(E) = |h\nu_{mn} - h\nu_{m'n'}|$ instead, the linear structure (triangular points) in Fig. 1 was obtained. Similar results were obtained earlier[6] using "end-on" and "side-on" ICPs in combination with different IDES spectrometer systems. These results show that the fluctuation data correlate much better to an intensity equation with a photon energy exponential than to the standard equation based on the assumption of LTE.

By studying R - D graphs for different element combinations, it was found that combinations from different elements (analysis line/analysis line or analysis line/iron line) show greater fluctuations than combinations from the same elements (iron line/iron line). Theoretical work[13,14] by Yngström led the author to apply the fluctuation analysis method to line pairs from different elements with $D(E) = |J^{\mathrm{a}} - J^{\mathrm{b}} + h\nu^{\mathrm{a}}_{mn} - h\nu^{\mathrm{b}}_{m'n'}|$ in equation (4) (where J is ionisation energy). It was then discovered that the data were organised linearly in the R - D plot with this expression for $D(E)$. This can be seen in Fig. 2 for an ICP measurement ("side-on"), where $R(I^{\mathrm{a}}_{mn}/I^{\mathrm{b}}_{m'n'})$ is plotted *versus* $D(E)$ for spectral line pairs from various element combinations. Note that the slope of the Fe lines ($J^{\mathrm{a}} - J^{\mathrm{b}} = 0$) is the same between the curves in Figs. 1 and 2. To illustrate the influence of $J^{\mathrm{a}} - J^{\mathrm{b}}$ in equation (4), a

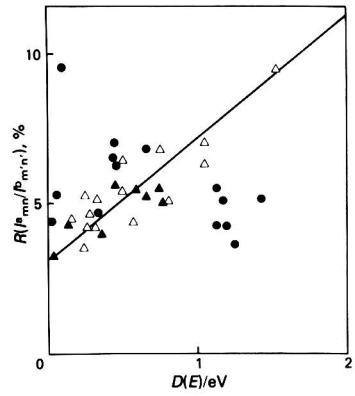

Fig. 1. Relative fluctuations of spectral line pair intensity ratios plotted *versus* $D(E) = |E_m - E_{m'}|$ (circles) and $D(E) = |h\nu_{mn} - h\nu_{m'n'}|$ (triangles) as defined in the text. This data set was obtained from 20 repeated measurements of Fe I line intensity ratios with a "side-on" ICP

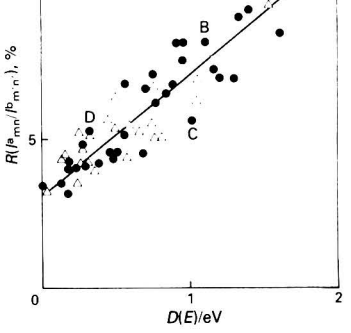

Fig. 2. Relative fluctuations of spectral line pair intensity ratios plotted *versus* $D(E) = |J^{\mathrm{a}} - J^{\mathrm{b}} + {}^{\mathrm{a}}h\nu_{mn} - {}^{\mathrm{b}}h\nu_{m'n'}|$ for a "side-on" ICP. The triangular points are the same as in Fig. 1. The circular points describe data from line pairs originating from two different kinds of metal atoms. These line pairs were selected from spectra of Cr, Mn, Fe, Co, Ni, Cu and Mo. The points A, B, C and D describe data from the line pairs Co 345.3 nm - Cr 425.4 nm, Cr 425.4 nm - Fe 427.1 nm, Ni 341.5 nm - Fe 516.7 nm and Mo 386.4 nm - Fe 516.7 nm, respectively. They represent positive and negative translations along the $D(E)$ axis in comparison with Fig. 3 and are described in the text

comparison between Figs. 2 and 3 has been made for different element combinations. In Fig. 3 $J^a - J^b$ has been put equal to zero for all element combinations. It can be seen that the circular points in Fig. 3 do not represent an ordered pattern as in Fig. 2, where a linear pattern is obvious with a good correlation coefficient ($r = 0.90$).

By using $D(E) = |E^a_m - E^b_{m'} - \bar{E}^a + \bar{E}^b|$ according to the standard intensity equation (1) instead, no linear relationship was obtained ($r = -0.17$), which is shown in Fig. 4 for the ICP. To illustrate the separation between the points in Fig. 3, four examples (points A, B, C and D) in these plots were chosen. Point A represents the combination between the line pair Co 345.3 nm - Cr 425.4 nm with $J^{Co} - J^{Cr} = 1.11$ eV, and point B represents the combination between Cr 425.4 nm - Fe 427.1 nm with $J^{Cr} - J^{Fe} = -1.10$ eV. These two examples illustrate large positive translations along the $D(E)$ axis, where the same element (Cr) has been combined with different elements. Points C and D represent the combination Ni 341.5 nm - Fe 516.7 nm and Mo 386.4 nm - Fe 516.7 nm, respectively, and illustrate negative translations along the $D(E)$ axis, where $J^{Ni} - J^{Fe} = -0.23$ eV and $J^{Mo} - J^{Fe} = -0.48$ eV.

The points in Fig. 2 were obtained from ten repeated analyses of NBS 363 on different occasions with the ICP light source at concentrations of 1 and 5 g per 100 ml ($n = 20$). This means that each point in Fig. 2 represents two concentrations. In this way the $D(E)$ dependence is more pronounced because the intensity ratio fluctuations are "collected" from two different samples with different concentrations and the mean value of $R(I^a_{mn}/I^b_{m'n'})$ is calculated and plotted *versus* $D(E)$. This means that each point in the graph has "collected" intensity ratio fluctuations from 20 repeated measurements. From this data set it is possible to compare the two exponents in the graphs. Again the data correlate badly to the old LTE equation (1) (see Fig. 4), whereas they show a good correlation to an intensity equation with the factor $\exp[-(J^a + h\nu^a_{mn})/kT]$.

Plots similar to that in Fig. 2 for the ICP are shown in Fig. 5 for a hollow-cathode lamp for flat metal samples. The data seem to follow a linear relationship as in Fig. 2, and indicate that it is possible to obtain such plots with other types of plasmas having different temperatures and plasma densities to those of the ICP.

By using $D(E) = |E^a_m - E^b_{m'} - \bar{E}^a + \bar{E}^b|$ according to the standard intensity equation (1) instead, one obtains for the FSHC lamp a non-linear plot (Fig. 6) similar to that in Fig. 4.

In the FSHC lamp a polished flat steel sample is sputtered together with a conical graphite electrode. Therefore, a very stable plasma is achieved. Two different steel samples (NBS 1261 and 1262) were run ten times each, which gave $n = 20$ for each point in Figs. 5 and 6. The spectral lines used in these analyses with the ICP and FSHC lamps are given in Table 2.

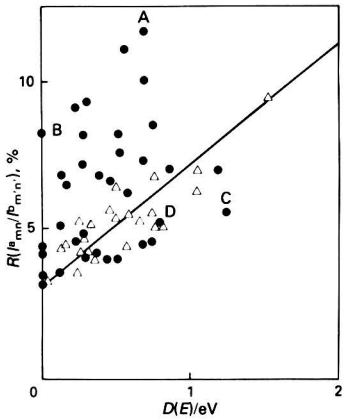

Fig. 3. Relative fluctuations of spectral line pair intensity ratios plotted *versus* $D(E) = |h\nu_{mn} - h\nu_{m'n'}|$ with the same spectral line data as used in Fig. 2 (ICP). This plot is an illustration of the fact that no linear relationship is obtained without the atomic part $J^a - J^b$ in $D(E)$

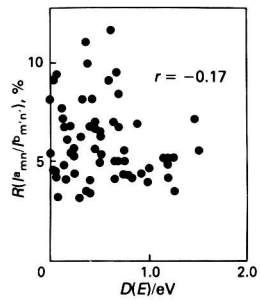

Fig. 4. Relative fluctuations of spectral line pair intensity ratios plotted *versus* $D(E) = |E^a_m - E^b_{m'} - \bar{E}^a + \bar{E}^b|$. The same spectral lines as in Fig. 2 (ICP) were used

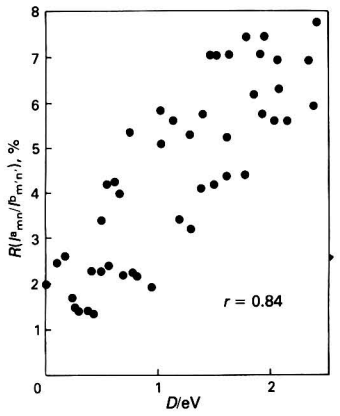

Fig. 5. R - D plot for the FSHC lamp. This figure should be compared with Fig. 2 with $D(E) = |J^a - J^b + h\nu^a_{mn} - h\nu^b_{m'n'}|$; it was obtained from 20 repeated measurements on two flat metal samples

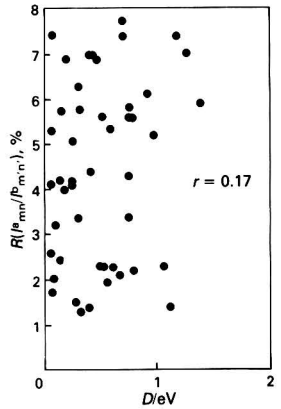

Fig. 6. Relative fluctuations of spectal line pair intensity ratios plotted versus $D(E) = |E^a_m - E^b_{m'}|$ for the FSHC lamp. As the contribution from the partition sum $(-\bar{E}^a + \bar{E}^b)$ is very small for this lamp, it can be neglected here

Table 2. Spectral lines used

Line	Wavelength/nm	Line	Wavelength/nm
Cu	324.754	Fe	385.991
Ni	341.477	Fe	344.061
Cr	425.433	Fe	323.622
Mn	403.449	Fe	516.749
Al	396.152	Fe	357.010
Al	309.284	Fe	427.176
Mo	386.411	Fe	392.291
Co	345.351	Fe	298.729

It is concluded from Figs. 2 and 5 that in analytical work it is necessary to select line pairs with $D(E)$ values as small as possible in order for them to be independent of temperature. This can easily be done with the IDES system, where line pairs with $D(E)$ values in the range 0.01–0.30 eV were selected without any difficulty because of the high resolution. In this way very good precision was obtained when various light sources and the IDES system were combined.

The results of this investigation show that linear relationships are obtained for various light sources and elements when using the exponent $\exp[-(h\nu^{a}_{mn} + J^{a})/kT]$ instead of the LTE-based factor $[\Sigma g_i \exp[-E^{a}_{i}/kT]^{-1}\exp(-E^{a}_{m}/kT)]$ in the spectral line intensity equation. These results are also in agreement with those of a recently published study by Thelin and Yngström[15] of absolute intensities from standard intensity tables for 17 elements.

The author thanks Dr. S. Yngström at KGI for valuable discussions and crucial theoretical suggestions and Prof. B. Hultqvist for his kind support of this project. The author also thanks the staff at the Swedish Institute for Metals Research in Stockholm for providing laboratory facilities.

References

1. Gerlach, W., *Z. Anorg. Allg. Chem.*, 1925, **142**, 383.
2. Barnett, W. B., Fassel, V. A., and Kniseley, R. N., *Spectrochim. Acta, Part B*, 1968, **23**, 643.
3. Suckewer, S., *Spectrochim. Acta, Part B*, 1971, **26**, 515.
4. Thelin, B., Preprint 063, Kiruna Geophysical Institute, Kiruna, Sweden, 1983.
5. Thelin, B., *ICP Inf. Newsl.*, 1985, **10**, 835.
6. Thelin, B., *Analyst*, 1986, **111**, 419.
7. Thelin, B., "Jernkontorets Forskning, Series D," Swedish Institute for Metals Research, Stockholm, 1981, No. 365.
8. Danielsson, L., and Thelin, B., "Proceedings of the Fourth Commission Europiénne d'Etude et d'Application de Travaux d'Analyse en Siderugie Meeting, Liege, Belgium, 1981".
9. Thelin, B., "Jernkontorets Forskning Series D," Swedish Institute for Metals Research, Stockholm, 1981, No. 355.
10. Thelin, B., *Analyst*, 1981, **106**, 54.
11. Danielsson, A., and Lindbolm, P., *Appl. Spectrosc.*, 1976, **30**, 151.
12. Meggers, W. F., Corliss, C. H., and Scribner, F., *Natl. Bur. Stand. (U.S.) Monogr.*, No. 32, Part I, 1961.
13. Yngström, S., and Thelin, B., Preprint 062, Kiruna Geophysical Institute, Kiruna, Sweden, 1983.
14. Yngström, S., *ICP Inf. Newsl.*, 1985, **10**, 818.
15. Thelin, B., and Yngström, S., *Spectrochim. Acta, Part B*, 1986, **41**, 403.

Paper A6/42
Received February 11th, 1986
Accepted October 27th, 1986

Determination of Tungsten in Ores and Concentrates by Atomic Absorption Spectrometry: Suppression of Atomisation Interferences from Calcium

Chow Chong* and Nik Meriam
Geological Survey Laboratory, Scrivenor Road, P.O. Box 1015, 30820 Ipoh, Perak, Malaysia

A simple and rapid method for the determination of tungsten in ores and concentrates by atomic absorption spectrometry is described. A dinitrogen oxide - acetylene flame was used and the absorbance was measured at 400.9 nm. The samples were decomposed using fused potassium hydrogen sulphate, which was found to be a suitable flux for opening tungsten minerals. The potassium hydrogen sulphate also proved to be a powerful enhancing agent for the tungsten absorbance signal while eliminating many reported interferences. Eighteen elements were examined for interferences and only calcium was found to interfere seriously when present in concentrations greater than 0.1 mg per 100 ml. The depressive effect of calcium could be easily suppressed and the absorbance signal wholly restored to the original level by the addition of a sodium silicate solution such that the minimum ratio of the concentration of Si : Ca was 1.5 : 1. The method has been applied to the determination of tungsten in wolframite, scheelite, wolframite - cassiterite and heavy mineral stream concentrate samples.

Keywords: *Tungsten determination; atomic absorption spectrometry; calcium interferences; ores; concentrates*

In this laboratory the determination of tungsten as a major constituent in ores and concentrates is carried out by using a classical gravimetric method[1] involving the precipitation of tungstic acid with cinchonine followed by subsequent ignition to tungsten trioxide. For samples containing low levels of tungsten, the spectrophotometric method based on the extraction of a tungsten - dithiol complex into amyl acetate[2] is used. These procedures are time consuming, tedious and unsuitable for large numbers of samples. In addition, they are subject to interferences, particularly from niobium, tantalum, titanium and molybdenum in the former instance and from molybdenum in the latter.

In general, atomic absorption spectrometric methods for the determination of tungsten have poor sensitivity[3] and suffer from interferences[4,5] by a large number of cations. Various techniques[4,6-10] have been developed to overcome these limitations. Recently, Roy and Das[6] determined tungsten in rocks and minerals by the chelate extraction of tungsten with *N*-benzoylphenylhydroxylamine in toluene followed by atomic absorption spectrometry. Edger[5] and Raoot *et al.*[11] used sodium sulphate and potassium persulphate, respectively, for the dual purpose of enhancing the tungsten absorbance signal and to act as releasing agents in the atomic absorption spectrometric determination of tungsten in alloys, ores and concentrates. Sprenz and Prager[12] determined tungsten in ores and concentrates using sodium carbonate fusion followed by the addition of sodium sulphate to eliminate interferences.

This paper describes a simple and rapid atomic absorption spectrometric method for the determination of tungsten in ores and concentrates using potassium hydrogen sulphate as a flux for opening up the sample and to enhance the tungsten absorbance signal and release it from interferences. Eighteen cations tested at various concentrations were found not to interfere in the determination. However, calcium in concentrations greater than 0.1 mg per 100 ml very seriously depressed the tungsten absorbance signal. It was found that the absorbance depression by calcium could be completely eliminated and the absorbance restored to its original value by the addition of a sodium silicate solution.

* To whom correspondence should be addressed.

Experimental

Apparatus

A Varian Techtron Model AA 875 atomic absorption spectrometer, equipped with a 6-cm dinitrogen oxide - acetylene burner was used for all measurements. A standard hollow-cathode tungsten lamp was used as a line source. A reducing fuel-rich dinitrogen oxide - acetylene flame was used in all absorbance measurements with the dinitrogen oxide and acetylene flows set at 24 and 88, respectively. These settings are equivalent to flow-rates of 10 and 5.5 l min^{-1}, respectively, according to the manufacturer's operating manual. The aspiration rate was 6 ml min^{-1} and the absorbance read-out integration time was 2 s. Other conditions were: lamp current, 20 mA; wavelength, 400.9 nm; spectral band pass, 0.5 nm; and burner height, 10 mm.

Reagents

Tungsten standard solution, 1000 μg ml^{-1}. Prepared by fusing 0.6305 g of Specpure tungsten trioxide (WO_3) (Johnson Matthey Chemicals) with 5 g of sodium hydroxide over a Bunsen burner flame in a platinum crucible. The melt was dissolved in water and accurately diluted to 500 ml with distilled water.

Calcium solution, 1 mg ml^{-1}. Prepared by dissolving 1.38 g of $CaCl_2$ (Merck Chemicals) in distilled water and diluting to 500 ml.

Sodium silicate solution, 1% *m/V*. Prepared by dissolving 12.7 ml of sodium silicate solution (BDH Chemicals) of density 1.57 g ml^{-1} in distilled water and diluting to 2 l. On standardisation the solution was found to contain 1.49 mg ml^{-1} of Si.

Tartaric acid solution, 10% *m/V*. Prepared by dissolving 50 g of (+)-tartaric acid (AnalaR grade) in distilled water and diluting to 500 ml.

Fused potassium hydrogen sulphate, solid. Prepared by heating potassium hydrogen sulphate ($KHSO_4$, pro analysi, Merck Chemicals) over a Bunsen burner flame in a silica dish until completely melted. The solid was cooled, broken into small pieces using a pestle and mortar and was stored in an air-tight bottle. Water was removed in order to obtain a quiet fusion without any loss of sample through spattering.

Calibration Graph

Pipette 5, 10, 15, 20, 25 and 30 ml of the tungsten standard solution into a series of 100-ml calibrated flasks. Add 10 ml of 10% tartaric acid solution to each flask followed by 5 ml of potassium hydrogen sulphate solution (containing 1 g of $KHSO_4$). Dilute accurately to the mark with distilled water and prepare a blank in the same manner. These solutions are then aspirated into the spectrometer in the absorbance mode under the described conditions. A typical calibration graph is shown in Fig. 1.

Procedure

Determination of tungsten in ores and concentrates

Accurately weigh 0.1–0.25 g (depending on the tungsten content) of the finely ground sample into a silica crucible. Fuse the sample over a Bunsen burner flame with 1 g of fused potassium hydrogen sulphate for about 30–40 min. Start with a very low flame until all the potassium hydrogen sulphate has melted and then slowly increase the intensity of the flame to medium strength. After fusion and cooling, pour 10 ml of 10% tartaric acid solution into the crucible. The tartaric acid prevents the precipitation of any tungsten and other elements. With the lid on, carefully warm the contents of the crucible on a thin asbestos sheet on a hot-plate to dislodge the cake and occasionally stir the cake with a glass rod to help dislodge it. Transfer the contents of the crucible into a 100-ml beaker with distilled water and warm over the hot-plate to dissolve the cake completely. Add a little paper pulp and filter (Whatman No. 40, 9 cm) into a 100-ml calibrated flask. Wash the beaker and the residue with distilled water. Dilute to the mark and measure the absorbance under the described conditions.

For samples of unknown composition which are suspected to contain calcium, a rough determination of the calcium content is required. This is to permit the addition of a suitable volume of 1% sodium silicate solution to the sample solution in order to obtain the minimum ratio of Si:Ca required (1.5:1). For scheelite concentrates ($CaWO_4$), take a suitable aliquot from the 100-ml sample solution and dilute to the desired volume after adding the appropriate amount of sodium silicate, potassium hydrogen sulphate and tartaric acid solutions. The sodium silicate solution should be added to give a Si:Ca ratio of 1.5:1, and the other two reagents should have concentrations adjusted to match the calibration standards. Scheelite samples from a particular source usually show no great variation in the calcium content. Hence, if the calcium content of one sample is known, it is possible to approximate its concentration in other samples. If approximation is not possible, pre-analysis for calcium is required.

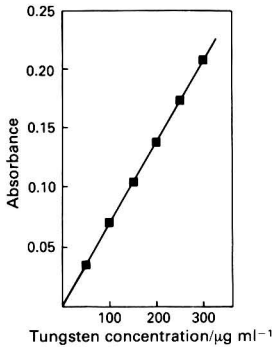

Fig. 1. Typical calibration graph for tungsten. Correlation coefficient = 0.9999. Regression equation: $y = 0.0007x - 0.0001$

Results and Discussion

Enhancement Effect

At the 100 μg ml^{-1} tungsten level, the addition of potassium hydrogen sulphate raised the absorbance reading from 0.030 to 0.069. This was an enhancement of about 130% compared with the 46% enhancement at the 100 μg ml^{-1} tungsten level obtained by Edger[5] using sodium sulphate in acidic medium at 255.1 nm and the 75% enhancement obtained at the 400 μg ml^{-1} tungsten level obtained by Raoot *et al.*[11] using potassium persulphate in alkaline medium at 400.9 nm. Under our experimental conditions, it was observed that potassium persulphate gave an improvement of about 120% in the 100 μg ml^{-1} tungsten absorbance signal. The enhancement in absorbance for other tungsten concentrations can be seen in Fig. 2.

The general enhancement of the tungsten absorbance signal by sodium sulphate, potassium persulphate and potassium hydrogen sulphate seems to suggest that the sulphate anion is one of the necessary and preferential enhancing agents. Tests were carried out using sulphuric acid or potassium chloride in place of potassium hydrogen sulphate. It was found that sulphuric acid gave an enhancement equal to that given by potassium hydrogen sulphate, whereas the enhancement obtained with potassium chloride was much lower (Fig. 2). Hence the sulphate anion is a better enhancing agent than the potassium cation. Further tests were carried out using inorganic sulphate salts such as $NiSO_4.6H_2O$, $MgSO_4.7H_2O$, $LiSO_4.H_2O$, $MnSO_4.H_2O$ and K_2SO_4 in amounts giving a sulphate concentration equal to that given by 1 g of $KHSO_4$. It was found that all these salts enhanced the signal of the 100 μg ml^{-1} tungsten solution to a level similar or equal to that given by potassium hydrogen sulphate. One possible explanation of this phenomenon is similar to that advanced by Price[13] for the enhancement of the rhodium signal. Under the reducing conditions of the dinitrogen oxide - acetylene flame, some of the sodium tungstate is reduced to tungsten metal, which has a boiling-point of greater than 5900 °C. Such a high vaporisation temperature is not achieved in a dinitrogen oxide - acetylene flame, thus leading to incomplete atomisation. In the presence of sulphate anions, the formation of metallic tungsten clotlets is prevented. A reaction between the free tungsten atoms and the solid solution of sulphate particles may occur. As the solid solution is vaporised in the flame, the tungsten atoms are released as an atomic vapour.

In this work we used 1 g of potassium hydrogen sulphate as a standard amount but the addition of 0.5 or 2 g of potassium hydrogen sulphate had no adverse effect on the tungsten absorbance. The presence of 10 ml of 10% tartaric acid also had no adverse effect.

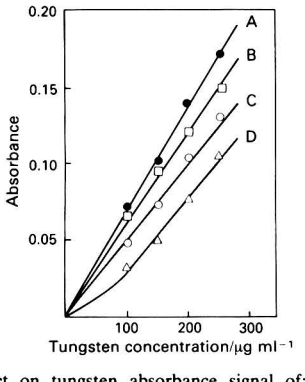

Fig. 2. Effect on tungsten absorbance signal of: A, 1% *m/V* potassium hydrogen sulphate or 0.4% *V/V* sulphuric acid; B, 0.1% *m/V* potassium persulphate; C, 0.57% *m/V* potassium chloride; and D, direct dilution from tungsten stock solution

Interferences

Eighteen elements were investigated for interference effects at various concentrations (Table 1). It was observed that in the presence of potassium hydrogen sulphate as a releasing agent, only calcium at concentrations greater than 0.1 mg per 100 ml interfered with tungsten by seriously depressing the absorbance signal (Fig. 3). A similar interference was observed by Sprenz and Prager[12] who overcame the problem by fusing the sample with sodium carbonate yielding calcium carbonate which is insoluble in basic media. In this work it was found that the calcium interference could be completely eliminated and the tungsten absorbance wholly restored to its original value by the addition of a 1% sodium silicate solution such that the minimum ratio of Si to Ca was about 1.5:1 (Fig. 4). One explanation of the depression of the tungsten absorbance by calcium was the formation of a refractory calcium tungstate compound in the flame that inhibited the release of tungsten atoms. It is suggested that sodium silicate competes with tungsten for calcium atoms forming the more stable calcium silicate and releasing the tungsten as free atoms.

The effect of 18 selected cations on a 100 μg ml^{-1} tungsten solution is shown in Table 1. These cations were selected on the basis that they are likely to be present in major or minor amounts in most samples containing tungsten. The tolerance limit listed in this table was set as the amount of foreign cation causing a ±2% error in the determination of tungsten. The salts used in this study were dissolved in a fixed volume of tartaric acid, if they were soluble. If they were insoluble in tartaric acid, the salts were fused with a fixed mass of fused potassium hydrogen sulphate and subsequently dissolved in a fixed volume of tartaric acid. The concentrations of tungsten, potassium hydrogen sulphate and tartaric acid in all solutions analysed as part of this interference study were matched with the standard tungsten solution.

Table 1. Effect of foreign ions. Amount of W taken = 100 p.p.m. Some of these tolerance limits are not likely to be exceeded in routine analytical applications but they indicate the potentiality of the method in other applications

Foreign ion	Added as	Tolerance limit/mg
Al^{3+}	$AlCl_3.6H_2O$	200
Ti^{4+}	TiO_2	200
Fe^{3+}	Fe_2O_3	200
Mn^{2+}	$MnSO_4.H_2O$	200
Nb^{5+}	Nb_2O_5	100
Ta^{5+}	Ta_2O_5	5
Mo^{6+}	MoO_3	200
Sb^{3+}	Sb_2O_3	200
Ni^{2+}	$(CH_3COO)_2Ni.4H_2O$	50
Bi^{3+}	Bi_2O_3	50
Mg^{2+}	$MgSO_4.7H_2O$	200
Pb^{2+}	$Pb(NO_3)_2$	2
Co^{2+}	$(CH_3COO)_2Co.4H_2O$	200
Ag^{+}	$AgNO_3$	200
Zn^{2+}	$(CH_3COO)_2Zn.2H_2O$	50
Cu^{2+}	$CuSO_4.5H_2O$	200
Sn^{2+}	$SnCl_2.2H_2O$	100
Ca^{2+}	$CaCl_2$	0.1

Table 2. Determination of tungsten in ores and concentrates

Sample	Tungsten, % Present method	Other methods
Wolframite	29.7	29.8*
Scheelite	59.5	59.4*
Scheelite rock	1.00	1.00†
Wolframite - cassiterite (Sn, 60.7%)	1.43	1.46†
Wolframite - cassiterite (Sn, 6.7%)	0.69	0.71†
Stream concentrate	0.88	0.86†
Stream concentrate	0.40	0.37†

* Gravimetric method, reference 1.
† Spectrophotometric method, reference 2.

Analysis of Ores and Concentrates

The proposed method has been applied to the analysis of a number of tungsten-bearing minerals, ores and concentrates and the results are as shown in Table 2. It can be seen that they agree well with those obtained by the spectrophotometric and classical gravimetric methods. Problems arising from a depression in absorbance by the presence of calcium, as occurs in samples containing scheelite, have been successfully eliminated.

Recovery Test

In order to test the validity of the proposed method, the standard additions method was used. Ten separate 0.10-g samples from a wolframite ore were accurately weighed and analysed by the proposed procedure. To each of five of these were added 10.000 mg of tungsten solution before diluting to the mark. Table 3 shows the recovery and precision results obtained. The recoveries ranged from 90 to 100% and the relative standard deviation of 4.2% shows that the proposed method has good reproducibility.

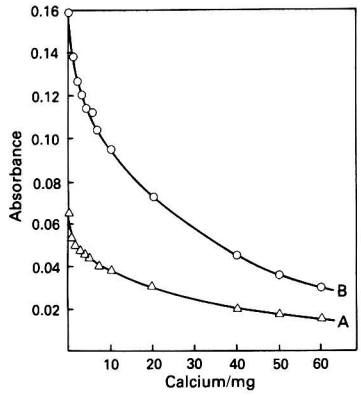

Fig. 3. Effect of calcium on tungsten absorbance. A, 100 p.p.m.W; B, 250 p.p.m. W

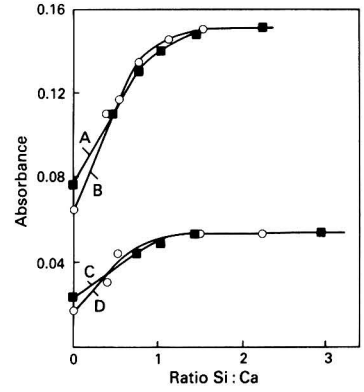

Fig. 4. Effect of silica on calcium interference in tungsten absorbance. A, 250 p.p.m. W, 10 mg of Ca; B, 250 p.p.m. W, 20 mg of Ca; C, 100 p.p.m. W, 10 mg of Ca; D, 100 p.p.m. W, 20 mg of Ca

Table 3. Determination and recovery of tungsten from 0.1 g of sample

W in sample/mg	W added to sample/mg	Total W found/mg	W recovered/ mg	Recovery, %
30.000	10.000	39.500	9.500	95
30.000	10.000	39.000	9.000	90
29.700	10.000	39.500	9.800	98
29.500	10.000	39.500	10.000	100
29.500	10.000	39.500	10.000	100
	Mean			9.660 mg
	Standard deviation			0.422 mg
	RSD, %			4.2

Conclusion

Potassium hydrogen sulphate has been shown to be an effective flux and also a powerful enhancing and releasing agent in the determination of tungsten in ores and concentrates. If a sodium silicate solution is added to suppress calcium interferences, the method is free of interferences and is applicable to most tungsten ores and concentrates.

We thank the Director-General of the Geological Survey, Malaysia, for his permission to publish this paper.

References

1. Li, K. C., and Wang, C. Y., "Tungsten, Its History, Geology, Ore-Dressing, Metallurgy, Chemistry, Analysis, Applications, and Economics," Chapman and Hall, London, 1955, p. 314.
2. Elwell, W. T., and Wood, D. F., "Analytical Chemistry of Molybdenum and Tungsten," Pergamon Press, Oxford, 1971, p. 116.
3. Manning, D. C., *At. Absorpt. Newsl.*, 1966, **5**, 127.
4. Rooney, R. C., and Pratt, C. G., *Analyst*, 1972, **97**, 400.
5. Edger, R. M., *Anal. Chem.*, 1976, **48**, 1653.
6. Roy, N. K., and Das, A. K., *Talanta*, 1986, **33**, 277.
7. Rao, P. D., *At. Absorpt. Newsl.*, 1970, **9**, 131.
8. Yudelevich, I. G., and Shabrova, N. P., *Chemist Analyst*, 1974, **19**, 941.
9. Welcher, G. G., and Kriege, O. H., *At. Absorpt. Newsl.*, 1969, **8**, 97.
10. Husler, J., *At. Absorpt. Newsl.*, 1971, **10**, 60.
11. Raoot, S., Athavale, S. V., and Rao, T. H., *Analyst*, 1986, **111**, 115.
12. Sprenz, E. C., and Prager, M. J., *Analyst*, 1981, **106**, 1210.
13. Price, W. J., "Analytical Atomic Absorption Spectrometry," Heyden, New York, 1974, p. 90.

Paper A6/397
Received October 20th, 1986
Accepted December 15th, 1986

Determination of Low Concentrations of Tungsten and Molybdenum in Geological Materials Using Inductively Coupled Plasma Atomic Emission Spectrometry with Pre-concentration on Activated Charcoal*

Gwendy E. M. Hall, Jean-Claude Pelchat and K. Nimalasiri de Silva
Geological Survey of Canada, 601 Booth Street, Ottawa, Ontario K1A 0E8, Canada

A practical and efficient method is described for the determination of W and Mo at concentrations of 0.5–100 μg g^{-1} in geological materials. The sample is first decomposed by alkaline fusion with sodium carbonate - sodium nitrate and the melt is leached with water to solubilise the elements as their oxy-anions. Concentration and separation of the analytes are achieved by selective adsorption of their 8-hydroxyquinolinates on to activated charcoal, which is then ashed and the metals solubilised. The acidic solution is analysed by inductively coupled plasma atomic emission spectrometry. The application of this method to determine levels as low as 0.4 μg g^{-1} of W and 0.2 μg g^{-1} of Mo is demonstrated by the analysis of 22 international reference materials.

Keywords: *Tungsten determination; molybdenum determination; pre-concentration on activated charcoal; inductively coupled plasma atomic emission spectrometry; geological materials*

The application of inductively coupled plasma atomic emission spectrometry (ICP-AES) to the determination of W and Mo in geological materials has so far been limited as these elements are normally present in igneous and sedimentary rocks at levels below 5 μg g^{-1}, too low to be measured directly by ICP-AES.[1] For example, inadequate determination limits of 7 μg g^{-1} for W and 3 μg g^{-1} for Mo have been reported by Church[2] in a multi-element analytical scheme in which a 1-g sample is decomposed by a mixture of acids (HF + $HClO_4$ + HNO_3) and diluted by a factor of 100 prior to nebulisation into the ICP. Brenner and Erlich[3] reported a rapid and efficient method of determining W by ICP-AES but the element was present at the percent. level in the ores, concentrates and alloys analysed.

Most methods capable of determining these elements at low levels have been based on two techniques, *i.e.*, spectrophotometry and neutron activation. In the former technique, the complexing agents most frequently used are dithiol[4,5] and thiocyanate.[6,7] Although detection limits as low as 0.1 μg g^{-1} have been reported for both elements,[4] the steps taken to ensure selectivity and sensitivity are numerous and the analysis of one solution for both elements is impossible as they mutually interfere. Similarly, methods based on the latter technique,[8–10] neutron activation, require complex radiochemical procedures to minimise interferences. However, very low detection limits, such as 0.01 μg g^{-1} for W[9] and 0.04 μg g^{-1} for Mo,[10] have been attained.

Leinz and Grimes[11] reported a determination limit of 0.2 μg g^{-1} for W using an emission spectrographic (d.c. arc) method. The sample was first fused with KOH and W was then separated from the aqueous leach by complexation with thiocyanate and extraction into ether. The solution was pipetted into a graphite electrode and the emission spectrum recorded on film for visual measurement. Thompson and Zao[12] have devised a procedure capable of detecting Mo at levels down to 0.06 μg g^{-1} by ICP-AES in soils, sediments and rocks. The sample was decomposed in 6 M HCl at 120 °C (Br_2 was added to oxidise the sulphide minerals) and the analyte was extracted under optimum conditions into heptan-2-one for subsequent nebulisation into the ICP.

A method of determining B in rocks and sediments by ICP-AES was recently developed at the Geological Survey of Canada[13] and it was shown that the procedure could also be used to determine W down to 5 μg g^{-1} and Mo down to 2 μg g^{-1}. Briefly, a 200-mg sample is fused with 1 g of a 5 + 1 mixture of Na_2CO_3 - $NaNO_3$ and the melt is leached with water to solubilise the analytes as their oxy-anions. The solution presented to the ICP for analysis contains about 4% dissolved salts and the sample dilution factor is 125. Thus, in order to lower the detection levels for these elements, a means of concentration and separation from this high salt matrix is required. Recent success[14] in this laboratory in the use of activated charcoal as a medium to separate Au led the authors to investigate its application to the separation of W and Mo from a Na_2CO_3 matrix.

In an attempt to pre-concentrate about 20 trace metals in waters by adsorption on to activated charcoal, Vanderborght and Van Grieken[15] measured the adsorption isotherms of 8-hydroxyquinoline and several metal 8-hydroxyquinolinates. It was clearly shown that the adsorption of metal 8-hydroxyquinolinates is much more effective than the adsorption of free ions and the steepness of the isotherms indicated that the collection of 8-hydroxyquinolinates at low initial concentrations would be more efficient than that for free metal ions. As 8-hydroxyquinolinate molecules are not formed with the alkali and alkaline earth elements to any significant extent, effective separation and enrichment of the heavy metals were achieved, with recoveries in the range 85–100% at pH 8. A later publication[16] described the pre-concentration of W and Mo in chloralkali brines by chelation with 8-hydroxyquinoline and adsorption on to activated charcoal at pH 5–6 over an equilibration time of 3 h; the filtered charcoal was then analysed by X-ray fluorescence. The application of such a separation technique appeared desirable in this study as the Na^+ ions originating from the flux would not be appreciably adsorbed. The optimum conditions for the efficient separation and concentration of W and Mo from the alkaline leach were investigated in this work and a procedure was designed to recover these elements from the charcoal in a minimum volume of solution amenable to analysis by ICP-AES. Internal standardisation with scandium was pursued in an attempt to improve the precision of measurement obtained by ICP-AES. Twenty-two international reference materials were analysed by the proposed procedure.

Experimental

Reagents

De-ionised, distilled water was used throughout. Sodium carbonate, sodium nitrate, hydrochloric acid, 8-hydroxyquinoline and ethanol were all of Baker Analyzed

* GSC contribution 52786.

reagent grade. The activated charcoal (Darco, G-60) was obtained from Matheson, Coleman and Bell, Cleveland, OH, USA. Standard stock solutions of 1000 μg ml^{-1} of W and Mo were obtained from Spex Industries, Metuchen, NJ, USA. All glassware was washed in 30% nitric acid and repeatedly rinsed with de-ionised, distilled water.

Instrumentation

A Jobin-Yvon (ISA, Metuchen, NJ, USA) Model 38 high resolution sequential ICP atomic emission spectrometer was used. Details of the instrumentation and operating conditions are given in Table 1. The path from the viewing zone of the argon plasma to the entrance of the spectrometer, and the spectrometer itself, was flushed with nitrogen, allowing the measurement of emission in the low ultraviolet region of the spectrum. The nebuliser gas flow was regulated with a mass flow controller for better precision and a humidifier was used with the nebuliser.

Procedure

Preliminary investigation of separation procedure

The synthetic solution to be used in the recovery studies was prepared by spiking 30-ml volumes of aqueous leaches of fused blank ($Na_2CO_3 + NaNO_3$) with aliquots of standard W and Mo solutions (as sodium tungstate and ammonium molybdate) such that the final concentration of analyte to be measured was 1.0 μg ml^{-1}. The following parameters were then investigated: (a) the amount of 8-hydroxyquinoline in ethanol (25 mg ml^{-1}) added; (b) the amount of activated charcoal added; (c) the pH adjustment of the aqueous leachate; (d) the time of stirring; (e) the ashing temperature; and (f) the final dissolution medium.

In order to study the effect of pH, excess amounts of 8-hydroxyquinoline (2 ml of 25 mg ml^{-1}) and charcoal (300 mg) were added and the stirring time was longer than that reasonably required (2 h). The ashing temperature chosen was the minimum required to achieve a clean ash and maintain an acceptable recovery of W and Mo. Three reagents were tested for their ability to solubilise W and Mo in the ash: potassium hydroxide solution, nitric acid and hydrochloric acid. The final volume was kept to 5 ml, thus producing a dilution factor of 25 based on a 200 mg sample mass. The international reference materials GXR-4 and GSD-6 were used to verify the results obtained with the synthetic solutions. These were chosen because their W and Mo contents are higher than the concentrations for which this method was being designed and, hence, they would indicate deficiencies in the amounts of reagents used. The recoveries were measured against synthetic solutions made up in the medium under investigation in the final dissolution step.

Recommended procedure

Mix 200 mg of sample with 1 g of Na_2CO_3 - $NaNO_3$ (5 + 1) flux in a nickel crucible and fuse at 870 °C for 15 min. Leach the melt with 10 ml of H_2O and let it stand overnight, and then transfer the contents of the crucible, with warming, into a test-tube. Rinse the crucible with 10 ml of H_2O. Heat the test-tube in a hot water-bath at 90 °C for 1 h with frequent shaking. After cooling, centrifuge and decant the clear solution into a 50-ml beaker. Add about 10 ml of H_2O and adjust the pH to 1.5–2.0 with HCl (initially with 12 M HCl, and then with 1.2 M HCl). With the volume at about 45 ml, add 1 ml of 8-hydroxyquinoline dissolved in ethanol (25 mg ml^{-1}) and 200 mg of activated charcoal. Stir for 1 h with a magnetic stirrer. Filter off the activated charcoal residue through a 0.45-μm membrane filter (Millipore, HAWP) under vacuum and transfer into a porcelain crucible. Ash at 650 °C for 2 h. Transfer the ash into a calibrated test-tube. Rinse the crucible, first with 0.5 ml of 12 M HCl and then with about 1 ml of H_2O and add the washings to the test-tube. Heat the test-tube and contents for several minutes with shaking. After cooling, adjust to approximately 4 ml with H_2O and centrifuge. Decant the solution and make up to 5 ml with H_2O. Analyse this final solution by ICP-AES.

Calibration

Blanks and calibration standards, in duplicate, were taken through procedures identical to the sample decomposition and separation using Eppendorf microlitre pipettes to deliver accurate amounts of standard stock solutions directly on to the flux itself. Aliquots of standard solutions were chosen such that they would be equivalent to 0, 2.5, 5.0, 10.0 and 50.0 μg g^{-1} W or Mo in the original sample. Three measurements for each solution were taken and the relative standard deviation (RSD) recorded.

Analysis of International Reference Materials

Twenty-two reference materials from the US Geological Survey (USGS), the Canadian Certified Reference Materials Project (CCRMP) and the Institute of Geophysical and Geochemical Prospecting, China (IGGE) were analysed by the proposed method. Four separate decompositions were carried out for each sample at random intervals over a 3-month period.

Results and Discussion

Sample Preparation Procedure

The recovery of W and Mo was not significantly affected by the following experimental conditions: 0.5, 1.0, 2.0 and 3.0 ml of 8-hydroxyquinoline; 150, 200, 250 and 300 mg of activated charcoal; and 0.5, 1.0 and 2.0 h of stirring. Thus, the values

Table 1. Hardware and operating conditions of inductively coupled plasma atomic emission spectrometer

Inductively coupled plasma:	
RF generator	2.5 kW, frequency 27.12 MHz
Nebuliser	Meinhard C concentric glass
Spray chamber	Scott-type
Torch	JY de-mountable quartz
Observation zone	12 mm above initial radiation zone
RF power	1.05 kW
Plasma Ar flow-rate	13 l min^{-1}
Auxiliary Ar flow-rate	0.15 l min^{-1}
Nebuliser pressure	38 lb in^{-2}
Solution uptake rate	1.4 ml min^{-1}
Atomic emission spectrometer:	
Slit widths	Entrance, exit = 50 μm
Grating	Holographic, 3600 grooves mm^{-1}
Wavelengths	Mo II 202.030 nm with background correction at −0.016 nm and +0.019 nm W II 207.911 nm with background correction at +0.024 nm
Data acquisition parameters	Integration time = 500 ms, three measurements on each solution

Table 2. Recovery of 5 μg of W in the ash using a variety of dissolution reagents. Final volume made up to 5 ml with H_2O

Dissolution reagent	W recovered, %
2 ml of 2 M KOH	73
2 ml of 1 M KOH	71
5 ml of 0.1 M HNO_3	63
5 ml of 1 M HNO_3	61
5 ml of 0.5 M HNO_3	69
1 ml of 12 M HCl	98
0.5 ml of 12 M HCl	93

cited in the recommended procedure were selected as optimum. However, both the pH of the analyte solution in the adsorption step and the reagent used in the dissolution of the ash were found to be highly critical.

At a pH of 2 for the separation stage, various concentrations of KOH, HNO_3 and HCl were investigated for their ability to dissolve W in the ash with heating. Mo was not considered to be as problematic as W, the latter being known to precipitate out as the white α-acid, $WO_3.2\,H_2O$, or the yellow β-modification, $WO_3.H_2O$. The results shown in Table 2 clearly indicate that dissolution in 1 ml of 12 M HCl with subsequent dilution to 5 ml achieves the maximum recovery of W. This solution was found to be stable over a 7-d period. The poor recovery exhibited by the use of the alkaline solution is surprising and, indeed, the contrasting good recovery using HCl was unexpected. It is possible that W is converted to its carbide form during ashing and this is more easily dissolved in concentrated HCl. The aqueous blank leachate was spiked with increasing amounts of W to determine the point at which the solubility of the W species would be exceeded under these dissolution conditions (1 ml of 12 M HCl diluted to 5 ml). The point at which the recovery became low was on the addition of 100 μg of W, equivalent to 500 μg g^{-1} of W in the original sample, much higher than necessary in light of the objective of this work. Studies carried out in duplicate for both elements in the low concentration range, equivalent to 2.5, 5.0 and 10.0 μg g^{-1} in the sample, resulted in recoveries of 97 ± 2% for W and 98 ± 2% for Mo.

Using the above recommended dissolution procedure, the pH of the aqueous blank leachate containing 5 μg of W and 5 μg of Mo was varied from 0.8 to 7 and the recoveries measured. The results obtained are shown graphically in Fig. 1. There is a dramatic decrease in recovery for both elements from a plateau region of about 96–99% at pH 1–3 to less than 40% above pH 5. This is further evidenced by the results shown in Table 3 for reference materials GXR-4 and GSD-6 at pH values of 1.5 and 5.0. This phenomenon of the critical effect of pH is in sharp contrast to the work described by Verbeeck *et al.*[16] where the natural pH of 5–6 in brines was used; however, low results were reported for Mo and W in brines spiked to levels of 100 μg l^{-1} or more. Thus, a pH range of 1.5–2.0 was chosen for further determinations. At this pH, a concentration of only 3 μg ml^{-1} of Na was detected in the final solution, indicating the effective separation of the analytes from the solubilised salt matrix of the flux.

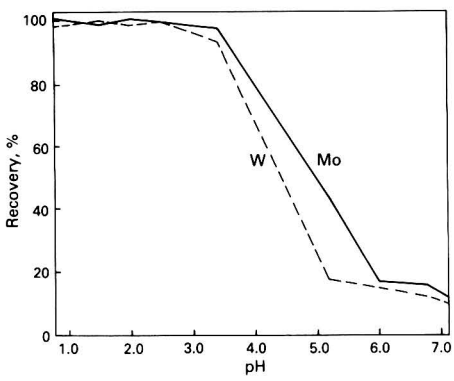

Fig. 1. Effect of pH in the separation procedure on the recoveries of W and Mo. Recoveries were measured at the following pH values: 0.8, 1.0, 1.5, 2.0, 2.5, 3.4, 5.2, 6.0, 6.8 and 7.1

The critical effect of pH on the separation of W and Mo by adsorption of their 8-hydroxyquinolinates on to activated charcoal prevents the application of this method to the determination of other elements such as Cr and V in the same solution. Recoveries at pH 1.5 for these elements were in the range 65–70% (measured with synthetic solutions, GXR-1, GXR-4, and GSD-6), whereas recoveries at pH 5 were 100 and 85% for Cr and V, respectively.

The blank values for W and Mo were consistent and were found to be equivalent to 0.3 and 0.7 μg g^{-1}, respectively, contributed by the activated charcoal and flux. Care must be taken when changing to a new batch of reagent as the contamination level can alter significantly. Methods to reduce these blank levels of W and Mo by clean-up of the reagents are currently under investigation.

Analytical Results for the International Reference Materials

The results of four separate analyses of 22 international reference materials by the proposed method are shown in Table 4. In general, the values obtained agree well with the literature values cited, with only a few exceptions. The W content of GXR-6 determined by this method appears high, whereas that for SCo-1 and for STM-1 seem low. However, these comparison values are mostly obtained from individual spectrophotometric or neutron activation methods and are not recommended values, as are those for the GSD series where agreement is excellent for W. The results obtained for Mo are slightly low for SCo-1 and high for SY-3. The concentration of 1.3 μg g^{-1} of Mo for SCo-1 lies between the 1.69 μg g^{-1} value reported by Aruscavage and Campbell[20] and 1.15 μg g^{-1} quoted by Terashima.[4]

As noted by Thompson and Zao[12] in the validation of their procedure to determine Mo at low levels in geological materials, interpretation of the data is impeded by the absence of certified results on reference materials for these elements. Only the IGGE standard samples, the GSD series of stream sediments, in Table 4 have recommended values with associated standard deviations. Thus, based on the good agreement between these sets of data for Mo and W, it can be concluded that the proposed method should provide accurate results. Validation of the ICP-AES determination has been carried out in-house by comparison with results obtained on the same sample solutions by ICP-MS. This study is included in a separate publication.[21]

Precision and Determination Limit

The precision, expressed as the RSD, of the over-all analytical procedure is shown in Table 4 for the international reference materials; the RSD is based on four separate decompositions. This value generally increases towards the determination limit for both W and Mo but also varies slightly from one sample to another at approximately the same concentration, probably

Table 3. Results of analyses of GXR-4 and GSD-6. Effect of pH in the separation procedure with activated charcoal.

	W/μg g^{-1}			Mo/μg g^{-1}		
Sample	This method, pH 1.5	This method, pH 5.0	Literature value[13]	This method, pH 1.5	This method, pH 5.0	Literature value[13]
GXR-4 (copper mill-head) . .	32.4/30.9	13.1/10.2	31	314/312	194/209	311
GSD-6 (stream sediment)	25.1/25.9	9.8/6.4	26	8.0/7.9	3.2/2.8	8.1

Table 4. Tungsten and molybdenum concentrations in international reference materials analysed by the proposed method. Each result is quoted as the mean ± standard deviation of four separate decompositions

Sample	W/ μg g^{-1}	RSD, %	W literature value/μg g^{-1}	Mo/ μg g^{-1}	RSD, %	Mo literature value/μg g^{-1}
AGV-1 (andesite)	0.6 ± 0.1	16	0.53*	2.1 ± 0.1	4.8	2.02‖
BHVO-1 (basalt)	<0.4		0.21†	1.1 ± 0.1	9.0	1.01‖
MAG-1 (marine sediment)	1.5 ± 0.2	13	1.67†	1.3 ± 0.1	7.7	1.46‖
QLO-1 (quartz latite)	0.6 ± 0.2	33	0.58†	2.5 ± 0.1	4.0	2.55‖
RGM-1 (rhyolite)	1.3 ± 0.2	15	1.6*	2.5 ± 0.1	4.0	2.44‖
SCo-1 (Cody shale)	1.1 ± 0.2	18	1.61†	1.3 ± 0.1	7.7	1.69‖
SDC-1 (mica schist)	0.8 ± 0.3	37	0.8*	0.4 ± 0.3	75	0.10‖
SGR-1 (petroleum shale)	2.5 ± 0.1	4.0	2.64†	34 ± 1	2.3	36.64‖
STM-1 (syenite)	3.1 ± 0.2	6.5	3.8*	4.9 ± 0.2	4.1	4.86‖
GXR-2 (soil)	1.5 ± 0.3	20	1.8 ± 0.5‡	1.5 ± 0.1	6.7	1.5 ± 0.2‡
GXR-5 (soil)	1.1 ± 0.2	18	1.1 ± 0.5‡	30 ± 1	3.3	28 ± 6‡
GXR-6 (soil)	1.8 ± 0.3	17	1.1‡	2.2 ± 0.2	9.1	2.1 ± 0.3‡
GSD-1 (stream sediment)	0.9 ± 0.2	22	1.04 ± 0.3§, ¶	0.8 ± 0.1	12	0.74 ± 0.20§,¶
GSD-3 (stream sediment)	4.7 ± 0.3	6.4	4.9 ± 0.7§, ¶	89 ± 4	4.5	92 ± 7§, ¶
GSD-4 (stream sediment)	2.3 ± 0.3	13	2.5 ± 0.8§, ¶	0.9 ± 0.1	11	0.86 ± 0.27§,¶
GSD-5 (stream sediment)	3.2 ± 0.4	12	3.2 ± 0.6§, ¶	1.3 ± 0.1	7.7	1.2 ± 0.3§, ¶
GSD-6 (stream sediment)	24 ± 2	8.7	25 ± 3§, ¶	8.0 ± 0.3	3.8	7.7 ± 1.2§,¶
GSD-7 (stream sediment)	5.3 ± 0.4	7.5	5.5 ± 1.0§, ¶	1.7 ± 0.2	11	1.4 ± 0.2§,¶
GSD-8 (stream sediment)	2.1 ± 0.3	14	1.95 ± 0.44§, ¶	0.6 ± 0.1	16	0.54 ± 0.19§,¶
SY-3 (syenite)	1.0 ± 0.1	10	1.27†	0.8 ± 0.2	25	0.58†
MRG-1 (gabbro)	0.4 ± 0.2	50	0.54†	0.9 ± 0.1	11	0.84†
FeR-1 (iron formation)	1.1 ± 0.3	27		3.3 ± 0.3	9.0	

* Reference 17.
† Reference 4.
‡ Reference 18.
§ Reference 19.
¶ Recommended values.
‖ Reference 20.

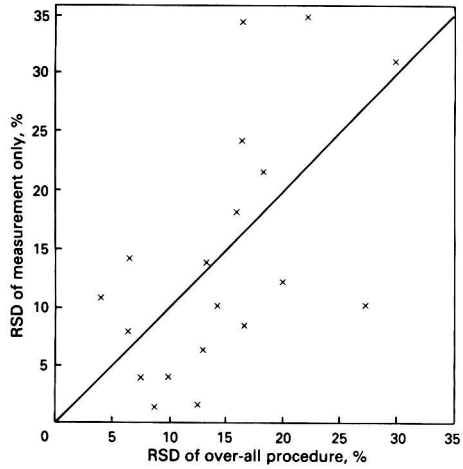

Fig. 2. Precision of analytical measurement *vs.* precision of the over-all procedure in the determination of W in the international reference materials

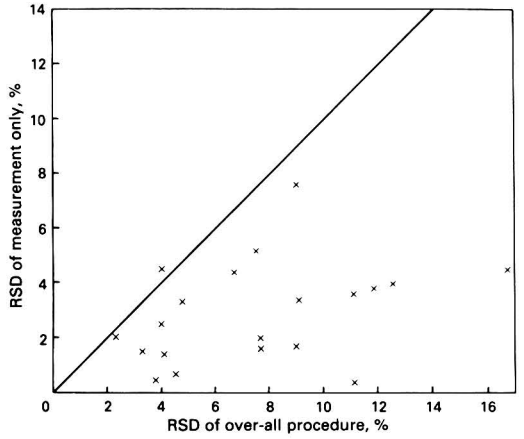

Fig. 3. Precision of analytical measurement *vs.* precision of the over-all procedure in the determination of Mo in the international reference materials

due to differences in sample homogeneity (*cf.*, FeR-1 and RGM-1). The average precision in the range 0.5–5 μg g^{-1}, computed from the data in Table 4, is 15% RSD for W and 8% RSD for Mo.

The reproducibility of the measurement step itself differs significantly for the two elements. The precision obtained on measurement every 2 min throughout a 60-min period of a 0.1 μg ml^{-1} calibration standard (equivalent to 2.5 μg g^{-1} in the sample) was 7.2% for W and 2.7% for Mo. At concentrations of W below 5 μg g^{-1} in the sample, the critical parameter affecting the analytical precision obtained is the measurement of the emission signal; the variation in results introduced by the decomposition and separation procedure is negligible by comparison. This is not so for Mo where much better precision is achieved in the measurement step itself. This is demonstrated graphically in Figs. 2 and 3 where the RSD of the determination step, based on three measurements for each sample solution, is plotted against the RSD of the entire sampling and analytical procedure, based on four separate decompositions for each sample, thereby reflecting errors in

the sampling itself, preparation procedure and analysis. The 45° line is included simply to illustrate the difference in behaviour of the two elements. The fact that all points except one lie to the right of this line in Fig. 2 indicates that the RSD of the over-all sampling and analytical procedure for Mo is significantly greater than that of the measurement step itself, a common occurrence in analytical chemistry. However, the reasonably even distribution of points about the 45° line in Fig. 2 indicates that the predominant source of noise in the data for W is the uncertainty in the determination step itself.

The determination limit (DL) is defined by DL = dilution factor (25) × analytical detection limit × constant. The constant reflects the variability introduced by the preparation procedure prior to analysis. The detection limit is defined as that concentration of the element which gives an emission signal equal to three times the standard deviation of the blank; this value is 0.015 μg ml^{-1} for W and 0.004 μg ml^{-1} for Mo. As the limiting factor in precision is the analytical measurement itself for W, the constant equals one and, therefore, the determination limit is 0.4 μg g^{-1}. However, this constant is given a value of two for Mo as the variability introduced in the preparation procedure is significant (Fig. 3) and about twice that of the measurement itself; therefore, the determination limit for Mo is estimated to be 0.2 μg g^{-1}.

Conclusions

This study has demonstrated that the analysis of geological materials by ICP-AES for low levels of W and Mo (<100 μg g^{-1}) is practical, accurate and efficient with concentration by adsorption of the metal 8-hydroxyquinolinate on to activated charcoal. A determination limit of 0.4 μg g^{-1} for W is obtained, with a typical precision at 5 μg g^{-1} of W of 6–7%. The determination limit for Mo is lower (0.2 μg g^{-1}) and the precision is also improved, typically 4% RSD at 5 μg g^{-1} of Mo.

References

1. Thompson, M., and Walsh, J. N., "A Handbook of Inductively Coupled Plasma Spectrometry," Blackie, London, 1983, pp. 102 and 104.
2. Church, S. E., *Geostand. Newsl.*, 1981, **V**, 133.
3. Brenner, I. B., and Erlich, S., *Appl. Spectrosc.*, 1984, **38**, 887.
4. Terashima, S., *Geostand. Newsl.*, 1980, **IV**, 9.
5. Aruscavage, P., and Campbell, E. Y., *U.S. Geol. Surv. J. Res.*, 1978, **6**, 697.
6. Lillie, E. G., and Greenland, L. P., *U.S. Geol. Surv. J. Res.*, 1973, **1**, 555.
7. Lillie, E. G., and Greenland, L. P., *Anal. Chim. Acta*, 1974, **69**, 313.
8. Simon, F. O., and Rollinson, C. L., *U.S. Geol. Surv. J. Res.*, 1975, **3**, 475.
9. Gladney, E. S., *Anal. Lett.*, 1978, **A11**, 429.
10. Nadkarni, R. A., and Morrison, G. H., *Anal. Chem.*, 1978, **50**, 294.
11. Leinz, R. W., and Grimes, D. J., *U.S. Geol. Surv. J. Res.*, 1978, **6**, 259.
12. Thompson, M., and Zao, L., *Analyst*, 1985, **110**, 229.
13. Hall, G. E. M., and Pelchat, J. C., *Analyst*, 1986, **111**, 1255.
14. Hall, G. E. M., Vaive, J. E., and Ballantyne, S. B., *J. Geochem. Explor.*, 1986, **26**, 191.
15. Vanderborght, B.M., and Van Grieken, R. E., *Anal. Chem.*, 1977, **49**, 311.
16. Verbeeck, J., Vanderborght, B., Van Grieken, R., and Ex, G., *Anal. Chim. Acta*, 1981, **128**, 207.
17. Govindaraju, K., *Geostand. Newsl.*, 1984, Special Issue, 3.
18. Gladney, E. S., Burns, C. E., and Roelandts, I., *Geostand. Newsl.*, 1984, **2**, 119.
19. Xie, X., Yan, M., Li, L., and Shen, H., *Geostand. Newsl.*, 1985, **II**, 83.
20. Aruscavage, P. J., and Campbell, E. Y., *Geostand. Newsl.*, 1984, **II**, 119.
21. Hall, G. E. M., Park, C. J., and Pelchat, J. C., *J. Anal. At. Spectrom.*, 1987, **2**, 189.

Paper A6/359
Received September 22nd, 1986
Accepted December 18th, 1986

Proof of a Pine Wood Origin for Pitch from Tudor (Mary Rose) and Etruscan Shipwrecks: Application of Analytical Organic Chemistry in Archaeology

Neil Robinson, Richard P. Evershed,* W. James Higgs, Katherine Jerman and Geoffrey Eglinton
Organic Geochemistry Unit, School of Chemistry, University of Bristol, Cantock's Close, Bristol BS8 1TS, UK

Six samples of tar and pitch from the wreck of the Mary Rose (Tudor, AD 1509–45) and a sample of pitch from an Etruscan shipwreck (*ca.* 600 BC) have been analysed by a number of modern analytical techniques (elemental analysis, IR and NMR spectroscopy, GC and GC - MS). Similar analyses were performed on samples of contemporary tars, derived from natural sources, for comparative purposes. The major constituents of the archaeological samples were observed to be alkyl-substituted, tricyclic diterpenoids based on the abietane and pimarane skeletons. Similar molecular compositions and spectral properties were found for Stockholm tar (a good quality wood tar obtained by the destructive distillation of *Pinus sylvestris*), and Tudor and Etruscan pitches, thus providing conclusive evidence for the derivation of the archaeological samples from pine wood. The analytical techniques utilised are compared for their relative usefulness in chemical archaeology.

Keywords: *Nuclear magnetic resonance; gas chromatography - mass spectrometry; chemical archaeology; pine wood tar; pitch*

Relatively few chemical archaeological investigations have been concerned with organic materials in contrast to the large number of studies carried out on the inorganic components of, for example, building materials, pottery, coins and weapons.[1] This is probably largely due to the comparative ease with which organic matter can decay, whereas many inorganic materials remain unchanged even after hundreds of years of weathering. In certain circumstances, however, when protected from the degradative effects of oxygen and sunlight, organic-based plant and animal products may survive for centuries, in a form little altered from the original. Indeed, sedimentary organic matter can resist decomposition to such an extent that, even after millions of years, source organisms can be assigned on the basis of molecular structure.[2]

A wide variety of modern analytical techniques are available to tackle studies of organic materials in archaeology. Studies which have been performed include infrared (IR) analyses of ancient dyes,[3] amber[4] and tar from a thirteenth century Norwegian shipwreck,[5] a ^{13}C nuclear magnetic resonance (NMR) spectroscopy investigation of non-metallic seals,[6] examination by gas chromatography (GC) of animal fats from peat bogs[7] and Eskimo dwelling sites[8] and investigations of natural resins of art and archaeology, including GC and GC - mass spectrometry (GC - MS) studies.[9–11] These studies have been concerned with the determination of the chemical composition of the organic constituents with a view to establishing such features as: (i) source, (ii) early technological practices and (iii) the extent and nature of decomposition (particularly important in the conservation and restoration of valuable artifacts).

This study reports the detailed chemical investigation of tars and pitches from two shipwrecks, namely, the Tudor Mary Rose (King Henry VIII's flagship; AD 1509–45) and an Etruscan vessel. The wreck of the Mary Rose was raised from the bed of the Solent in 1981. The preservation of the ship and the many Tudor relics that were found is attributed to the anaerobic conditions prevailing within the sediments during much of the period of burial and, in some instances, to the large amounts of pitch that permeated the ship and certain of the relics. The second wreck to provide pitch samples was that of an Etruscan vessel that sank *ca.* 600 BC off the Island of Giglio, about 80 miles north west of Rome.[12] Excavation began in 1983 and led to the discovery of a large amount of pitch from amphorae carried as cargo that had oozed down over the rocks on the sea bed.

The production and use of tars and pitches as protective hydrophobic coatings is well documented. To our knowledge, however, the study reported here represents the first detailed chemical investigation of the origins of such materials; preliminary results of this study have been reported elsewhere.[13] Pitch from the Giglio shipwreck and six samples of pitch and pitch-impregnated materials from the Mary Rose were selected for analysis (sample details given in Table 1). Five tarry substances derived from natural sources were obtained for comparison, *viz.*, coal tar, peat tar, North Sea crude oil and two wood tars, one derived from Norway spruce (*Picea abies*), the other Stockholm tar (a good quality pine tar obtained by the destructive distillation of *Pinus sylvestris* or Scots Pine, the only pine native to Great Britain).

We analysed the samples by a variety of analytical organic chemical techniques in order to (i) establish their origins and (ii) evaluate the different analytical methodologies in terms of their applicability to archaeology.

Experimental

The archaeological samples investigated and the examples of tarry substances derived from natural sources (analysed for comparison) are described in Table 1. Care was taken to keep the contamination to a minimum; water was doubly distilled and all the solvents were re-distilled prior to use. Where the pitches were neither adhered to, nor incorporated into, any other materials, no extraction was necessary. For the caulking, "luting" and rope samples, their associated pitch required extraction before analysis, and this was achieved by placing the sample in an elution tube plugged with pre-washed cotton-wool and washing with dichloromethane (DCM; *ca.* 200 ml). Extraction was continued until no further colouration appeared in the solvent washings.

Fractions for GC and GC - MS analyses were obtained by

Table 1. Description of tars and pitches investigated

Sample	Appearance and odour	Origin
*Mary Rose**—		
Tarred rope (MR AC)	20 strands 0.5–20 cm long, impregnated with tar	Anchor cable
Pitch (82 S 1298)	Shiny black conchoidally fractured fragments with strong "tarry" odour	Barrel in hold
Luting (MR 82 S1274/12)	Small pieces of damp tarred wood with a strong "tarry" odour	Main deck
Caulking (MR 82 S126)	Rope-like material composed of hair fibres impregnated with tar	Between the timbers forming the outer frame
Tar (82 S1296/7)	Thick black tarry material with "tarry" odour	Barrel in hold
Solid (81 S300)	Soft dark brown solid, smelling strongly "tarry"	Inside chest/box of longbows (probably intrusive)
Others—		
Giglio pitch	Gravel - sand conglomerate, bound by shiny black solid with a slight "tarry" odour	Oozed over sea bed from amphorae carried as cargo
Stockholm tar	Viscous black tar	Destructive distillation of *Pinu sylvestris*
Norway spruce wood tar	Thick black tar	Destructive distillation (750–800 °C)
Peat tar	Dark brown solid with "tarry" odour	Destructive distillation (600 °C)
Coal tar pitch	Black solid with characteristic coal tar odour	Product of coking process (Avenue coal, 1100 °C)
North Sea oil	Low viscosity black liquid	Kimmeridge crude oil

* Bracketed codes were used by the Mary Rose Trust to document the samples.

Mary Rose samples and Stockholm tar, the fractionation was achieved by successive elution with hexane, toluene, DCM, ethyl acetate and methanol (100 ml each). The Giglio pitch was fractionated by successive elution with hexane (150 ml), hexane - diethyl ether (9 + 1, 100 ml) and ethyl acetate - methanol (2 + 1, 300 ml). Further fractionation of Giglio pitch was performed using thin-layer chromatography [TLC; silica gel G; hexane - diethyl ether (9 + 1) developer]. The acidic components were isolated from the neutral components by partitioning between DCM and aqueous potassium hydroxide (5%). Neutralisation (5 M hydrochloric acid) of the aqueous extract, and extraction (DCM, 3 × 20 ml) produced the acids, which were converted to their corresponding methyl ester derivatives by refluxing with boron trifluoride - methanol (14%) or by treatment with ethereal diazomethane. The hydroxyl groups were converted to trimethylsilyl ethers with *N,O*-bis(trimethylsilyl)trifluoroacetamide prior to analysis by GC.

The elemental analyses were performed on a Perkin-Elmer Model 240 CHN analyser. IR spectra were recorded as either melted films or as solutions in DCM, using a Perkin-Elmer 197 infrared spectrophotometer. NMR spectra were obtained by dissolving aliquots of total sample (*ca.* 50 mg) in deuterated chloroform and filtering. Tetramethylsilane was used as a reference and the spectra were recorded on a Jeol FX200 instrument operating at 199.5 MHz.

The GC analyses were performed on an Erba Science 4160 GC using on-column injection with the samples dissolved in DCM. Either a 25 m × 0.3 mm (Chrompak) or a 50 m × 0.3 mm (Hewlett-Packard) OV-1 coated (0.17-μm film thickness) flexible silica column was used. Hydrogen was used as the carrier gas at a flow-rate of 50 cm s^{-1} and the GC oven was programmed over 80–300 °C at 4–6 °C min^{-1} and the eluting compounds were monitored by flame-ionisation detection. The GC runs were acquired on a VG Analytical Minichrom data system. GC - MS analyses were carried out using a Finnigan 4000 quadrupole MS coupled to either a Finnigan 9160 GC or an Erba Science 5160 GC. The spectra were recorded over the range *m/z* 50–500 every second; the data were acquired and processed using a Finnigan INCOS 2300 data system. The GC conditions were similar to those described above, except that the column was replaced by a 25 m × 0.3 mm SE-54 coated column (0.25-μm film thickness) and helium was used as the carrier gas.

Results

Elemental Composition

The percentages, by mass, of carbon, hydrogen and nitrogen in the various samples are given in Table 2. Owing to the differing proportions of inorganic residue, a more significant parameter is the H : C atomic ratio, which provides a measure of the degree of unsaturation of the sample. Similar values were obtained for all of the samples, with the exception of the coal tar. The Mary Rose pitch (82 S 1298) exhibited a lower H : C value than Mary Rose tar (82 S 1296/7).

Infrared Spectroscopy

The IR spectra of all the Mary Rose samples were similar, displaying absorptions which could be assigned to carboxylic acid groups and aliphatic and aromatic moieties. Striking similarities were observed among the Mary Rose samples, Giglio pitch and Stockholm tar, the spectra of which were comparable in almost every respect (wavenumber and absorption intensity) (Fig. 1A, B and C, respectively). Of the Mary

Table 2. Elemental composition of the tars and pitches

Sample	Mass percentage C	H	N	H : C ratio
Mary Rose—				
MR AC	77.1	8.8	0.0	1.4
82 S 1298	78.2	7.8	0.2	1.2
MR 82 S1274/12	67.4	7.6	0.2	1.3
MR 82 S126	82.1	9.3	0.0	1.4
82 S1296/7	67.4	9.0	0.0	1.6
81 S300	66.4	8.3	0.0	1.5
Others—				
Giglio pitch	65.5	7.5	0.0	1.4
Stockholm tar	79.5	9.1	0.0	1.4
Norway spruce wood tar	71.3	7.2	0.1	1.2
Peat tar	67.3	7.0	1.0	1.2
Coal tar pitch	91.4	4.4	1.3	0.6
North Sea oil	86.5	13.8	0.2	1.9

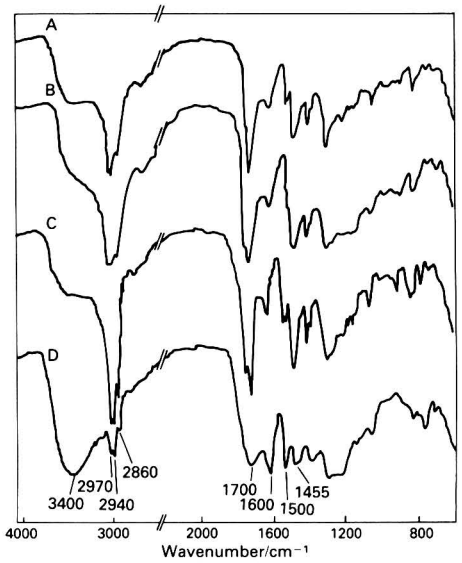

Fig. 1. Infrared spectra of (A) Giglio pitch (melted film); (B) Mary Rose tar (82 S1296/7; thin film); (C) Stockholm tar (thin film) and (D) Norway spruce wood tar (thin film). Marked signals: 3400 cm^{-1} = H-bonded O–H stretch; 2970 cm^{-1} = CH_3 C–H stretch and =C–H stretch; 2940 cm^{-1} = CH_2 asymmetric C–H stretch; 2860 cm^{-1} = CH_2 symmetric C–H stretch; 1700 cm^{-1} = carbonyl stretch of aromatic ester; 1600, 1500 cm^{-1} = aromatic stretching; and 1455 cm^{-1} = CH_2 C–H bend

Rose samples, the pitch from the barrel (82 S 1298) most closely matched the Giglio pitch. The infrared spectrum of peat tar also resembled that of the Mary Rose samples, but to a lesser extent. The spectrum of wood tar (Norway spruce) displayed the same principal absorptions as the Mary Rose samples, but with much stronger absorptions from aromatic moieties and hydroxyl groups (Fig. 1D). Although the coal tar pitch and North Sea crude oil had many absorptions in common with the Mary Rose samples, their spectra were very different, coal tar pitch exhibiting absorptions principally due to aromatic moieties and the North Sea crude oil displaying absorptions mainly due to aliphatic C–H vibrations. It should be noted, however, that coal tars from the fifteenth century would have been produced at lower temperatures than 1100 °C and consequently would have contained a larger amount of lighter ends and more functional groups.

Table 3. Assignment of ^1H NMR resonances

Signal range (δ), p.p.m.	Resonances
0.6–1.2	Methyl protons in aliphatic and alicyclic systems
1.2–1.3	Methyl resonances α or β to an aromatic ring, or other electron-withdrawing substituents, and aliphatic methylene protons
0.6–2.4	Methylene - methine envelope
2.4–3.0	Methylene - methine protons adjacent to an electron-withdrawing group
3.5–6.0	Vinylic protons
6.8–9.0	Aromatic protons

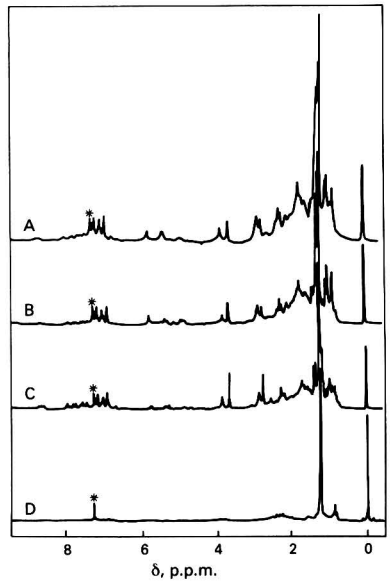

Fig. 2. ^1H NMR spectra of (A) Mary Rose pitch (82 S1298); (B) Giglio pitch; (C) Stockholm tar and (D) peat tar. Assignments of the resonances are proposed in Table 3. * = resonance due to residual proton resonances from solvent

Nuclear Magnetic Resonance Spectroscopy

The NMR spectra of the Mary Rose samples, Giglio pitch and Stockholm tar were virtually identical except for minor differences in the relative intensities of certain signals. The spectra of Mary Rose tar, Giglio pitch and Stockholm tar are compared in Fig. 2; assignments for the observed resonances are proposed in Table 3. Although the spectrum of peat tar exhibited similar signals to the above samples, the relative intensities were significantly different (Fig. 2D). The spectrum of Norway spruce wood tar contained strong signals due to aliphatic methylene groups. It also showed strong signals due to hydrogens adjacent to carboxylic acid groups, esters, aldehydes and ketones, thus producing an over-all spectrum differing greatly from that of Giglio pitch. The coal tar and North Sea crude oil could clearly be distinguished from Giglio pitch, the spectrum of the coal tar being dominated by resonances of aromatic protons, whereas that of North Sea crude oil was very simple, consisting solely of signals due to aliphatic methylene and methyl groups.

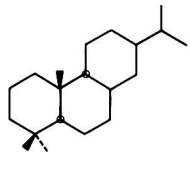

I

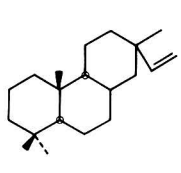

II

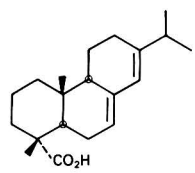

III

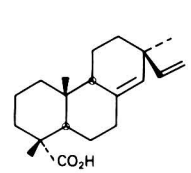

IV

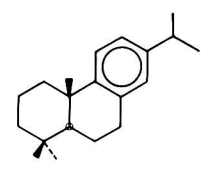

V

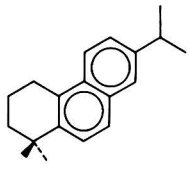

VI

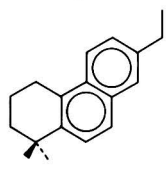

VII

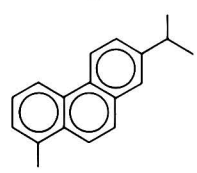

VIII

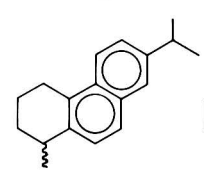

IX

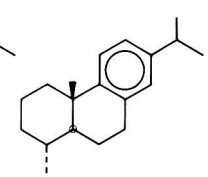

X

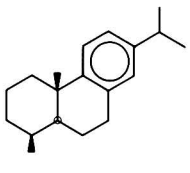

XI

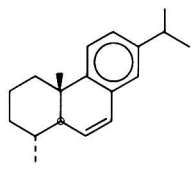

XII

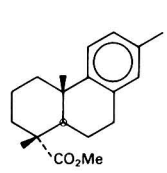

XIII

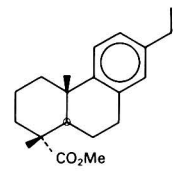

XIV

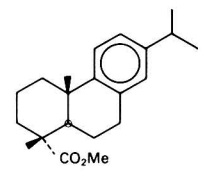

XV

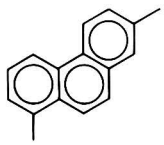

XVI

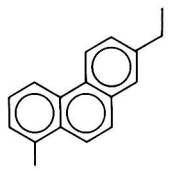

XVII

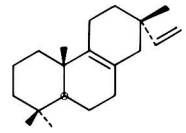

XVIII

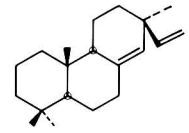

XIX

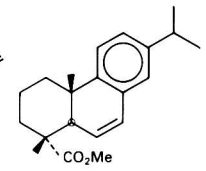

XX

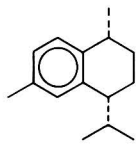

XXI

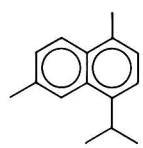

XXII

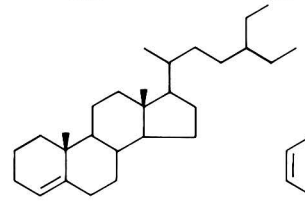

XXIII

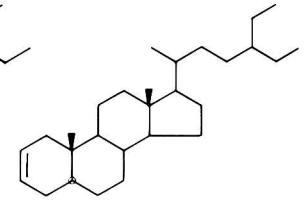

XXIV

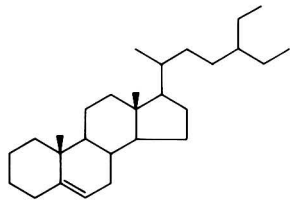

XXV

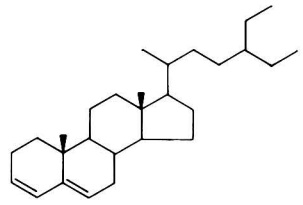

XXVI

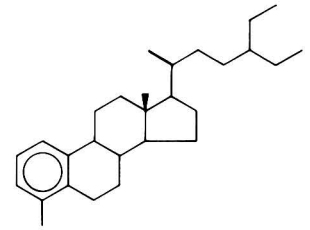

XXVII

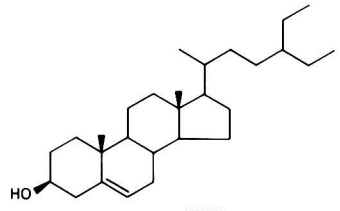

XXVIII

Gas Chromatography

Fractions of differing polarities, obtained by column chromatography and TLC of Stockholm tar, Giglio pitch and the Mary Rose samples, were analysed by GC. The homogeneous pitch and tar contained in barrels from the Mary Rose (82 S 1298 and 82 S 1296/7, respectively) produced chromatograms closely resembling those of corresponding fractions of Stockholm tar. The hydrocarbon fractions (hexane and hexane - diethyl ether eluents) produced the most complex distributions. Pitches from the Mary Rose already in their intended site of application (for example, luting, caulking and anchor rope) had more variable hydrocarbon patterns. The chromatograms of the Giglio pitch fractions resembled those of the corresponding Stockholm tar fractions, although to a lesser extent than for the samples from barrels of the Mary Rose. In general, the chromatograms of the Giglio pitch fractions were more complex than those of the Stockholm tar. This was particularly apparent with the methylated acid fractions, where Giglio pitch produced a more complex distribution of minor constituents, otherwise the pattern of methylated acids in each was very similar. Co-chromatography of the Giglio pitch and Stockholm tar fractions resulted in co-elution of the major peaks present in both, suggesting that they contained common constituents, although in slightly different relative amounts.

Gas Chromatography - Mass Spectrometry

Selected fractions from Stockholm tar (hexane, hexane - diethyl ether), Giglio pitch (hexane, hexane - diethyl ether, neutrals, methylated acids) and the Mary Rose samples (MR 82 S 1298 hexane and methylated acids and MR 82 S 1296/7 hexane) were analysed by GC - MS. The principal constituents (Fig. 3) were found to be alkyl-substituted tricyclic diterpenoids, those based on abietane (**I**) dominating compounds with a pimarane (**II**) skeleton. For the fractions analysed, Stockholm tar, Giglio pitch and the Mary Rose samples proved to be composed of the same basic mixture of compounds. The distribution of the Mary Rose pitch and tar (82 S 1298 and 82 S 1296/7, respectively) closely resembled that of Stockholm tar.[13] Giglio pitch contained a complex series of hydrocarbons resembling the distribution of Stockholm tar (Fig. 4; peak assignments and relative abundances are presented in Table 4). In addition to the tricyclic diterpenoid hydrocarbons, two sesquiterpenoids, calamenene (**XXI**) and cadalene (**XXII**), were identified by comparison with published spectra[14,15] in both Giglio pitch and Stockholm tar. Low levels (<1% of the most abundant hydrocarbon) of a series of C_{29} steroidal hydrocarbons were recognised in Mary Rose and Giglio pitches and Stockholm tar; the series consisted of 24-ethylcholest-4-ene (**XXIII**), its Δ^2 and Δ^5 isomers (**XXIV** and **XXV**), 24-ethylcholesta-3,5-diene (**XXVI**) and 4-methyl-24-ethyl-19-norcholesta-1,3,5(10)-triene (**XXVII**).

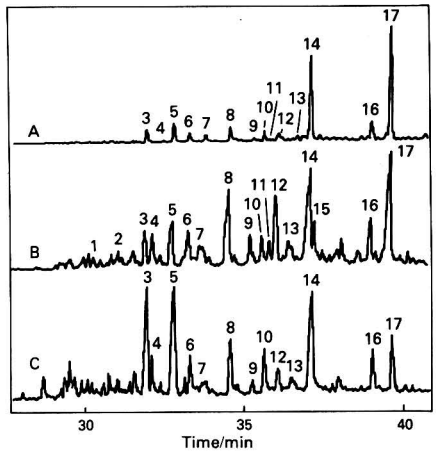

Fig. 4. Partial reconstituted ion chromatograms of total hydrocarbons (hexane and hexane - diethyl ether or toluene eluents combined) of (A) Mary Rose pitch (82 S1298), (B) Giglio pitch and (C) Stockholm tar. Peak assignments are given in Table 4

Table 4. Relative abundances of selected compounds in the hydrocarbon fraction of Mary Rose and Giglio pitches and Stockholm tar

			Relative abundance, %		
Component*	Assignment†	Structure	Mary Rose pitch	Giglio pitch	Stockholm tar
1	$\Delta^{8,9}$-Sandaracopimaradiene	**XVIII**	ND¶	6.0	ND
2	13-Isopimaradiene	**XIX**	ND	9.3	1.9
3	19-Norabieta-8,11,13-triene	**X**	10.1	22.6	87.6
4	19-Norabieta-4,8,11,14-tetraene	**XII**	0.8	22.1	23.5
5	18-Norabieta-8,11,13-triene	**XI**	14.5	35.6	100.0
6	1,7-Dimethylphenanthrene‡	**XVI**	7.9	11.4	16.8
	+ $C_{18}H_{26}$		0.5	11.5	4.2
7	Dehydroabietane	**V**	2.0	10.4	4.1
8	Norsimonellite	**VII**	10.9	65.2	31.2
9	Simonellite	**VI**	2.1	17.7	6.6
10	1-Ethyl-7-methylphenanthrene‡	**XVII**	7.2	15.1	25.2
11	$C_{19}H_{26}O_2$		0.8	12.5	1.5
12	1,2,3,4-Tetrahydroretene	**IX**	2.4	52.9	10.5
	+ $C_{19}H_{26}O_2$		Trace	52.9	Trace
	+ ethylmethylphenanthrene		5.2	52.9	5.2
13	$C_{19}H_{24}$		1.4	12.0	6.0
14	Retene§	**VIII**	70.0	90.7	94.1
15	$C_{19}H_{26}O_2$		Trace	21.9	Trace
16	$C_{19}H_{20}$, a higher retene homologue		16.1	25.8	22.3
17	Methyl dehydroabietate	**XV**	100.0	100.0	30.6

* Refers to peak number in Fig. 4.
† Based on comparison of mass spectra and relative retention times with published data.[14–16, 25]
‡ Position of substituents tentatively assigned based on comparison with published data.[14]
§ Assignment confirmed by co-chromatography with an authentic standard.
¶ ND = Not detected.

The neutral fraction of the ethyl acetate - methanol eluent of both the Giglio pitch and Stockholm tar was dominated by methyl dehydroabietate (**XV**), with methyl 16,17-bisnordehydroabietate (**XIII**) and methyl 17-nordehydroabietate (**XIV**) also major constituents (Table 5). Similarly, the methylated acid fractions were dominated by methyl dehydroabietate and, for Giglio pitch, were also found to contain the two lower homologues and methyl 13-isopropyl-5α-podocarpa-6,8,11,13-tetraen-16-oate (**XX**) as major components (Table 5). A series of alkanoic acids was detected as a significant component of the Giglio pitch. The series was dominated by the C_{16} homologue and had a strong even over odd predominance; a monounsaturated C_{18} acid was also recognised as a major constituent.

Discussion

Origins of Pitches

The results of analysis by IR and NMR spectroscopy, GC and GC - MS suggest that the pitches found at the Mary Rose and Giglio shipwrecks are of a similar generic origin. Comparison with a variety of naturally derived contemporary pitches revealed a remarkably close similarity to modern Stockholm tar, produced by the destructive distillation of *Pinus sylvestris*. The major constituents of the archaeological samples were characterised by GC - MS as being alkyl-substituted mono- and diaromatic tricyclic diterpenoids based on the abietane and pimarane skeletons. Such compounds are widespread among higher plants and are particularly abundant in conifer resins.[16] Although diagenetic products such as retene (1-methyl-7-isopropylphenanthrene, **VIII**), dehydroabietane (**V**) and dehydroabietic acid can occur as minor constituents of bleed resin,[16] their presence in the tars and pitches arises largely through thermal dehydrogenation and, to a lesser extent, decarboxylation of abietic acid (**III**) and pimaric acid (**IV**), the principal resin acids of conifers, during the retorting process used to produce the initial wood tar. A similar suite of diterpenoids is commonly observed in aquatic sediments, where they are proposed to originate mainly from *in situ* microbial alteration of abietic and pimaric acids derived from conifers.[14] Abietic acid is a more abundant constituent of conifer resin than pimaric acid. This is reflected in the tars and pitches by the lower proportion of 1,7-dimethylphenanthrene and 16,17-bisnordehydroabietic acid, derived from pimaric acid,[14,15] than retene and dehydroabietic acid, the analogous products of the decomposition of abietic acid.

24-Ethylcholesterol (**XXVIII**) is the major sterol of higher plants.[17] The presence of a series of steroidal hydrocarbons based on this skeleton in a Stockholm tar type of material is, therefore, to be expected. 24-Ethylcholest-4-ene, its Δ^2 and Δ^5 isomers and the $\Delta^{3,5}$-diene would be formed by dehydration of the parent sterol and, probably, the related 5α(H)-stanol, during the retorting process. 4-Methyl-24-ethyl-19-norcholesta-1,3,5(10)-triene is a known diagenetic product of 24-ethylcholesta-3,5-diene in sediments,[18,19] a transformation that may be effected in the laboratory by treatment of the latter with acid[19] and which may occur under the conditions prevailing in the retorting process.

Wood pitch is formed from wood tar, the initial pyrolysate, by boiling, which drives off some of the volatiles, increases the extent of aromatisation and decarboxylation and effects a degree of polymerisation. Thus, pitch would be expected to have a lower H : C ratio than the precursor tar, as observed for the Mary Rose pitch (82 S 1298) and tar (82 S 1296/7). Moreover, the greater abundance of retene relative to the less aromatised tricyclic diterpenoids in the pitch[13] is consistent with further heating. The differences in hydrocarbon distribution between the Mary Rose pitches in their intended sites of application and of those contained in barrels may be due to differing degrees of microbial alteration, weathering, water washing and exposure to oxygen and sunlight during the ship's 36-year active life and subsequent 437-year submergence and burial.

The variations in molecular distribution between the Giglio pitch and Stockholm tar may similarly reflect a different extent of degradation. Alternatively, they may be due to differences in the retorting process (time, temperature, exposure to oxygen), species of tree used or presence of adulterants, commonly used to reduce the cost of the pitch and to alter its physical properties (*e.g.*, consistency, softening point).

Today Stockholm tar or similar tars are imported into the United Kingdom from Russia, Eastern Europe, Scandinavia, China, America and India. At the time of the Mary Rose, it is known that trade developed between Russia and England, and among the first cargos were tar and pitch.[20,21] The similarity in chemical composition between the Mary Rose samples and the modern Russian Stockholm tar is consistent with the former having originated from one such cargo, although a local source of manufacture cannot be excluded. These chemical data are in agreement with the historical and geographical evidence for the probable sources of the Mary Rose tars and pitches.[22]

The pitch found on the Giglio shipwreck was most probably locally produced in Etruria, which in the 6th and 7th centuries BC was well wooded,[23] with oak, beech and pine being important trees.[24] Much of the Etruscans' wealth came from the exploitation of their mineral reserves of copper, tin, lead, silver, mercury and especially iron. They must have produced vast amounts of charcoal for iron smelting, utilising the surrounding forests; wood tar is an important by-product of charcoal production.

Table 5. Relative abundances of major components in the neutral and methylated acid fractions of Giglio pitch and Stockholm tar

Compound	Relative abundance* Giglio pitch	Stockholm tar
Methyl esters—		
Methyl hexadecanoate	10.8	
$C_{18:1}$ FAME†	8.6	
Methyl 16,17-bisnordehydroabietate	5.5	
Monoaromatic C_{18} tricyclic diterpenoidal methyl ester	12.0	
$C_{20}H_{30}O_2$ methyl ester	4.9	
Methyl 17-nordehydroabietate	2.0	
Methyl 13-isopropyl-5α-podocarpa-6,8,11,13-tetraen-16-oate	3.1	
Methyl dehydroabietate	100.0	100.0‡
Neutrals—		
Monoaromatic C_{18} tricyclic diterpenoidal methyl ester	12.5	2.9
Methyl 16,17-bisnordehydroabietate	2.5	5.3
Monoaromatic C_{18} tricyclic diterpenoidal methyl ester	3.3	4.1
$C_{15}H_{14}O_2$ methyl ester	26.7	1.8
Methyl 17-nordehydroabietate	4.5	3.8
Methyl dehydroabietate	100.0	100.0

† FAME = fatty acid methyl ester. Number of carbon atoms refers to parent acid.

‡ Components not characterised by GC - MS, dominant component assigned on basis of GC co-chromatography with Giglio pitch neutrals fraction.

Historical Roles of Tars and Pitches

The analytical data have revealed very similar chemical compositions and hence similar generic origins for the pitches found on the Mary Rose and Giglio wrecks. There is evidence, however, to suggest that the pitches were intended to serve

Table 6. Comparison of analytical methodologies

Method (amount taken)	Advantages	Disadvantages
Elemental analysis (*ca.* 5 mg)	Fast, simple and cheap	Little information; does not readily distinguish between different tars and pitches
IR (1–5 mg)	Fast and cheap. Spectra are easily interpreted, give information on functional groups present and provide "fingerprints"	Does not provide unambiguous differentiation of all samples. Little information on structures of constituents
NMR (5–50 mg)	Fast and simple. Spectra are fairly easily interpreted, give information on structure of constituents and provide unambiguous "fingerprints" of all samples studied	Structural information limited, little information on functional groups present
GC (*ca.* 10 μg)	Chromatograms provide good "fingerprints"	Slow. Results depend on reproducible chromatographic conditions. Little information on composition of samples
GC - MS (*ca.* 10 μg)	Excellent method of differentiating tars and pitches. Provides a great deal of information on structures of individual constituents	Slow, expensive and facilities not normally readily available. Results can be difficult to interpret

rather different functions. The pitches originating from the Mary Rose were undoubtedly used for their hydrophobic properties as water-proofing agents in the vessel's construction and maintenance. Whether or not the Giglio pitch was intended for use in this role is arguable. Certainly pitch was important to the Roman and Greek shipbuilders.[21] Pitches, however, were also used for other purposes at this time. For instance, wines flavoured with liquid pitch were popular amongst the Romans.[21] The fact that the Giglio pitch had flowed from the amphorae suggests that it originally possessed an appreciably lower viscosity than the tars and pitches encountered on the Mary Rose. In addition to their use in flavouring wines, pitches were used to seal terracotta amphorae used in the export and storage of wines.[21] Although the chemical data provide a powerful means of determining the generic origin of pitches it cannot, in this instance at least, reveal such subtleties as intended use.

Comparison of Analytical Methods

Of the methods described herein, elemental analysis is the least informative. The archaeological tars and pitches could only be distinguished from the coal tar (and possibly the crude oil), the rest of the samples having H : C values lying in a fairly narrow range. Infrared spectroscopy provided fingerprints of each sample and demonstrated a strong similarity among the various archaeological samples and Stockholm tar, a slightly poorer fit with peat tar, some resemblance to Norway spruce wood tar and a significantly different fingerprint for coal tar pitch and North Sea crude oil. Information was also obtained on the main functional groups present; however, as the functional groups that give strong absorptions, such as carboxylic acid groups and aliphatic moieties, were common to nearly all the samples, these could only be differentiated to a limited extent.

More conclusive results were obtained by NMR. The Giglio pitch, Stockholm tar and the Mary Rose tars and pitches produced very similar spectra and were clearly distinct from the other samples. Whereas infrared spectra are largely dependent on the main functional groups present, NMR spectra are more dependent on the structure of the components within the sample. The intensity of the signals in ^{1}H NMR are proportional to the number of protons resonating; infrared spectroscopy, however, does not exhibit the same proportionality, the intensity of the signal depends on the change in dipole moment as a bond vibrates. This results in a dominance of the spectra by signals due to, for instance, vibrations of carbonyl bonds. The narrower width of ^{1}H NMR than infrared signals means that NMR produces higher resolution spectra. GC was found to provide very informative fingerprints of the different samples, but the preparation involved was relatively lengthy and the results were dependent on achieving reproducible chromatographic conditions.

Further characterisation of the samples required detailed molecular analysis by GC - MS. This method provided by far the most informative data, not only clearly indicating a pine wood origin for the Giglio pitch and Mary Rose tars and pitches, but also allowing details of their molecular composition to be unravelled, thus revealing subtle differences between the samples, perhaps related to minor variations in their manufacture. In situations where little is known of the origins of an archaeological sample, or if no standards are available for comparison, GC - MS would be the preferred method. It does, however, have the significant disadvantage of being slow and, probably, of very limited access to archaeologists. In the study described in this paper, NMR, which is intrinsically faster, provided an unambiguous fingerprint match of the archaeological samples to pine wood tar. The advantages and disadvantages of each of the analytical techniques investigated is summarised in Table 5.

Conclusions

The bulk chemical, chromatographic and spectral properties of samples of pitches and tars from the Mary Rose and Giglio shipwrecks are consistent with an origin from pine wood. Detailed molecular analysis by GC - MS provided conclusive evidence for such a source. GC - MS yielded the most informative data and is the preferred method for analysis of this type of material. In this study, NMR provided a facile means of unambiguously characterising the samples.

The unambiguous identification of the sources of pitches and tars, even after submergence for up to 2500 years, demonstrates the potential use of analytical organic chemistry in archaeology, when favourable conditions for preservation of organic matter have prevailed.

We thank the Mary Rose Trust for provision of samples and especially Mr. I. Oxley and Dr. M. Rule for valuable discussions. We also thank Mr. M. Bound and the World Ship Trust for pitch from the Giglio wreck (courtesy of the Superintendency of Archaeology for Tuscany); Dr. W. Ladner and colleagues of the Coal Research Establishment for reference samples of coal and peat tars; Mr. M. I. Danischewsky of the White Sea and Baltic Tar Company, Mr. D. W. Kelly of Carbotech and Dr. S. C. Brassell for valuable discussions; Dr. T. M. Peakman for running the NMR spectra; Mrs. A. P. Gowar, Ms. L. Dyas and Mr. C. L. Saunders for assistance with GC-MS facilities; NERC for grants (GR3/2951 and GR3/3758) providing GC-MS and MS computing facilities; and British Petroleum plc for financial support (R. P. E.). The investigation reported in this paper represents in part work performed by W. J. H. and K. J. for their BSc Theses.

References

1. Goffer, Z., "Archaeological Chemistry," Wiley, Chichester, 1980.
2. Mackenzie, A. S., Brassell, S. C., Eglinton, G., and Maxwell, J. R., *Science,* 1982, **217**, 491.
3. Saltzmann, M., *in* Carter, G. F., *Editor,* "Archaeological Chemistry II: Analysis of Dyes," American Chemical Society, 1978, p. 172.
4. Beck, C. W., Wilbut, E., and Meret, S., *Nature* (*London*), 1964, **201**, 256.
5. Plahter, U., *Saertr. Fra, Univ. Oldsaksamlings Arbok,* 1969, 217.
6. Cassar, M., Robins, G. V., Fletton, R. A., and Alstin, A., *Nature* (*London*), 1983, **303**, 238.
7. Thornton, M. D., Morgan, E. D., and Celoria, F., *Sci. Archaeol.,* 1970, **2–3**, 20.
8. Morgan, E. D., Titus, L., Small, R. J., and Edwards, C., *Arctic,* 1983, **36**, 356.
9. Mills, J. S., and White, R., *Stud. Conserv.,* 1977, **22**, 12.
10. Mills, J. S., and White, R., *Natl. Gallery Tech. Bull.,* 1982, **6**, 3.
11. White, R., and Castle, S. A., *Britannia,* 1978, **9**, 383.
12. Marsh, B., *Sunday Express Mag.,* 7th October, 1984, 22.
13. Evershed, R. P., Jerman, K., and Eglinton, G., *Nature* (*London*), 1985, **314**, 528.
14. Simoneit, B. R. T., *Geochim. Cosmochim. Acta,* 1977, **41**, 463.
15. Simoneit, B. R. T., and Mazurek, M. A., *Atmos. Environ.,* 1982, **16**, 2134.
16. Simoneit, B. R. T., Grimalt, J. O., Wang, T. G., Cox, R. E., Hatcher, P. G., and Nissenbaum, A., *Org. Geochem.,* 1986, **10**, 877.
17. Huang, W.-Y., and Meinschein, W. G., *Geochim. Cosmochim. Acta,* 1976, **40**, 323.
18. Hussler, G., and Albrecht, P. A., *Nature* (*London*), 1983, **304**, 262.
19. Hoffman, C. F., *PhD Thesis,* University of Bristol, 1984.
20. Danischewsky, M. I., "Post-Medieval Archaeology," Volume 9, Society for Post-Medieval Archaeology, 1975.
21. Meiggs, R., "Trees and Timber in the Ancient Mediterranean World," Clarendon, Oxford, 1982.
22. Forbes, R. J., "Bitumen and Petroleum in Antiquity," Brill, Leiden, 1936.
23. Macnamara, E., "Everyday Life of the Etruscans," Batsford, London, 1973.
24. Shullard, H. H., "The Etruscan Cities and Rome," Camelot Press, 1967.
25. Philp, R. P., "Fossil Fuel Biomarkers: Applications and Spectra," Elsevier, Amsterdam, 1985.

Paper A6/440
Received November 17th, 1986
Accepted December 18th, 1986

Spectrofluorimetric Determination of Beryllium in Rocks, Alloys and Steels with Nuclear Fast Red

Francisco Salinas, Arsenio Muñoz de la Peña and Francisco Muñoz de la Peña
Department of Analytical Chemistry, University of Extremadura, 06071 Badajoz, Spain

A spectrofluorimetric method is described for the determination of trace amounts of beryllium, based on its reaction with Nuclear Fast Red. The detection limit is 3 ng ml^{-1} and the method can be used to determine between 10 and 80 ng ml^{-1} of beryllium. The stoicheiometry of the complex is 1 : 1. The method has been satisfactorily applied to the determination of beryllium in rocks, alloys and steels.

Keywords: *Beryllium determination; spectrofluorimetry; rocks; alloys; steels*

Nuclear Fast Red (sodium 1,3-dihydroxy-4-aminoanthraquinone-2-sulphonate) has been used as a photometric reagent for determination of calcium,[1-3] lanthanum[4] and zirconium,[4] and it has been proposed as a qualitative reagent for the fluorimetric detection of aluminium.[5] Of anthraquinone derivatives,[6] 1,4-dihydroxyanthraquinone (quinizarin), quinizarin-2-sulphonic acid, 5,8-dichloroquinizarin, 1-amino-4-hydroxyanthraquinone, 1,4,5,8-tetrahydroxyanthraquinone and 1-hydroxy-2-carboxyanthraquinone have been proposed for the fluorimetric determination of beryllium.

In all the above examples, the reagents have hydroxy or amino groups in the 1 and 4 positions, except 1-hydroxy-2-carboxyanthraquinone, and the reactions are developed in water or in an ethanol - water medium with a high percentage of ethanol. Nuclear Fast Red also has this structural characteristic and also the advantage of a sulphonate group in the molecule, which makes the reagent and its complex with beryllium soluble in water.

This paper describes the fluorescent characteristics of the complex formed between Nuclear Fast Red and beryllium and a spectrofluorimetric method for the determination of this ion. The proposed method has been applied satisfactorily to the determination of beryllium in rocks, alloys and steels.

Experimental

Reagents

All experiments were performed with analytical-reagent grade chemicals and pure solvents. Doubly distilled, de-mineralised water was used throughout.

The Nuclear Fast Red solution (2.5×10^{-4} M) was prepared by dissolving an exact mass of sodium 1,3-dihydroxy-4-aminoanthraquinone-2-sulphonate (Aldrich Chemicals) in water.

A 1.000 g l^{-1} standard beryllium solution was prepared from $BeSO_4.4H_2O$ in 0.2 M hydrochloric acid. More dilute solutions were prepared from this standard by dilution with the acid.

Apparatus

All fluorimetric measurements were performed on a Perkin-Elmer MPF-43 fluorescence spectrophotometer, equipped with an Osram BO 150-W xenon lamp, excitation and emission grating monochromators, 1-cm quartz cells, an R-508 photomultiplier and a Perkin-Elmer 056 recorder. A standard fluorescent stick (equivalent to a 3×10^{-4} M solution of Rhodamine B) was used daily to adjust the spectrofluorimeter to compensate for changes in source intensity. No correction was made to the instrumental response. A Selecta 382 thermostatic water-bath circulator was used for temperature control. The pH measurements were carried out using a Crison Digit 74 pH meter employing a glass - saturated calomel combination electrode.

Determination of Beryllium

Appropriate volumes of the sample solution (giving a final Be^{II} concentration between 10 and 80 ng ml^{-1}), 3 ml of 1 M acetic acid - acetate buffer solution (pH 6.25) and 6 ml of 1.0×10^{-4} M reagent solution were mixed in a 25-ml calibrated flask. The solution was diluted to the mark with distilled water. The fluorescence intensity ($\lambda_{ex.}$ = 495 nm, $\lambda_{em.}$ = 560 nm) was measured at 20 °C. A correction for a reagent blank was applied and a calibration graph was prepared in the same way.

Results and Discussion

Spectral Characteristics of the Complex

Nuclear Fast Red reacts with beryllium ions to give a fluorescent complex. The uncorrected excitation and emission fluorescence spectra of the complex and the reagent are shown in Fig. 1. The wavelengths chosen were 495 and 560 nm for excitation and emission, respectively, as these are the wavelengths at which the differences between the emission of the complex and the reagent are at a maximum.

Effect of Experimental Variables

The effect of pH was studied using sodium hydroxide solution and hydrochloric acid for adjustment. The fluorescence intensity was at a maximum and was independent of pH in the range 5.9–6.4 [Fig. 2(*a*)]. The pH can be suitably adjusted by the addition of a pH 6.25 acetic acid - acetate buffer solution. Under these conditions, the complex formation is instantaneous and the complex remains stable for at least 8 h.

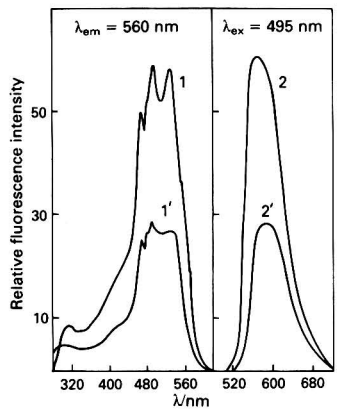

Fig. 1. Uncorrected fluorescence excitation and emission spectra of the complex Nuclear Fast Red - Be^{II} (1,2) and of the reagent alone (1', 2'). pH = 6.0; [Be^{II}] = 8.8×10^{-6} M; [reagent] = 4.0×10^{-5} M

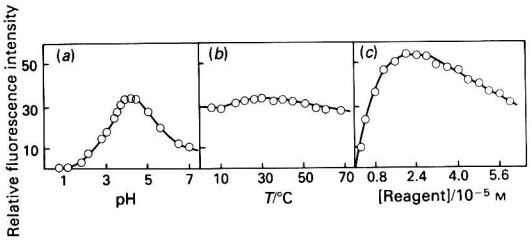

Fig. 2. Influence of (*a*) acidity, (*b*) temperature and (*c*) concentration of Nuclear Fast Red on the fluorescence intensity of the Nuclear Fast Red - Be^{II} complex

Variations in the order of mixing of the solutions had no influence on the fluorescence.

The effect of temperature on the fluorescence was studied over the range 5–70 °C [Fig. 2(*b*)]. The fluorescence intensity is not appreciably affected by changes in the temperature between 20 and 40 °C. At higher temperatures there is a gradual decrease in the fluorescence with increasing temperature.

The effect of reagent concentration on the fluorescence intensity of solutions containing a constant beryllium concentration of 8.8×10^{-6} M was studied under conditions similar to those of the recommended method [Fig. 2(*c*)]. The fluorescence intensity increased with increasing reagent concentration up to 2.0×10^{-5} M, remained constant between this value and 2.8×10^{-5} M and then decreased above this concentration. In accordance with this, a 2.4×10^{-5} M reagent concentration was chosen as the optimum.

The stoicheiometry of the complex was studied under the established conditions by the classical methods of Job[7,8] and Yoe and Jones.[9] From these studies the composition of the complex was concluded to be 1 : 1 (ligand to metal).

Analytical Parameters

Under the operating conditions outlined in the proposed procedure, there is a satisfactory linear relationship between fluorescence intensity and Be^{II} concentration over the range 10–80 ng ml^{-1}. For two series of ten measurements on 20 and 60 ng ml^{-1} of Be^{II}, relative errors of 1.42 and 0.44% and relative standard deviations of 0.39 and 0.37%, respectively, were obtained (95% confidence level).

The sensitivity of the method, reported as the slope of the calibration graph of fluorescence intensity *versus* concentration (in ng ml^{-1}) obtained by linear regression is 1.0 (r = 0.9988) and the detection limit is 3 ng ml^{-1} when defined as the analyte concentration leading to a fluorescence intensity that is three times the blank standard deviation.[10,11]

Interferences

The effects of 50 foreign ions on the proposed method were examined. For these studies, different amounts of the ionic species were added to 60 ng ml^{-1} of beryllium by first testing a 100-fold *m/m* ratio of interferent to beryllium, and, if interference occurred, this ratio was progressively reduced until the interference ceased. The tolerance criterion was a variation of fluorescence intensity of not more than 5% from the value expected for beryllium alone. The tolerance limits for these ions are given in Table 1. The interference of Cu^{II} is eliminated in the presence of $S_2O_3^{2-}$ as a masking agent and those of Fe^{III} and Al^{III} are reduced in the presence of EDTA and tartrates, respectively. The low tolerance to ions such as Y^{III}, La^{III} and Th^{IV} is due to the formation of complexes between these ions and the reagent at the pH of the determination. Al^{III} also forms a fluorescent complex, but the reaction is time dependent. As can be seen from Table 1, the proposed method is relatively free from interferences.

Table 1. Effect of various ions on the determination of 60 ng ml^{-1} of Be^{II}

Ion added	Tolerance ratio of ion to Be^{II}
Li^{I}, Na^{I}, K^{I}, Ag^{I}, Mg^{II}, Ca^{II}, Hg^{II}, Cd^{II}, Sr^{II}, Ba^{II}, Pb^{II}, Co^{II}, Ni^{II}, Zn^{II}, Cu^{II},* Mn^{II}, V^{V}, Ge^{IV}, Cr^{VI}, W^{VI}, Mo^{VI}, NH_4^+, NO_3^-, NO_2^-, IO_3^-, ClO_3^-, $S_2O_3^{2-}$, CO_3^{2-}, SO_4^{2-}, SCN^-, Cl^-, Br^-, I^-, EDTA, tartrates	100 : 1
Hg^{I}, Bi^{III}	75 : 1
PO_4^{3-}	50 : 1
Fe^{III}†	40 : 1
F^-, Al^{III},‡ In^{III}	10 : 1
Citrates, Th^{IV}	5 : 1
Sn^{II}, Y^{III}, Ce^{III}, Cr^{III}, Ti^{IV}, La^{III}	1 : 1

* In the presence of $S_2O_3^{2-}$ (400 μg ml^{-1}).
† In the presence of EDTA (6 μg ml^{-1}).
‡ In the presence of tartrates (90 μg ml^{-1}).

Table 2. Determination of beryllium in beryl*

Be added/ ng ml^{-1}	Be found/ ng ml^{-1}	Recovery, %
0.0	21.5	—
12.0	33.5	100
20.0	41.0	98.8
28.0	50.5	102
32.0	53.0	99.1
48.0	69.5	100

* Sample supplied by the Geology Department of the University of Extremadura. The amount of beryllium found in the sample was 5.37%. The stoicheiometric amount of beryllium in natural beryl is 5.03% ($3BeO.Al_2O_3.6SiO_2$).

Applications

The recommended procedure has been applied satisfactorily to the determination of beryllium in a beryl, two copper - nickel alloys and a steel.

Determination of beryllium in beryl

Fuse 0.1 g of sample in a platinum dish with 0.4 g of sodium carbonate for 30 min. Dissolve the melt in 5 ml of 1 + 1 hydrochloric acid. Add 10 ml of hydrochloric acid and evaporate to dryness. Bake at 110–120 °C for 30 min. Moisten the residue with 5 ml of hydrochloric acid and add 70 ml of water. Bring to the boil, filter and dilute to 1 l. Take an aliquot of 0.1 ml and determine beryllium by the proposed procedure.

The procedure was verified by the method of standard additions. The results obtained are summarised in Table 2, including the recoveries obtained in the determination of beryllium; 5.37% of beryllium was found in the sample.

Determination of beryllium in copper - nickel alloys

Copper base alloys containing beryllium find extensive use[12] in springs of all kinds and in diaphragms of pressure-sensitive instruments because of their fatigue resistance. They are also used in the manufacture of dies for pressing plastics, electrodes and other components for resistance-welding work and sparkless tools for use in mines, refineries and similar industries. Beryllium is also used as an alloying agent in nickel[12] to produce a high-strength alloy that is resistant to corrosion and wear, and which is used for instrument springs, hypodermic needles and surgical instruments.

Table 3. Determination of beryllium in copper - nickel alloys

Standard sample	Certified composition, %	Total Be added/μg	Be found/ μg	Recovery, %
Copper - nickel alloy (BCS No. 180/2)	Cu 68.12, Ni 30.35, Fe 0.68, Mn 0.75, C 0.04, S 0.006, Si 0.018, Pb 0.003, Co 0.005	200	192	96
		100	98	98
		50	51	102
Monel Alloy 400 (BAS No. 363/1)	Cu 31.90, Ni 64.7, Fe 1.86, Mn 1.26, C 0.140, Si 0.028, Al 0.027, Co 0.032, Cr 0.047, Pb <0.002, Ti 0.033	225	220.5	98
		150	144.4	96
		75	74.3	99
		37.5	36.0	96

Table 4. Determination of beryllium in steel

Standard sample	Certified composition, %	Total Be added/μg	Be found/ μg	Recovery, %
High speed steel (BAS No. 64b)	C 0.90, Cr 4.55, V 1.99, Mo 4.95, W 7.05	20	19.5	97.5
		20	20.0	100
		20	19.3	96.5

Table 5. Comparison with other related ligands

Reagent	Quantitation limit/ μg ml^{-1}	References
Quinizarin	0.02	15–19
Quinizarin-2-sulphonic acid	0.001	20
5,8-Dichloroquinizarin	0.1	16
1,4,5,8-Tetrahydroxyanthraquinone	0.1	16
1-Amino-4-hydroxyanthraquinone	0.02	15, 16, 21
1-Hydroxy-2-carboxyanthraquinone	0.03	22
Nuclear Fast Red	0.01	This work

For the determination of beryllium in copper - nickel base alloys, take about 0.1 g of the sample, add 5 ml of nitric acid and heat until the evolution of nitrogen oxides ceases. Cool, adjust the pH to 5 and dilute the solution to 1 l in a calibrated flask. Take an aliquot of this solution and determine beryllium by the proposed procedure, adding 400 μg ml^{-1} of $S_2O_3^{2-}$ to avoid the interference produced by the copper present.

The recoveries of known amounts of beryllium added to two copper - nickel base alloys are summarised in Table 3.

Determination of beryllium in steels

Beryllium steels with various amounts of Ni, Co, Cr and Mo are extensively used for springs (some high-temperature) and where good resistance to corrosion and wear is required (valve discs, pump impellers and gears).[12]

In order to avoid the interference from iron in the determination of beryllium in steels by the proposed procedure, we separated beryllium by extraction with acetylacetone into chloroform in the presence of EDTA.[13]

The recovery of beryllium was determined by the addition of a known amount of beryllium to a solution of stainless steel. The steel is dissolved by the following procedure. Dissolve a 0.1 g amount of high-speed steel (BAS No. 64b) of the composition given in Table 4 in 4 ml of 50% of sulphuric acid to which 1 ml of nitric acid has been added; evaporate the mixture with the evolution of sulphur trioxide. Dissolve the residue in 10 ml of water, filter and wash the filter with hot dilute sulphuric acid and hot water. Add solution equivalent to 20 μg of beryllium, followed by 50 ml of 10% EDTA and then concentrated ammonia solution until the yellow Fe^{III} - EDTA complex changes to red.[14] Dilute to 100 ml, pipette 25 ml of the solution into a separating funnel and add 5 ml of 5% aqueous acetylacetone. Adjust the pH to 7–8 by the addition of 0.1 M sodium hydroxide. Allow the solution to stand for 5 min and then extract with three 10-ml aliquots of chloroform, shaking vigorously for 2 min. Combine the extracts in a platinum dish. Cover the chloroform extracts with about 15 ml of water, 2.0 ml of concentrated nitric acid and 2.0 ml of 60% perchloric acid.

Evaporate off the chloroform on a water-bath and then transfer the dish to a hot-plate and continue to evaporate to about 0.5 ml. Repeat the evaporation with a further 2.0 ml of nitric and perchloric acids, after which no organic material should remain.[13] Dilute the solution to 250 ml in a calibrated flask.

Aliquots of the above solution were taken and beryllium was determined as described. The results obtained are given in Table 4.

Discussion

The results obtained show that the method can be reliably applied to the determination of beryllium in various samples. The proposed method is simple, sensitive and selective and it was compared with other methods previously reported that use related ligands (Table 5). The method using quinizarin-2-sulphonic acid involves development in 95% ethanol, resulting in a quantitation limit higher than that reported in Table 5. The method of extraction of beryllium, as acetylacetonate in chloroform, used for its determination in steels, is the usual way of separating this ion from interferences.

We thank the Comision Asesora Cientifica y Tecnica del Ministerio de Educacion y Ciencia de España for supporting this study (Project No. 2903-83).

References

1. McGee-Russell, S. M., *Nature (London)*, 1955, **175**, 301.
2. Baar, S., *Clin. Chim. Acta*, 1957, **2**, 567.
3. Kingsley, G. R., and Robnett, O., *Anal. Chem.*, 1961, **33**, 552.
4. Popa, G., Baiulescu, G., Paralescu, I., and Mircea, D., *An. Univ. Bucuresti, Ser. Stiint. Nat. Chim.*, 1962, **11**, 77.
5. Malowan, L. S., *Ciencia (Mex.)*, 1956, **1**, 11.
6. Fernandez-Gutierrez, A., and Muñoz de la Peña, A., *in* Schulman, S. G., *Editor*, "Molecular Luminescence Spectroscopy: Methods and Applications, Part I," Wiley, New York, 1985, Chapter 4.
7. Job, P., *Ann. Chim.*, 1927, **9**, 114.
8. Vosburgh, W. C., and Cooper, G. R., *J. Am. Chem. Soc.*, 1941, **63**, 437.
9. Yoe, J. H., and Jones, A. L., *Ind. Eng. Chem., Anal. Ed.*, 1944, **16**, 111.
10. "Nomenclature, Symbols, Units and their Usage in Spectrochemical Analysis—II," *Spectrochim. Acta, Part B*, 1978, **33**, 242.
11. "Guidelines for Data Acquisition and Data Quality Evaluation in Environmental Chemistry," *Anal. Chem.*, 1980, **52**, 2242.

12. American Society for Testing and Materials, "Methods of Chemical Analysis of Metals," ASTM, Philadelphia, 1956, p. 536.
13. Adam, J. A., Booth, E., and Strickland, J. D., *Anal. Chim. Acta*, 1952, **6**, 462.
14. Sill, C. W., and Willis, C. P., *Anal. Chem.*, 1959, **31**, 598.
15. Hyshop, F., Palmes, E. D., Alford, W. C., Monaco, A. R., and Fairhall, L. T., *Natl. Inst. Health Bull.*, 1943, **181**, 49.
16. Prezeheval'skii, E. S., Belyavskaya, T. A., and Golovina, A. P., *Vestn. Mosk. Univ., Ser. II, Ser. Mat. Mekh. Fiz.* Khim., 1956, **1**, 191.
17. Fletcher, M. H., White, C. E., and Sheftel, M. S., *Ind. Eng. Chem., Anal. Ed.*, 1946, **18**, 179.
18. Bosa, M. J., *J. Indian Chem. Soc., Ind. News Ed.*, 1951, **14**, 61.
19. Dressel, W. M., and Ritchey, R. A., *US Bur. Min., Inf. Circ.*, 1960, 7946.
20. Guiraum, A., and Vilchez, J. L., *Quim. Anal.*, 1975, **29**, 265.
21. White, C. E., and Lowe, C. S., *Ind. Eng. Chem., Anal. Ed.*, 1941, **13**, 809.
22. Capitan, F., Salinas, F., and Franquelo, L. M., *Anal. Lett.*, 1975, **8**, 753.

Paper A6/312
Received September 5th, 1986
Accepted October 27th, 1986

Fluorimetric Determination of Aluminium and Beryllium in Mixtures by Synchronous Derivative Spectrometry

Francisco García Sánchez, Jose C. Márquez Gómez and Miguel Hernández López
Department of Analytical Chemistry, Faculty of Sciences, The University, Malaga-29071, Spain

Morin (2',3,4',5,7-pentahydroxyflavone) has been used as a ligand in the fluorimetric determination of beryllium and aluminium in binary mixtures. A synchronous derivative spectrofluorimetric method has been developed for the determination of beryllium and aluminium at ng ml^{-1} levels. The precision of the method, expressed as relative standard deviation, is better than 5%. This paper reports the testing of a graphical model used to measure derivative amplitudes. The method is based on the interference-free character of the isodifferential points in the derivative calibration graphs.

Keywords: *Beryllium determination; aluminium determination; synchronous derivative spectrometry; fluorimetry; morin*

Several organic ligands have been proposed for the separate determination of Be and Al that take advantage of the fact that these two ions, and other cations with empty *d* and *f* orbitals, give sensitive fluorogenic reactions with a wide range of organic reagents,[1,2] in particular in co-ordination processes. One of these reagents, morin, is especially suitable for the determination of beryllium because of its high sensitivity.

Fluorimetry is often used, even in routine laboratory work, to determine both Be and Al alone. However, to differentiate them in mixtures is more difficult because of their broad and featureless emission spectra, and the fact that their spectra strongly overlap.

This is to be expected for lumiphores in solution at room temperature especially if the emission is produced from metal chelates with organic ligands which have rigid skeletons. In these compounds, the introduction of metal ions produces changes in the structural configuration of the ligand and associated spectral differences are seen which are very similar to those seen in the interactions of protons with ligands. Consequently, small differences of only a few nanometres between the spectral shapes of the different complexes may be expected.

However, synchronous fluorimetry[3-5] and its associated band-narrowing effect, together with derivative spectrometry[6,7] (with additional spectral information), provides a satisfactory method of resolving these mixtures.

The graphical method used in this work is based on the spectral interference-free character of the derivative amplitudes measured from a common point (which may be termed isodifferential) on the base line to the break with the actual derivative curve. This approach offers acceptable levels of precision in the determination of Ga and Al with quinolin-8-ol[8] and in the resolution of pesticide residue mixtures.[9] This paper describes the use of morin in the determination of Al and Be in mixtures.

Experimental

Apparatus

All the fluorimetric measurements were carried out on a Perkin-Elmer LS-5 luminescence spectrometer, equipped with a xenon discharge lamp (9.9 W) pulsed at line frequency, F/3 Monk - Gillieron monochromators and 1 × 1-cm quartz cells. The spectrometer was connected to a Perkin-Elmer Model 3600 data station, provided with PECLS II applications software. The system responds to spectral derivatives and the structure calculates the first and second derivative of a spectrum. The analogue output to a chart recorder is digitally filtered using a Savitzky - Golay quadratic smoothing function and five operator-selectable widths to provide an optimum recorder output under the scanning conditions. In order to compare all the fluorimetric measurements and to ensure reproducible experimental conditions, the LS-5 fluorimeter was checked daily. A polymer fluorescence sample of *p*-terphenyl (10^{-7} M) gives a relative fluorescence intensity of 90% at $\lambda_{em.}$ = 340 nm and $\lambda_{ex.}$ = 295 nm, slit widths 2.5/2.5 and a sensitivity factor of 0.593. All the fluorimetric measurements were made at v_{scan} = 240 nm min^{-1}, a time constant of 1 s, slit widths of 2.5/2.5 and a sensitivity factor of 3.833.

Reagents

Morin was purchased from UCB, Brussels, Belgium, and was recrystallised twice from ethanol. Reagent solutions (0.05%) were prepared in absolute ethanol.

A 0.1 M Be stock solution was prepared from analytical-reagent grade $Be(NO_3)_2.4H_2O$ in distilled, de-mineralised water and standardised gravimetrically.

A 1 g l^{-1} Al stock solution was prepared from $Al(NO_3)_3.9H_2O$ (Sigma) in 1 M nitric acid. This solution was standardised with EDTA using Xylenol Orange as an indicator. Lower concentrations were obtained by dilution with de-mineralised water.

A pH 5.5 buffer solution was prepared from 2 M acetic acid and 2 M sodium acetate.

General Procedure

Place an aliquot of sample containing 0–0.8 μg of Al and Be in a 10-ml calibrated flask. Add 0.5 ml of 0.05% ethanolic morin solution, 0.5 ml of absolute ethanol and 2 ml of pH 5.5 acetate buffer solution and dilute to the mark with de-ionised water. Record the first and second derivative synchronous spectra between 340 and 500 nm against a reagent blank, with the following fixed instrumental parameters: $\Delta\lambda$ = 96 nm, a scan speed of 120 nm min^{-1}, a response time of 1 s and an integer factor of 20. Measure the first and second derivative values as the vertical difference on the dI_F or d^2I_F scale from the corresponding isodifferential point to the break with the first or second derivative curve. The concentration of Al and Be in the binary mixture is determined from the corresponding calibration graph run previously under similar conditions to those of the mixture.

Results and Discussion

Morin is frequently cited as one of the most sensitive reagents for the fluorimetric determination of Be[1,2] but it is not very selective as it forms fluorescent chelates with a large number of metals, including Al. Be has many similar properties to Al

and its compounds, and hence organic reagents that are used for the determination of Al frequently find application in the analytical chemistry of Be.

As suggested above, the emission spectra of both chelates are similar showing maxima at 510 and 517.5 nm, respectively. Both spectra are broad, with half band-widths of 66.4 and 60.4 nm, respectively. In Fig. 1 the emission spectra and the synchronous spectra recorded with $\Delta\lambda = 96$ nm (Stokes shift), and the corresponding first derivative spectra are shown. The synchronous spectra show a modest reduction in band width, are symmetric and produce symmetric first and second derivatives.

The chelation of Al and Be with morin occurs in a wide pH range, the maximum fluorescence intensity for the Al and Be chelates occurring at pH 3.5 and 12, respectively (Fig. 2). An increase in pH causes a linear increase in the fluorescence of morin measured at the same frequency. At pH 5.5 the three lumiphore species co-exist in the media with a suitable relative fluorescence intensity (I_F) to give good signal to noise ratios (SNR). A 10% ethanol concentration is adequate for the determination and a morin concentration below 5×10^{-4} M does not show fluorescence inversion phenomena; the order of addition of the reagents is immaterial. Under these conditions the fluorescence remains stable for at least 1 h.

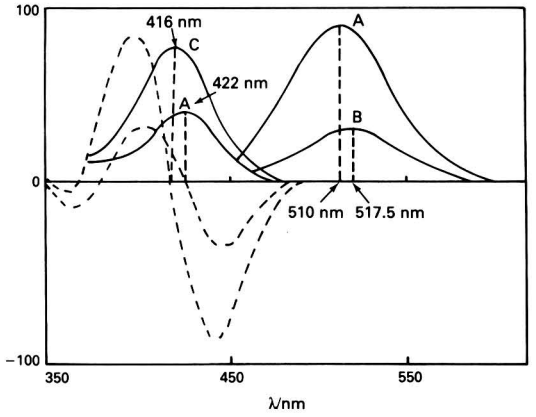

Fig. 1. Solid lines: emission spectra of (A) aluminium chelate and (B) beryllium chelate at $\lambda_{ex.} = 415$ nm, and synchronous spectra of (C) aluminium and (D) beryllium chelates at $\Delta\lambda = 96$ nm. Broken lines: first derivative of the synchronous spectra. Arrows indicates $\lambda_{max.}$. [Morin] = 1.4×10^{-4} M, pH 5.5; [Be] = 80 ng ml^{-1} [Al] = 60 ng l^{-1}

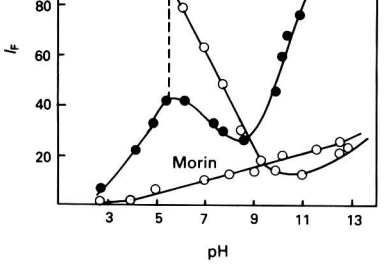

Fig. 2. Effect of pH on fluorescence intensity of morin - aluminium, morin - beryllium and morin alone. Initial concentrations: morin, 1.4×10^{-4} M; Al and Be, 300 ng ml^{-1}

Selection of Instrumental Parameters

In the synchronous derivative approach, two sets of parameters, which affect the derivative and synchronous signals in different ways may be optimised and selected.

As discussed elsewhere[10] the main parameters affecting the shape of the derivative spectra are the wavelength scan speed (ν_{scan}), the response time (t_r) and the derivative order. In general, a high value of ν_{scan} gives peaks with high amplitudes but small resolution, whereas a high t_r gives small amplitudes but a good SNR. Other instrumental parameters that must be optimised are the number of data points, which affects a digital derivative or the size of the wavelength increment over which the derivative is taken, $\Delta\lambda'$, if the derivative is analogue. In the LS-5 spectrofluorimeter, numbers of data points ranging from 5 to 81 are possible. Higher numbers give better SNR in both first and second derivatives,[8] thus 81 data points, corresponding to an integer factor of 20, were chosen for the experimental work.

For the selection of the appropriate constant difference in wavelength ($\Delta\lambda$)[11] between the two monochromators, various synchronous spectra at various wavelength differences near the Stokes shifts of both chelates were recorded. Maximum differences in the synchronous peaks corresponding to Al and Be chelates are obtained for $\lambda_{em.} - \lambda_{ex.} = 96$ nm.

A $\Delta\lambda$ of 96 nm, a scan speed of 120 nm min^{-1}, a response time of 1 s and an integer factor of 20 were employed in all further work.

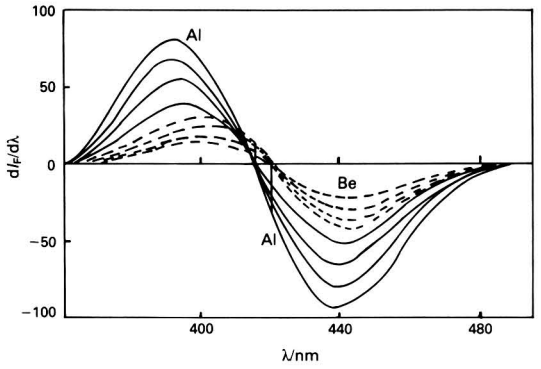

Fig. 3. Synchronous first-derivative spectra of complexes of Al (solid lines) and Be (broken lines). [Al]: 20, 40, 60, 80 ng ml^{-1}. [Be]: 20, 40, 60, 80 ng ml^{-1}. [Morin] = 1.4×10^{-4} M; pH 5.5; $\Delta\lambda = 96$ nm; scanning speed, 120 nm min^{-1}; slit width, 2.5 nm; response 1 s

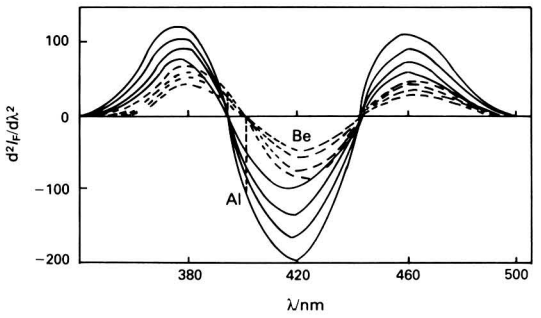

Fig. 4. Synchronous second-derivative spectra of complexes of Al (solid lines) and Be (broken lines). [Al] 20, 40, 60, 80 ng ml^{-1}. [Be]: 20, 40, 60, 80 ng ml^{-1}. [Morin] = 1.4×10^{-4} M; pH 5.5; $\Delta\lambda = 96$ nm; scanning speed, 120 nm min^{-1}; slit width 2.5 nm; response, 1 s

Table 1. Analytical parameters

Element	Method	Analytical sensitivity/ng ml^{-1}	Detection limit ($k = 3$)/ng ml^{-1}	Linear dynamic range/ng ml^{-1}	R.s.d.,%
Beryllium	1st derivative	1.40	3.80	12.5–100	5.0
	2nd derivative	4.71	5.70	19.0–100	5.0
Aluminium	1st derivative	1.40	1.45	5–100	3.6
	2nd derivative	2.00	2.80	10–100	4.2

Table 2. Determination of aluminium and beryllium in binary mixtures

Method	Ratio Al : Be	Concentration of Al/ng ml^{-1}		Error, %	Concentration of Be/ng ml^{-1}		Error, %
		Taken	Found		Taken	Found	
1st derivative	1:4	20	20.6	+3.0	80	76.8	−4.0
	1:1	40	39.0	−2.5	40	41.5	+3.7
	1:1.5	40	42.0	+5.0	60	58.5	−2.5
	1.5:1	60	62.4	+4.0	40	38.7	−3.2
	4:1	80	82.0	+2.5	20	20.3	+1.5
2nd derivative	1:4	20	21.1	+5.5	80	77.0	−3.7
	1:1	40	41.2	+3.0	40	38.7	−3.2
	1:1.5	40	41.0	+2.5	60	61.2	+2.0
	1.5:1	60	57.3	−4.5	40	41.5	+3.7
	4:1	80	81.8	+2.2	20	18.8	−6.0

Quantitative Analysis

As is seen in Fig. 1, the emission spectra of Be and Al chelates overlap, hence the quantification of mixtures is not possible even if the synchronous spectra are recorded. However, as shown in Figs. 3 and 4, the first and second derivatives of the synchronous spectra corresponding to the same component at different concentrations have values of zero on the ordinate scale (differential fluorescence). This so-called isodifferential point shows that the contribution of this component to the over-all derivative signal is equal to zero. Consequently, the amplitudes of the derivative spectra from this wavelength to the break with the experimental derivative curve of the mixture are independent of this component. Fig. 3 shows that the isodifferential point corresponding to the Al series is at 446 nm, whereas that of the Be series is at 422 nm. As pointed out previously,[8,9] the isodifferential method which is used to discriminate closely related spectral bands is based on the assumption that a linear relationship is obeyed between the analyte concentration and the fluorescence signal in the over-all concentration range studied and that the derivative of a profile is equivalent to the sum of the derivatives of its component bands.

Following the same reasoning as in references 8 and 9, the following equations may be derived:

$$\text{At } \lambda_1,\ dI_F/d\lambda_1 = k\phi_{F1}c_1\frac{d\varepsilon_1}{d\lambda_1} + k\phi_{F2}c_2\frac{d\varepsilon_2}{d\lambda_1}$$

$$\text{At } \lambda_2,\ dI_F/d\lambda_2 = k\phi_{F1}c_1\frac{d\varepsilon'_1}{d\lambda_2} + k\phi_{F2}c_2\frac{d\varepsilon'_2}{d\lambda_2}$$

where ϕ_F = fluorescence efficiency, c = concentration of the sample, I_F = fluorescence intensity and ε = molar absorptivity (1 mol^{-1} cm^{-1}).

When $d\varepsilon_1/d\lambda_1 = 0$ (zero crossing at this λ), the contribution of component 1 to the over-all derivative amplitude is zero and, consequently, component 2 may be measured as it is free from interferences from component 1. The same may be applied to component 2 when $d\varepsilon_2/d\lambda_2 = 0$.

The accuracy and precision of quantitative determinations of binary mixtures depend essentially on three variables in the fundamental emission spectra: the relative fluorescence intensity of both components, the relative band width and half maximum height and distance band maxima.[8,9]

Analytical Parameters

Based on this graphical model for quantitative analysis, linear relationships between dI_F or d^2I_F and the concentration of Al and Be were established in the concentration range 0–0.08 μg ml^{-1} of Al and between 0 and 0.08 μg ml^{-1} of Be. The calibration graphs obtained by the least-squares treatment were as follows:

1st derivative:

$dI_F/d\lambda = 0.165\ [\text{Be}] - 1.36,\ r = 0.993,\ \lambda = 416$ nm

$dI_F/d\lambda = 0.298\ [\text{Al}] + 7.17,\ r = 0.992,\ \lambda = 422$ nm

2nd derivative:

$d^2I_F/d\lambda^2 = 0.216\ [\text{Be}] + 0.22,\ r = 0.985,\ \lambda = 441$ nm

$d^2I_F/d\lambda^2 = 0.488\ [\text{Al}] + 5.29,\ r = 0.996,\ \lambda = 447$ nm

where the ion concentration is expressed in μg ml^{-1}.

The calculated analytical sensitivity, S_A, and detection limit[12] ($k = 3$), together with other details about precision, are given in Table 1. The results obtained in the determination of each ion in binary mixtures with different concentration ratios are shown in Table 2. It can be seen that the reported method gives satisfactory results for the determination of Al and Be in the binary mixtures outlined.

Conclusion

The usefulness of spectrofluorimetric analysis has been extended to the quantification of binary mixtures of metal chelates with strongly overlapped emission - excitation spectra. The method, based on a graphical model to measure derivative amplitudes, gives satisfactory precision levels (below 5% in r.s.d.) and accuracy (errors from 1.5 to 6%).

We thank the Comisión Asesora de Investigación Cientifica y Tecnica for supporting this study (Project No. 3007/83 C02-02).

References

1. Holzbecher, Z., Divis, L., Kral, M., Sucha, L., and Vlacil, F., *in* Chalmers, R. A., *Editor*, "Handbook of Organic Reagents in Inorganic Analysis ," Ellis Horwood, Chichester, 1976.
2. Fernandez Gutierrez, A., and Muñoz de la Peña, A., *in* Schulman, S. G., *Editor*, "Molecular Luminescence Spectroscopy: Methods and Applications," Part I, Wiley, New York, 1985.
3. Vo-Dinh, T., *Anal. Chem.*, 1978, **50**, 396.
4. Vo-Dinh, T., *Appl. Spectrosc.*, 1982, **36**, 576.
5. Garcia Sanchez, F., Cruces, C., and Ramos Rubio, A. L., *J. Mol. Struct.*, 1986, **143**, 473.
6. Talsky, G., Mayring, L., and Kreuzer, H., *Angew. Chem., Int. Ed. Engl.*, 1978, **17**, 785.
7. O'Haver, T. C., and Begley, T., *Anal. Chem.*, 1981, **53**, 1876.
8. Garcia Sanchez, F., Hernandez Lopez, M., and Marquez Gomez, J. C., *Spectrochim. Acta, Part A*, 1987, **43**, 101.
9. Garcia Sanchez, F., and Cruces, C., *Anal. Chem.*, in the press.
10. Medinilla, J., Ales, F., and Garcia Sanchez, F., *Talanta*, 1986, **33**, 329.
11. Cruces, C., and Garcia Sanchez, F., *Anal. Chem.*, 1984, **56**, 2035.
12. Garcia Sanchez, F., and Cruces, C., *Anal. Chem.*, 1986, **58**, 73.

Paper A6/355
Received September 22nd, 1986
Accepted November 20th, 1986

Spectrophotometric Determination of Pyridoxine Hydrochloride

V. Nirmalchandar, Rajganesh Viswanathan and N. Balasubramanian*
Department of Chemistry, Indian Institute of Technology, Madras-600 036, India

A spectrophotometric method is described for the determination of pyridoxine hydrochloride based on an oxidative coupling reaction with 4-aminoantipyrine in the presence of ammonium persulphate. The stable yellow colour obtained is measured spectrophotometrically at 420 nm. Minerals, sugars and several vitamins do not interfere when present in amounts usually found in pharmaceutical preparations. Modification of the method with boric acid can be used to distinguish pyridoxine from pyridoxal and pyridoxamine. Interference from ascorbic acid was eliminated by pre-separation as lead ascorbate. The molar absorptivity of the colour system is 5.41×10^3 l mol^{-1} cm^{-1} at 420 nm and Beer's law is obeyed in the range 0–250 μg of pyridoxine hydrochloride. The procedure is simple, rapid and suitable for routine determinations.

Keywords: *Pyridoxine hydrochloride determination; spectrophotometry; vitamins*

Pyridoxine hydrochloride was the first vitamin to be isolated from the B_6 group of vitamins and a comprehensive review of methods for the determination of pyridoxine has been given by Hashmi.[1] A direct spectrofluorimetric method[2] has been described by Soderhjelm and Lindquist, whereas a spectrophotometric method for the determination of pyridoxine in combination with other vitamins using 2,6-dichloroquinone chlorimide is the official method given in the USP.[3] In the USP method a boric acid modification is used to distinguish pyridoxine from pyridoxal and pyridoxamine. The principal drawback of the method is the poor colour stability, which makes rapid measurement of the developed colour necessary.

The method described here is a simple and sensitive spectrophotometric procedure based on the oxidative coupling of pyridoxine with 4-aminoantipyrine in the presence of ammonium persulphate followed by the measurement of the absorbance of the complex formed at 420 nm. The yellow colour formed is stable for 24 h. The concentration of pyridoxine in the presence of pyridoxal and pyridoxamine is generally established by the addition of boric acid to bleach the developed colour. The bleaching of the colour is attributed to the formation of a boric acid complex with the primary alcohol groups present in the pyridoxine. The addition of boric acid has been slightly modified in this study to distinguish pyridoxine in the presence of pyridoxal and pyridoxamine.

Experimental

Apparatus

A Carl Zeiss PMQ II spectrophotometer with 1-cm cells was used for the absorbance measurements.

Reagents

Analytical-reagent grade reagents were used throughout.

Standard pyridoxine solution, 50 p.p.m. Dissolve 0.1 g of pyridoxine hydrochloride in 100 ml of distilled water in a calibrated flask to give a 1000 p.p.m. solution. Dilute 5 ml of this solution to 100 ml to obtain a 50 p.p.m. working solution.

Sodium carbonate, 1%. Dissolve 1 g of anhydrous sodium carbonate in 100 ml of distilled water.

4-Aminoantipyrine, 0.4%. Dissolve 0.4 g of 4-aminoantipyrine hydrochloride in 100 ml of distilled water.

Ammonium persulphate, 1%. Dissolve 1 g of ammonium persulphate in 100 ml of distilled water.

Lead acetate, 1%. Dissolve 1 g of lead acetate in 100 ml of distilled water.

Boric acid, 1%. Dissolve 1 g of boric acid in 100 ml of distilled water.

Cation exchanger. Dowex 50-X8, Na^+ form.

Calibration Graph

To a series of 10-ml calibrated flasks add 0–5 ml of the 50 p.p.m. pyridoxine solution. Adjust the volume of the solution to 5 ml by adding the required amount of distilled water. To this solution add 1 ml of 1% sodium carbonate solution followed by 1 ml of 0.4% 4-aminoantipyrine and 1 ml of ammonium persulphate. Dilute the solution to 10 ml with distilled water and allow it to stand for 20 min for maximum colour development. Measure the absorbance at 420 nm against a reagent blank using 1-cm cells. Plot the absorbance against the concentration of pyridoxine hydrochloride to obtain a calibration graph.

Procedure

Determination of pyridoxine hydrochloride in pure solution

Treat 5 ml of a sample containing not more than 250 μg of pyridoxine hydrochloride as described under Calibration Graph and determine the concentration by reference to the calibration graph.

Determination of pyridoxine hydrochloride in pharmaceutical preparations

Suitable aliquots of aqueous samples can be used directly for the determination. For the analysis of tablets, representative samples of the ground tablets are stirred with 30 ml of distilled water and the residual solid is filtered off. The resulting aqueous solution is used for the determination of pyridoxine hydrochloride. For capsules containing oily preparations the contents should be partitioned between light petroleum and water and the aqueous layer used for the determination. A 5-ml aliquot of the aqueous sample solution containing not more than 250 μg of pyridoxine hydrochloride is treated as described under Calibration Graph and the concentration established by reference to the calibration graph.

If ascorbic acid (up to 50 mg) is present in the sample, take an aliquot of the sample and add 10 ml of lead acetate solution. Adjust the pH to 7.6 with ammonia solution. Filter off the precipitate and remove the excess lead as the carbonate by the addition of 5 ml of 1% sodium carbonate solution. Filter and make up the filtrate to a known volume. Use a suitable aliquot for the determination of pyridoxine hydrochloride.

For multivitamin preparations containing coloured dyes, take an aliquot of the sample and adjust the pH to 3. Pass the

* To whom correspondence should be addressed.

sample through a Dowex 50-X8 column (cationic, Na^+ form) at a flow-rate of 2 ml $min.^{-1}$ Wash the column with distilled water (adjusted to pH 3). Elute the pyridoxine with 0.1% sodium carbonate solution and use the eluate for the determination. Using this separation procedure the interference of ascorbic acid is also eliminated.

If the samples contain species such as pyridoxal and pyridoxamine, which undergo oxidative coupling with 4-aminoantipyrine, take two 5-ml aliquots of the sample containing not more than 250 μg of pyridoxine hydrochloride and to one of these add 1 ml of 1% boric acid solution and adjust the pH to 7 with sodium carbonate solution. Add 1 ml of 1% sodium carbonate solution followed by the other reagents as described under Calibration Graph and measure the absorbance. The absorbance of the sample in the presence of boric acid will be less than that of the sample without boric acid owing to the formation of a complex between the boric acid and pyridoxine, resulting in no colour development. The difference in absorbance between the two aliquots is used to determine the concentration of pyridoxine.

Results and Discussion

Various parameters were optimised to give maximum colour development. Although potassium or ammonium persulphate could be used for colour development, ammonium persulphate was chosen based on solubility considerations. The absorbance was found to be constant in the pH range 7.5–9. Although various reagents such as sodium hydroxide, aqueous ammonia and sodium carbonate could be used to adjust the pH, sodium carbonate was selected because the use of 1 ml of 1% sodium carbonate was sufficient to maintain the pH in the range 8 ± 0.5. It was also found that a minimum period of 20 min is required for maximum colour development. The developed colour was found to be stable for 24 h. It was further established that the concentration of 4-aminoantipyrine should be in the range 0.75–2 ml of a 0.4% solution in order to obtain the maximum colour development with minimum blank values. The ammonium persulphate concentration should be in the range 0.75–1.25 ml of a 1% solution. The species responsible for the colour is a phenazene - pyridoxine dye[4] (Fig. 1). The absorption spectrum of the colour system is shown in Fig. 2 and the absorbance of the sample against a blank is found to be constant in the range 410–430 nm. Hence all absorbance measurements were carried out at 420 nm. The calculated molar absorptivity is 5.41×10^3 l mol^{-1} cm^{-1} at 420 nm. The system obeys Beer's law in the concentration range 0–250 μg of pyridoxine hydrochloride.

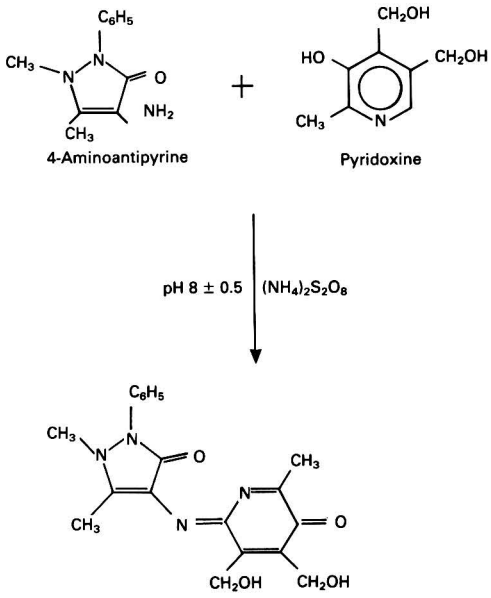

Fig. 1. Reaction scheme

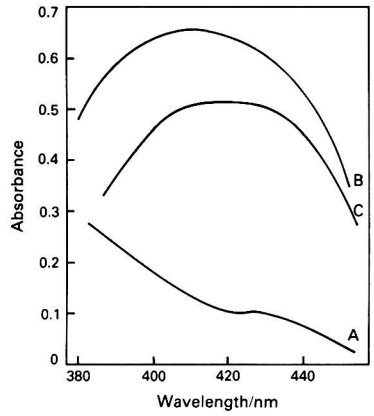

Fig. 2. Absorption spectra. A, Blank; B, 200 μg of pyridoxine hydrochloride; and C, 200 μg of pyridoxine hydrochloride against blank

Interference Studies

The interference of various cations, anions and organic compounds usually associated with pyridoxine was studied and the results are shown in Table 1. A deviation of more than ±0.02 from the absorbance of the solution without any interfering species was taken to indicate interference.

The interference of ascorbic acid, which is usually found in high concentrations in pharmaceutical preparations, is eliminated by separating it as lead ascorbate at a pH of 7.6 (adjusted with aqueous ammonia).

Pyridoxal and pyridoxamine interfere in the determination of pyridoxine when they are present at concentrations of 100 μg. The interference from up to 1000 μg of these compounds can be overcome by modification with boric acid. When boric acid was added after colour development to a system containing pyridoxine, no bleaching of the colour was observed. This is unexpected and can be explained by the fact that the primary alcohol groups responsible for the formation of complexes with boric acid are oxidised by the persulphate.

By changing the order of addition it is possible to distinguish pyridoxine from pyridoxal and pyridoxamine. When boric acid was added prior to the addition of persulphate to samples containing pyridoxine alone and to mixtures containing pyridoxal and pyridoxamine together with pyridoxine, no colour development was observed in the samples containing pyridoxine alone. This clearly indicates that the boric acid complex formation resists the oxidation of primary alcohol groups by persulphate. Hence, pyridoxine can be determined even when present with pyridoxal and pyridoxamine (Table 2).

Application of the Method

The method was applied to the determination of pyridoxine hydrochloride in various multivitamin formulations (Table 3). Common excipients such as talc, lactose, starch and magne-

Table 1. Results of interference study. Amount of pyridoxine hydrochloride present, 200 μg

Interfering species	Concentration/ μg	Remarks
Oxalic acid, citric acid, tartaric acid, urea, thiourea, D-glucose, sucrose, starch, ethanol, glycerol, EDTA, Zn^{2+}, Co^{2+}, Mg^{2+}, nicotinic acid, calcium pantothenate	10000	No interference
Ascorbic acid, thiosulphate, thiamine hydrochloride, Fe^{2+}	3000	No interference
Riboflavin, folic acid, pyridoxamine dihydrochloride, pyridoxal-5-phosphate	100	Interferes by increasing the absorbance
Ascorbic acid*	10000	No interference
Riboflavin, folic acid†	5000	No interference
Pyridoxal, pyridoxamine‡	1000	No interference

* Pre-separated as lead ascorbate.
† Pyridoxine separated using Dowex 50-X8 resin.
‡ Modification with boric acid.

Table 2. Determination of pyridoxine hydrochloride in the presence of pyridoxal and pyridoxamine

Pyridoxine hydrochloride/ μg	Pyridoxal-5-phosphate/ μg	Pyridoxamine dihydrochloride/ μg	Absorbance
100	—	—	0.26
—	100	—	0.06
—	—	100	0.09
100*	—	—	0.00
—*	100	—	0.056
—*	—	100	0.09
100	100	100	0.41
100*	100	100	0.15
100	1000	1000	1.60
100*	1000	1000	1.35

* Sample treated with 1 ml of 1% boric acid and pH adjusted to 7 before the addition of sodium carbonate solution.

Table 3. Application of the proposed method to the determination of pyridoxine in various multivitamin formulations

Sample	Manufacturer's specification/ mg	Pyridoxine found* Proposed method/ mg	Pyridoxine found* USP method/ mg
Abdec drops (Parke Davis)	1.0	1.02	1.01
Digiplex (Teddington Chemical Factory)	0.5	0.55	0.54
B Complex Oral (Teddington Chemical Factory)	0.5	0.56	0.55
Beplex forte (Glaxo)	3.0	3.15	3.10
Becadexamin (Glaxo)	2.0	2.12	2.15
Becozym C forte (Roche)	3.0	3.2	3.15

* Average of five determinations.

sium stearate do not interfere in the determination. Recovery studies were carried out by spiking pyridoxine hydrochloride solution into the pharmaceutical preparations and determining the concentration of pyridoxine hydrochloride. The recovery of pyridoxine was found to be in the range 99–99.5%. The results were also compared with those obtained by the USP method.[3]

Conclusion

The proposed method has several advantages over existing procedures, the major advantage being the high stability of the colour system. The method is comparable in sensitivity to existing methods. The selectivity is further enhanced by boric acid modification by which means the concentration of pyridoxine can be determined in the presence of pyridoxal and pyridoxamine. The method is simple and rapid and can be used for the routine determination of pyridoxine.

References

1. Hashmi, M. V. H., "Assay of Vitamins in Pharmaceutical Preparations," Wiley, London, 1973, pp. 188–212.
2. Soderhjelm, P., and Lindquist, J., *Acta Pharm. Suecica*, 1974, **11**, 621.
3. "United States Pharmacopeia," 20th Revision, 15th Edition United States Pharmacopeial Convention, Rockville, MD, 1980, p. 198–199.
4. Mohler, E. F., Jr., and Jacob, L. N., *Anal. Chem.*, 1957, **29**, 1369.

Paper A6/319
Received September 10th, 1986
Accepted November 11th, 1986

Gas Chromatographic Method for the Determination of Isomeric Bromoisobutyric Acids and Their Chlorides

Anna Mayer, István Simonyi and József Reiter
EGIS Pharmaceuticals, P.O. Box 100, H-1475 Budapest, Hungary

A GC method for the determination of 3-bromoisobutyric acid and the isomeric 2-bromoisobutyric acid, 2,3-dibromoisobutyric acid and methacrylic acid as their trimethylsilyl esters was developed. The determination of the corresponding acid chlorides was performed after their conversion to the corresponding morpholides.

3-Bromoisobutyric acid (**2**) and its acid chloride (**6**) are important intermediates, produced by the addition of hydrogen bromide to methacrylic acid (**1**) in non-aqueous media (Scheme 1). 3-Bromoisobutyric acid is converted into

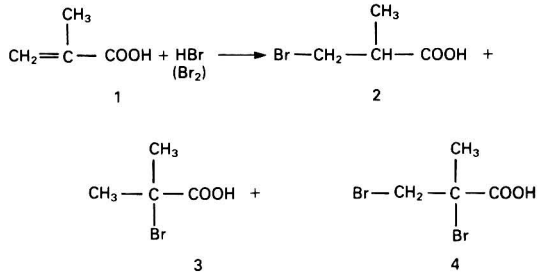

Scheme 1

its acid chloride (**6**) by the reaction with thionyl chloride (Scheme 2). The further work-up of the 3-bromoisobutyroyl chloride obtained leads, however, to some problems that could be explained by its insufficient purity.

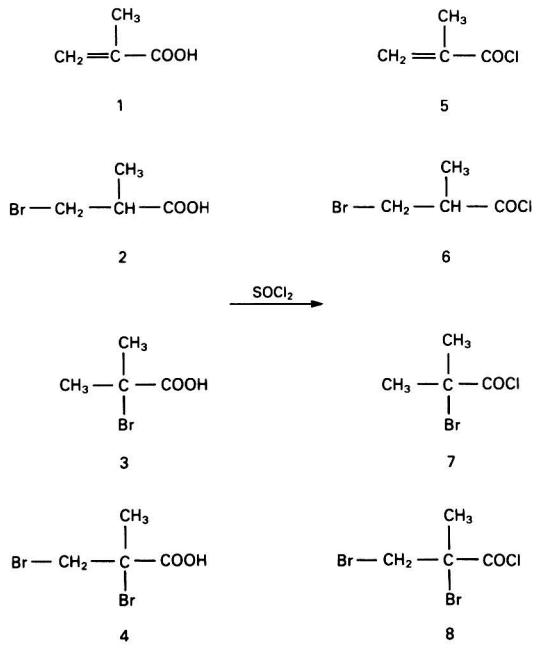

Scheme 2

As the addition of hydrogen bromide to methacrylic acid (**1**) proceeds *via* the anti-Markownikoff rule, first of all the formation of the Markownikoff product, *i.e.*, 2-bromoisobutyric acid (**3**) and its acid chloride (**7**) have to be taken into account as impurities in the above reactions. Hence a rapid, selective and quantitative method was required for the determination of the amount of **3** in **2** and that of **7** in **6**. Acids **1–4** were previously determined by titration to the acid and halogen and assay via the double bond, which made their selective determination impossible. We have developed a GC method for the determination of the isomeric bromoisobutyric acids **2** and **3** using reference samples of checked purity prepared by us for this purpose.

Derivatives **2** and **3** were chromatographed after their conversion into the corresponding trimethylsilyl esters[1] using Tri-Sil reagent in pyridine as solvent. In addition, further impurities in the 3-bromoisobutyric acid, namely unreacted methacrylic acid (**1**) and 2,3-dibromoisobutyric acid, namely unreacted methacrylic acid (**1**) and 2,3-dibromoisobutyric acid (**4**) (probably formed by the addition of bromine present as an impurity in the hydrobromic acid used in Scheme 1), were also determined as their trimethylsilyl esters by this method.

With the corresponding isomeric bromoisobutyroyl chlorides **6** and **7** it seemed to be reasonable to convert them into their methyl esters. However, this reaction was sluggish for analytical purposes, so the reaction of the acid chlorides with morpholine in benzene as solvent to yield the corresponding morpholides (**10** and **11**, respectively) was chosen as it offered a rapid and quantitative method for the determination of the isomeric bromoisobutyroyl chlorides and their impurities, namely the methacryloyl chloride (**5**) and the 2,3-dibromoisobutyroyl chloride (**8**) in the form of the corresponding morpholides **9** and **12**, respectively (Scheme 3). The determination was not affected by large amounts of thionyl chloride (5–10%) present in the sample.

Experimental

Reagents

All reagents were of analytical-reagent grade, unless indicated otherwise.

Methacrylic acid (**1**). Commercial product, triply distilled. B.p. 70 °C (12 mmHg) [Lit.[2] b.p., 72 °C (14 mmHg)].

2-*Bromoisobutyric acid* (**2**). Prepared as described.[3] M.p. 48–49 °C (Lit.[3] m.p., 48 °C).

3-*Bromoisobutyric acid* (**3**). Commercial product, triply distilled. B.p. 105 °C (12 mmHg), m.p. 22–23 °C after recrystallisation from light petroleum (Lit.[4] m.p., 22 °C).

2,3-*Dibromoisobutyric acid* (**4**). Prepared as described.[5] M.p. 47–48 °C after two recrystallisations from carbon disulphide (Lit.[5] m.p., 48 °C).

Methacryloyl morpholide (**9**). Prepared from methacryloyl

chloride and morpholine in benzene as described below. B.p. 96 °C (2 mmHg) [Lit.[6] b.p., 94.5 °C (1 mmHg)].

2-*Bromoisobutyroyl morpholide* (**10**). Prepared from 2-bromoisobutyroyl chloride and morpholine in benzene as described below. M.p. 66–67 °C (Lit.[7] m.p., 66 °C).

3-*Bromoisobutyroyl morpholide* (**11**). Prepared from 3-bromoisobutyroyl chloride and morpholine in benzene as described below. Purified by chromatography on a silica gel column with benzene - ethyl acetate (2 + 1) as eluent. Honey-like product. **11:** pmr ($CDCl_3$): δ, p.p.m., 1.19 (d, 3H, CH_3), 3.33 (t, 4H, NCH_2), 3.38 (m, 1H, CH), 3.67 (t, 4H, OCH_2), 3.16 (q, 2H, $BrCH_2$).

2,3-*Dibromoisobutyroyl morpholide* (**12**). Prepared from 2,3-dibromoisobutyroyl chloride and morpholine in benzene as described below. Purified by chromatography on a silica gel column with benzene - ethyl acetate as eluent. Honey-like product. **12:** pmr ($CDCl_3$): δ, p.p.m., 1.03 (s, 3H, CH_3), 3.32 (t, 4H, NCH_2), 3.44 (d, 2H, $BrCH_2$), 3.68 (t, 4H, OCH_2).

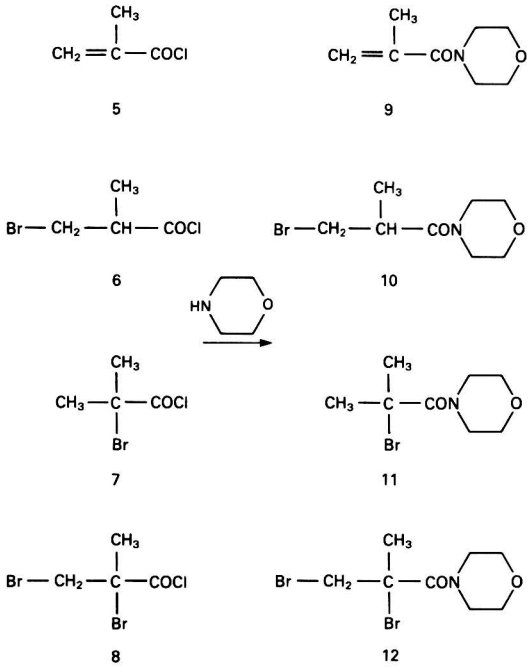

Scheme 3

Fumaric acid.

Tri-Sil reagent. Tri-Sil concentrate, Pierce Eurochemie.

Pyridine, silylation-grade solvent. Pierce Eurochemie.

Benzene, anhydrous.

Morpholine, anhydrous.

Magnesium sulphate.

Apparatus

A Hewlett-Packard 5840A reporting gas chromatograph was used for the GC measurements. Fumaric acid trimethylsilyl ester was used as an internal standard.

Preparation of Trimethylsilyl Esters of the Acids 1–4

To a mixture of 0.150 g of the appropriate acid samples and 0.015 g of fumaric acid in a Reacti-Vial (Pierce Eurochemie) were added 1 ml of pyridine and 0.4 ml of Tri-Sil reagent and the vial was shaken well and allowed to stand at room temperature for 15 min. A 1-μl volume of the solution obtained was injected directly on to the GC column.

Preparation of Morpholides of the Acid Chlorides 5–8

A solution of 3.7 g (± 0.05 g) of the appropriate acid chloride sample in 20 ml of benzene was added while stirring in one portion to a solution of 11 ml of morpholine in 60 ml of benzene. The temperature of the reaction mixture raised to 40–50 °C and a large amount of white crystalline material was precipitated. The mixture was stirred for a further 3 min at this temperature, then cooled with tap water to 20 °C. The crystals precipitated were dissolved by adding 30 ml of distilled water. Two clear phases were obtained, which were separated and the benzene layer was washed with 30 ml of water and the combined aqueous phases were extracted with 10 ml of benzene. The benzene phases obtained were combined, dried over anhydrous magnesium sulphate, filtered through a filter-paper impregnated with silica into a 100-ml calibrated flask and the volume was adjusted with benzene to 100 ml. A 1-μl volume of the solution obtained was injected directly on to the GC column.

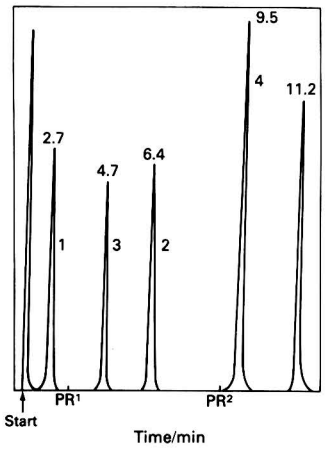

Fig. 1. Chromatograms of acids **1–4** as their trimethylsilyl esters

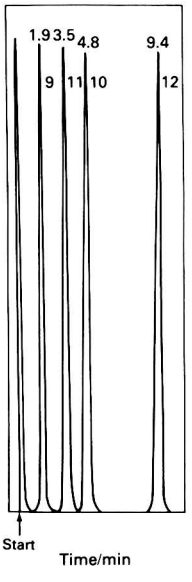

Fig. 2. Chromatograms of morpholides **9–11**

GC Conditions for the Determination of the Acids 1–4

Column. 1.8 m × 2 mm i.d. filled with 10% OV-101.
Temperature. 105 °C for 3.6 min, then increased (PR[1]) at 30 °C min^{-1} to 145 °C, kept at this temperature for 9.0 min, then increased (PR[2]) at 20 °C min^{-1} to 165 °C and kept at this temperature until the end of the determination
Detector. FID; carrier gas, nitrogen; flow-rate, 23 ml min^{-1}.
Injection. Directly on-column.
Retention times.
Methacrylic acid (**1**) trimethylsilyl ester . . t_{R1} = 2.7 min;
2-Bromoisobutyric acid (**3**) trimethylsilyl ester t_{R2} = 4.7 min;
3-Bromoisobutyric acid (**2**) trimethylsilyl ester t_{R3} = 6.4 min;
2,3-Dibromoisobutyric acid (**4**) trimethylsilyl ester t_{R4} = 9.5 min;
Fumaric acid trimethylsilyl ester (internal standard) t_{R5} = 11.2.

GC Conditions for the Determination of the Acid Chlorides 5–8

Column. 1.8 m × 2 mm i.d. filled with 5% SE-30.
Temperature. 175 °C.
Detector. FID; carrier gas, nitrogen; flow-rate, 25 ml min^{-1}.
Injection. Directly on-column
Retention times.
Methacryloyl morpholide (**9**) . . . . t_{R1} = 1.9 min;
2-Bromoisobutyroyl morpholide (**11**) . . t_{R2} = 3.5 min;
3-Bromoisobutyroyl morpholide (**10**) . . t_{R3} = 4.8 min;
2,3-Dibromoisobutyroyl morpholide (**12**) t_{R4} = 9.4 min.

Results and Discussion

Determination of the Acids 1–4

Compounds **1–4** were well chromatographed after converting them into their trimethylsilyl esters (see Fig. 1). The method is suitable for the determination of the above derivatives using fumaric acid trimethylsilyl ester as an internal standard even when the ratio of the above components is up to 1000, *e.g.*, when **1**, **2** and **4** are present in **3** as impurities at levels up to 0.1%.

For calibration, a mixture of 0.020 g of **1**, 0.050 g of **2**, 0.050 g of **3**, 0.050 g of **4** and 0.015 g of fumaric acid was converted into a mixture of trimethylsilyl esters by the method described above. The relative standard deviation was 1.22%.

Determination of the Acid Chlorides 5–8

As **5–8** were converted into their morpholides, the determination was not affected even by the large amounts (5–10%) of thionyl chloride often present in samples of **7**. The thionyl chloride is decomposed by the water present during the preparation of samples, giving hydrochloric and sulphuric acids, which are extracted in the form of their morpholinium salts into the aqueous phase so they do not interfere in the determination carried out on the benzene layer. After a simple and rapid preparation of samples, the morpholides obtained could be injected directly on to the column and are well and very rapidly separated (see Fig. 2). By this means quantitative information can be obtained within 10 min on the quality of 3-bromoisobutyroyl chloride (**7**) and impurities present in it in amounts down to 0.2%. The relative standard deviation was 1.4%.

The authors express their thanks to Lászloné Nyikos for technical assistance.

References

1. Pierce, A. E., "Silylation of Organic Compounds," Pierce Chemical, Rockford, IL, 1979, p. 160.
2. Autenrieth, C., and Pretzell, K., *Chem. Ber.*, 1903, **36**, 1272.
3. Hell, K., and Waldbauer, A., *Chem. Ber.*, 1877, **10**, 448.
4. Fittig, R., and Engelhorn, W., *Justus Liebigs Ann. Chem.*, 1880, **200**, 65.
5. Kolbe, C., *J. Prakt. Chem.*, 1895, **51**, 553.
6. *Belg. Pat.*, No. 650965; *Chem. Abstr.*, 1965, **63**, 17368e.
7. Canceill, J., Brienne, M. J., and Jacques, J., *Bull. Soc. Chim. Fr.*, 1966, 3612.

Paper A6/323
Received September 15th, 1986
Accepted November 19th, 1986

High-performance Liquid Chromatographic Determination of Artemisinine (Qinghaosu) in Human Plasma and Saliva

Shishan Zhao
Institute of Chinese Materia Medica, Academy of Traditional Chinese Medicine, Dongzhimen, Beijing, People's Republic of China

A liquid chromatographic method for the determination of artemisinine in human plasma and saliva is described. Artemisinine was extracted from plasma and saliva samples with ethyl acetate and then converted to a strongly UV-absorbing compound, Q260, by a known pre-column reaction. The samples were chromatographed on a C_{18} column with a 0.010 M NaH_2PO_4 - Na_2HPO_4 buffer solution (water - methanol = 6 + 4) as the mobile phase. The purity and identity of the peaks of interest were examined. The detection limit of artemisinine in plasma and saliva was about 2.5 ng ml^{-1}. Over the concentration range 10–1000 ng ml^{-1}, the recovery and relative standard deviation were >95% and 1.2–18%, respectively. Plasma and saliva concentration - time profiles were determined in two healthy volunteers after the administration of artemisinine.

Keywords: *Artemisinine determination; antimalaria herbal drug; human plasma and saliva; high-performance liquid chromatography; concentration - time profiles*

In two earlier papers,[1,2] Zhao and Zeng reported the pre-column reaction of artemisinine (Qinghaosu), a promising antimalaria constituent of the Chinese herbal drug *Artemisia annua* L.[3,4] During the pre-column reaction, artemisinine, which does not possess any sensitive and specific spectrophotometric characteristics, is converted to a UV-absorbing compound, Q292, which has an absorbance maximum at 292 nm. Q292 can be converted further to another strongly UV-absorbing compound, Q260, which has an absorbance maximum at 260 nm and can be determined by liquid chromatography owing to its stability. This paper describes a liquid chromatographic method based on this pre-column reaction for the determination of artemisinine in human plasma and saliva.

Experimental

Apparatus and Chemicals

The HPLC system consisted of an LC-4A chromatograph, an SPD-2AS detector, a SIL-1A LC injector, a CTO-2AS column oven, a 4 mm i.d. × 25 cm stainless-steel column packed with LiChrosorb RP-18 (10 μm, obtained from E. Merck, FRG) and a CR-2AX Chromatopac microprocessor, all manufactured by Shimadzu, Japan. The liquid vortex mixer used for extraction was a Jiangxi Clinical Apparatus Plant Model YKH-1 made in China.

The artemisinine standard material was purified and dried at 80 °C. It had a melting-point of 152–153 °C. All the chemicals used were of analytical-reagent grade. Distilled, de-ionised water was used in all the experiments.

Sampling and Preparation of Plasma and Saliva Samples

Artemisinine was administered orally in the form of capsules or via the rectum in the form of suppositories. The healthy volunteers, who were male and aged from 25 to 35, received a single dose 30 min after a light breakfast. Each dosage form contained the drug at 10 mg kg^{-1}. Plasma and/or saliva were sampled at frequent time intervals after the administration of the drug.

For plasma analysis, 4-ml blood samples were drawn from an arm vein into a heparinised 5-ml syringe and transferred into a centrifuge tube. After being cooled in an ice-bath for 5 min, the tube was centrifuged at 2800 rev min^{-1} for 8 min in order to separate the plasma. An 1.5-ml aliquot of the plasma sample was pipetted into a 5-ml centrifuge tube containing 0.5 ml of 0.9% *m/V* NaCl solution.

For saliva analysis, each sample was collected in a test-tube with the aid of a funnel. A 1.5-ml aliquot of the saliva sample was then pipetted into a 5-ml centrifuge tube containing 0.5 ml of 0.9% *m/V* NaCl solution.

Both the plasma and saliva samples were extracted with 2.5 ml of ethyl acetate on a vortex mixer with no pH adjustment. After being centrifuged at 2800 rev min^{-1} for about 3 min to facilitate the separation of the two solvent phases, the samples were stored in a refrigerator at about 4 °C for no longer than 40 h. Experiments showed that the plasma and saliva samples could be stored for at least 72 h without any change in the concentration of the drug.

For further treatment, each extract was transferred into a small centrifuge tube and each sample was extracted twice more with 2.5 ml of ethyl acetate. The extracts were combined in a centrifuge tube and evaporated to dryness at room temperature by a gentle stream of compressed air blowing on the surface of the solvent. The residue was dissolved in 0.1 ml of ethanol. After the addition of 0.4 ml of 0.2% *m/V* aqueous NaOH solution, the mixture was heated in a water-bath at 50 °C for 30 min. The tube was then quickly chilled in water and the mixture extracted twice with 0.5 ml of ethyl acetate using the vortex mixer, followed by centrifugation to facilitate the separation of the solvent layers. The organic phases were discarded. The trace amount of ethyl acetate remaining on the surface of the sample solution was evaporated with a gentle stream of compressed air at room temperature. The sample solution was then acidified with 40 μl of 2.5 M acetic acid solution in ethanol and transferred into a 0.5-ml tube. Methanol - water (2 + 8) was used to rinse the tube and adjust the sample volume to 0.5 ml. The whole procedure, from the alkaline reaction to the acidification with acetic acid solution, should be completed within 90 min, otherwise there is some loss of the unstable product of the alkaline reaction, Q292.[1]

Aliquots of 200 μl of each sample solution (equivalent to 0.6 ml of plasma or saliva) were injected on to the column for chromatographic separation.

Calibration Graph and Linearity

A stock ethanolic solution of 50.0 μg ml^{-1} (A) of artemisinine was prepared. Two artemisinine standard solutions with concentrations of (B) 5.00 and (C) 0.500 μg ml^{-1} were prepared by diluting an aliquot of stock solution A with ethanol. An aliquot (0.4 ml) of each of the solutions A, B and

C were pipetted into centrifuge tubes and 1.6 ml of 0.2% *m/V* NaOH solution were added to each tube. The reaction mixtures were heated in a water-bath at 50 °C for 30 min. After being cooled in water, the solutions were immediately extracted twice with 2 ml of ethyl acetate and the organic phases were discarded. The trace amount of ethyl acetate remaining on the surface of each solution was evaporated with a gentle stream of compressed air. To each solution was then added 0.16 ml of 2.5 M acetic acid in ethanol, after which the solutions were transferred into 2-ml tubes. Methanol - water (2 + 8) was used to rinse the tubes and to adjust accurately the volumes of the solutions. The final concentrations of the solutions used for preparing the calibration graphs were 10.0, 1.00 and 0.100 μg ml^{-1}.

Depending on the concentrations of the plasma and saliva samples being analysed, two calibration solutions were selected as calibration standards from the above three solutions. The injection volume was 200 μl. The calibration graph was calculated and stored by a CR-2AX Chromatopac microprocessor.

In order to determine the linear range of the method, standard solutions with initial drug concentrations ranging from 0.050 to 1 μg ml^{-1} were prepared and chromatographed in triplicate according to the procedure described above.

Recovery

In order to study the recovery of the proposed method, an appropriate volume of artemisinine standard solution A, B or C was added to separate tubes to give 15.0–1500 ng per tube. After the solvent had been evaporated with compressed air, 0.50 ml of 0.9% *m/V* NaCl solution and 1.50 ml of blank plasma or saliva (sampled from a volunteer) were added. The mixture was vortexed thoroughly. The samples were then extracted and treated according to the proposed sample preparation procedure. The recovery ratios were obtained by comparing the peak response of each test solution with that of a standard solution with the same concentration prepared according to the procedure for calibration solutions.

Precision

Five 1.5-ml aliquots of each plasma or saliva sample covering the concentration range 10–1000 ng ml^{-1} were simultaneously analysed according to the proposed procedure for the preparation of plasma and saliva samples. A comparison was made between the concentrations determined and the nominal concentrations.

Confirmation of the Sample Peaks

Three 1.5-ml aliquots of plasma or saliva taken from a volunteer during the high concentration period after the administration of artemisinine were sampled and extracted according to the sample preparation procedure. The solvents in each tube were removed by evaporation. The first aliquot was not subjected to the pre-column reaction treatment but was prepared directly as a 0.5-ml solution by adding 0.1 ml of ethanol and 40 μl of 2.5 M acetic acid solution followed by about 360 μl of 0.2% *m/V* NaOH solution. The second aliquot was mixed with 150 ng of artemisinine standard and treated simultaneously with the third aliquot according to the procedure for sample preparation. A 200-μl aliquot of each sample solution was taken for chromatographic determination and the chromatograms obtained were compared with one another.

Response Ratio Technique[5]

An adequate amount of plasma or saliva sample solution was obtained by collecting several sample solutions that had been analysed according to the preparation procedure for plasma and saliva samples. The sample solution collected and a standard solution with a concentration of 200 ng ml^{-1} were prepared as calibration standards and were chromatographed at 240, 260, 280 and 300 nm. The ratios between their respective responses at any two different wavelengths were calculated.

Chromatographic Conditions

Mobile phase, 0.01 M Na_2HPO_4 - NaH_2PO_4 buffer solution (water + methanol = 6 + 4); flow-rate, 1.3 ml min^{-1}; oven temperature, 35 ± 1 °C; detection wavelength, 260 nm; detection sensitivity, 0.005 a.u.f.s.; and method for quantitation, two-point calibration graph method using peak-height data.

Results and Discussion

Extraction and Chromatography

The extraction characteristics of artemisinine and the product (Q260) of its pre-column reaction in the ethyl acetate - water system were examined.[1] Artemisinine could be easily extracted from the aqueous phase by ethyl acetate over a very broad pH range. Because Q260 is a carboxylic acid, most of the impurities present in plasma or saliva samples were removed from its solution by the extraction with ethyl acetate under alkaline conditions directly after the alkaline reaction. This extraction treatment could prevent possible interference from the fat-soluble impurities and prolong the life of the analytical column.

Figs. 1 and 2 show the chromatograms obtained with human plasma and saliva samples, respectively, treated as described under Experimental. It can be seen in Figs. 1 and 2 that the remaining impurities, which should be water-soluble, were eluted before the sample peak of interest and, unfortunately, formed a large tailing peak under the proposed chromatographic conditions. The sample peak of interest eluted close to the tail-end of the impurity peak; however, there are no peaks close to the sample peak and the quantitation of the sample peaks could therefore be accomplished both accurately and easily.

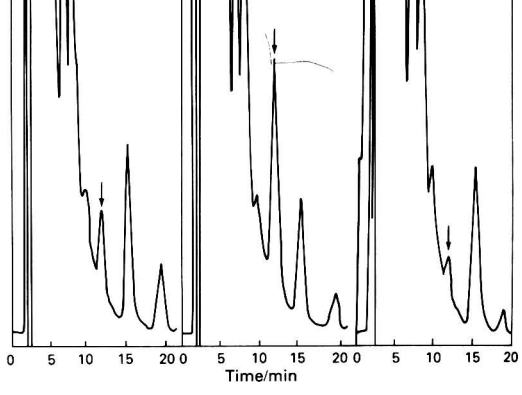

Fig. 1. Chromatograms of human plasma samples taken from a volunteer at different time intervals after the rectal administration of an artemisinine suppository. Dose: 10 mg kg^{-1}. (*a*) 2 h; (*b*) 7 h; and (*c*) 24 h

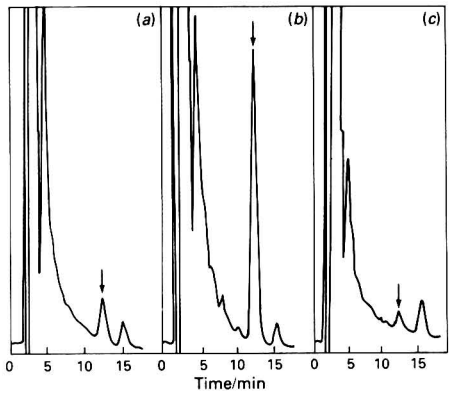

Fig. 2. Chromatograms of human saliva samples taken from a volunteer at different time intervals after the oral administration of an artemisinine capsule. Dose: 10 mg kg^{-1}. (*a*) 1 h; (*b*) 3 h; and (*c*) 12 h

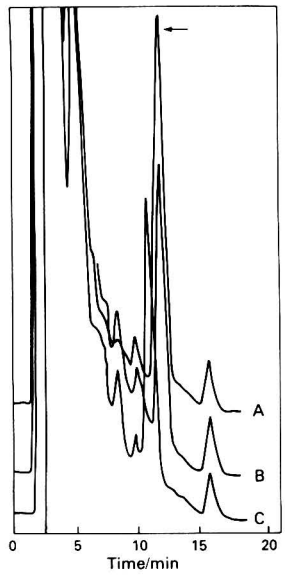

Fig. 3. Chromatograms of a human plasma sample before and after the pre-column reaction in comparison with that of the aliquot with standard. A, Sample with standard after the pre-column reaction; B, sample after the pre-column reaction; and C, sample before the pre-column reaction

Confirmation of the Sample Peaks

Before its quantitation, the reliability and purity of the sample peak under consideration were examined. The pre-column reaction for the conversion of artemisinine, initially to Q292 under weakly alkaline conditions and then to Q260 under weakly acidic conditions, is specific. Therefore, this process can be utilised for the confirmation of the reliability of the sample peak of interest in a similar manner to a derivatisation reaction. Figs. 3 and 4 show the chromatograms of plasma and saliva samples, respectively, before and after the pre-column reaction compared with those of a standard sample solution. At the retention time of the standard peak there were no peaks in the chromatograms of the plasma and saliva samples that did not undergo the pre-column reaction (lines C in Figs. 3 and 4), whereas there were corresponding peaks in those

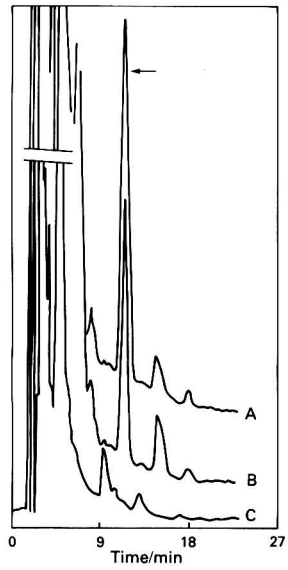

Fig. 4. Chromatograms of a human saliva sample before and after the pre-column reaction in comparison with that of the aliquot with standard. A, Sample with standard after the pre-column reaction; B, sample after the pre-column reaction; and C, sample before the pre-column reaction

Table 1. Response ratios of plasma and saliva samples and standards

Sample	H_{260}/H_{240}	H_{260}/H_{280}	H_{260}/H_{300}
Plasma sample	4.02	1.92	7.72
Saliva sample	3.83	1.94	7.91
Standard solution	3.98	1.95	7.78

samples that underwent the pre-column reaction (lines B in Fig. 3 and 4). In addition, the chromatograms obtained with blank samples of plasma and saliva after the pre-column reaction did not show any peaks at the retention time of the standard peak. It can be concluded that the peaks of interest in Figs. 3B and 4B represent the product of the pre-column reaction of artemisinine in plasma (Fig. 3) and saliva samples (Fig. 4).

In order to confirm further the sample peaks of interest and observe their purity, the response ratio technique[5] was used. Assuming that the absorbance of Q260 obeys the Beer-Lambert law, the absorbance ratio $A_{\lambda 1}/A_{\lambda 2}$ and the peak response ratio $H_{\lambda 1}/H_{\lambda 2}$ obtained after chromatographic separation at any two different wavelengths λ_1 and λ_2 should be independent of concentration. In Table 1 the response ratios of the plasma and saliva samples and the standard solutions are listed. The data in Table 1 further support the identification of the sample peaks under consideration and confirm their purity.

Recovery and Precision

The recovery and precision were investigated over the concentration range covered by the plasma and saliva samples used in this work. The results are summarised in Table 2. Both the recovery ratio and the precision are satisfactory and an internal standard was therefore considered to be unnecessary. The between-batch precision was examined at 100 ng ml^{-1}.

Table 2. Recovery and precision of the determination of artemisinine in plasma and saliva samples

Sample	Concentration of artemisinine added/ ng ml^{-1}	n	Concentration of artemisinine found/ ng ml^{-1}	RSD ($s/\bar{x}$), %
Plasma	1000	4	983	7.9
	100	4	97.3	1.4
	10.0	4	9.49	18
		5	879	6.5
		5	159	1.2
		5	23.1	15
Saliva	200	4	197	6.9
	100	4	97.0	7.9
	10.0	4	9.59	7.6
		5	220	6.9
		5	59.9	2.2
		5	16.0	7.2

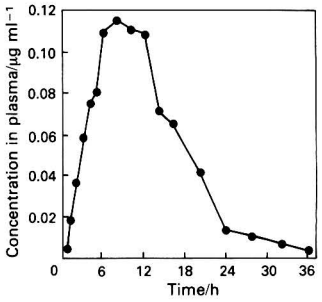

Fig. 5. Plasma concentration - time profile in a volunteer after the rectal administration of an artemisinine suppository. Dose: 10 mg kg^{-1}. Age, 26 years; sex, male; and mass, 58 kg

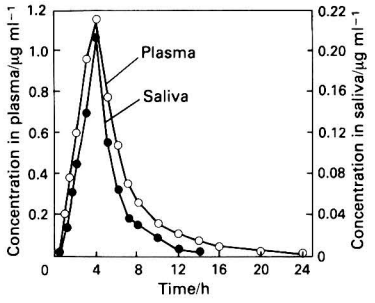

Fig. 6. Plasma and saliva concentration - time profiles in a volunteer after the oral administration of an artemisinine capsule. Dose: 10 mg kg^{-1}. Age, 28 years; sex, male; and mass, 60 kg

Three batches, each in duplicate, were analysed on three consecutive days. The between-batch relative standard deviation ($s/\bar{x}$) was <8% for both plasma and saliva samples and was similar to the within-batch relative standard deviation.

Linearity

Over the observed range of standards (6–600 ng) the peak response was found to be proportional to the amount injected on to the column. The detection limit under the proposed chromatographic and detection conditions is 1.5 ng ($S = 4\sigma$), giving an effective detection limit in plasma and saliva samples of about 2.5 ng ml^{-1}.

Plasma and Saliva Concentration - Time Profiles

The plasma and/or saliva concentration - time profiles of two volunteers who had received a dose of the drug by rectal administration of a suppository, and on a separate occasion by oral administration of a capsule, are shown in Figs. 5 and 6, respectively. The ages and masses of the volunteers are given in the captions. The maximum concentration in plasma after oral administration of the capsule was much higher than that after rectal administration of the suppository, despite the fact that each contained the drug at 10 mg kg^{-1}. It can be seen from Fig. 6 that the concentration - time profile of artemisinine in saliva was similar to that in plasma over the period monitored. However, the latter was about seven times higher than the former, *i.e.*, the mean plasma to saliva concentration ratio was 8.0 (± 2.7 s.d.).

Conclusions

In summary, the proposed method can be used to monitor the concentration of artemisinine in human plasma and saliva after the administration of the drug and can be employed in pharmacological and clinical studies. The preliminary data tentatively suggest that there is a constant relationship between the concentrations of the drug in plasma and saliva, and therefore that saliva samples alone might be adequate for studying pharmacokinetics, thereby avoiding drawing blood samples from the subjects.

References

1. Zhao, S., and Zeng, M.-Y., *Anal. Chem.*, 1986, **58**, 289.
2. Zhao, S., and Zeng, M.-Y., *Planta Med.*, 1985, **3**, 233.
3. Qinghaosu Antimalaria Coordinating Research Group, *Chin. Med. J.*, 1979, **92**, 811.
4. Qinghaosu Antimalaria Coordinating Research Group, *Yaoxue Tongbao*, 1979, **14**, 49.
5. Thomas, M. V., "Liquid Chromatography Detector," Marcel Dekker, New York, 1983, p. 65.

Paper A6/293
Received August 20th, 1986
Accepted October 23rd, 1986

Determination of Inorganic Anions by Non-suppressed Ion Chromatography with Indirect Ultraviolet Absorption Detection

Frank G. P. Mullins*
Department of Instrumentation and Analytical Science, University of Manchester Institute of Science and Technology, Manchester M60 1QD, UK

Reversed-phase high-performance liquid chromatography (HPLC) using a hexadecyltrimethylammonium bromide (CTAB) conditioned stationary phase is shown to provide efficient separation of iodate, phosphate, bromate, chloride, nitrite, bromide, nitrate and chlorate in 11 min. The anions were detected using an eluent containing sodium hydrogen phthalate by the indirect ultraviolet absorption (IUA) technique. The mechanism of separation of the anions is attributed to their interaction with the surface electrical double layer (formed by the initial adsorption of CTAB on the stationary phase) followed by conditioning with sodium hydrogen phthalate. Systems peaks could be induced by increasing the pH or the ionic strength of the eluent.

The application of ion chromatography with IUA detection to the determination of anions is demonstrated via the determination of nitrate and chloride in both a domestic water sample and a river water sample. The limits of detection for nitrate and chloride were 3 and 4 nmol of anion injected, respectively.

Keywords: *Inorganic anions; high-performance liquid chromatography; hexadecyltrimethylammonium bromide; indirect ultraviolet absorption detection; system peaks*

Following the development of ion chromatography by Small *et al.*[1] in 1975, the method has become widely accepted for the quantitative determination of anions in aqueous samples.[2] Single column or non-suppressed ion chromatographic techniques have been successful in a variety of applications.[2] Of particular interest is the development of an ion analysis method which would be compatible with inexpensive commercially available instrumentation. One such technique was that reported by Mullins and Kirkbright[3] which involved the separation of five UV-absorbing inorganic anions by high-performance liquid chromatography (HPLC) using micellar hexadecyltrimethylammonium chloride in the mobile phase. The determination of inorganic anions by non-suppressed ion chromatography generally involves the use of a low-capacity anion-exchange column combined with an eluent containing a UV-absorbing aromatic acid such as benzoate or phthalate. The detection systems most commonly employed are those involving conductivity or indirect ultraviolet absorption (IUA). The IUA technique involves the use of UV-absorbing eluent ions, such as the phthalate ion, in an ion-exchange mode. This enables sample ions to appear as "negative peaks" in the base-line absorbance as transparent sample ions substitute for the UV-absorbing displacing ions. For convenience the recorder polarity is usually arranged so that a positive peak corresponds to a decrease in absorbance. The retention times of the peaks vary with the ion injected and their areas are proportional to the amount injected. The IUA technique of detection is popular because of its high sensitivity and the ease with which it can be incorporated into inexpensive HPLC equipment. Unfortunately, there are problems associated with this type of detection.

Chromatograms obtained using the IUA technique may contain one or more extraneous peaks. The first peak generally elutes at the solvent front and is referred to as the injection peak. The second peak, the system peak, elutes further into the chromatogram and may result in incorrect peak identification, co-elution with solute peaks[4] and erroneous quantification of some eluting solutes. The occurrence of system peaks therefore imposes a severe limitation on the use of the IUA technique in ion chromatography. Denkert *et al.*[5] observed that when the UV-absorbing components were either naphthalene-2-sulphonate or 1-phenethyl-2-picolinium bromide, the samples injected gave either positive or negative peaks depending on their charge and retention behaviour. Small and Miller[6] reported the separation of ions using the IUA technique but no mention was made of system peaks. Cochrane and Hillman[7] described the separation of anions using potassium hydrogen phthalate in the eluent but did not discuss the occurrence of any system peaks. Bidlingmeyer and Warren[8] discussed the effect of ionic strength and detector response in ion-pair liquid chromatography with IUA detection. These workers observed the existence of system peaks and described them as concentration perturbations arising from injection of ionic or neutral samples. Haddad and Heckenberg[9] reported the separation of non-UV-absorbing anions on a low-capacity, high-efficiency, ion-exchange column with IUA, conductivity and refractive index detection. System peaks were observed with the three types of detection. Barber and Carr[10] described the use of UV-absorbing eluents with "ion-interaction" chromatography. System peaks were observed and their presence could be altered by addition of an alkyl sulphonate to the mobile phase. Warren and Bidlingmeyer[11] demonstrated that an eluent of high ionic strength provides superior stability of peak area and retention time when using a hydrophobic cationic reagent in the mobile phase. Barber and Carr[12] reported a study of the factors that affect and control the sensitivity and detection of nine anions. An "ion-interaction" separation was described and the system peaks were observed. Simulations were described which predicted the existence of two system peaks. The occurrence of both an injection peak and a system peak in non-suppressed ion chromatography was reported by Jackson and Haddad.[13] These workers attributed the system peak to adsorption and desorption of neutral eluent molecules from the stationary phase on the unfunctionalised portions of the anion-exchange surface. Naish[14] mentions system peaks in her study but did not discuss their origin in detail. Dreux *et al.*[15] described the use of a non-buffered ion-pair chromatographic system to determine inorganic anions. A system peak or "induced peak" was observed in their anion separation.

In this report, a study of the effects controlling the retention of anions is presented. These anions were separated on a column "dynamically loaded" with CTAB, therefore confer-

* Present address: Medeval Ltd., University of Manchester, Coupland III Building, Oxford Road, Manchester M13 9PL, UK.

ring anion exchange capabilities on the stationary phase. Phthalate anion was subsequently loaded on the anion-exchange surface to form a surface adsorbed anion layer. No system peaks were noted in the chromatogram obtained using the conditions described. System peaks could be induced by increasing the ionic strength of the mobile phase or by increasing the pH. These results were explained in terms of a reduction of the outer Helmholtz potential on the modified stationary phase surface that results in adsorption of the solute anions. This adsorption results in desorption of the phthalate anion causing system peaks in the chromatogram.

Experimental

Apparatus

A Waters Associates M6000A pump equipped with a Rheodyne 7125 valve injector (20 or 200-μl loop) connected to a Waters Lambda Max variable-wavelength UV detector was used in conjunction with a 250 × 5 mm i.d. 5 μm particle size Spherisorb ODS-2 column (Phase Separations, Queensferry, UK). Retention times and peak heights were measured using a recording integrator (Hewlett-Packard, Model 3390A).

Reagents

Inorganic salts. All the salts used were of AnalaR grade (BDH Chemicals, Poole, UK), except potassium iodate, which was of analytical-reagent grade (General Pharmaceuticals, Sudbury, UK).

Methanol. HPLC-grade methanol was supplied by Rathburn Chemicals, Walkerburn, UK.

De-ionised water. Distilled from glass and further de-ionised using a Waters I de-ioniser (Gelman Sciences, Ann Arbor, MI, USA).

Procedure

Mobile phases were prepared by adding the appropriate amount of CTAB to the selected mobile phase and filtering through a 0.22 μm filter (Duropore). The column was conditioned, before each set of experiments, by passage of the mobile phase for 90 min at a flow-rate of 1.5 ml min^{-1}. The CTAB adsorbed was determined by the breakthrough method.[3] The same conditioning procedure was used with phthalate. After each series of experiments, the surfactant was removed from the column by flushing with methanol for 90 min at 2 ml min^{-1}. The column was regenerated before each set of experiments. Stock solutions of the anions were prepared in water and diluted to the appropriate concentrations with water. pH values were obtained by dropwise addition of 0.13 M NaOH with constant stirring until the required value was obtained.

Results and Discussion

Mechanism of Anion Retention

Charged surfactants have been widely used as mobile phase modifiers to improve the partitioning characteristics of ionisable solutes in reversed-phase HPLC. Mullins and Kirkbright[3] have previously discussed the various mechanisms proposed to account for the retention behaviour of charged solutes in the presence of CTAB. When strongly hydrophobic cationic surfactants are present in the mobile phase in HPLC, the hydrophobic surface of the stationary phase becomes conditioned with the surfactant. This confers anion-exchange properties on the stationary phase. Cantwell and Puon[16] have shown by distribution isotherm and microelectrophoresis measurements that adsorption of organic cations on to a non-ionic surface produces a constant surface potential. The subsequent interaction of counter and sample ions with this surface can be quantitatively explained in terms of the Stern - Gouy - Chapman (SGC) theory of the electrical double layer. These authors[16] also reported that the electrical potential of the adsorbent surface must be kept constant if linear sorption isotherms and symmetrical chromatographic peaks are desired. These conditions are achieved by either including a potential-determining ion in the mobile phase throughout the analysis[17] or by using low sample concentrations. Cassidy and Elchuk[18,19] reported the use of cetylpyridinium chloride to condition the stationary phase and used tetrabutyl- and tetramethylammonium salts in the mobile phase. Barber and Carr[9] reported the use of UV-absorbing ion-interaction reagents to determine low levels of non-UV-absorbing anions. Neither of these studies presented detailed discussions on the significance of including potential-determining ions in the mobile phase other than to control retention of the sample anions.

Cationic surfactants such as CTAB are known to be readily adsorbed at the interface between two immiscible liquids of greatly differing polarity such as a water - methanol mobile phase and a hydrocarbon bonded stationary phase. The adsorbed ions are oriented such that the ionic head groups project into the aqueous phase and the hydrocarbon tails into the hydrocarbon stationary phase. The adsorbed ions are referred to as the potential-determining ions. As an approximation, the charges of the adsorbed potential-determining ions (CTA^+) are viewed as smeared out over the ODS-2 hydrocarbon stationary phase surface, with the plane passing through them identified as the charge surface. The plane of closest approach by the adsorbed counter ions to the charge surface is called the outer Helmholtz plane (OHP). The ions closer to the surface than the OHP are considered "contact adsorbed" in an inner Helmholtz plane (IHP). For the purpose of this study, the IHP is considered to be located at the charge surface so that the electrical potential of the IHP is identical with the surface potential. The "compact part" of the electrical double layer extends from the charge surface to the OHP and includes the IHP whereas the "diffuse part" includes the OHP and extends from it into the bulk solution.

Regardless of the way the surface charge arises, there are two principal mechanisms by which an ion can interact with a surface of opposite charge. The first mechanism is one of ion exchange where the ion exchanges with other counter ions in the electrical double layer. The second mechanism involves surface adsorption of the ion. Surface adsorption is strongly dependent on the electrical potential of the surface[17] whereas ion exchange is independent of surface potential.

Adsorption of CTAB and Phthalate on the ODS-2 Stationary Phase

Fig. 1 shows the variation in CTAB adsorbed as the concentration of methanol in the "loading" mobile phase was increased, and the subsequent loading of phthalate on to the CTAB conditioned ODS-2 stationary phase. The graph shows

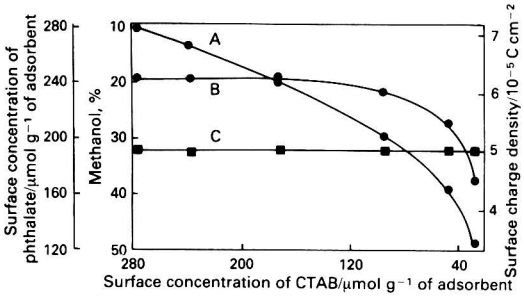

Fig. 1. (A) Variation of concentration of CTAB adsorbed on the stationary phase with percentage of methanol in the mobile phase. (B) Variation of concentration of phthalate adsorbed with concentration of CTAB adsorbed. (C) Variation of surface charge density with concentration of adsorbed ions on the stationary phase. For loading conditions see under Experimental

that the concentration of adsorbed CTAB decreased as the concentration of methanol was increased. This graph can be

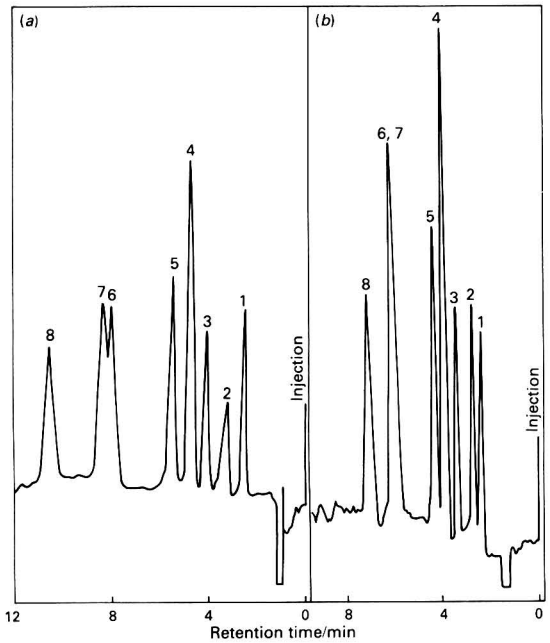

Fig. 2. (*a*) Ion chromatogram with indirect ultraviolet detection. Solutes: 1, iodate (320 μg l^{-1}); 2, phosphate (370 μg l^{-1}); 3, bromate (310 μg l^{-1}); 4, chloride (30 μg l^{-1}); 5, nitrite (310 μg l^{-1}); 6, bromide (350 μg l^{-1}); 7, nitrate (330 μg l^{-1}); 8, chlorate (350 μg l^{-1}). Mobile phase, 5 × 10^{-3} M sodium hydrogen phthalate in water; pH, 4.19; flow-rate, 2 ml min^{-1}; detection, IUA at 300 nm, 0.02 a.u.f.s; injection volume, 20 μl; stationary phase loading conditions, CTAB loaded from a 10 + 90 *V/V* MeOH - H_2O solution 1 × 10^{-2} M in CTAB. (*b*) As in (*a*) but mobile phase 1 × 10^{-2} M sodium hydrogen phthalate

used to predict the modifier concentration necessary to achieve a particular surface concentration of both adsorbed CTAB and phthalate. The bonded stationary phase used in this study was an end-capped Spherisorb ODS-2 phase. The maximum surface coverage by CTAB obtained was 1.27 μmol g^{-1} (280 μmol m^{-2}). For comparison, Knox and Laird[20] observed CTAB surface coverage of 0.25 μmol m^{-2} on SAS silica and Terweij-Groen *et al.*[21] noted up to 1.5 μmol m^{-2} (330 μmol g^{-1}). The surface coverages observed for CTAB in this study and other comparable studies[3] indicate high surface coverage by CTAB approaching those of the chemically bonded groups themselves.

Separation of the Anions

When Spherisorb ODS-2 stationary phase was loaded with CTAB, it acquired a positive surface charge density. The anion phthalate was also surface adsorbed as a potential-determining ion. The net surface charge density was not important and depended on the concentration of phthalate adsorbed. Fig. 2(*a*) illustrates separation of eight anions using phthalate in the mobile phase with the IUA technique. The conditions used are as indicated. Base-line resolution was obtained for all the anions except bromide and nitrate. Only one system peak appeared and this occurred at the solvent front. The phthalate concentration in the aqueous mobile phase was 5 × 10^{-3} M. Fig. 2(*b*) illustrates separation of eight anions using a 1 × 10^{-2} M phthalate aqueous mobile phase. The retention times of the anions were decreased as the phthalate anion concentration was increased, but the resolution of the anions was not as good as the previous separation

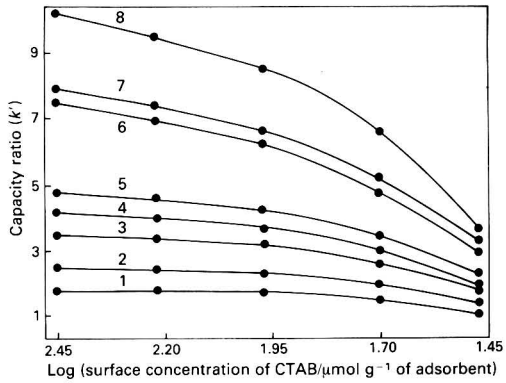

Fig. 3. Variation of capacity ratios for the anions with decrease in the concentration of CTAB adsorbed on the stationary phase. Conditions and solutes as in Fig. 2

conditions. The effect of variation of the surface coverage conditions previously described on the retention of the anions is illustrated in Fig. 3. A decrease in the capacity ratios with a decrease in CTAB adsorbed was observed. The elution order of the anions remains constant. Knox and Hartwick[22] concluded that the degree of retention of the anions is directly related to the surface charge density arising from the adsorbed ions. The variation of surface charge density with loading of CTAB and phthalate is illustrated in Fig. 3, and remains constant over the range of surface loadings investigated.

Ion Interactions with the Conditioned Stationary Phase

For the early eluting anions, *i.e.*, iodate, phosphate, bromate, chloride and nitrate, the capacity ratios were almost linear over an order of magnitude of surface coverage, only decreasing at low surface coverages. These anions contain primary hydration shells and have strong ion - water interactions.[23] They show a preference for the dilute aqueous phase over the modified stationary phase for the reason that there is more "free" water available in the former phase with which to solvate. Hence, on this basis alone, ions in an exchange situation will prefer the aqueous phase, but the smaller or more highly charged ion has the greater need for solvation and so will win the competition and induce the other ion, with less need for hydration, into the modified stationary phase. Essentially in the transfer of ions from water to a modified surface, there is always a loss of entropy and the enthalpy transfer from water sometimes opposes and sometimes reinforces the effect of this loss. The exo- or endothermicity of the transfer depends on the nature of the anion. The endothermic transfers occur from water with anions such as Cl^-, which is a strong hydrogen bond acceptor and which therefore interacts strongly with water, a strong hydrogen bond donor. These enthalpies and entropies of transfer combine to produce the well known increase in free energy which is observed when small anions are transferred from water to dipolar aprotic solvents.[23] An interesting example in which the size of the ions and the effects of specific ion hydration, as measured by the strength of the parent acid, combine to give an unambiguous order is provided by the pair NO_2^- and NO_3^-. The NO_2^- is derived from the weaker acid and is more hydrated (it shows a lower limiting equivalent conductivity).[24] The expected order of selectivity would be $NO_2^- < NO_3^-$, and this is the observed order.

The enthalpies of transfer of those anions that are weak hydrogen bond acceptors and polarisable, *i.e.*, Br^-, NO_3^- and ClO_3^-, are exothermic. These less highly hydrated anions are preferentially pushed by the water structure into the modified

stationary phase and into contact with the CTA^+ ions on the surface which have not interacted with a phthalate anion. With large polarisable anions the disturbance of the water structure causes their transfer to the modified stationary phase hence forming "water structure enforced ion pairs."[24] Such ion pairing is observed with tetrabutylammonium iodide in a water solution as dilute as 1×10^{-3} M.[24] From Fig. 1 it is seen that the adsorption of phthalate anion remains fairly high even when the adsorption of CTAB decreases. At low CTAB surface coverages, there are more phthalate molecules on the surface which will more effectively compete for the cationic sites, and hence compete in the ion-pairing process. The effect of this competition is a decrease in retention of the polarisable anions at lower surface coverages of CTAB. This is indeed shown in Fig. 3.

Effect of the Eluent pH on Anion Retention and Separation

Fig. 4 illustrates the variation in capacity ratio with increase in pH of the mobile phase. A slight decrease in retention in changing from pH 4.19 to 5.5 is observed for iodate, phosphate, bromate, chloride and nitrite. The nitrate shows a slight decrease and then a sharp increase in retention. When the nitrate peak appeared, it was negative to those of the other anions. The chlorate retention decreased slightly and then increased considerably. Fig. 5 illustrates the separation achieved at pH 5.5. Raising the pH of the mobile phase alters the degree of ionisation of the phthalate in both the mobile phase and also on the modified stationary phase. Using the equations derived by Cantwell and Puon[16] and Afrashtefar and Cantwell,[17] the outer Helmholtz plane potential (OHPP) was derived. Fig. 6 illustrates the variation of the OHPP with increase in pH of the mobile phase; the OHPP falls considerably as the pH is raised. As surface adsorption is strongly dependent on the electrical potential of the surface, a decrease in OHPP should result in a change in retention behaviour of the anions involved in a "surface adsorption" type interaction. The decrease in OHPP does not affect the retention of the anions iodate, phosphate, bromate, chloride, nitrite and bromide. As stated previously, the nitrate appeared negative with respect to the other anions. With the IUA technique the negative peak obtained is acutally a "positive" peak. A possible explanation for this is that as the pH is raised, a higher percentage of the phthalate anions becomes divalent. The OHPP decreases and the divalent phthalate has a higher water solubility, and can be more easily displaced by an anion seeking to form a "water structure enforced ion pair." The displaced phthalate will act as a concentration perturbation through the column and will elute as a "negative" peak in the chromatogram. The increase in retention of the chlorate can also be explained by energetically favoured ion-pair formation. The peak obtained for chlorate remains positive, so this anion cannot displace any phthalate anion in its interaction with the modified surface.

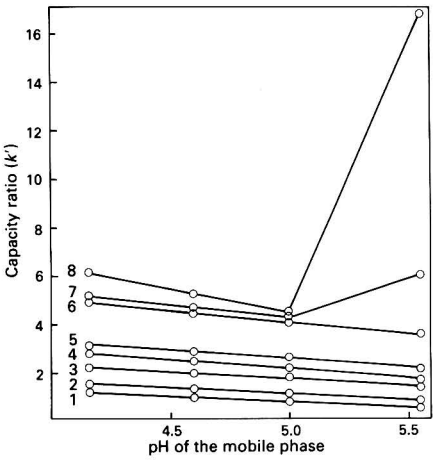

Fig. 4. Variation of the capacity ratios with pH of the mobile phase. Conditions as in Fig. 2

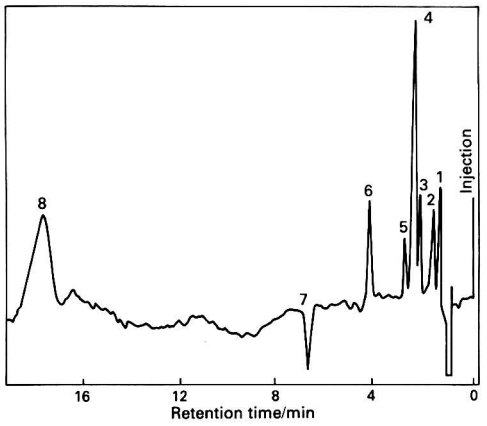

Fig. 5. Ion chromatogram with indirect ultraviolet detection. Conditions as in Fig. 2

Effect of the Eluent Ionic Strength on Anion Retention and Separation

It was decided also to investigate the effects of an increase in ionic strength using sodium chloride on the separation of the anions. Warren and Bidlingmeyer[11] studied the UV detection of sodium valproate and reported that a mobile phase containing 5×10^{-3} M potassium chloride provided optimum chromatographic performance. Bidlingmeyer and Warren[8] also advised that working at extremes of ionic strength yields reproducible chromatographic data when using the UV detection technique. Fig. 7 illustrates the adsorption of phthalate anions on to the modified stationary phase with increase in ionic strength. As was expected,[8] increasing the ionic strength of the mobile phase resulted in an increase in the concentration of phthalate adsorbed. The variation in the OHPP with increase in ionic strength as shown in Fig. 8. The OHPP drops substantially with an increase in the ionic strength of the mobile phase. The decrease in the OHPP will directly affect the anions that prefer to surface adsorb rather than ion exchange.

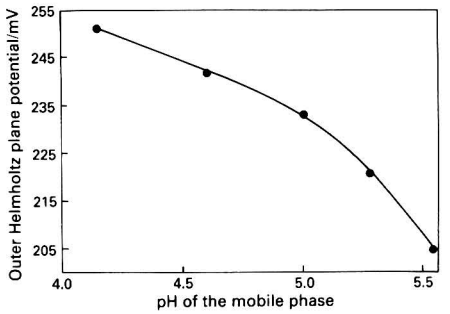

Fig. 6. Variation of outer Helmholtz plane potential with increase in pH

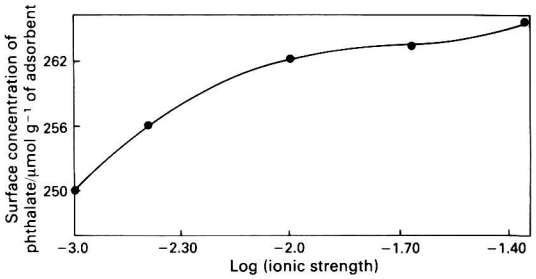

Fig. 7. Variation of concentration of phthalate adsorbed with increase in the ionic strength of the mobile phase. Surface loading conditions as in Fig. 2

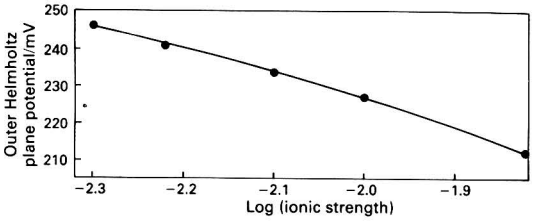

Fig. 8. Variation in outer Helmholtz plane potential with increase in ionic strength

System Peak Formation

Fig. 9(*a*)–(*d*) illustrates the effect of increasing the ionic strength in the mobile phase on the separation of the selected anions. Obviously, for this chromatographic system, increasing the ionic strength results in unusual system peak formation. At high ionic strength, Fig. 9(*d*), the chromatogram obtained shows peaks which are negative, *i.e.*, elute as UV-absorbing species rather than UV-transparent troughs in the mobile phase as is normally expected when the IUA technique is used. It was decided to investigate the effect of individual injections of anions on the "negative system peaks." Fig. 10 illustrates that for nitrite, both the system peak at the solvent front and the second system peak are negative. For the more polarisable anions, bromide, nitrate and chlorate, the system peaks at the solvent front are positive but the second system peaks are negative. An important feature of an ion-exchange process is the Donnan potential and the theory behind the exclusion of ions from a surface.[24] In this situation the Donnan potential on the modified stationary phase arises from the fact that the CTA^+ and phthalate anions are immobile, fixed on the stationary phase surface and so are not free to diffuse into the external solution. The phthalate anions will tend to diffuse into the modified stationary phase where their concentration is lower than in the mobile phase. Such a distribution of anions of the same charge in the stationary phase will attract ions of opposite charge from the mobile phase. This violation of electroneutrality in the two phases results in the establishment of a potential difference at the interface. Non-adsorbed phthalate anions will be repelled from the modified stationary phase by the potential established so that their concentration there remains lower than in the mobile phase. The efficiency of the exclusion of the non-adsorbed phthalate depends on the magnitude of the Donnan potential, and so is a function of the ion concentrations and charges in the two phases. The Donnan potential and the OHPP previously discussed may be considered identical for the purpose of this discussion. A highly charged sample anion will be more efficiently excluded by a high OHPP or Donnan potential. Reduction of the OHPP by increasing the pH of the solution results in a situation where

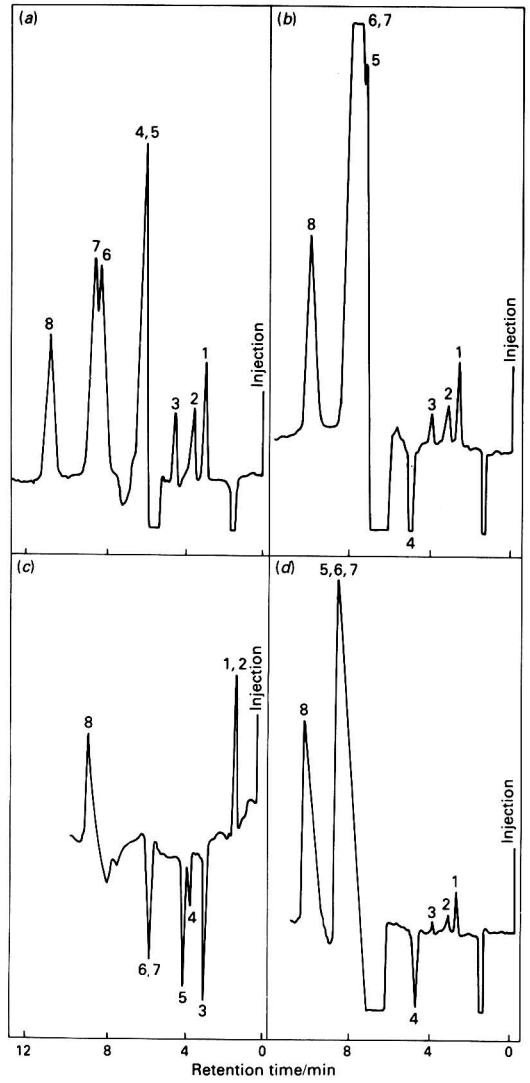

Fig. 9. Ion chromatogram with indirect ultraviolet detection. Conditions as in Fig. 2 except ionic strength of the mobile phase was (*a*) 1×10^{-3}, (*b*) 3×10^{-3}, (c) 5×10^{-3} and (d) 0.18, controlled by sodium chloride

the sample anions are not as efficiently excluded from the modified stationary phase as in the case of the nitrate anion in Fig. 5; it can exclude phthalate from the stationary phase and a negative peak occurs in the chromatogram. However, the importance of the phenomenon of the Donnan exclusion for this work is the fact that exclusion is known to become poorer as the external ionic strength is increased.[24] As a result, the modified stationary phases in contact with solutions of high ionic strength no longer show equivalent exchange, but will also show non-equivalent adsorption of ions or invasion of the stationary phase by ions. As the ionic strength is increased, the less hydrated anions begin to invade the modified stationary phase and exclude the phthalate anions. Only the less hydrated ions do this at low ionic strengths, but as the ionic strength is increased, even the well hydrated ions begin to participate in the exclusion, hence the pulses of UV-absorbing material in the chromatograms (seen as negative peaks).

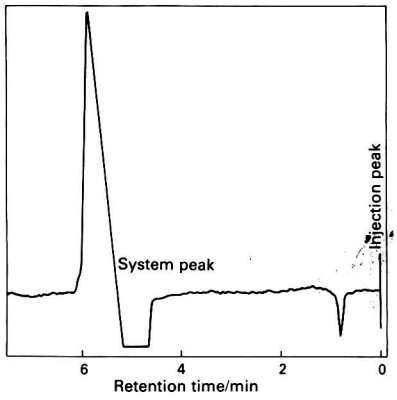

Fig. 10. Ion chromatogram of nitrate at high ionic strength, see Fig. 9(*d*).

Table 1. Regression parameters for peak height *versus* nanomoles of anion injected. $n = 10$. Conditions as in Fig. 2

Anion	Slope/A nmol^{-1}	Intercept, A	Correlation coefficient
(*a*) Cl^-	2.19×10^{-4}	1.23×10^{-3}	0.999
NO_3^- ..	1.32×10^{-4}	2.94×10^{-4}	0.998
(*b*) Cl^-	9.06×10^{-5}	6.92×10^{-3}	0.996
NO_3^- ..	8.05×10^{-5}	2.28×10^{-3}	0.995

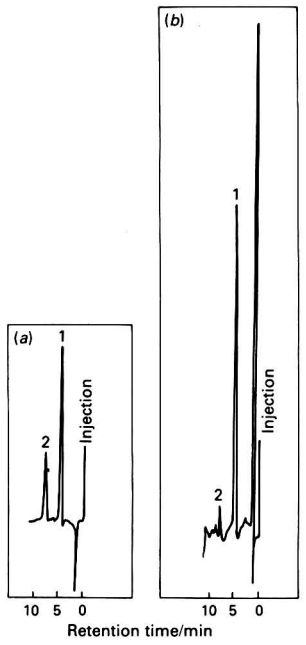

Fig. 11. Ion chromatogram of (*a*) river water sample with (1) chloride and (2) nitrate. (*b*) Domestic tap water sample with (1) chloride and (2) nitrate. Conditions as in Fig. 3, 0.02 a.u.f.s., for the tap water sample, 0.05 a.u.f.s. for the river water. Injection volume, 200 µl. The river water sample was pumped through a Sep-Pak cartridge to remove interferences before chromatography. The domestic water sample was used without any further treatment.

Linearity and Sensitivity

The regression parameters for peak height *versus* nanomoles of anion injected are shown in Table 1. Good linearity is obtained from 8 to 40 nmol of chloride and from 6 to 46 nmol of nitrate, as shown in Table 1(*a*). At higher concentrations of anions injected, a noticeable drop in the expected peak height is observed, resulting in a change in the slope and the intercept of the calibration graph. This can be explained by the fact that the peaks become asymmetric as the injected anion concentration increases, hence reducing the peak height. Barber and Carr[11] observed similar results with their UV detection system. Table 1(*b*) shows regresssion data for higher concentrations of the anions. Good linearity is obtained for chloride from 70 to 205 nmol and for nitrate from 70 to 205 nmol. The detection limits for nitrate and chloride were 3 and 4 nmol, respectively (signal to noise ratio = 3 for both anions). No serious attempt was made to optimise the detection limit in this work. Fig. 11 illustrates a chromatogram obtained for (*a*) domestic tap water and (*b*) river water. The analysis shows the presence of nitrate at 2.86 mg l^{-1} (2.86 p.p.m.) and chloride at 84.00 mg l^{-1} (84 p.p.m.) in the domestic tap water sample. The nitrate concentration in the river water was 7.00 mg l^{-1} (7 p.p.m.) and the chloride concentration was 57.00 mg l^{-1} (57 p.p.m.).

Conclusions

CTAB and phthalate adsorption on to the stationary phase results in the formation of an electrical double layer with which the anions interact. The optimum conditions for the anion separation involve the initial conditioning of the ODS-2 stationary phase with a methanol - water (10 + 90 *V/V*) mobile phase containing 1×10^{-2} M CTAB. The mobile phase for the anion separation was 5×10^{-3} M sodium hydrogen phthalate. The early eluting anions, iodate, phosphate, bromate, chloride and nitrite, ion exchange with the electrical double layer. The later eluting anions, bromide, nitrate and chlorate, surface adsorb on to the stationary phase. The ion-exchange process is not dependent on the surface potential, whereas surface adsorption is dependent on the surface potential. When the surface potential was reduced by increasing the pH or the ionic strength of the mobile phase, the interaction of the later eluting anions, bromide, nitrate and chlorate, with the stationary phase resulted in negative peak formation. This was explained in terms of a Donnan-type exclusion of the adsorbed phthalate by the incoming anion. This resulted in a pulse of desorbed phthalate appearing as a negative peak in the chromatogram.

In this type of ion chromatography, mobile phases employing high ionic strengths or high pH values are not recommended and only increase the complexity of the analysis. Alternative mobile phases incorporating anions other than phthalate are currently under investigation.

References

1. Small, H., Steven, T. S., and Bauman, W. C., *Anal. Chem.*, 1975, **47**, 1801.
2. Wetzel, R. A., Pohl, C. A., Riviello, J. M., and McDonald, J. C., *in* McDonald, J. C., *Editor*, "Inorganic Chromatographic Analysis," Chemical Analysis, Volume 78, Wiley, New York, 1985, p. 355.
3. Mullins, F. G. P., and Kirkbright, G. F., *Analyst*, 1984, **109**, 1217.

4. Heckenberg, A. L., and Haddad, P. R., *J. Chromatogr.*, 1984, **299**, 301.
5. Denkert, M., Hackzell, L., Schill, G., and Sjogen, E., *J. Chromatogr.*, 1981, **218**, 31.
6. Small, H., and Miller, T. E., *Anal. Chem.*, 1982, **54**, 462.
7. Cochrane, R. A., and Hillman, D. E., *J. Chromatogr.*, 1982, **241**, 392.
8. Bidlingmeyer, B. A., and Warren, F. V., *Anal. Chem.*, 1982, **54**, 2351.
9. Haddad, P. R., and Heckenberg, A. L., *J. Chromatogr.*, 1982, **252**, 177.
10. Barber, W. E., and Carr, P. W., *J. Chromatogr.*, 1984, **316**, 211.
11. Warren, F. V., and Bidlingmeyer, B. A., *Anal. Chem.*, 1984, **56**, 487.
12. Barber, W. E., and Carr, P. W., *J. Chromatogr.*, 1983, **260**, 89.
13. Jackson, P. E., and Haddad, P. R., *J. Chromatogr.*, 1985, **346**, 125.
14. Naish, P. J., *Analyst*, 1984, **109**, 809.
15. Dreux, M., Lafosse, M., Agbohazoume, P., Chabaane, B., Gilbert, M., and Levi, Y., *J. Chromatogr.*, 1986, **254**, 119.
16. Cantwell, F. F., and Puon, S., *Anal. Chem.*, 1979, **51**, 623.
17. Afrashtefar, S., and Cantwell, F. F., *Anal. Chem.*, 1982, **54**, 2422.
18. Cassidy, R. M., and Elchuk, S., *J. Chromatogr.*, 1983, **262**, 311.
19. Cassidy, R. M., and Elchuk, S., *J. Chromatogr. Sci.*, 1983, **21**, 454.
20. Knox, J. H., and Laird, G. R., *J. Chromatogr.*, 1976, **122**, 17.
21. Terweij-Groen, C. P., Heemstra, S., and Kraak, J. C., *J. Chromatogr.*, 1978, **161**, 69.
22. Knox, J. H., and Hartwick, R. A., *J. Chromatogr.*, 1981, **204**, 3.
23. Cox, B. G., Hedwig, G. R., Parker, A. J., and Watts, D. W., *Aust. J. Chem.*, 1974, **27**, 477.
24. Diamond, R. M., and Whitney, D. C., *in* Marinsky, J. A., *Editor*, "Ion Exchange," Volume 1, Marcel Dekker, New York, 1966, p. 277.

Paper A6/365
Received September 24th, 1986
Accepted November 28th, 1986

Inter-laboratory Calibration for the Quality Control of Pesticide Residue Analyses (1984–85)

Pieter R. de Beer, Louis P. van Dyk, Susan M. Prinsloo, Awie J. Viljoen and Laurraine H. Lotter
Task Group ICE, Working Group on Pesticide Analysis, Private Bag X134, Pretoria 0001, South Africa

Five inter-laboratory calibration exercises (ICEs) carried out in South Africa during 1984 and 1985 are described. Analyses were carried out on solutions of pesticides and on residues in butter, maize meal, soil, eggs and grape juice. The results seem to indicate an improvement in the quality of pesticide residue analysis since the inception of the ICE programme.

Keywords: *Inter-laboratory calibration; pesticide residue analyses; quality assurance; co-operative trial*

Pesticide residue analysis "is still an art, and especially not a simple science to be entrusted to untrained, inexperienced personnel."[1] A confidential survey conducted in South Africa by the Task Group ICE during 1984 showed that several laboratories in this country employed untrained and inexperienced analysts, a phenomenon that has been confirmed by previous inter-laboratory calibration exercises (ICEs).[2,3] According to Bantjies,[4] the universities and polytechnics do not specifically train analytical chemists. Therefore, the Task Group ICE continued its programme of ICEs with the primary objective of improving the quality of residue analyses and giving each laboratory the opportunity to prove its analytical capability. Presentation of all the data for each exercise also gives participants the opportunity to compare their results with others and careful analysis of the results has allowed the Task Group to identify training needs.

Procedure

Programme

The organisation of ICEs has been described previously.[2,3] The first parts of the exercises were relatively easy and consisted of a sample solution containing one or more pesticides of either known or unknown identity, but always of unknown concentration.

The second parts of the exercises were more advanced and for the 1984–85 period consisted of substrates such as butter, maize meal, soil, eggs or fruit juice fortified with one or more pesticides at unknown concentration levels. The participating laboratories were expected to quantify, identify and confirm the pesticides present. The confirmation technique used had to be based on a principle other than gas chromatography.

Samples were prepared by two experienced analysts who are also members of the Task Group ICE. After sample fortification, the recommended extraction method was tested to ensure a result within 10% of the spiked concentration. Any problems with the method were resolved at this stage. Samples were also analysed for homogeneity. A protocol was drawn up, detailing the handling, extraction, analysis and reporting of the results. For each ICE, participating laboratories were supplied with relevant standard solutions of known concentration, with the identity of each pesticide remaining unknown.

Each participating laboratory was given 1 month in which to complete the ICE and submit its results to the Task Group. The Task Group's results were compared with those of the participants in an attempt to identify their problems. The relevant laboratory supervisors were subsequently informed of the Task Group's conclusions.

ICE 2/84

This exercise was divided into two parts. A sample solution containing diazinon and dieldrin was supplied at concentration levels of 2.01 and 1.01 ng μl^{-1}, respectively. The concentration and identity of both compounds had to be determined.

A butter sample was analysed beforehand to establish whether it was free from pesticide residues. This sample was then fortified with diazinon and dieldrin at concentration levels of 0.20 and 0.10 mg kg^{-1}, respectively. The concentration and identity of both compounds had to be determined and confirmed. The multi-residue method for fatty foods of the WGPA[5] was recommended, but each laboratory was free to use its method of choice on condition that this was reported.

ICE 3/84

The exercise consisted of two parts. First, the concentration of malathion and pirimiphos-methyl solution (at concentration levels of 12 and 40 ng μl^{-1}, respectively) had to be determined. The identities of both pesticides were known.

Secondly, white maize meal fortified with the same pesticides at concentration levels of 7.5 and 2.5 mg kg^{-1}, respectively, was supplied. The identities of both pesticides were known and their concentration had to be determined.

A Soxhlet extraction method[6] was recommended, in which 20 g of the maize meal were extracted with acetonitrile for a minimum of 2 h with a minimum of 30 solvent exchanges per hour. The resultant extract was evaporated to 10 ml and analysed on a gas chromatograph.

ICE 1/85

Firstly, the concentration of a herbicide solution of 5 ng μl^{-1} of tebuthiuron had to be determined. The identity of the component was known.

Secondly, air-dried, sifted loamy soil fortified with tebuthiuron at a level of 2 mg kg^{-1} was supplied. The identity of the tebuthiuron was known and the herbicide had to be extracted and quantified.

It was recommended that the sample be analysed according to the method of Lok *et al.*,[7] but again each laboratory was free to use a different method, which then had to be reported.

ICE 2/85

p,p'-DDE and dieldrin were dissolved in hexane at concentrations of 0.52 and 0.2 ng μl^{-1}, respectively. The participants had to identify and quantify both compounds.

The second part of the exercise consisted of egg pulp fortified with the two organochlorines at 0.31 and 0.13

mg kg^{-1}, respectively. About 3 kg of eggs were beaten in a stainless-steel bowl using a commercial food mixer, after which a sample of the egg pulp was analysed to establish whether it was free from organochlorine residues. After fortification, samples were analysed to test homogeneity. The analysis method of Van Dyk *et al.*[8] was recommended, which included a fat clean-up by size exclusion chromatography. The alternative method of Horwitz[9] was also recommended. The results of the analyses had to be reported on a whole sample basis and the identity of the organochlorines had to be confirmed.

ICE 3/85

Firstly, participants had to identify, confirm and quantify chlorpyrifos and fenchlorphos at concentration levels of 32.5 and 22.0 ng µl^{-1}, respectively, in a solution. The second part consisted of unfortified commercial grape juice, containing no pesticides.

The grape juice had to be extracted according to a recommended method and screened for pesticides. The identity, confirmation of identity and concentration of pesticides present had to be reported. The recommended extraction involved adding 100 ml of hexane - ethyl acetate (60 + 40) solution to 50 g of juice in a separating funnel, followed by vigorous shaking. This was repeated three times. The extracts were combined and evaporated to dryness and the residue was dissolved in toluene - ethyl acetate (1 + 3) and cleaned up by size-exclusion chromatography, if necessary.

Evaluation of the Results

A serious problem for the Task Group was to determine what the magnitude of the deviation from the spiked concentration should be for the results to be acceptable. The small number of participants involved made a full-scale statistical evaluation of the results difficult. The evaluation method used by the Environmental Protection Agency (EPA)[10] was tested against a number of our own ICEs, but it was concluded that the quantification part of the method was not sensitive enough to distinguish between "good," "fair" or "unacceptable" results. The main problem lies with the calculation of the compound quantitative score, where in practice a maximum of 2 points can be lost for each compound.

In accordance with a previous decision, the results were therefore not evaluated and laboratories were provided with a summary of all the results, the true value and the percentage

Table 1. Results of ICE 2/84—diazinon and dieldrin in solution and butter. Abbreviations: P, packed column; NI, not identified; ND, not detected; NPD, nitrogen - phosphorus detector; ECD, electron-capture detector; FPD, flame photometric detector

	Solution				Butter						
	Diazinon (unknown)		Dieldrin (unknown)		Diazinon (unknown)		Dieldrin (unknown)				
Laboratory code	Concentration/ ng µl^{-1}	Relative error, %	Concentration/ ng µl^{-1}	Relative error, %	Concentration/ mg kg^{-1}	Relative error, %	Concentration/ mg kg^{-1}	Relative error %	Column used	Detector used	Method of confirmation
R06	1.41	30	1.10	9	0.26	30	0.05	50	P	NPD + ECD	Retention times on different columns and detectors
R09	1.99	1	0.99	2	ND	—	0.14	40	P	ECD	Relative retention times on two columns
R12	1.93	4	0.95	6	0.14	30	0.14	40	P	ECD	GC - MS
R14	1.90*	6	0.71	30	No results submitted				P	ECD + FPD	Retention times on different columns and detectors
R17	2.02	0	1.07	6	No results submitted				P	ECD + FPD	Retention times on different columns and detectors
R18	19.32NI†	—	9.75NI†	—	0.23NI	15	0.22NI	120	P	ECD + FPD	—
R23	1.98†	2	0.97	4	No results submitted				P	ECD	Retention times on different columns and detectors
R34	2.12	6	1.01	0	0.21	5	0.12	20	P	ECD + NPD	Retention times on different columns and detectors
R35A . .	1.84	9	0.97	4	0.23	15	0.16	60	P	ECD + NPD	GC - MS
R35B . .	1.88	7	1.22	21	0.21	5	0.13	30	P	ECD + NPD	GC - MS
Mean . .	1.90		1.00		0.21		0.14				
Standard deviation	0.20		0.14		0.04		0.05				
Relative standard deviation, % of spiked concentration . .	10%		14%		20%		50%				
Spiked concentration . .	2.01		1.01		0.20		0.10				

* Identified as disulfoton.
† Outliers.
‡ Identified as aldrin.

relative error for each participant (appearing under a code). The reason for this presentation was described previously.[3] Those questionable values which, if included, would exert a significant effect on the standard deviation, were calculated and rejected as described by Sherma.[10]

Results

Not all the participating laboratories provided results with each exercise so that the total number of analyses reported is sometimes less than the expected figure. Laboratories often participated only in the analysis of the relatively easy first part of a given exercise, in spite of having the necessary infrastructure to analyse the matrix part of the exercise.

ICE 2/84

Results of the exercise are given in Table 1. Only 10 out of the 16 laboratories that originally indicated they would participate supplied results. Of this number, only seven participated in the second part of the exercise.

The results of the analysis of the solution showed that one participant (R18) produced outliers for both pesticides. Closer examination of the results revealed that the analyst made a 10-fold calculation error. No effort was made to identify the pesticides. One of the analysts presented results with a relative error of >20% for diazinon and two with a relative error of >20% for dieldrin.

Butter analyses produced results showing an even greater deviation from the true values. This could be expected owing to the more complicated nature of the extraction procedure. Six participants reported results for diazinon whilst eight reported results for dieldrin. Participant R09 did not detect diazinon owing to a broad, tailing solvent peak. R18 did not identify any of the pesticides. No participant reported a result with a relative error of >30% for diazinon. Two participants reported results with relative errors of >50% for dieldrin.

The participants had to confirm the identities of the two pesticides using a technique other than gas chromatography. Three participants used gas chromatography - mass spectrometry (GC - MS) but others used only GC, which was unacceptable. Participants R14 and R23 both incorrectly identified diazinon in the solution as disulfoton and aldrin, respectively.

All participants used electron-capture detectors (ECDs) to detect the compounds, sometimes in combination with a nitrogen - phosphorus detector (NPD) or flame photometric detector (FPD). All participants used packed columns.

ICE 3/84

The results of this exercise are given in Table 2. Samples were supplied to 12 laboratories with 14 potential participants. Of these, 9 laboratories with 11 analysts eventually participated, and 9 analysts took part in the matrix part of the exercise.

The identities of both pesticides were known and only a quantitative analysis of the solution and maize meal was required. One participant (R38) produced outliers for both the solution and the matrix. This was possibly due to incorrect calculation as a re-calculation of the results showed the values to be close to the spiked concentrations. The result reported under pirimiphos (solution) was considered to be anomalous.

With the solution, no participant reported a relative error of >25%. No matrix analysis result showed a deviation of >50%. This may be due to the relatively high pesticide concentration levels in both parts of the exercise.

Only one participant made use of a capillary column with an FID; others used packed columns with either an FID, FPD or NPD.

In spite of the low number of participants, the exercise seemed to be highly successful.

ICE 1/85

The results of this exercise are given in Table 3. Twelve laboratories wished to participate but only seven submitted results. Of these, only five analysed the matrix. The identity of the herbicide was known and only quantitative analyses of the solution and soil were required.

Table 2. Results of ICE 3/84—malathion and pirimiphos-methyl in solution and maize meal. Abbreviations as in Table 1; WCOT, wall-coated open-tubular column; FID, flame-ionisation detector

	Solution				Maize meal					
	Malathion (known)		Pirimiphos (known)		Malathion (known)		Pirimiphos (known)			
Laboratory code	Concentration/ ng µl^{-1}	Relative error, %	Concentration/ ng µl^{-1}	Relative error, %	Concentration/ mg kg^{-1}	Relative error, %	Concentration/ mg kg^{-1}	Relative error, %	Column used	Detector used
R06A	10.88	9	41.54	4	8.22	10	2.31	8	P	NPD
R06B	10.73	11	44.37	11	8.40	12	2.71	8	P	NPD
R09	11.58	4	37.10	7	8.42	12	2.74	10	P	FPD
R13	13.91	16	39.16	2	7.05	6	2.17	13	P	FPD
R15A	11.50	4	39.40	2	No results submitted				WCOT	FID
R15B	10.00	17	37.10	7	No results submitted				P	FID
R18	13.64	14	36.11	10	5.75	23	3.74	50	P	FPD
R23	13.54	13	43.04	8	6.64	12	2.17	13	P	NPD
R34	12.90	8	38.70	3	7.79	4	2.60	4	P	FPD
R35	14.40	20	48.70	22	5.76	23	2.64	6	P	NPD
R38	58.19*	—	42.15	5	0.18*	—	0.06*	—	P	FPD
Mean	12.31		40.67		7.25		2.64			
Standard deviation	1.55		3.75		1.12		0.05			
Relative standard deviation, % of spiked concentration	13%		9%		15%		20%			
Spiked concentration	12.00		40.00		7.50		2.50			

* Outliers.

Table 3. Results of ICE 1/85—tebuthiuron in solution and soil. Abbreviations as in Tables 1 and 2; FPD(S), FPD in sulphur mode

	Tebuthiuron (known)					
	Solution		Soil			
Laboratory code	Concentration/ ng µl^{-1}	Relative error, %	Concentration/ mg kg^{-1}	Relative error, %	Column used	Detector used
R08	2.80	44	No results submitted		WCOT	FID
R09	4.85	3	1.97	2	P	NPD
R18	5.57	11	1.76	12	P	FPD(S)
R24	3.00	40	No results submitted		P	NPD
R28	4.81	4	1.03	49	P	NPD
R34	5.05	1	1.95	3	P	NPD
R36	5.03	1	0.93	54	P	FPD(S)
Mean	4.40		1.53			
Standard deviation	1.09		0.51			
Relative standard deviation, % of spiked concentration	22%		26%			
Spiked concentration	5.00		2.00			

Table 4. Results of ICE 2/85—DDE and dieldrin in solution and eggs. Abbreviations as in Tables 1 and 2

	Solution				Egg pulp						
	p,p'-DDE (unknown)		Dieldrin (unknown)		*p,p'*-DDE (unknown)		Dieldrin (unknown)				
Laboratory code	Concentration/ ng µl^{-1}	Relative error, %	Concentration/ ng µl^{-1}	Relative error, %	Concentration/ mg kg^{-1}	Relative error, %	Concentration/ mg kg^{-1}	Relative error %	Column used	Detector used	Method of confirmation
R02A	0.54	4	0.20*	0	No results submitted				P	ECD	Retention times. No confirmation
R02B	0.52	0	0.11*	45	No results submitted				P	ECD	Retention times. No confirmation
R06A	0.50	4	0.22	10	0.34	10	0.09	31	P	ECD	Retention times. No confirmation
R06B	0.49	6	0.20	0	0.25	19	0.11	15	P	ECD	Retention times. No confirmation
R09	0.50	4	0.19	5	0.31	0	0.12	8	P	ECD	GC - MS
R11	0.37	29	0.20	0	No results submitted				P	ECD	GC - MS
R17	0.50	4	0.18	10	0.16	48	0.06	54	P	ECD	Retention times on three columns
R18	Unable to separate these compounds				No results submitted				P	ECD + FID	—
R26A	0.76	46	0.27	35	0.24	23	0.11	15	WCOT	ECD	Chemical conversion, WCOT column
R26B	0.50	4	0.21	5	0.26	16	0.12	8	WCOT	ECD	Chemical conversion, WCOT column
R27A	0.49	6	0.15	25	0.17	45	0.08	39	WCOT	ECD	Ultraviolet conversion
R27B	0.44	15	0.08	60	0.27	13	0.11	15	WCOT	ECD	Ultraviolet conversion
R30A	0.53	2	0.22	10	No results submitted				P	ECD	No confirmation
R30B	0.55	6	0.23	15	No results submitted				P	ECD	No confirmation
R34	0.52	0	0.18	10	0.20	36	0.12	8	P	ECD	GC - MS
R35	0.87†	—	0.28	40	0.21	32	0.08	39	P	ECD	GC - MS
Mean	0.52		0.20		0.24		0.10				
Standard deviation	0.08		0.05		0.06		0.02				
Relative standard deviation, % of spiked concentration	15%		25%		19%		15%				
Spiked concentration	0.52		0.20		0.31		0.13				

* Identified as *o,p*-DDT.
† Outliers.

Although there were no outliers, results from R08 and R24 showed relative errors of >25% for the solution section of the exercise. One result (R36) showed a relative error of >50% for the matrix part of the exercise.

Six participants used packed columns and one used a capillary column. NPDs, FIDs and FPDs (in the sulphur mode) were used.

The exercise cannot be regarded as a success owing to the small number of participants and the fact that only three participants reported results in both sections that were close to the spiked concentration.

ICE 2/85

Although 17 laboratories with a total of 22 participants requested to participate, only 11 laboratories with 16 analysts submitted results. Of the 16 analysts, 10 also submitted results for the matrix section of the exercise. The results are given in Table 4.

Only one outlier (R35) was identified. Results from R11 and R26A showed relative errors of >25% for the solution (*p,p'*-DDE) and for dieldrin four results showed relative errors of >25%.

In the egg pulp analysis for *p,p'*-DDE, no result showed a relative error of >50%. With dieldrin, only one result (R17) had a relative error of >50%. Considering the relatively low organochlorine concentrations in the matrix, the exercise can be regarded as successful.

Whilst most of the laboratories still made use of packed columns, it was noteworthy that four analysts in two laboratories used capillary columns fairly successfully. All the laboratories used ECDs.

Four analysts in separate laboratories used GC - MS for confirmation of pesticide identity, whereas four analysts used ultraviolet irradiation and chemical conversion instead. The remaining participants used retention times and relative retention times for confirmation on one or more columns.

ICE 3/85

Results of the exercise are presented in Table 5. Seventeen laboratories indicated their interest in participating with seven submitting results, involving a total of ten analysts.

No outliers were identified and the low relative standard deviation indicated a successful exercise. No results showed a relative error of >25%, which may be due to the relatively high pesticide concentrations and the simplicity of the analysis of the solution.

Three participants identified some or all of the pesticides incorrectly by using retention times or relative retention times with one or more columns. Five analysts in three laboratories used either GC - MS or a mass-selective detector (MSD) to identify the pesticides.

Only one participant (R13A) reported the presence of malathion in the grape juice sample at a concentration level of 0.15 mg kg^{-1}.

The detectors used for the analysis included FPDs, NPDs, ECDs and FIDs.

Table 5. Results of ICE 3/85—chlorpyrifos and fenchlorphos in solution and unfortified grape juice. Abbreviations as in Tables 1 and 2; MSD, mass-selective detector

	Solution							
	Chlorpyrifos (unknown)		Fenchlorphos (unknown)					
Laboratory code	Concentration/ ng μl^{-1}	Relative error, %	Concentration/ ng μl^{-1}	Relative error, %	Unfortified grape juice	Column used	Detector used	Method of confirmation
R06A	33.91	2	24.30*	11	—	P	FID/NPD	Retention times on different columns and detectors
R06B	37.20	12	20.50	7	—	P	NPD	Retention times on different columns
R08A	35.10	6	20.90	5	—	WCOT	FID	GC - MS
R08B	33.70	2	21.30	3	—	WCOT	FID	GC - MS
R09	32.02	3	22.30	1	—	P	FPD	Relative retention times
R13A	32.56	2	21.39	3	Malathion 0.15 mg kg^{-1}	P	FPD	MSD
R13B	32.18	3	22.45	2	—	P	ECD	MSD
R18	29.40	11	21.60	2	—	P	FPD/ECD	Relative retention times
R23	33.52†	1	23.42‡	7	—	P	NPD	Relative retention times
R35	31.33	5	21.84	1	—	P	NPD	GC-MS
Mean	33.09		22.00					
Standard deviation ..	2.14		1.16					
Relative standard deviation, % of spiked concentration	7%		5%					
Spiked concentration	32.50		22.00					

* Identified as pirimiphos.
† Identified as formothion.
‡ Identified as dimethoate.

Discussion

Residue results from ICEs undertaken during the past 2 years, and previous results,[2,3] indicate a gradual and definite improvement in analysts' expertise. Some of the laboratories have participated on a regular basis and the high quality of their results was probably due to their regular participation in ICEs. Regrettably, some laboratories still appear to view an ICE as a possible threat to their profession, thereby foregoing the benefits obtained from participating.

The major causes of errors by participants in this series of ICEs were identified by the Task Group as follows. The first cause was a lack of training and experience. Where this was identified, the relevant laboratory supervisor was notified. Second, sporadic calculation errors occurred in most of the exercises, probably owing to inexperience. Quantification was sometimes carried out with peaks too small for accurate quantification, particularly when peaks were measured manually and not by integrator. Third, the difference between the peak size of the standard injection and the sample injection was too large for accurate quantification of the sample peak. This error usually occurred with analysts using proportional quantification techniques. Fourth, inaccurate results were produced by analysts working outside the linear range of the detectors when standards were used at excessive concentrations. This was so particularly with ECDs. Finally, the identification and confirmation techniques used by most of the participants were not acceptable to the Task Group. Participants using retention and relative retention times for confirmation often reported erroneous compounds. Identifying compounds with only gas chromatographic retention data was strongly discouraged as superior alternative identification and confirmation techniques were available.[11,12] The increase in the use of GC - MS and GC - MSD is to be commended and should be encouraged.

Appendix: Participating Laboratories

Laboratories of the following organisations participated in this series of ICEs: Agricultural Products Standards Division, Department of Agriculture Economics; Agrihold (Pty) Ltd.; Animal and Dairy Science Research Institute, Department of Agriculture and Water Supply; Applied Science Research Laboratories (Pty) Ltd.; Chromtek (Pty) Ltd.; City Health Department, Johannesburg City Council; Echalaz and Osborne (Pty) Ltd.; F.B.C. Holdings (Pty) Ltd.; Food and Nutritional Products SA (Pty) Ltd.; Government Chemical Laboratory, Department of Health; Malawi Bureau of Standards; Maize Board; Marine Pollution Group, University of Port Elizabeth; National Institute for Water Research, Council for Scientific and Industrial Research (two laboratories); Oil Seeds Board; Plant Protection Research Institute, Department of Agriculture and Water Supply; Premier Quality and Research; South African Bureau of Standards; South African Transport Services; and Union Carbide (Pty) Ltd.

References

1. Snelson, J. T., "The Quantity and Quality of Residues Data Required for the Establishment and Enforcement of Maximum Residues Limits," *in* Miyamoto, J., and Kearney, P. C., *Editors*, "Pesticide Chemistry, Volume 4, Pesticide Residues and Formulation Chemistry," Pergamon Press, Oxford, 1983, p. 13.
2. Van Dyk, L. P., Lotter, L., De Beer, P. R., De Klerk, A., Viljoen, A. J., and Prinsloo, S. M., *Analyst*, 1983, **108**, 748.
3. Van Dyk, L. P., Lotter, L., De Beer, P. R., Reyskens, D. H. J. P., Viljoen, A. J., and Prinsloo, S. M., *Analyst*, 1985, **110**, 1053.
4. Bantjies, N. V., *Chemsa*, 1984, **10**, 539.
5. Van Dyk, L. P., Wiese, I. H., and Mullen, J. E. C., *Residue Rev.*, 1982, **82**, 42.
6. Bowman, M. C., Beroza, M., and Harding, J. A., *J. Agric. Food. Chem.*, 1969, **17**, 138.
7. Lok, A., West, S. D., and Macy, T. D., *J. Agric. Food. Chem.*, 1978, **26**, 410.
8. Van Dyk, L. P., Breedt, B. C., and De Beer, P. R., *Agrochemphysica*, 1978, **10**, 47.
9. Horwitz, W., *Editor*, "Official Methods of Analysis of the Association of Official Analytical Chemists," Thirteenth Edition, Association of Official Analytical Chemists, Washington, DC, 1980.
10. Sherma, J., "Manual of Analytical Quality Control for Pesticides in Human and Environmental Media," US Environmental Protection Agency, Research Triangle Park, NC, 1976.
11. "Pesticide Analytical Manual," Volume 1, US Department of Health and Human Services, Food and Drug Administration, Washington, DC, 1986.
12. "Manual of Analytical Methods for the Analysis of Pesticides in Human and Environmental Samples," US Environmental Protection Agency, EPA-600/8-80-038, Washington, DC, 1980.

Paper A6/419
Received November 3rd, 1986
Accepted December 11th, 1986

Recommendations for the Conduct and Interpretation of Co-operative Trials

Analytical Methods Committee*
Royal Society of Chemistry, Burlington House, Piccadilly, London W1V 0BN, UK

In a co-operative trial, six or more laboratories analyse a series of specimens by any method that is appropriate. The results are collated and examined by a nested analysis of variance procedure, with a view to making a realistic quantification of random and systematic errors in the system. The performance of the laboratories as a whole and individually can be assessed. The information can be used to initiate remedial action in laboratories producing discrepant results, or to select laboratories for particular tasks. Suggestions for the conduct of these trials is given in respect of the choice, preparation and analysis of the specimens, the recording and reporting of data, and the statistical evaluation of the data.

Keywords: *Co-operative trials; accuracy, precision, repeatability, reproducibility; analysis of variance*

The Analytical Methods Committee has received and has approved for publication the following report from its Statistical Sub-Committee.

Report

The constitution of the Sub-Committee responsible for the preparation of this report was Dr. M. Thompson (Chairman), Mr. H. M. Bee, Mr. P. M. G. Broughton, (the late) Mr. R. V. Cheeseman, Dr. W. H. Evans, Dr. E. J. Greenhow (from June 1986), Mr. D. W. Lord, Prof. B. D. Ripley and Dr. R. Wood with Mr. J. J. Wilson as Secretary.

Introduction

Co-operative Trials

A co-operative trial is a concerted activity undertaken by six or more laboratories in which a number of specimens are analysed in each laboratory for a specified analyte, by a method that is not prescribed. Each specimen is a sub-sample from a bulk material held by the organising body. Each participating laboratory analyses a specimen from each bulk material one or more times. The data so produced are then statistically analysed with a view to making a realistic quantification of the random and systematic errors in the whole "system." Thus the co-operative trial has elements in common with the "round robin" trial, but is distinct from the collaborative trial in which the analytical procedure is prescribed in considerable detail.

This paper proposes recommendations for the conduct of co-operative trials and for the statistical interpretation of the data produced. At the time of writing, no British nor internationally recognised body had issued recommendations for such trials. The statistical methods recommended here are based on the normal principles of the analysis of variance, with three nested levels consisting of the variances (i) between laboratories; (ii) within laboratories but between analytical batches; and (iii) within analytical batches. There are two themes that are specifically emphasised. Firstly, many features of co-operative trials as currently practised tend to underestimate the variability that would be encountered in routine analysis. Secondly, it is felt that insufficient attention is paid at present to the way that both random and systematic errors vary with the concentration of the analyte.

* Correspondence should be addressed to the Secretary, Analytical Methods Committee, Analytical Division, Royal Society of Chemistry, Burlington House, Piccadilly, London W1V 0BN, UK.

Where an analytical method has been standardised and tested, and has been found to be suitable for a specific task, that method alone should be used for contractual or legal testing so that strict comparability can be maintained. In principle, only by using such a common yardstick can different laboratories minimise their relative biases. However, in many instances no such single method exists, and different laboratories use their own favoured methods. Such methods can differ in respect of the physical principle involved in the measurement (*e.g.*, atomic absorption spectrometry and X-ray fluorescence spectrometry) or can consist merely of a family of similar procedures based on a common measurement principle. In these circumstances co-operative trials are appropriate for the quantification of errors.

The recommendations in this paper are intended to form the basis for a protocol for the statistical analysis of the results of co-operative trials. The use of such a protocol would make it possible to arrive at a definitive interpretation of the data. However, there is an important qualification to this intention. During this study it was quickly realised, from the examination of case histories, that data from some trials were virtually beyond interpretation. It was clear that unless a trial were properly designed and executed, no definitive interpretation could be obtained. Accordingly, this paper includes recommendations for the design and conduct of co-operative trials, as well as for their interpretation.

Reasons for conducting co-operative trials

As no method is specified in a co-operative trial, only two features of the system can be tested, namely, (i) the performance of laboratories, as a whole and individually, and (ii) the test specimens.

The main concern of a co-operative trial is to provide a synopsis of the pattern of error in the trial and thereby to identify laboratories producing discrepant results. The outlying results can be identified separately as bias (systematic error) or precision (random error), the latter being subdivided into within batch, between batch and between laboratories. It should be noted that, in a hierarchical system of analysing errors, the usual distinction between accuracy (lack of bias) and precision may break down. For example, between-batch precision can be regarded as due to the variations in bias from batch to batch, in other words due to a systematic error of magnitude peculiar to each batch, which is added to the within-batch precision. The synopsis of error in the trial can be used to ensure that any legislation or contractual arrangements based on analysis is within the capabilities of the laboratories to provide. Further, the significance of an individual analytical result can be assessed in relation to any such legal requirement.

The quality of performance of an individual laboratory can be assessed and compared with that of other laboratories, or with an arbitrary standard of performance. Where individual laboratories fall outside performance requirements, they can be notified so that remedial action can be taken. Laboratories can be selected for future use on the basis of their performance in the trial.

When the participating laboratories can be divided into two or more groups based on the analytical methods used, the results can be compared on a method basis. For this purpose it is recommended that sufficient information on the methods used be provided by the laboratories involved in co-operative trials.

When the "true values" of the specimens are known, an assessment of the over-all accuracy can be obtained. When the "true values" for the specimens are not known, the results obtained from a successfully completed co-operative trial may be used to produce a consensus value for the material, which can subsequently be used in quality control procedures. It should be noted that the production of consensus values normally involves an element of judgement based on known foibles of particular analytical methods.

Whereas co-operative trials are a valuable general method of testing laboratories, it is recognised that they are not necessarily the optimum design for routine inter-laboratory quality control. Procedures such as the Harmonised Monitoring Scheme[1] for Inland Fresh Water and others have a different design and depend in part on pre-determined targets of performance. They therefore represent features that are more suitable for specific areas of application.

Collaborative Trials

In contrast to co-operative trials, collaborative trials have been widely studied and used. In a collaborative trial, the procedure at all stages is specified in considerable detail, so that differences in methodology between different laboratories and between individual analysts will be minimised. Many bodies, such as the BSI,[2] AOAC[3] and the Laboratory of the Government Chemist[4] have issued detailed recommendations for this purpose. Collaborative trials are primarily used to examine methods proposed as official or standardised tests. Only laboratories experienced in the test method would participate in such a trial. The results obtained enable the performance characteristics of the test method to be specified and its suitability for a particular task to be assessed. The format of the collaborative trial is also suitable for the assessment of laboratories using a particular test method, although it may not be the best procedure for routine quality control.

Procedures given in BS 5497[2] for the analysis of results from collaborative trials enable estimates of only two extreme types of variability to be obtained, namely reproducibility and repeatability. In the Standard, the terms reproducibility (R) and repeatability (r) are defined as the corresponding 95% confidence intervals for the absolute difference between a single pair of results duplicated under the appropriate conditions.

The co-operative trial, however, is distinct from the collaborative trial, in that each participating laboratory is free to use any appropriate method to determine the analyte. In a collaborative trial the procedure is specified in detail, so that a reasonable initial assumption is that (incompetence aside) the data comprise a single population. In a co-operative trial, however, significant differences between different laboratories in respect of the within-laboratory variations and laboratory bias might be encountered. In suitable instances it might be both possible and advisable to separate the laboratories into two or more groups, each using a particular method, before the analysis of variance is undertaken.

Choice, Preparation and Analysis of Specimens

Composition of the Specimens

Specimen matrix

The specimens must all consist of a material that falls into a narrowly defined class. Examples of suitable classes might be cereal grains, meat products, calcareous soils, etc. This may permit valid relationships to be established between the estimated errors and the analyte concentration, within the class of material, without undue concern about specific biases for particular specimens due to circumstances such as unique matrix effects. It is also important that a single analytical procedure will cope with the whole range of specimens within such a class without any deviations for particular specimens.

Analyte concentration range

The concentrations of analyte in the specimens should cover the range of interest fairly uniformly. Where the analyte range is to cover several orders of magnitude above the detection limit, a uniform spread on a logarithmic scale should be attempted. A bunching of the analyte concentrations towards the ends of the range will improve the standard errors in a regression on analyte concentration, but this practice may entail a loss of confidence about the middle range.

Specimen homogeneity

There is a special problem relating to homogeneity in analytical trials. The normal practice is to produce specimens with the greatest possible degree of homogeneity by very fine grinding and mixing. This is carried out to reduce sub-sample variations to a low level in relation to the errors accumulating in the analytical phases of the trial, and to minimise the segregation of parts of the material during storage and handling. The comminution and mixing of trial specimens is characteristically more thorough than that applied to samples in routine analysis. Thus the trial specimens may be unrepresentative of routine analysis in two respects, (i) the sub-sampling error will be lower and (ii) chemical decomposition may be more effective on the finer material of the trial specimen. Both of these features will tend to underestimate errors. We therefore recommend that the trial specimens be homogenised to a degree no greater than that in routine use where possible. The homogeneity of specimens should be tested beforehand by a laboratory not involved in the main trial.

Specimen stability

The specimens should be stored and transported in a manner which ensures the stability of the analyte concentration. Specific instruction for pre-analysis preparation (such as drying to constant mass) must be given, unless it is deemed that variations from this source are to be included in the analytical error between laboratories.

Role of true values

A knowledge of the true values of the concentration of the analyte in the specimens is highly desirable in co-operative trials and is essential if bias is to be estimated. If true values are not available, the over-all mean results can be used as estimates of them, but in this instance only random errors can be evaluated. In some instances the true values are defined only in terms of a specific test. In such instances, the concept of bias does not arise. Likewise, only the collaborative test can be applied, as there can be only one test method.

The concentrations in the distributed specimens must, however, be at least broadly known by the organising body for two reasons, (i) so that the participating analysts can use appropriate methods, and (ii) so that the range of analyte concentrations in the specimens is appropriate for the purpose of the trial.

Generally, specimens with known values are not readily available, and certified reference materials may well be too costly to use in large trials. Under these conditions, the technique of spiking may have to be resorted to. In this method a base material is fortified (or spiked) with known concentrations of the analyte. It might therefore be assumed that the true values are known in the specimens. This optimistic assumption depends for its validity on several conditions which may not be fulfilled. For instance, it is necessary to assume that the concentration of the analyte in the base material is either negligible or known.

In addition, it must be ensured that the mixing is completely satisfactory, so that the production of specimens for analysis is not subject to a significant degree of sampling error. However, the most serious limitation of spiking is that the spiked analyte may not be present as the same chemical species, or incorporated in the same physical environment, as it is in the natural material. This may give rise to bias because of varying behaviour of the analyte in its different forms, in response to a chemical decomposition or an instrumental determination. Therefore spiking should be used only when no other course of action is available, and with due consideration given to its shortcomings.

Conduct of the Analysis

Analysts participating in a trial may encounter a professional dilemma. Clearly they wish to demonstrate their competence by producing their best possible accuracy and precision on the test material. In contrast, the trial organiser normally wants to discover the bias and precision that is appropriate for typical conditions rather than the best possible conditions. This apparent conflict of requirements can be resolved by attention to the points outlined in this section. Deviation from these suggestions, however, may give rise to estimates of errors that are smaller than typical levels.

Randomness and anonymity of specimens

We make the assumption that laboratories participating in a co-operative trial will analyse batches of material similar to the specimens as a routine task. A batch is regarded as a group of samples in which each sample is treated in a close sequence according to a particular stage of the analytical procedure, before the analyst passes to the next stage. It is essential that the specimens should be inserted at random positions into the sequence of samples constituting such a routine batch, and not specially marked. In this way the specimens will receive the least possible amount of special attention, *i.e.*, they will be treated as routine samples. Any deviation from this practice will tend to underestimate errors. Any means by which samples can be identified will further tend to reduce variability. An alternative possibility would be for the trial organisers to supply the specimens within a bigger group of dummy specimens. This would necessarily increase the cost of the trial.

Prevention of data selection

The participating laboratories should be instructed to produce only the specified number of replicate determinations for each specimen. Over-production of data combined with the selective reporting of favoured results will inevitably result in underestimated errors in the results of the trial. This can be rigorously prevented by supplying the participating laboratories with only a small excess of the specimens for the trial specification, say 1.2 times the mass required. In co-operative trials this would require extra planning, as each laboratory will have to state in advance what sample mass is required for use by their nominated method.

Use of normal conditions

Participating laboratories must be encouraged to execute the analysis in a manner that does not give special attention to the specimens, *i.e.*, attention beyond that given to routine samples. When the samples are analysed blind, or the data logging is completely automatic, this is usually a straightforward task. In manual work, however, it is difficult for the analyst to avoid taking extra care when the trial specimens are being analysed.

In many procedures the analyst is expected to exercise a degree of judgement when manually recording analytical data. For example, in atomic absorption spectrometric determinations, the analyst may watch the digital ouput until a steady reading is obtained and then record the steady value. In practice, some noise is often visible in the last digit of the reading and the analyst may record a mental average of the last few readings.

Where a judgement of this kind is an intrinsic part of the analytical method used in a trial, the analysis must be blind. If the analyst is aware that a trial specimen is under examination, it is virtually impossible for him or her to avoid giving extra attention to the specimen, for instance by waiting longer to ensure signal stabilisation, or by mentally averaging more than the usual number of results. In automatic systems, however, the data reading sequence is completely determined, so that the special treatment of trial specimens is impossible.

Possible Effects of In-house Data Quality Control

Many laboratories employ routine quality control schemes involving every batch of analysis, including presumably those containing co-operative trial specimens. If measures of batch bias or within-batch precision fall outside of the control limits the analytical batch may be rejected. Overall this will produce a data sample from a "culled" distribution. In a collaborative trial data from outlying batches will be lost unless the laboratory is allowed to repeat the analysis of the specimen in a subsequent batch. It is recommended that this practice be permitted within the co-operative trial, because the culling and re-analysis constitutes a normal component of the analytical system being used by that individual laboratory. In other words, the quality control scheme and its consequences are as much a part of the analytical system as are the procedure, the instruments, the analyst, the environment, etc. However, it is important that the normal control limits are used for the batch containing the trial specimens.

A practice that is not desirable in the context of co-operative trials is the retrospective adjustment of trial data on the basis of information obtained from the quality control scheme. Whereas this practice may provide an improvement in batch accuracy, it will produce flawed data for a trial.

It is recognised that in certain analytical procedures a factor is applied to adjust the figures initially obtained to allow for recovery errors. The recovery is estimated in a separate experiment. Where this practice is an intrinsic part of the procedure that is applied to every sample, it is permissible in a trial. This is quite distinct from the previously discussed situation involving quality control data.

Recording and Reporting of Data

Number of Significant Figures

The advent of the digital output in analytical instrumentation has given the analyst the capacity to select the number of significant figures produced during the analysis. In many instances of such instrumentation, an output with a fixed number of digits is combined with a sensitivity control that is variable over a wide range. The analyst, for example, might elect to output and record a signal of say 4.231 . . . as 4.23, 4.2, or 4, as seems appropriate.

In methods where a steady analogue signal is presented digitally, the output commonly displays two features, namely a part of the number where the digits are invariant with time and a second moiety where the digits are rapidly changing. Some analysts regard the latter part as "mere noise," and excise it completely from their recorded data. The mere noise, however, is part of the error that a trial is designed to quantify. Clearly then, enough of the noise must be retained to enable an estimate of its magnitude to be made.

In order to achieve this, the analyst should record at least the first digit showing variation, and preferably the second such figure as well. Failure to include these variable digits will tend to produce an underestimated variability.

At first sight this suggestion seems to diverge from the stated aim of these recommendations, which is to estimate errors that occur under normal conditions of routine analysis. Any special data recording requirements for inter-laboratory trials seems difficult to reconcile with the idea of normal practice. No such inconsistency is intended, however. It is suggested that the recommendation should be implemented under all conditions when data are being recorded, *i.e.*, both in trials and in normal working. For routine analysis the data can be rounded to an appropriate degree as the last stage of calculations before the data are presented to the client. For inter-laboratory trials, and for in-house data quality assurance, however, the data should be reported and used as recommended, *i.e.*, with at least one and preferably two significant figures showing uncertainty.

The same practice of recording figures representing noise is similarly required for data that are read directly from an analogue output. Interpolation between the finest divisions of a scale should always be attempted, and the figures recorded.

Censoring of Data

In this paper, the term censoring refers to the practice of modifying the recorded data on the basis of a pre-conceived notion on the part of the analyst as to the possible range of analyte concentration. It occurs, then, at the extremes of the concentration range. Censoring can be illustrated by an imaginary example, in which a chalk sample is analysed for calcium. Pure calcium carbonate contains 40.04% *m/m* of calcium. Thus an analyst encountering a determined value that is greater than this figure might be inclined to report a default value of 40.04%, on the grounds that the determined value was impossible and therefore likely to draw undue criticism from the client.

The high determined value may spring from one of several possible causes namely, (i) there may actually be more than 40.04% of calcium in the sample, due to the unsuspected presence of a species with a higher calcium content than that of $CaCO_3$, (ii) there may be a positive bias in the analytical method, tending generally to produce determined values that are too high and (iii) the random errors in the analysis may have combined to give a chance value above the theoretical limit, although the population mean of the results is below the limit.

The argument against censoring

Clearly censoring should not be applied within a trial, because the practice tends to obscure the very factors (*i.e.*, bias and random error) that the trial is designed to quantify. This suggestion, however, may seem to diverge from the basic principle that the conditions of a trial should resemble normal routine practice as closely as possible.

Again the apparent conflict can be resolved by recommending that censoring should be applied neither to trial data nor to the first stage of routine analysis. There may be compelling reasons to censor data produced for a client. If this is so, it should be carried out by the analyst as the ultimate stage of data handling. Data produced for trials or for in-house data quality assurance should not be censored at all. The reported value should be exactly the value that is produced by the method, without any intervention or post-analysis exercise of judgement by the analyst.

Censoring at low analyte levels

In practice analysts are more likely to censor data at the lower end of the concentration scale. In that circumstance, there are two theoretical lower limits (i) the detection limit, below which (however it is defined) there is considerable uncertainty as to whether any analyte is present and (ii) the zero point, as there is no reality corresponding to a negative concentration. Despite these two limits, it is recommended that no censoring should be applied at low levels of analyte to data produced for trials or for in-house quality assurance. Values falling below a putative detection limit should be reported as they occur and not as "less than detection limit." Even negative values should be recorded as they occur.

It is anticipated that many analysts will resist this recommendation initially. However, the case against censoring at low levels is as clear as it is at high levels. In regard to the detection limit, there is no consensus on the definition of this term, and therefore censoring practice would vary from laboratory to laboratory. More significantly, values reported as "less than" do not fall on a continuous scale, and thus cannot be incorporated into statistical calculations except as a default value (*e.g.*, as an arbitrary fraction of the detection limit).

Sub-zero observations are seldom encountered on actual samples if an unbiased analytical method is used, but are common in blank determinations (unless they are suppressed by a data-processing or recording practice). This fact springs from the ordinary distribution of random errors. If the analyte concentration in the blank is virtually zero, about one half of the blank readings should be negative. Setting these values to zero would bias the mean blank value positively. A subtraction of the biased blank would bias the sample values negatively.

In addition to this factor, the analytical method may have a negative bias at the lower end of the concentration scale. If this is so, then it is important that the trial should be able to detect the bias. The bias may be manifested in part by the appearance of some negative values for specimens with low analyte concentrations. If these low values are censored, however, the existence of the bias may be partly or completely hidden.

Analyte concentration ranges in trial samples

It might be argued that the whole problem of low-level censoring could be avoided by the use of specimens with concentrations well above the detection limit of the methods employed. This is certainly so where the analyte is a major component of the specimens. Where the analyte is a trace constitutent, the use of low-level specimens may be unavoidable if the trial is to be realistic.

Many laboratories that are participating in co-operative trials will be using methods close to their detection limits. This is partly an economic effect, as laboratories will tend to use the cheapest method that can do the job. In addition to this, statutory limits for toxic analytes are often set unreasonably low in relation to general analytical capabilities, presumably on the grounds that the only safe level is zero. Thus it is often necessary to include in trials specimens that contain analyte levels not much greater than the detection limit, because these are the very concentration ranges that are of principal interest. In addition, the inclusion of low-level specimens is an important point of experimental design when there is an interest in the magnitude of errors as a function of concentration.

Excess Data

An excess of data results from a participating laboratory providing more information than requested (*e.g.*, a triplicated result rather than the required duplicated result). In collaborative trials this can be prevented if the specimens are restricted in amount to just sufficient for the analysis. Co-operative trials cannot be easily controlled in this way, because no particular procedure or sample mass is specified. However, this control could be exerted if laboratories were asked to supply statements of their procedures before the distribution of specimens. This would necessarily involve the distributing agency in extra work, but would avoid the underestimation of errors due to the reporting of selected data. In any event, participating laboratories must be emphatically instructed to carry out only the specified number of determinations. If excess data are nevertheless reported by a laboratory, the situation can be recovered (in the absence of contra-indications) by deleting the excess data at random.

Missing Data

When a laboratory fails to supply data in accordance with the experimental design, several courses of action are available to the organising agency. When the lack of data is due to the loss of specimens in transit, or to loss through an accident during the course of analysis, substitute specimens can usually be supplied to the laboratory without compromising the experimental design, so long as the deadlines can still be met.

When data items are omitted from the reported data set without an acceptable explanation, two possibilities are available, (i) to fill in the missing data items with appropriate data to balance the experimental design or (ii) to eliminate the data from the appropriate laboratories either partly or completely from the study. If the proportion of missing data is large, the second course of action is preferred. Unless the amount of missing data is very small, a statistical expert should be consulted before a quantitative evaluation of the data is attempted.

Statistical Evaluation of the Data

Minimum Numbers for Each Level of the Trial

The number of laboratories participating in the trial should not be less than six, and should be selected at random from a pool of laboratories when the whole pool is not to be involved.

The number of different specimens (*i.e.*, levels of analyte) should not be less than six, and the number of batches should not be less than two. The replication for each specimen in a batch should be exactly two (although the identity of the duplicate pairs should be withheld from the participating laboratories).

Treatment of Outliers

The definition and detection of outliers or stragglers and how to treat them has long been a contentious matter among analytical chemists and statisticians. Most of the literature has been concerned with the effect of outliers on measures of location (that is, measures of the centre of a distribution such as a sample average or median). In the present context we are equally interested in measures of spread such as a standard deviation.

The practice among analytical chemists in the context of collaborative trials has been to use outlier tests and reject outliers (either discrepant means or cells with too large a variability). The effect of outlier rejection on measures of spread is to reduce them; a simulation experiment described below shows that the effect can be fairly serious. Estimating variability after rejecting outliers amounts to estimating variability under perfect conditions with no errors in techniques. We found these to be compelling arguments against outlier rejection and thus recommend that for the present purposes outliers must be retained. The effect of this recommendation is to overestimate variability occasionally, but this is safer than the consistent underestimation which we suspect happens all too frequently.

There is one exception to this rule, that of a spurious value. This is a result that has been corrupted during the reporting stage, for example by a transcription error. The statistical analysis should report possible outliers so they can be checked against the original record of the result. If the possible outlier proves to be a spurious value it should be corrected and the statistical analysis repeated. Transcription errors are surprisingly common. Huber[5] suggests that 5–10% of wrong values in a data set seem to be the rule rather than the exception. Where possible results should be recorded and transferred automatically to avoid this.

A small simulation experiment was performed to show the effect of outlier rejection on typical sample variances. In the simulated trial six laboratories analysed a specimen twice each. The Dixon and Cochran tests were used once each, and outliers detected at the 5% level were rejected. Table 1 shows the results obtained.

The experiment was performed for three different distributions of the errors. For line 1 the random error on each sample and the random difference between laboratories was normally distributed. The normal distribution is known to produce fewer extreme values than most real error distributions. For lines 2 and 3 we assumed a distribution with longer tails, the *t*-distribution with 10 and 5 degrees of freedom, respectively. It would probably not be noticed that these errors were not normally distributed, but the effect of outlier rejection is to underestimate variability markedly.

Sources of Variation

In the general design of a co-operative trial discussed above, there are three sources of random variation for an analyte in each specimen. These are assumed to be statistically independent.

(a) Variation between replicates. We assume each measurement has a measurement error of variance σ_e^2.

(b) Variation between analytical batches. Different batches will be analysed under different conditions. The effect of the conditions on a particular batch, the batch effect, is random with variance σ_B^2.

(c) Inter-laboratory variation. Each laboratory will have a systematic bias ξ_i. As the laboratories are regarded as a random effect in statistical parlance, ξ_i is regarded as random with variance σ_L^2.

Consider a single additional measurement. This is made up of the true value + laboratory bias + batch effect + measurement error and so has variance of $\sigma_L^2 + \sigma_B^2 + \sigma_e^2$. Let

$$D = 2\sqrt{(\sigma_L^2 + \sigma_B^2 + \sigma_e^2)}$$

Then

$$P(|\text{measurement} - \text{true value}| < D) \approx 95\%$$

and D measures the attainable precision and is the most important result of a co-operative trial.

Table 1. Bias of a sample variance after outlier rejection

	Variance, %	
Distribution	Between-laboratory	Within-laboratory
Normal	0	−6
t_{10}	−2	−9
t_5	−10	−16

Table 2. The analysis of variance between laboratories, within laboratories - between batches and within batches - between replicates. The "mean square" equals (sum of squares)/(degrees of freedom), and E(MS) is the expected value of the mean square. Variances are estimated by equating the last two columns

Source of variation	Degrees of freedom	Sum of squares	Mean square	E(MS)
Between laboratories	$l-1$	$br\sum_i(\bar{y}_i - \bar{y})^2$	MS_L	$\sigma_e^2 + r\sigma_B^2 + br\sigma_L^2$
Within laboratories - between batches	$l(b-1)$	$r\sum_{i,j}(\bar{y}_{ij} - \bar{y}_i)^2$	MS_B	$\sigma_e^2 + r\sigma_B^2$
Within batches - between replicates	$lb(r-1)$	$\sum_{ijk}(y_{ijk} - \bar{y}_{ij})^2$	MS_e	σ_e^2

Table 3. Trial data set used as an example. Analyte concentration (g kg^{-1}) found in seven specimens. Six laboratories analysed the specimens three times each, with duplication on each occasion

		Laboratory					
Specimen	Batch	1	2	3	4	5	6
1	1	0.29	0.40	0.40	0.9	0.44	0.38
		0.33	0.40	0.35	1.3	0.44	0.39
	2	0.33	0.43	0.38	0.9	0.45	0.40
		0.32	0.36	0.32	1.1	0.45	0.46
	3	0.34	0.42	0.38	0.9	0.42	0.72
		0.31	0.40	0.33	0.9	0.46	0.79
2	1	0.13	0.22	0.25	1.7	0.23	0.24
		0.14	0.22	0.20	1.3	0.24	0.20
	2	0.16	0.24	0.16	1.5	0.22	0.15
		0.11	0.19	0.16	1.5	0.23	0.16
	3	0.14	0.21	0.25	0.6	0.24	0.35
		0.13	0.22	0.18	0.4	0.18	0.42
3	1	0.68	1.03	0.83	1.3	1.1	1.03
		0.71	1.05	0.66	1.7	1.0	0.88
	2	0.86	1.05	0.89	1.5	1.1	1.06
		0.76	1.16	0.92	1.5	1.2	1.16
	3	0.72	0.97	0.75	2.1	1.2	1.1
		0.73	1.12	0.75	1.9	1.1	1.2
4	1	0.50	0.81	0.50	1.3	0.48	0.31
		0.47	0.57	0.50	1.3	0.47	0.31
	2	0.64	0.67	0.58	1.3	0.57	0.69
		0.53	0.60	0.67	1.1	0.56	0.73
	3	0.49	0.66	0.50	0.2	0.55	1.1
		0.50	0.80	0.50	0.2	0.55	0.90
5	1	6.60	8.40	6.9	7.6	8.0	7.7
		7.08	8.60	6.7	7.8	7.8	6.8
	2	7.56	7.54	7.1	7.9	8.0	9.4
		7.14	8.50	7.1	7.5	7.9	9.9
	3	7.19	8.74	6.3	7.8	8.3	9.2
		6.64	8.22	6.7	7.4	8.3	9.0
6	1	1.36	2.12	1.5	2.4	1.9	1.7
		1.34	2.44	1.5	2.6	1.9	1.8
	2	1.51	1.49	1.5	2.2	1.9	2.0
		1.44	1.70	1.6	2.8	1.9	2.1
	3	1.52	1.73	1.3	2.2	1.8	1.5
		1.30	1.64	1.5	1.7	1.9	1.5
7	1	1.06	1.50	1.0	1.5	1.3	1.5
		0.88	1.07	1.0	1.9	1.4	1.5
	2	1.01	1.23	1.1	2.4	1.3	1.3
		1.09	0.93	1.1	1.9	1.3	1.4
	3	0.87	1.32	0.75	1.7	1.2	1.5
		1.02	1.25	0.90	2.0	1.2	1.8

A complication arises in that σ_L^2, σ_B^2 and σ_e^2 are functions of the analyte concentration. Thus the statistical analysis should include graphs of σ_L, σ_B and σ_e against concentration. These may be roughly linear, of the form $\sigma = a + b \times$ concentration. The variances σ_L^2, σ_B^2 and σ_e^2 are regarded as the fundamental quantities, from which other quantities may be computed as shown below.

Statistical Analysis

In this procedure each level is analysed separately by a nested analysis of variance. The residuals for each analysis are then checked for possible outliers and any spurious values found are corrected. Finally the values of σ_L, σ_B and σ_e from each analysis are plotted against concentration and a line fitted if possible.

Table 4. Calculated statistics for the data set shown in Table 3

Specimen	$\bar{y}$	MS_L	MS_B	MS_e	$\hat{\sigma}_L$	$\hat{\sigma}_B$	$\hat{\sigma}_e$
1	0.51	0.378	0.017	0.0063	0.25	0.07	0.079
2	0.37	0.933	0.116	0.0062	0.37	0.23	0.079
3	1.08	0.645	0.037	0.0097	0.32	0.12	0.098
4	0.64	0.128	0.168	0.0051	0.0	0.28	0.072
5	7.76	3.266	0.600	0.0967	0.67	0.50	0.311
6	1.79	0.633	0.109	0.0261	0.30	0.20	0.161
7	1.31	0.731	0.039	0.0270	0.34	0.08	0.164

Analysis of variance

Suppose that there are l laboratories, b batches and $r = 2$ replicates in each batch. Let y_{ijk} denote the result for the kth replicate of batch j at laboratory i. Let

$$\bar{y}_{ij} = \frac{1}{r}\sum_k y_{ijk},\ \bar{y}_i = \frac{1}{b}\sum_j \bar{y}_{ij},\ \bar{y} = \frac{1}{l}\sum_i \bar{y}_i$$

Then the analysis of variance is shown in Table 2.

We can estimate the variances by equating the last two columns in the table. We obtain

$$\hat{\sigma}_e^2 = MS_e$$
$$\hat{\sigma}_B^2 = r^{-1}(MS_B - MS_e)$$
$$\hat{\sigma}_L^2 = (br)^{-1}(MS_L - MS_B)$$

There is a complication if either $\hat{\sigma}_B^2$ or $\hat{\sigma}_L^2$ turns out to be negative, in which instance it is set to zero. The results (y, $\hat{\sigma}_L^2$, $\hat{\sigma}_B^2$, $\hat{\sigma}_e^2$) are carried forwards.

Outlier checking

As previously recommended, we test for outliers only to allow correction of spurious values and to report unusual performances of particular laboratories.

(i) Compute

$$\alpha_i = (\bar{y}_i - \bar{y})/\sqrt{[(l-1)MS_L/lbr]}$$

for each laboratory i. Values of $|\alpha_i| > 2.5$ suggest a laboratory with an unusual systematic bias.

(ii) Compute

$$\alpha_{ij} = (\bar{y}_{ij} - \bar{y}_i)/\sqrt{[(b-1)MS_B/br]}$$

Values of $|\alpha_{ij}| > 2.5$ suggest a discrepant batch.

(iii) Compute

$$\alpha_{ijk} = (y_{ijk} - \bar{y}_{ij})/\sqrt{[MS_e/2]}$$
$$\beta_{ijk} = (y_{ijk} - \bar{y}_i)/\sqrt{\left[\left(\frac{b-1}{b}\right)(MS_e + MS_B/2)\right]}$$

and note which measurements produce an absolute value of one or both that is greater than 2.5.

Laboratories discrepant at more than one level should be reported. Laboratories with several discrepant batches should be reported as having a large within-laboratory variation.

Table 5. Absolute values of test statistics α_{ij}, α_{ijk} and β_{ijk} falling above the critical value of 2.5, calculated from the data of Table 3. No value of α_i fell above 2.5. The parenthesised figures are the indices for the test statistic, of which the value follows. Thus (411) is the value of α_{411}, *i.e.*, the first sample in the first batch from the fourth laboratory

Specimen	α_{ij}	α_{ijk}	β_{ijk}	Comment
1	—	(411) (412) 3.57	(412) 3.03	Lab. 4, batch 1, too variable, esp. 2nd result
1	(63) 3.07	—	(632) 2.68	Lab. 6, batch 3, too high
2	—	(411) (412) 3.59	(411) 2.58	Lab. 4, batch 1, first result too high
2	(43) 3.39	—	(431) 2.74 (432) 3.70	Lab. 4, batch 3, lower than 1 and 2
3	—	(411) (412) 2.88	(411) 2.68	Lab. 4, batch 1, value 1 low
3	(43) 3.01	—	(431) 3.17	Lab. 4, batch 3, value 1 high
4	(43) 2.96	—	(431) 2.87 (432) 2.87	Lab. 4, batch 3, both values low
5	(61) 3.09	—	(612) 3.47	Lab. 6, batch 1, value 2 low
6	—	—	(212) 2.53	Lab. 2, batch 1, value 2 high
6	—	(421) (422) 2.63	—	Lab. 4, batch 1, value 2 high
6	—	—	(432) 2.66	Lab. 4, batch 3, value 2 low
7	—	—	(421) 2.84	Lab. 4, batch 2, value 1 high

Results with large $|\alpha_{ijk}|$ or $|\beta_{ijk}|$ are suspect spurious results. They should be checked against the original record and corrected if necessary.

Summary graphs

Each of the $\hat{\sigma}_L$, $\hat{\sigma}_B$ and $\hat{\sigma}_e$ is plotted against $\bar{y}$. If no consistent pattern is seen, then the average value is reported as applying to all concentrations in the range of the trial. Normally each standard deviation, σ, will appear to increase with mean concentration $\bar{y}$. Then a straight line should be fitted using a standard regression program, and its equation reported, e.g.,

$$\hat{\sigma}_L = 0.205 + 0.595 \times \text{concentration}$$

If a negative intercept is found, re-fit with the line constrained to pass through the origin or use a non-linear relationship such as a quadratic in concentration.

Assumptions involved

The main assumption of the analysis of variance is the equality of variances within laboratories and batches. If some laboratories are more variable than others, the results represent the average variability. As such the estimates of standard errors are reliable but the confidence intervals (as derived below) will be too short.

If the performance of different laboratories is indeed very different the whole purpose of a co-operative trial is called into question. A sign of this will be that the most variable laboratories will have many discrepant batches.

Sometimes laboratories can be grouped by their method of analysis. When the groups are not too small (four or more) a separate statistical analysis should be performed for each group. Groups of similar precision can then be combined.

Worked Example of the Statistical Calculation

The set of results shown in Table 3 consists of the results of a co-operative trial in which seven different materials of a particular class were analysed. Six laboratories analysed the specimens for a single analyte, with the analyses being repeated in three batches with blind duplication in each batch.

For specimen 1, the various $\bar{y}$ values and the mean squares are calculated from the individual y_{ijk} values as follows:

y_{ijk}	0.29	0.40	0.40	0.9	0.44	0.38
	0.33	0.40	0.35	1.3	0.44	0.39
	0.33	0.43	0.38	0.9	0.45	0.40
	0.32	0.36	0.32	1.1	0.45	0.46
	0.34	0.42	0.38	0.9	0.42	0.72
	0.31	0.40	0.33	0.9	0.46	0.79
$\bar{y}_{ij}$	0.31	0.40	0.375	1.1	0.44	0.385
	0.325	0.395	0.35	1.0	0.45	0.43
	0.325	0.41	0.355	0.9	0.44	0.755
$\bar{y}_i$	0.32	0.4017	0.36	1.0	0.4433	0.5233
$\bar{y}$	0.5081					

$SS_L = 6[(0.32 - 0.5081)^2 + \ldots . + (0.5233 - 0.5081)^2] = 1.89$

$MS_L = SS_L/5 = 0.378$

$SS_B = 2[(0.31 - 0.32)^2 + \ldots . + (0.755 - 0.5233)^2] = 0.20$

$MS_B = SS_B/12 = 0.017$

$SS_e = [(0.29 - 0.31)^2 + \ldots . + (0.79 - 0.755)^2] = 0.11$

$MS_e = SS_e/18 = 0.0063$

The statistics for all seven specimens, including the estimated standard deviations, are given in Table 4.

Outliers were detected by calculating values of α_i, α_{ij}, α_{ijk} and β_{ijk}. Values falling above the critical level of 2.5 are listed in Table 5. Laboratory 4 was repeatedly flagged, with occasional discrepant batches and analyses from other laboratories.

Fitting summary lines gave

$$\hat{\sigma}_L = 0.205 + 0.0595 \times \text{concentration}$$

$$\hat{\sigma}_B = 0.123 + 0.0466 \times \text{concentration}$$

$$\hat{\sigma}_e = 0.063 + 0.0311 \times \text{concentration}.$$

Application of Results

Confidence intervals

We have so far deviated from the provisions of BS 5497 in not using the terms "repeatability" (r) and "reproducibility" (R).

These parameters are less transparent when the batch effect introduces an extra layer of random variation. The quantity

$$D = 2\sqrt{(\hat{\sigma}_L^2 + \hat{\sigma}_B^2 + \hat{\sigma}_e^2)}$$

introduced previously is the half-width of a 95% confidence interval for the true value of a single measurement. We could define $R = \sqrt{2}D$ for the difference between two measurements taken at different laboratories. It would, however, seem wise only to compare results from the same laboratory. Then the relevant half-width is

$$r_e = 2\sqrt{2}\hat{\sigma}_e$$

for the difference between two measurements in the same batch and

$$r_B = 2\sqrt{[2(\hat{\sigma}_B^2 + \hat{\sigma}_e^2)]}$$

for the difference between two measurements in different batches.

Comparison with known values

Occasionally the true values of the analyte concentrations will be available. In such instances we can compute the systematic bias of each laboratory. Let the true value be μ. Then the estimate of laboratory bias is $(\bar{y}_i - \mu)$ with standard error

$$\sqrt{\left(\sigma_L^2 + \frac{1}{b}\sigma_B^2 + \frac{1}{br}\sigma_e^2\right)}$$

estimated by $\sqrt{(MS_L/br)}$. If several specimens of known concentration are available it may be instructive to plot bias against concentration.

Selection of laboratories

The outlier checks will often reveal one or more laboratories whose results are suspect. From the remaining laboratories one can choose on the basis of systematic bias [$(\bar{y}_i - \mu)$ if μ is known] and within-laboratory variability. The latter can be assessed by

$$\hat{\sigma}_i^2 = \frac{1}{(b-1)}\sum_j (\bar{y}_{ij} - \bar{y}_i)^2$$

which estimates $(\sigma_B^2 + 1/r\,\sigma_e^2)$ for that laboratory. One would select laboratories with small values of $\hat{\sigma}_i^2$ at all levels of the analyte in the specimen.

References

1. Simpson, E. A., *J. Inst. Water Eng. Sci.*, 1978, **32**, 45.
2. British Standard 5497, Part 1, "Precision of Test Methods," 1979.
3. Youden, W. J., and Steiner, E. H., "Statistical Manual of the Association of Official Analytical Chemists," Association of Official Analytical Chemists, Washington, DC, 1975.
4. "Guidelines for the Development of Standard Methods by Collaborative Study," Laboratory of the Government Chemist, London, 1986.
5. Huber, P. J., "Robust Statistical Procedures," SIAM, Pennsylvania, 1976.

SHORT PAPERS

Rapid Enzyme-linked Immunosorbent Assay (ELISA) with a Visual End-point for Detecting Opiate Narcotics in Urine

David Laurie, Andrew J. Manson, Andrew Mounsey and Frederick J. Rowell
Department of Pharmaceutical Chemistry, Sunderland Polytechnic, Sunderland SR2 7EE, UK
and John Seviour
Department of Clinical Biochemistry, Newcastle General Hospital, Newcastle-upon-Tyne NE4 6BE, UK

A simple ELISA technique has been developed for detecting opiate narcotics in urine. The assay employs a visual end-point and has a limit of sensitivity of 3 μg l^{-1} using 5-μl samples. No cross-reactivity is observed with non-opiate drugs commonly found in urine. The assay was used to identify opiates in urine from 38 addicts that had been screened using Toxi-Lab, EMIT and radioimmunoassay techniques. Only one false negative result was observed using the ELISA method. The assay may find application as an alternative to current screens where no sophisticated equipment is available for end-point detection.

Keywords: *Enzyme immunoassay; opiate drug screen; urine narcotic analysis*

A simple, rapid screen is required to determine the presence of the narcotic opiates morphine, codeine and dihydrocodeine in the urine of suspected drug abusers. Such a screen should be sensitive, rapid and specific for these opiate agonists and simple enough to be reliably performed by unskilled operators without sophisticated equipment. The current methods of screening these compounds are based on chromatographic technqiues[1,2] (GC, HPLC, TLC), immunoassays, including radioimmunoassay (RIA),[3–8] and non-isotopic enzyme immunoassays.[9,10] These methods require sophisticated equipment and/or skilled personnel, which renders them unsuitable for use as screens outside centralised laboratories. We have therefore developed a simple, specific screen for these narcotic opiates that requires only basic pipetting skills. The method employs a visual end-point and is sensitive and rapid.

Experimental

Apparatus

The assay was carried out on polystyrene microtitre plates (M-420, Atom Medical, Sussex). Absorbance measurements were recorded on a Dynatech Microreader II.

Reagents

All reagents, unless specified otherwise, were purchased from Sigma Chemical, Poole, Dorset. The buffer salts were of analytical-reagent grade (BDH Chemicals, Poole, Dorset).

Coating buffer, pH 9.0. 50 mM sodium hydrogen carbonate - carbonate.

Phosphate-buffered saline with 0.05% *Tween* 20 (*PBST*), *pH* 7.4. Prepared from 36.0 g of NaCl, 2.15 g of KH_2PO_4, 7.40 g of Na_2HPO_4, 2.5 ml of Tween 20 and 0.5 g of NaN_3, made up to 5 l with distilled water.

Glycine buffer, pH 10.4. Prepared from 4.12 g of glycine, 3.22 g of NaCl, 45 ml of 1.0 M NaOH solution and 0.1 g of NaN_3, made up to 1 l with distilled water.

Enzyme substrate solution, 1 mg ml^{-1}. 4-Nitrophenyl phosphate in glycine buffer was made up immediately prior to use.

Synthetic urine. Prepared from 22 g of urea, 1.1 g of Na_2HPO_4, 1.8 g of $NaH_2PO_4.2H_2O$, 8.25 g of NaCl, 5.2 g of KCl, 1.5 g of creatinine and 0.1 g of NaN_3, made up to 1 l in distilled water.

Urine Samples

Urine samples were taken from 38 patients attending Parkwood House Regional Unit for Alcohol and Drug Dependency, St. Nicholas' Hospital, Newcastle. These had been previously assayed by a morphine-specific RIA (Diagnostic Products, Wallingford, Surrey), subjected to a Toxi-Lab screen (Mercia Diagnostics, Weybridge) and screened using an EMIT Drug Abuse Urine assay for opiates and other drugs of abuse (Syva UK, Maidenhead, Berkshire) following the manufacturer's protocols.

Preparation of Immunogen

6-Succinylmorphine was prepared from a morphine-free base by the method of Simon *et al.*[12] in 70% yield; m.pt. 230 °C (decomposes); *m/z* 385 (M^+).

Porcine thyroglobulin (PTG) and bovine serum albumin (BSA) were each coupled to 6-succinylmorphine via a carbodiimide method described previously.[13] The resulting conjugates contained 6 mol of morphine per mole of PTG and 23 mol of morphine per mole of BSA. The amount of morphine bound to the protein was determined by RIA[8] and the protein concentrations by the standard Lowry test.

Antiserum

Three New Zealand white rabbits were immunised with the morphine - BSA conjugate following a previously described protocol.[8]

Assay

The wells of microtitre plates were coated by passive adsorption from 250 μl of a 1 μg ml^{-1} solution of morphine - PTG conjugate in coating buffer. After standing overnight at 4 °C, the plates were washed twice with distilled water, dried at 37 °C and stored at room temperature. The plates were washed four times with PBST immediately prior to assay.

Urine samples or morphine standard solutions in synthetic urine (5 μl) and PBST (15 μl) were added to each well followed by 40 μl of morphine antiserum, 1 + 599 dilution in PBST. The mixture was incubated for 15 min at room temperature, washed three times with PBST then 60 μl of alkaline phosphatase - anti-rabbit IgG conjugate solution (1 + 249 dilution in PBST) added to each well. After 15 min, the plate was again washed three times with PBST and 100 μl of enzyme substrate solution were added. The absorbance at 410 nm was recorded after 15 min development at room temperature or the wells were inspected visually for development of yellow colour.

Each urine sample was assayed in duplicate and each plate contained quadruplicate samples of both positive and negative

Table 1. Cross-reactivity of opiates in synthetic urine at 10^{-5} M solution in the ELISA

Opiate*	Cross-reactivity†	Opiate*	Cross-reactivity†
Morphine	+++	Naloxone	+
Dihydrocodeine	+++	Narcotine	−
Methadone	+	Norcodeine	+++
Morphine-3-glucuronide	+++	Papaverine	−
Heroin	+++	Thebaine	++

* Other compounds tested at 10^{-5} M concentrations in synthetic urine were alprazolam, amitriptyline, chlorpromazine, chlorpromazine sulphoxide, cocaine, cotinine, diazepam, didesmethylchlorpromazine, flupenthixol, fluphenazine, haloperidol, 5-hydroxytryptamine, LSD, mesoridazine, nitrazepam, nortriptyline, oxazepam, pentobarbitone, phenobarbitone, primidone, prochlorpromazine and propranolol. None of these gave inhibition of colour development in the assay.

† +++ Indicates the same absolute inhibition of colour development as morphine in the assay, ++ indicates moderate inhibition, + indicates some inhibition and − indicates no inhibition.

standards. A negative result is indicated by a visual yellow colour, absorbance greater than 0.1 (410 nm), and a positive result by the absence of colour after 15-min development.

The cross-reactivity of a range of drug substances was investigated by including 10^{-5} M solutions of the drugs in synthetic urine in place of the urine samples.

Results

The cross-reactivity of the antiserum is limited to the opiate narcotics (Table 1). Interference from other classes of drug substances including LDS, cocaine, neuroleptics, tricyclic antidepressants, antiepileptics and the nicotine metabolite cotinine is not observed at 10^{-5} M concentrations. The presence of urine (5 μl in the assay volume of 60 μl) has no effect on the assay.

The calibration graph for the assay gives a sharp change in absorbance between 0.3 and 3 μg l^{-1}. This corresponds to a distinctly yellow colour in the absence of morphine (absorbance > 0.15) and no visually discernible colour in the presence of 3 μg l^{-1} of morphine (absorbance > 0.07). The limit of sensitivity is 3 μg l^{-1}, this being the concentration of morphine corresponding to the mean absorbance for 20 drug-free urine samples minus three standard deviations as determined from the calibration graph. Hence the assay will visually detect the presence of morphine in urine for samples with concentrations exceeding 3 μg l^{-1}.

The assay successfully identified 37 of the 38 opiate-positive urine samples. However, the false negative result was for a sample with a morphine concentration of 2 μg l^{-1} as determined by RIA and was therefore outwith the sensitivity of the assay. All samples registered positive in the EMIT opiate screen. In addition EMIT drugs of abuse assays detected the presence of methadone in 11 samples, methadone plus benzodiazepine metabolite in 12 samples, benzodiazepine metabolite in 3 samples and benzodiazepine plus amphetamine in 3 samples. The morphine-specific RIA also identified "free" morphine in every sample, the range of morphine being 2–1000 μg l^{-1} within these samples. The Toxi-Lab screen gave 10 positives, out of the 38 samples, for morphine (4), codeine (1) or dihydrocodeine (5). The mean concentration of "free" morphine in these Toxi-Lab negative samples as determined by RIA was 179 μg l^{-1} (range 2–1000 μg l^{-1}).

Discussion

The assay is a standard ELISA format[14] in which binding of the anti-morphine IgG to the immobilised hapten (morphine - PTG) is visualised after binding of a second enzyme-labelled antibody to the anti-morphine IgG, via the enzyme hydrolysis of colourless 4-nitrophenyl phosphate to yellow 4-nitrophenol. Morphine or structually similar opiates competitively inhibit binding of the anti-morphine IgG to the morphine - PTG coating.

Incubation times for the assay have been minimised without sacrificing reliability or sensitivity by optimising reagent concentration and reducing the total assay volume. The total assay time for processing urine samples is typically 90 min for a full 96-well plate.

The microtitre plates coated with morphine - PTG and stored dry (not desiccated) at room temperature are stable for at least 6 months.

The ELISA assay was able to positively detect opiates in 37 of the 38 samples whereas the Toxi-Lab screen failed to detect opiates in 28 of these samples. Hydrolysis of the samples to generate additional free opiates would probably have produced more positives in the Toxi-Lab screen. Our results support those of others[15] that Toxi-Lab screening may only be sufficiently sensitive for the detection of drugs in urine in overdose situations.

The ELISA assay has advantages over the current EMIT and RIA methods for opiate screening in that it is simple, robust, does not use radioactive tracers and requires no sophisticated equipment, relying on the presence or absence of colour for end-point detection. It may therefore find application as a preliminary screen for opiates at locations where sophisticated equipment is not available.

This investigation received financial support from Cambridge Life Sciences plc.

References

1. Gough, T. A., and Baker, P. B., *J. Chromatogr.*, 1982, **20**, 289.
2. Gough, T. A., and Baker, P. B., *J. Chromatogr.*, 1983, **21**, 145.
3. Wainer, B. H., Fitch, F. W., Rothberg, R. R., and Freid, J., *Science*, 1972, **178**, 647.
4. Wainer, B. H., Fitch, F. W., Rothberg, R. R., and Freid, J., *Science*, 1972, **176**, 1143.
5. Stanski, D. R., Paalzon, L., and Edlund, P. O., *J. Pharm. Sci.*, 1982, **71**, 314.
6. Spector, S., *J. Pharmacol. Exp. Ther.*, 1971, **178**, 253.
7. Spector, S., and Parker, C. W., *Science*, 1970, **168**, 1347.
8. Spector, S., and Vessell, E. S., *Science*, 1971, **174**, 421.
9. Rowley, G. L., Rubenstein, K. E., Huisjen, J., and Ullman, E. F., *J. Biol. Chem.*, 1975, **250**, 3759.
10. Turner, S. J., *Aust. J. Med. Lab. Sci.*, 1981, **2**, 117.
11. Litman, D. J., Lee, R. H., and Jeong, H. J., *Clin. Chem.*, 1983, **29**, 1598.
12. Simon, E. J., Dole, W. P., and Hiller, J. M., *Proc. Natl. Acad. Sci. USA*, 1972, **69**, 1835.
13. Colbert, D. L., Smith, D. S., Landon, J., and Sidki, A. M., *Ann. Clin. Biochem.*, 1986, **23**, 37.
14. Schuurs, A. H. W. M., and Weeman, B. K., *Clin. Chim. Acta*, 1971, **81**, 1.
15. Jarvie, D. R., and Simpson, D., *Ann. Clin. Biochem*, 1986, **23**, 76.

Paper A6/322
Received September 11th, 1986
Accepted November 24th, 1986

Selective and Sensitive Extraction Spectrophotometric Method for the Determination of Palladium in Titanium Base Alloys

Yerramilli Anjaneyulu,* Chandra S. Kavipurapu and Manda Raviprakasa Reddy
Department of Chemistry, Nagarjuna University, Nagarjuna Nagar 522 510, India

and B. V. Rao
Defence Metallurgical Research Laboratories, Kanchanbagh, Hyderabad 500 258, India

A rapid, highly selective and sensitive extraction spectrophotometric method for the determination of palladium in titanium base alloys (0.1–0.8%) is described involving extraction of the Pd^{II} - PAR - XMH ion pair into chloroform.

Keywords: *Xylometazoline hydrochloride; ion pair; palladium determination; extraction spectrophotometry; titanium alloys*

Titanium and its alloys possess an unusual combination of intrinsic properties that assure their place as prominent structural metals and they find very important and extensive uses in aero engines, chemical plants and nuclear programmes owing to their high strength and corrosion resistance. For example, Ti - 6Al - 4V alloys, specially heat treated for maximum strength, are used in large amounts in jet engines and air frames. Titanium and its alloys are also extensively used for equipment such as reactors, heat exchangers exposed to chloride, chlorine and sulphuric acid and desalinators.

It is well recognised that the high strength and low density titanium alloys used in aerospace and hydrospace applications require palladium additions for increased stress corrosion resistance. Palladium (0.1–0.2%) has been added to naturally corrosion-resistant titanium alloys in order to increase their resistance to stress corrosion cracking,[1,2] particularly in environments such as chloride, bromide and iodide solutions, nitric acid systems and methanol - halide - water systems.

Variations in the critical levels of palladium in these alloys impart detrimental effects and analytical procedures that are simple, rapid, selective and reproducible for the determination of palladium at trace levels in the titanium matrix are of great importance for quality control.

Many wet chemical techniques such as gravimetry, titrimetry and spectrophotometry have been used[3–5] for the determination of minor and trace elements in titanium alloys. However, these conventional techniques are time consuming and generally involve complicated procedures for the separation or isolation of the element to be determined from the interfering species. Non-destructive multi-element analysis is possible by X-ray fluorescence spectrometry.[6] Although the method is simple and rapid, it requires certified standard titanium alloys as reference materials and these are often unavailable.

We have developed a direct and rapid method for the precise determination of palladium at trace levels in titanium alloys, extracting it as the Pd^{II} - 4-(2-pyridylazo)resorcinol - xylometazoline hydrochloride ion pair, the results of which are presented in this paper.

Experimental

Reagents

All reagents used were of analytical-reagent grade unless specified otherwise.

Palladium(II) stock solution. Prepared by dissolving 0.3402 g of palladium chloride (Johnson Matthey, London) in 500 ml of 0.2 M HCl. The resulting solution is standardised gravimetrically with dimethyl glyoxime.[7]

4-(2-Pyridylazo)resorcinol (PAR) stock solution, 0.01 M. Prepared by dissolving the compound (Riedel-de Haën, Hannover, FRG) crystallised twice from 1 + 1 ethanol - water in de-mineralised water. The purity is checked by spectrophotometric titrations.[8]

Xylometazoline hydrochloride [$C_4H_9C_6H_2(CH_3)_2CH_2$-$C_3H_5N_2.HCl$] *solution (XMH),* 0.01 M. Prepared from a pure sample (Fair-Deal, Bombay) and kept in an amber-coloured bottle.

Buffer solution, pH 7.6. Prepared by mixing 88.5 ml of 1/15 M sodium hydrophosphate solution with 11.5 ml of 1/15 M potassium hydrophosphate solution.

Apparatus

Absorbance measurements were made with a Systronics Model 106 MK(II) digital spectrophotometer. pH measurements were made on an Elico Model 335 expanded pH meter.

Dissolution of the Alloy

To 0.5 g of titanium alloy (containing 0.1–0.8% of palladium) placed in a 100-ml PTFE beaker, add 30 ml of 6 M hydrochloric acid and 1.0 ml of fluoroboric acid. Cover the beaker and warm slightly until the reaction ceases. Alternatively, 1.8 M sulphuric acid may be used instead of 6 M hydrochloric acid. Add concentrated nitric acid dropwise (10–20 drops) and warm until the titanium is oxidised and the solution is clear; the colour of the solution changes from purple to yellow or red - brown if an excess of palladium is present. Transfer this solution into a 100-ml calibrated flask and dilute to the mark, keeping the hydrochloric acid concentration at 2.5 M.

Extraction Procedure

Transfer an aliquot containing 5–50 μg of palladium into a 125-ml separation funnel. Add 1.0 ml of 0.01 M EDTA and neutralise the excess of acid by adding 3.0 ml of 0.1 M NaOH (ammonia solution should not be used, as it affects the formation of the palladium complex). To this mixture add 7.0 ml of pH 7.6 phosphate buffer, 2.0 ml of 0.001 M PAR and 2.0 ml of 0.01 M XMH. Equilibrate the mixture with 10.0 ml of chloroform for 1.0 min. After clear separation of the two phases, transfer the pinkish red organic layer into a 1-cm cell

* To whom correspondence should be addressed.

Table 1. Determination of palladium in some synthetic mixtures by the Pd^{II} - PAR - XMH ion-association method

Sample No.	Amounts of other metal ions added to Ti/μg g^{-1}													Palladium/ μg g^{-1}		Recovery, %
	Al	Mn	Cr	Cu	Mo	Sn	Ni	V	Mg	Zr	Fe	Nb	Ta	Added	Found	
1	250	100	0	1000	0	100	5	1000	50	50	5000	100	0	10	9.8	98.0
2	500	0	1000	250	25	500	10	500	0	0	0	250	0	15	4.9	98.0
3	0	250	5000	500	0	250	25	0	100	100	1000	500	0	50	48.0	96.0
4	1000	2000	500	0	0	0	50	250	0	0	0	0	500	20	20.3	101.5
5	2500	1000	100	0	250	0	0	0	250	0	2500	50	100	30	30.5	101.7
6	0	5000	0	1000	100	10	0	100	0	250	0	0	250	25	24.3	97.2
7	0	7500	0	0	50	0	0	0	10	500	1500	0	100	30	31.2	104.0

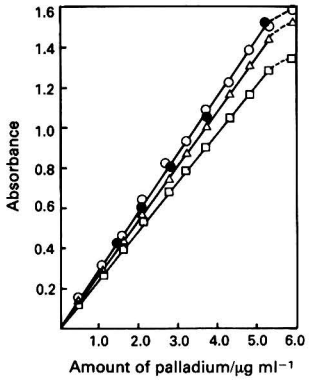

Fig. 1. Adherence of palladium(II) - PAR - XMH ion pair extracted into chloroform to Beer's law in the presence of the titanium matrix. ○, Without titanium matrix; ●, with titanium matrix (20 mg); △, with titanium matrix (40 mg); □, with titanium matrix (60 mg)

and measure the absorbance of the coloured extract at 520 nm against a chloroform blank. Determine the palladium content from the Beer's law graph constructed from different known concentrations of palladium following the same procedure.

Results and Discussion

Palladium can be extracted into chloroform as a pinkish red ion-association complex of the type Pd^{II} - PAR - XMH in the pH range 7.2–7.8 which has been proposed[9] earlier as a highly sensitive (ε = 33 400 l mol^{-1} cm^{-1}) and selective (in the presence of EDTA) spectrophotometric method for its determination.

To examine the applicability of this method to the determination of palladium in some important titanium alloys, the effect of the titanium matrix on the Beer's law behaviour (Fig. 1) of the Pd^{II} - PAR - XMH system was studied by carrying out the extraction with various additions of high-purity titanium sponge solution (2 g in 100 ml). Titanium matrix levels of up to 20 mg per 5–50 μg of palladium did not interfere in the method even though titanium hydroxide is formed in the aqueous phase. Although 40 mg of titanium matrix per 5–50 μg of palladium decreases the absorbance by 5%, the working solution suitable for titanium alloys containing 0.1–0.8% palladium can be prepared by dissolving 0.5–1.0 g of titanium alloy in 100 ml, which offers a titanium matrix in the range 5–10 mg of titanium per 5–50 μg of palladium only.

The precision was evaluated by analysing different amounts of palladium (5–50 μg) in the titanium sponge solution (20 mg per 20 ml) six times by the procedure described above, which gave values of the confidence limit with a standard deviation of 0.05 for 95% probability, indicating that this method is highly precise.

Table 2. Determination of palladium in titanium base alloys by Pd^{II} - PAR - XMH ion-association method

	Palladium found, %					
	C-349	C-350	C-353	C-354	C-357	C-358
	0.202	0.194	0.408	0.412	0.794	0.805
	0.198	0.196	0.405	0.392	0.800	0.823
	0.199	0.203	0.397	0.396	0.820	0.802
	0.206	0.205	0.406	0.410	0.815	0.814
	0.204	0.197	0.392	0.408	0.828	0.806
	0.195	0.192	0.402	0.394	0.808	0.812
Mean:	0.201	0.198	0.403	0.402	0.811	0.810
Standard deviation:	0.004	0.005	0.007	0.009	0.013	0.008
Certified value:	0.200	0.200	0.400	0.400	0.800	0.800

Standard solutions of 13 elements that are normally present in titanium alloys as alloying elements were prepared and mixed with palladium in different proportions and the palladium content was determined by the proposed method in order to establish its applicability to the determination of palladium in various titanium alloys.

Typical results obtained for the determination of palladium in the presence of various concentrations of different metal ions are given in Table 1 and show that this method can be applied directly to the precise determination of palladium in the range 5–50 μg g^{-1} in different titanium alloys.

This method has also been applied to the determination of palladium in certain titanium base alloys (Table 2), which yielded accurate results.

Conclusions

The proposed method is rapid, accurate and reasonably sensitive and selective and can be applied directly to the determination of palladium (5–50 μg g^{-1}) in titanium alloys, in contrast to other methods[10–14] which always require isolation of the element to be determined or removal of interfering species. The palladium - dimethylglyoxime method, although very selective, finds little use because of its very poor sensitivity[15] (ε = 170 l mol^{-1} cm^{-1}). The sample solutions and the standard solution can easily be prepared in the proposed method as no spectral interference is found from the titanium matrix at concentration levels of up to 20 mg of titanium per 5–50 μg of palladium.

The authors are grateful to the Ministry of Defence, Government of India, New Delhi, for their financial assistance through their Grant-in-Aid scheme and to the Director, Defence Metallurgical Research Laboratories (DMRL), Hyderabad, for the supply of analysed titanium alloy samples.

References

1. Gray, A. G., *Metall. Prog.*, 1968, **94**, 60.
2. Wood, R. A., "Review of Recent Developments in Titanium and Titanium Alloys," Batelle Memorial Institute, Defense Metals and Information Center, OH, 1968.
3. Beamish, F. E., "The Analytical Chemistry of Noble Metals," Pergamon Press, New York, 1966, p. 428.
4. Marczenko, Z., "Spectrophotometric Determination of Elements," Ellis Horwood, Chichester, 1976.
5. "ASTM Designation: E 120–71, Standard Methods for Chemical Analysis of Titanium and Titanium Base Alloys," American Society for Testing and Materials, Philadelphia, PA, 1973.
6. Matsumura, T., Kotani, N., and Goto, T., *Bunseki Kagaku,* 1970, **19**, 1393.
7. Vogel, A. I., "A Textbook of Quantitative Inorganic Analysis," Longman, London, 1968, p. 512.
8. Iwamoto, T., *Bunseki Kagaku,* 1961, **10**, 189.
9. Anjaneyulu, Y., Chandra Sekhar, K., Raviprakasa Reddy, M., and Sarma, R. N., *Mikrochim. Acta,* 1985, **III**, 23.
10. Sandell, E. B., "Textbook of Quantitative Inorganic Analysis," Third Edition, Macmillan, New York, 1952, p. 85.
11. Peshkova, V. M., Shlenskaya, V. I., and Rashevskaya, A. I., *Vestn. Mosk. Univ. Ser. Fiz. Mat. Estestv. Nauk,* 1954, **3**, 83.
12. Banks, C. V., and Smith, R. V., *Anal. Chim. Acta,* 1959, **21**, 308.
13. Pflaum, R. T., Wehking, M. W., and Jenson, R. E., *Talanta,* 1964, **11**, 1193.
14. Banerjee, S., and Dutt, R. K., *Fresenius Z. Anal. Chem.*, 1975, **277**, 379.
15. Sandell, E. B., "Textbook of Quantitative Inorganic Analysis," Third Edition, Macmillan, New York, 1952, p. 717.

Paper A6/427
Received November 11th, 1986
Accepted December 8th, 1986

Spectrophotometric Determination of Platinum(IV) with Potassium Butyl Xanthate

Nepal Singh* and Arvind K. Garg
Department of Chemistry, Hindu College, Moradabad, India

A simple, convenient and highly selective spectrophotometric method for the determination of platinum has been developed using potassium butyl xanthate. The optimum concentration range evaluated by Ringbom's method was found to be 4.87–9.75 ppm. The method of continuous variations and the molar ratio method confirmed a platinum to reagent ratio of 1 : 3 in the complex. The effect of pH, excess of reagent and foreign ions on the determination of platinum(IV) and the effect of time, temperature and the solubility of the complex with various solvents were studied.

Keywords: *Platinum(IV) determination; potassium butyl xanthate; visible spectrophotometry*

Numerous reagents[1–14] have been proposed for the determination of platinum, but most of these methods require a catalyst, pH control and/or heating, and a large number of non-platinum and platinum metals interfere in the determinations.

In this paper potassium butyl xanthate (KBX), previously used for the determination of selenium(IV),[15] is proposed as a spectrophotometric reagent for the quantitative determination of platinum(IV).

Experimental and Results

Apparatus

A Bausch and Lomb Spectronic 20 spectrophotometer was used for the absorbance measurements and a Philips PP 9040 pH meter with a glass - calomel electrode was used for the measurement of pH.

Reagent and Solutions

The potassium butyl xanthate reagent was prepared as described in reference 15. All solvents and reagents were of analytical-reagent grade.

Potassium butyl xanthate stock solution, 0.1882% *m/V*. Prepared by dissolving a known mass of the reagent in distilled water.

Chloroplatinic acid stock solution. Johnson Matthey, UK. Prepared by dissolving 1.0 g of chloroplatinic acid in 100 ml of doubly distilled water and standardising.[2] The stock solution was further diluted as required.

Acetic acid - sodium acetate buffer solution, pH 4.4.

Procedure

An aliquot of solution containing 20–88 μg of platinum(IV) was mixed with 5.0 ml of acetate buffer (pH 4.4) and 1.0 ml of potassium butyl xanthate (0.188% *m/V*) in a 25-ml glass-stoppered tube and allowed to stand for 30 min for completion of the reaction. The platinum butyl xanthate formed was shaken with 8 ml of carbon tetrachloride for 5 min. The two phases were separated and the absorbance of the organic layer was measured at the $\lambda_{max.}$ at 410 nm against a reagent blank prepared in the same way but without the addition of platinum.

* Address for correspondence: 42 Malviya Nagar, Moradabad-244001 India.

Composition of the Complex

Molar ratio method[14]

Equimolar solutions of chloroplatinic acid and the reagent of concentrations 5.0×10^{-4} and 2.5×10^{-4} M, respectively, were used. A series of solutions were prepared keeping the concentration of platinum ions constant (1 ml of 5×10^{-4} and 2.5×10^{-4} M) while varying the KBX concentration (1–8 ml of 5×10^{-4} and 2.5×10^{-4} M solutions). The pH of the solution was adjusted to 4.4 with acetate buffer. The mixture was allowed to stand for 30 min for the completion of the reaction. The platinum butyl xanthate was then extracted with 8 ml of carbon tetrachloride and the absorbance was measured at the $\lambda_{max.}$ at 410 nm against a blank obtained by the extraction of the reagent containing no platinum. A graph was plotted of absorbance *versus* amount of reagent and a break was observed where the platinum to reagent ratio was 1 : 3 (Fig. 1), although a ten-fold excess of the reagent was required for full complexation.

Jobs method of continuous variations[16,17]

Equimolar solutions of chloroplatinic acid and KBX were mixed in complementary proportions to a fixed total volume. The procedure adopted for the preparation of the solution was the same as described under *Molar ratio method*. The plot of absorbance *versus* molar fraction (M : M+R) produced a graph that indicated the formation of a complex with a platinum to reagent ratio of 1 : 3.

Effect of pH

Maximum absorbance was observed for yellow platinum butyl xanthate at pH 4.4 (Fig. 2). Vosburgh and Cooper's method[18] indicated the existence of a single complex with an absorption maximum at 410 nm at pH 4.4.

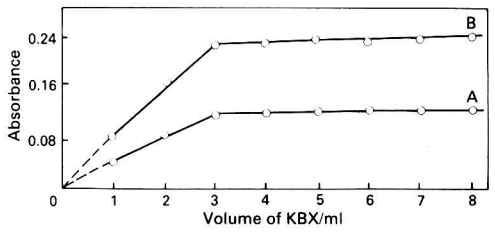

Fig. 1. Molar ratio graph for the Pt^{IV} - KBX system. A, Concentration of $Pt^{IV} = 2.5 \times 10^{-4}$ M in 1 ml of 2.5×10^{-4} M KBX solution; and B, concentration of $Pt^{IV} = 5 \times 10^{-4}$ M in 1 ml of 5×10^{-4} M KBX solution

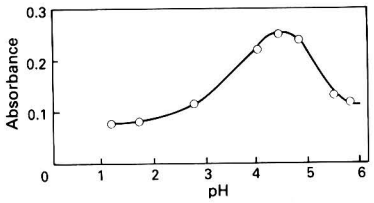

Fig. 2. Effect of pH on Pt^{IV} - KBX system

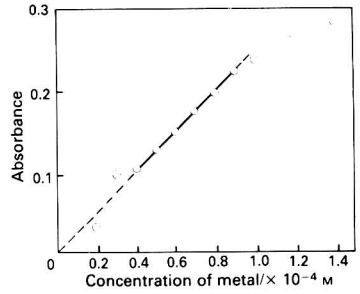

Fig. 3. Graph of Pt^{IV} concentration *versus* absorbance

Choice of Solvents

The nature of yellow platinum butyl xanthate was studied in carbon tetrachloride, chloroform, benzene,1,4-dioxane, pyridine, methanol, ethanol, butan-1-ol, decalin, diethyl ether and acetone solvents and it was observed that platinum butyl xanthate was soluble in all of these solvents, but only dissolved slowly in methanol. The haziness that appeared after 2 min with acetone is possibly due to the composition of the complex.

Linearity and Sensitivity

Under the experimental conditions described, it was observed that Beer's law was obeyed between 4.87 and 10.96 p.p.m. of platinum (Fig. 3). The molar absorptivity calculated from Beer's law was 4.002×10^3 l mol^{-1} cm^{-1} at 410 nm and the Sandell's sensitivity[19] of the colour reaction was 0.04875 μg cm^{-2}. The optimum concentration for the effective spectrophotometric determination of platinum(IV) evaluated by Ringbom's method[20,21] was found to be between 4.87 and 9.75 p.p.m.

Effect of Foreign Ions

The interference of several cations and anions with 10.968 p.p.m. of platinum(IV) was investigated. The interference of Fe^{III}, Ni^{II}, Co^{II}, chromate and molybdate ions could be avoided by using a mixture of EDTA and tartrate (1 : 1 molar ratio). Hg^{II} interfered seriously. Fe^{II}, Sn^{II}, Pb^{II} and Zn^{II} complexed with KBX but were not extracted with carbon tetrachloride and therefore did not interfere with the determination of platinum(IV).

The effect of foreign ions and the concentrations at which they interfered are shown in Table 1.

Table 1. Effect of foreign ions on the determination of platinum(IV) with KBX. The amount of platinum(IV) in each solution was 10.968 p.p.m.

Foreign ion	Amount added, p.p.m.	Platinum(IV) found, p.p.m.	Error,%
Fe^{III}	7.0	10.968	Nil
Co^{II}	7.94	10.858	−1.0
Ni^{II}	6.0	11.077	+1.0
Mg^{II}	6.0	10.968	Nil
As^{III}	37.5	10.86	−0.98
Ba^{II}	17.0	10.968	Nil
Sn^{II}	10.0	10.968	Nil
Pb^{II}	10.0	10.86	−0.98
Zn^{II}	16.0	10.968	Nil
V^{IV}	8.0	11.077	+1.0
V^{V}	8.0	10.968	Nil
Ca^{II}	16.0	10.86	−0.98
Ti^{IV}	16.0	10.968	Nil
Fe^{II}	25.0	11.077	+1.0
PO_4^{3-}	52.0	10.858	−1.0
NO_2^-	57.5	11.077	+1.0
Cl^-	50.0	10.968	Nil
Br^-	50.0	10.968	Nil
I^-	110.0	10.968	Nil
CN^-	150.0	11.077	+1.0
CH_3COO^-	150.0	10.968	Nil
SO_4^{2-}	50.0	10.968	Nil
MoO_4^{2-}	48.0	10.858	−1.0
CrO_4^{2-}	42.0	10.968	Nil
EDTA	121.0	10.86	−0.98
Citrate	5.0	10.86	−0.98

Discussion

When the complex was subject to paper chromatography in different organic solvents (benzene, diethyl ether, chloroform, ethyl acetate and 1,4-dioxane), only a single spot was developed on the paper, indicating the formation of only one complex. The colour of the spot remained unchanged in different solvents, but after about 4 h the colour of the spot on the paper became brown. Potassium butyl xanthate therefore forms a yellow complex with platinum(IV) in a weak acidic medium. The formation of the complex between platinum and KBX is complete within 30 min at 28 ± 1 °C, the temperature at which the determination was carried out. The absorbance of the complex in carbon tetrachloride remained stable up to 2.45 h and thereafter the absorbance changed slightly. The extracted complex was found to be stable in carbon tetrachloride up to 60 °C when it was heated for 1 min. After 1 min the absorbance decreased, possibly owing to the decomposition of the complex. At room temperature the extracted complex showed a constant absorbance for 2 h, after which the absorbance decreased slightly. The complex showed a greater stability in carbon tetrachloride, chloroform, pyridine, diethyl ether and benzene than in the other solvents in which the complex was found to be soluble. Carbon tetrachloride was chosen for all further studies as diethyl ether is highly volatile and pyridine has a higher cut-off point than carbon tetrachloride. Although the complex has a slightly stronger absorbance in chloroform that in carbon tetrachloride, $\lambda_{max.}$ is at a shorter wavelength in chloroform than in carbon tetrachloride (400 nm in $CHCl_3$, 410 nm in CCl_4). Foreign ions have a minimum interference in carbon tetrachloride. It may be concluded that the proposed methods are simple and sensitive and that no catalyst is required for the determination of platinum(IV) at room temperature.

References

1. Rakovskii, E. E., and Rabinovich, B. S., *Izv. Sib. Otd. Akad. Nauk SSSR, Ser. Khim. Nauk*, 1970, **9**, 498; *Anal. Abstr.*, 1971, **21**, 3423. .
2. Sandhwani, S. K., and Singh, P. R., *Talanta*, 1973, **20**, 248.
3. Gangopadhyay, P. K., Das, H. R., and Shome, S. C., *Anal. Chim. Acta*, 1973, **66**, 460.
4. Paria, P. K., and Majumdar, S. K., *Zh. Anal. Khim.*, 1976, **279**, 207.
5. Sankegowda, H., and Padmaji, K. A., *J. Indian Chem. Soc.*, 1979, **26**, 568.

6. Sankegowda, H., and Jagadeesh, K. S., *Microchim. Acta*, 1979, **1**, 183.
7. Sankegowda, H., and Jagadeesh, K. S., *Talanta*, 1978, **25**, 416.
8. Sankegowda, H., and Padmaji, K. A., *Fresenius Z. Anal. Chem.*, 1979, **295**, 413.
9. Bhoon, Y. K., Pandey, K. B., and Singh, P. R., *Chimica.*, 1974, **28**, 659; *Chem. Abstr.*, 1975, **82**, 51017.
10. Piercy, F. E., and Ryan, D. E., *Can. J. Chem.*, 1963, **41**, 667.
11. Marczenko, Z., and Kalinowski, K., *Anal. Chim. Acta*, 1983, **153**, 219.
12. Jaya, S., Prasada Rao, T., and Ramakrishna, T. V., *Analyst*, 1984, **109**, 1405.
13. Jayorama, D'souza, M. V., Yathirajan, H. S., and Ranjaswami, *Indian J. Chem.*, 1985, **24A**, 987.
14. Khan, H. M., *J. Chem. Soc. Pak.*, 1985, **7**, 129.
15. Singh, N., and Garg, A. K., *Analyst*, 1986, **111**, 247.
16. Job, P., *Am. Chem.*, 1928, **9**, 113.
17. Irving, H., and Pierce, T. B., *J. Chem. Soc.*, 1959, **5**, 256.
18. Vosburgh, W. C., and Cooper, G. R., *J. Am. Chem. Soc.*, 1941, **63**, 437.
19. Sandell, E. B., "Colorimetric Determination of Traces of Metals," Interscience, New York, 1959.
20. Ringbom, A., *Z. Anal. Chem.*, 1939, **115**, 332.
21. Ayres, G. H., *Anal. Chem.*, 1949, **21**, 652.

Paper A5/266
Received July 18th, 1985
Accepted August 14th, 1986

Determination of Nitrazepam and Flunitrazepam by Flow Injection Analysis Using a Voltammetric Detector

Elisa Ruiz, Manuel Hernández Blanco, Encarna Lorenzo Abad and Lucas Hernández*
Department of Analytical Chemistry, Faculty of Sciences, Autonomous University of Madrid, 28049 Madrid, Spain

Nitrazepam and flunitrazepam were determined by flow injection analysis using a glassy carbon electrode as a voltammetric detector. The sample solution (200 μl, 5.6–28.1 μg ml^{-1} and 6.3–31.3 μg ml^{-1} for nitrazepam and flunitrazepam, respectively) was injected into the carrier stream, which was a 0.1 M phosphate buffer solution (pH 7.0) containing 10% *V/V* of methanol. Nitrazepam and flunitrazepam were determined by reduction at the glassy carbon electrode; a 70 cm delay coil (0.58 mm i.d.) was incorporated before the detector and a flow-rate of 4 ml min^{-1} was used. The system was applied to the determination of 5 and 2 mg of nitrazepam and flunitrazepam, respectively, giving concentrations of 5.1 ± 0.25 and 1.9 ± 0.08 mg (n = 5).

Keywords: *Flow injection analysis; voltammetry; nitrazepam; flunitrazepam; drugs*

Numerous papers have been published on the determination of 1,4-benzodiazepines by polarography or voltammetry and the electrochemistry of compounds containing the azomethine group has been investigated at a dropping mercury electrode (DME) by several workers.[1–4] However, except for one method for the on-line determination of nitrazepam by direct reduction at a mercury-coated solid electrode,[5] little work has been carried out on the determination of 1,4-benzodiazepines by flow injection analysis (FIA) with electrochemical detection using the reduction that takes place at several different electrodes (*e.g.*, a DME, hanging mercury drop electode or a glassy carbon electrode), in spite of the high sample throughput and reduction in the volumes of reagents used that can be achieved.

Dropping mercury,[6,7] sessile mercury drop[8] and glassy carbon[9] electrodes have been used in FIA for the determination of various other organic compounds by using wall-jet type cells. Carbon electrodes have a wider potential range than mercury electrodes and can be used to determine compounds by either oxidation or reduction processes, the latter being applicable to compounds such as 1,4-benzodiazepines.

In this paper an FIA method is described for the determination of nitrazepam and flunitrazepam using an electrochemical detector based on a glassy carbon working electrode. This system has been used to determine nitrazepam and flunitrazepam in tablets.

Experimental

Apparatus

The arrangement of the apparatus used for flow injection analysis is shown in Fig. 1.

The carrier stream was pumped by the pump (B) (Watson Marlow 202 U/1 peristaltic pump) through the detector (D) and the stream was then discharged to waste. The sample was introduced into the carrier stream at M by a six-way injection valve (Rheodyne Type 50) and was transported as a plug by suitable lengths of 0.58 and 0.71 mm i.d. tubing to the detector (a Metrohm 656 detector with a Metrohm EA-1096 flow-through wall-jet cell). The working electrode was glassy carbon and the reference electrode was a silver - silver chloride electrode containing 3 M KCl. The auxiliary electrode was gold. The potential of the glassy carbon electrode was held at −0.9 V and the currents were monitored with a Metrohm 641 VA potentiostat and recorded on a Lineseis L-6512 y - t recorder (R).

Reagents

All reagents were of analytical-reagent grade and de-ionised water was obtained from Milli-Q and Milli-R systems (Millipore). The carrier stream was a 0.1 M phosphate buffer solution (pH 7.0) containing 10% *V/V* methanol to aid the dissolution of adsorbed electrochemical reaction products from the working electrode.

Nitrazepam and flunitrazepam were obtained from Productos Roche in both pure and tablet form.

Stock nitrazepam and flunitrazepam solutions (1.0×10^{-3} M) were prepared by dissolving the required amount of pure compound in absolute methanol. Less concentrated solutions were obtained by dilution of these stock solutions with the phosphate buffer (pH 7.0).

Procedure

The carrier stream, bubbled through with inert gas to remove oxygen, was first pumped through the electrochemical cell. When a steady background current was obtained, the analyte solution (also oxygen free) was introduced and the change in current recorded. When high currents were used a steady background current was obtained immediately, whereas for low ranges a period of 2–10 min was required to achieve steady values.

The samples contained 10% *V/V* of methanol in order to keep the compounds in solution.

The glassy carbon electrode was cleaned daily or as required with methanol on a polishing cloth followed by rinsing with de-ionised water.

Results and Discussion

Optimisation of Variables

The hydrodynamic d.c. voltammograms obtained in different carrier solutions (including acetate, Britton - Robinson and phosphate buffers) were compared and the best results were obtained in a 0.1 M phosphate buffer solution (pH 7.0). Under

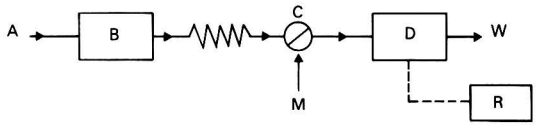

Fig. 1. Arrangement for voltammetric FIA. A = Carrier stream; B = peristaltic pump; C = injection valve; D = electrochemical detector; R = recorder; M = sample; W = waste

* To whom correspondence should be addressed.

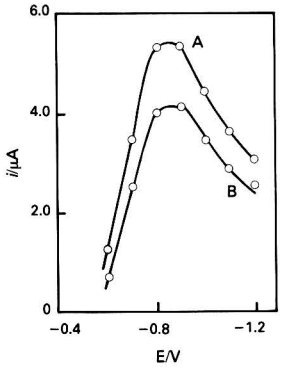

Fig. 2. Peak current as a function of working electrode potential. Mobile phase, 0.1 M phosphate buffer (pH 7.0) containing 10% *V/V* of methanol at a flow-rate of 4.0 ml min^{-1}; peak currents obtained by injection of 200 μl of (A) 1.0×10^{-4} M flunitrazepam and (B) 1.0×10^{-4} M nitrazepam

these conditions the voltammograms showed a current maximum around −0.9 V (Fig. 2).

The peak height and peak width in flow systems depend on the dispersion of the sample plug during its passage from the point of injection to the detector. Variables such as injection volume, coil length and flow-rate, which influence the dispersion of the sample, were adjusted according to the specific requirements of this system. The peak height and thus the sensitivity increased with increasing injection volume in the range 50–200 μl (Fig. 3), but decreased for coil lengths of 70 cm and above. The pumping rate was found to affect both peak width and height, the peak height reaching a maximum at a flow-rate of 4 ml min^{-1}, and the peak width, measured in seconds (Fig. 4), decreased with increasing flow-rate.

The combination of an injection volume of 200 μl with a coil length of 70 cm and a flow-rate of 4 ml min^{-1} was considered to be appropriate for routine work. Using this system the current reached its base-line value about 30 s after injection, allowing a maximum sampling frequency of about 100 samples per hour.

Determination of Nitrazepam and Flunitrazepam

The relationship between the current and the amount of analyte injected is shown in Fig. 5(*a*) and (*b*). This relationship is linear between 5.6 and 28.1 μg ml^{-1} for nitrazepam and between 6.3 and 31.3 μg ml^{-1} for flunitrazepam.

The detection and determination limits (three and ten times the standard deviation of the background noise[10]) were about 1.8 and 4.0 μg ml^{-1} for nitrazepam and 1.3 and 3.6 μg ml^{-1} for flunitrazepam. The accuracy and precision of the method were evaluated from ten determinations at each of four different concentrations of the drugs and the relative errors and relative standards deviations were −2.3 and 1.3% for nitrazepam and −1.8 and 1.2% for flunitrazepam.

The proposed voltammetric FIA method was tested by analysing a tablet formulation of nitrazepam and flunitrazepam. The sample was dissolved in 20 ml of methanol, stirring the solution for about 30 min. The insoluble constituents were decanted and an appropriate amount of the resulting solution was diluted to 25 ml with 0.1 M phosphate buffer (pH 7.0), keeping the concentration of methanol at 10%. The concentrations of nitrazepam and flunitrazepam were then determinated by the standard additions method and the results obtained are given in Table 1. It can be seen that there is good agreement between the results obtained by differential-pulse polarography and those obtained by the proposed method. The proposed FIA method has the advantage of a high sample throughput.

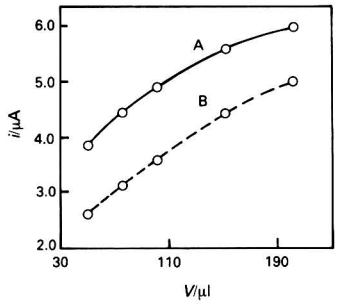

Fig. 3. Influence of injection volume on peak current for (A) 1.0×10^{-4} M flunitrazepam and (B) 1.0×10^{-4} M nitrazepam. The carrier stream was 0.1 M phosphate buffer containing 10% *V/V* of methanol at a flow-rate of 4.0 ml min^{-1}. Glassy carbon electrode held at −0.9 V

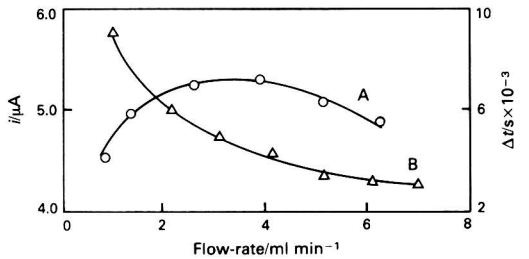

Fig. 4. Influence of flow-rate on (A) peak current and (B) peak width, measured in seconds. The carrier stream was 0.1 M phosphate buffer (pH 7.0) containing 10% *V/V* of methanol. Samples were 200 μl of 1.0×10^{-4} M nitrazepam

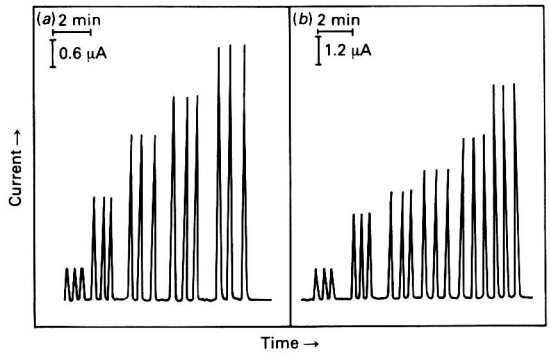

Fig. 5 (*a*) Calibration for nitrazepam by continuous flow monitoring of current at a fixed potential of −0.9 V for the concentration range 5.6–28.1 μg ml^{-1} (5.6, 11.3, 16.9, 22.5 and 28.1 μg ml^{-1}). Mobile phase, phosphate buffer (pH 7.0) containing 10% *V/V* of methanol at a flow-rate of 4.0 ml min^{-1}; injection volume, 200 μl. (*b*) Calibration for flunitrazepam by continuous flow monitoring of current at a fixed potential of −0.9 V for the concentration range 6.3–31.3 μg ml^{-1} (6.3, 12.5, 16.3, 18.8, 25.1 and 31.3 μg ml^{-1}). Other conditions as in (*a*)

Table 1. Comparison of results obtained for the determination of nitrazepam and flunitrazepam by the proposed FIA method and differential-pulse polarography (DPP). Working potential −0.9 V

Compound	Amount present/mg	Amount found/mg* FIA	DPP
Nitrazepam . .	5	5.1 ± 0.25	5.1
Flunitrazepam . .	2	1.9 ± 0.08	2.1

* Average obtained from five determinations.

The authors thank CAICyT for economic support grant No. 2077/83.

References

1. Senkowski, B. Z., Levin, M. S., Urbigkit, J. R., and Wollish, E. G., *Anal. Chem.*, 1964, **36**, 1991.
2. Oelschlager, H., Volke, J., and Lim, G. T., *Arch. Pharm. Ber. Dtsch. Pharm. Ges.*, 1969, **302**, 241.
3. Halvorsen, S., and Jacobsen, E., *Anal. Chim. Acta*, 1972, **59**, 127.
4. Clifford, J. M., and Smyth, F. W., *Fresenius Z. Anal. Chem.*, 1973, **264**, 149.
5. Ivaska, A., and Smyth, W. F., *Anal. Chim. Acta*, 1980, **114**, 283.
6. Alexander, P. W., and Shah, M. H., *Talanta*, 1979, **26**, 97.
7. Michel, L., and Zatka, A., *Anal. Chim. Acta*, 1979, **109**, 105.
8. Fogg, A. G., Summan, A. M., and Fernandez-Arciniega, M. A., *Analyst*, 1985, **110**, 341.
9. Fogg, A. G., Chamsi, A. Y., and Abdalla, M. A., *Analyst*, 1983, **108**, 464.
10. IUPAC, "Appendices of Tentative Nomenclature, Symbols, Units and Standards. II. Terms and Symbols Related to Analytical Functions and their Figures of Merit," No. 28, Pergamon Press, Oxford, 1972.

Paper A6/373
Received October 6th, 1986
Accepted October 31st, 1986

Determination of Sodium *N*-Methyldithiocarbamate (Metham Sodium) and Methyl Isothiocyanate in Aqueous Samples by High-performance Liquid Chromatography Using a Micellar Mobile Phase

Frank G. P. Mullins* and (the late) Gordon F. Kirkbright
Department of Instrumentation and Analytical Science, University of Manchester Institute of Science and Technology, P.O. Box 88, Manchester M60 1QD, UK

A high-performance liquid chromatographic procedure was developed for the simultaneous determination of the fungicides sodium *N*-methyldithiocarbamate and methyl isothiocyanate. These fungicides were separated on a reversed-phase octadecyl bonded column with micellar hexadecyltrimethylammonium bromide in an eluent of methanol - water (50 + 50 *V/V*) buffered to pH 6.8 (10 mM phosphate). Detection was carried out at 247 nm with a UV detector. Recoveries of standards added to pond water and untreated sewage were >92% and >88%, respectively, for both fungicides. The detection limits for sodium *N*-methyldithiocarbamate and methyl isothiocyanate are 70 μg dm^{-3} (p.p.b.) and 1 μg dm^{-3} (p.p.b.), respectively.

Keywords; *Micellar chromatography; sodium N-methyldithiocarbamate; methyl isothiocyanate; high-performance liquid chromatography*

Sodium *N*-methyldithiocarbamate is a soil fungicide, nematicide and herbicide with a fumigant action, applied at rates of approximately 3.88 × 10^3 mol $hectare^{-1}$ of soil surface. Its activity is thought to be due to its breakdown product, methyl isothiocyanate. It is phytotoxic and the planting of treated soil must be delayed until decomposition is complete. Methyl isothiocyanate is also applied to soil as a fumigant at the rate of 25 g m^{-2}, and decomposition occurs in about 3 weeks at a soil temperature of 12 °C.[1]

Earlier methods for the determination of these fungicides were relatively involved. Sodium *N*-methyldithiocarbamate is very polar, soluble in water (722 g l^{-1} at 20 °C), thermally unstable and pH-sensitive.[2] Techniques for the analysis of dithiocarbamate salts have been described elsewhere.[3-6] However, they are susceptible to interferences and require careful sample clean-up procedures prior to derivatisation before accurate and reproducible results may be obtained. There are two recommended methods for methyl isothiocyanate determination.[1] The first involves potentiometric titration. The second is a more specific and quantitative method involving the determination of methyl isothiocyanate by gas chromatography (GC) after extraction with a mixture of diethyl ether and 5% ethanol.[1] The GC method is susceptible to interferences. Crop materials containing a high level of organic sulphides and disulphides can lead to high blank values.

A new and inexpensive HPLC procedure is described here for the simultaneous determination of sodium *N*-methyldithiocarbamate and methyl isothiocyanate using a buffered mobile phase containing micellar hexadecyltrimethylammonium bromide (CTAB). This procedure permits the quantitative separation and determination of these fungicides in the low μg dm^{-3} (p.p.b.) range in pond water and untreated sewage effluent after standard additions of the fungicides.

Experimental

Apparatus

A Waters Associates M6000A pump equipped with a Rheodyne 7125 valve injector (20-μl loop) connected to a Waters Lambda Max variable-wavelength UV detector was used in conjunction with a 250 × 5 mm i.d., 5-μm particle size Spherisorb ODS column (Phase Separations, Queensferry, UK). Retention times and peak areas were measured using a recording integrator (Hewlett-Packard, Model 3390A).

Reagents

Inorganic salts. Potassium dihydrogen orthophosphate was of AnalaR grade, supplied by BDH Chemicals, Poole, UK. Disodium hydrogen orthophosphate was of analytical-reagent grade, supplied by Fisons Scientific Apparatus, Loughborough, UK.

Hexadecyltrimethylammonium bromide (CTAB). AnalaR grade, obtained from BDH Chemicals.

Methanol. HPLC grade, supplied by Rathburn Chemicals, Walkerburn, UK.

De-ionised water. Distilled from glass and further de-ionised using a Waters I de-ioniser (Gelman Sciences, USA).

Procedure

Mobile phases were prepared by adding the appropriate amount of surfactant to a water - methanol mixture (50 + 50 *V/V*) buffered to pH 6.8 (10 mM phosphate); these were filtered using a 0.22 μm filter (Duropore, Millipore). The column was conditioned by passage of the mobile phase for 90 min at a flow-rate of 1 ml min^{-1}. The mobile phase and the column were thermostated at 298 K by immersion in a water-bath (Gallenkamp). Efficiencies of up to 30 000 theoretical plates per metre for methyl isothiocyanate were obtained using this micellar mobile phase.

Table 1. Retention times and detection limits for sodium *N*-methyldithiocarbamate and methyl isothiocyanate. Conditions as for Fig. 1(*a*)

Analyte	Capacity factor	Detection limit*/ μg dm^{-3} (p.p.b.)
Methyl isothiocyanate	2.30	1
Sodium *N*-methyldithiocarbamate	7.44	70

* Signal to noise ratio = 3.

* Present address: Medeval Ltd., University of Manchester, Coupland III Building, Oxford Road, Manchester M13 9PL, UK.

Results and Discussion

Charged surfactants have been widely used as mobile phase modifiers to improve the partitioning characteristics of charged solutes in reversed-phase HPLC. Knox and Laird[7] showed that the use of CTAB proved remarkably effective for the resolution of sulphonic acids. Other workers[8-11] have described the use of micellar mobile phases and discussed their separating ability. We have reported[12] the separation of dithiocarbamate salts by HPLC using a buffered eluent containing micellar CTAB. A micellar mobile phase allows the separation of charged and uncharged solutes simultaneously. Fig. 1(*a*) illustrates a separation of sodium *N*-methyldithiocarbamate and methyl isothiocyanate following standard additions of these fungicides to pond water. The separation was achieved in 16 min using buffered (10 mM phosphate) methanol - water (50 + 50 *V/V*) as the mobile phase. Pond water was used initially to assess the potential of micellar chromatography for the determination of these fungicides in environmental samples. Phenol was used as an internal standard. The blank reading, Fig. 1(*b*), at 247 nm illustrates some interference at the void volume but this does not pose a problem. Standard additions of these fungicides to untreated sewage with subsequent analysis by HPLC is illustrated in Fig. 2(*a*). The blank reading is also included in Fig. 2(*b*). The retention times and detection limits are presented in Table 1. The limit of detection for methyl isothiocyanate is lower than previously reported.[1] Recoveries from pond water and untreated sewage effluent following standard additions of the fungicides are presented in Table 2.

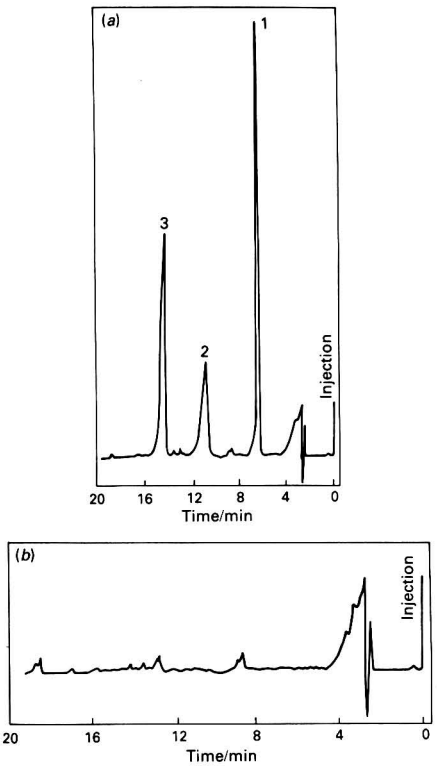

Fig. 1.(*a*) Micellar chromatogram of sodium *N*-methyldithiocarbamate and methyl isothiocyanate in pond water. Packing, octadecyl bonded silica (Spherisorb ODS); column, 250 × 5 mm i.d., 5 μm particle size; solvent, 50 + 50 *V/V* MeOH - H_2O containing 1×10^{-2} M CTAB buffered to pH 6.8 (10 mM phosphate); detection, UV at 247 nm (0.01 a.u.f.s.); flow-rate, 1.4 ml min^{-1}; pressure drop, 1800 lb in^{-2}; sample, (1) methyl isothiocyanate (10 mg dm^{-3}), (2) phenol (internal standard) (15 mg dm^{-3}), (3) sodium *N*-methyldithiocarbamate (10 mg dm^{-3}); injection volume, 20 μl. (*b*) Micellar chromatogram of pond water sample (prior to standard additions of the fungicides). Conditions as in (*a*)

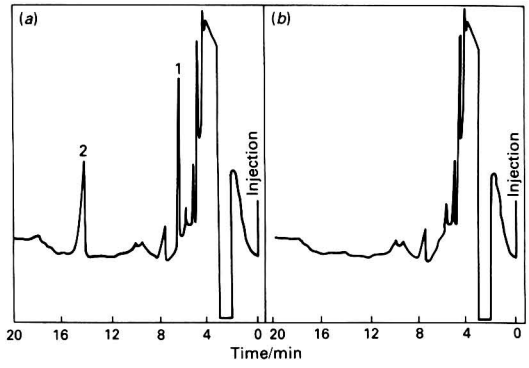

Fig. 2. (*a*) Micellar chromatogram of sodium *N*-methyldithiocarbamate and methyl isothiocyanate in untreated sewage effluent. Conditions as in Fig. 1(*a*). Solute, (1) methyl isothiocyanate (0.2 mg dm^{-3}), (2) sodium *N*-methyldithiocarbamate (0.2 mg dm^{-3}); injection volume, 200 μl; detection, UV at 247 nm (0.002 a.u.f.s.). (*b*) Micellar chromatogram of untreated sewage effluent (prior to standard additions of the fungicides). Conditions as in Fig. 1(*a*)

Table 2. Recovery of sodium *N*-methyldithiocarbamate and methyl isothiocyanate from pond water and untreated sewage effluent

	Standard additions to pond water			
Analyte	Concentration	Replicates	Average recovery, %	Relative standard deviation, %
Methyl isothiocyanate	237.0 μg dm^{-3}	7	93	0.14
	237.0 mg dm^{-3}	7	97	0.17
Sodium *N*-methyldithiocarbamate	0.7 mg dm^{-3}	7	102	0.12
	1.0 mg dm^{-3}	7	95	0.16
	Standard additions to untreated sewage effluent			
	Concentration	Replicates	Average recovery, %	Relative standard deviation, %
Methyl isothiocyanate	200.0 μg dm^{-3}	7	102	0.10
	200.0 mg dm^{-3}	7	104	0.12
Sodium *N*-methyldithiocarbamate	0.7 mg dm^{-3}	7	89	0.16
	1.0 mg dm^{-3}	7	91	0.11

The calibration graphs obtained for both sodium *N*-methyldithiocarbamate and methyl isothiocyanate were linear for injected masses between 100 μg and 200 ng (correlation coefficient, 0.997) for sodium *N*-methyldithiocarbamate, and 100 μg and 20 ng (correlation coefficient, 0.998) for methyl isothiocyanate.

This procedure permits the analyst to monitor the decomposition of sodium *N*-methyldithiocarbamate to methyl isothiocyanate by HPLC without the need to employ two different techniques.

We are grateful to Thames Water Authority for support of this work and partial funding.

References

1. Ottnad, M., Jenny, N. A., and Roder, C. H., *in* Zweig, G., and Sherma, J., *Editors*, "Analytical Methods for Pesticides and Plant Growth Regulators," Academic Press, New York, 1978, Volume 10, p. 563.
2. Joris, S. J., Aspila, K. I., and Chakrabarti, C. L., *Anal. Chem.*, 1969, **41**, 1441.
3. Newsome, W. H., *in* Zweig, G., and Sherma, J., *Editors*, "Analytical Methods for Pesticides and Plant Growth Regulators," Academic Press, New York, 1980, Volume 11, p. 197.
4. Raizman, P., and Thompson, Q. E., *in* Karchmer, J. H., *Editor*, "The Analytical Chemistry of Sulfur and its Compounds," Wiley–Interscience, New York, 1972, Part II, p. 491.
5. Ripley, B. D., Cos, D. F., Wieke, J., and Frank, R., *J. Agric. Food Chem.*, 1978, **26**, 134.
6. Keppel, G. E., *J. Assoc. Off. Anal. Chem.*, 1969, **52**, 162.
7. Knox, J. G., and Laird, G. R., *J. Chromatogr.*, 1976, **122**, 17.
8. Weinberger, R., Yarmchuck, P., and Cline Love, L. J., *Anal. Chem.*, 1982, **54**, 1552.
9. Yarmchuck, P., Weinburger, R., Hirsch, R. F., and Cline Love, L. J., *Anal. Chem.*, 1982, **54**, 2233.
10. Armstrong, D. W., and Nome, F., *Anal. Chem.*, 1981, **53**, 1662.
11. Armstrong, D. W., and Stine, G. Y., *J. Am. Chem. Soc.*, 1983, **105**, 2962.
12. Kirkbright, G. F., and Mullins, F. G. P., *Analyst*, 1984, **109**, 493.

Paper A6/28
Received January 31st, 1986
Accepted November 28th, 1986

Rapid Titrimetric Method for the Determination of Captan and Folpet in Fungicide Formulations

Balbir C. Verma, Narendra K. Sharma, Miss Anila Sud, Hari K. Thakur and Devender K. Sharma
Department of Chemistry, Himachal Pradesh University, Summer Hill, Shimla-171005, India

A simple, rapid titrimetric method for the determination of captan and folpet based on their reduction with potassium trithiocarbonate is described. The compounds in dimethylformamide - water are titrated with the reagent and the end-point determined by the appearance of a yellow colour (the reagent acting as a self indicator) or potentiometrically. The method has been successfully applied to the determination of captan and folpet in commercial formulations.

Keywords: *Captan determination; folpet determination; potassium trithiocarbonate; titrimetry; fungicide formulations*

Captan [*N*-(trichloromethylthio)-3a,4,7,7a-tetrahydrophthalimide] and folpet [*N*-(trichloromethylthio)phthalimide)] have found a variety of applications in agriculture as fungicides. They are recommended both as disinfectants and protectants

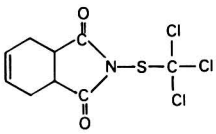

Captan

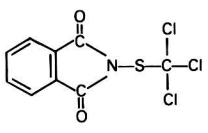

Folpet

of grains. The chemical method commonly employed for their determination in formulations involves a selective hydrolysis followed by the determination of halide.[1] This method is based on the differential rate of hydrolysis of the parent compound *versus* chloride-containing impurities derived from trichloromethanethiol. The thiol and other impurities derived from these chemicals hydrolyse very rapidly in acetone - methanol solution to yield chloride ions. The total chloride content is then determined by hydrolysis with sodium hydroxide solution. The difference between the total amount of chloride ion and impurity chloride ion present is calculated to give the concentration of pure captan or folpet. The method is tedious, time consuming and requires strict control of the experimental conditions. Also, the determination cannot be conducted with a single portion of the test solution; two similar aliquots are required.

A simple, rapid, accurate and reliable titrimetric method has been developed for the determination of captan and folpet at macro and semimicro levels and this has subsequently been adapted to the determination of these agrochemicals in pesticide formulations. The method is based on the reductive determination of these agrochemicals with potassium trithiocarbonate. The method consists in titrating each agrochemical in dimethylformamide - water with potassium trithiocarbonate. The end-point can be detected visually by the appearance of a yellow colour or potentiometrically. The most obvious property of the reagent is its bright yellow colour. This means that it is self-indicating in visual titrations. Although the visual end-point is adequate for most purposes, the potentiometric method is useful when the sample solution itself is coloured.

Experimental

Reagents

Dimethylformamide. Obtained from BDH Chemicals and purified by storing over anhydrous analytical-reagent grade sodium carbonate for 2 d. The solvent was decanted and distilled, and the fraction distilling at 148.5–149.5 °C was collected in coloured bottles.

Potassium trithiocarbonate solution. Prepared and standardised as described previously.[2]

Captan and folpet. Standards were supplied by the Environmental Protection Agency, NC, USA.

Apparatus

The potentiometric titrations were performed with a Toshniwal (India) Type CLO6A potentiometer equipped with a platinum - saturated calomel electrode assembly.

Procedure

Determination of captan and folpet

Aliquots (0.2–2.0 ml) of a dimethylformamide solution of each pure compound were placed into titration vessels and the volumes were diluted to 25 ml with dimethylformamide. Each solution was mixed with 25 ml of water and titrated at room temperature (*ca.* 25 °C) with both visual and potentiometric end-point detection. In the visual titrations the end-point was detected by the appearance of the yellow colour imparted to the solution by the first excess drop of reagent added. The initial stages of the titrations were characterised by the appearance and immediate disappearance of a light pink colour. The solution was, however, colourless before the end-point, which is extremely sharp. In the potentiometric titrations, a sharp drop in potential was observed at the end-point. The results obtained are given in Tables 1 and 2.

Table 1. Determination of captan with potassium trithiocarbonate

	Captan found*/mg		
	This method		
Captan taken/mg	Visual method	Potentiometric method	Hydrolysis method[1]
3.00	2.98 ± 0.019	3.01 ± 0.017	3.03 ± 0.041
6.00	6.04 ± 0.037	5.98 ± 0.035	6.05 ± 0.072
9.00	8.96 ± 0.053	9.04 ± 0.048	8.90 ± 0.092
12.00	11.92 ± 0.057	12.05 ± 0.050	12.10 ± 0.089

* Mean of ten determinations ± standard deviation.

Table 2. Determination of folpet with potassium trithiocarbonate

	Folpet found*/mg		
	This method		
Folpet taken/mg	Visual method	Potentiometric method	Hydrolysis method[1]
2.50	2.49 ± 0.018	2.50 ± 0.016	2.53 ± 0.035
5.00	5.04 ± 0.032	4.97 ± 0.030	4.93 ± 0.073
7.50	6.47 ± 0.038	7.53 ± 0.037	7.60 ± 0.074
9.00	9.04 ± 0.050	8.96 ± 0.048	9.10 ± 0.088

* Mean of ten determinations ± standard deviation.

Table 3. Determination of captan and folpet in some commercial formulations

Fungicide formulation	Active ingredient, %	Amount taken/mg	Amount found*/mg: This work: Visual method	Recovery, %	Potentiometric method	Recovery, %	Hydrolysis method[1]	Recovery, %
Captan	75	4.00	3.95	98.8 ± 0.34	3.96	99.0 ± 0.28	3.96	99.0 ± 0.30
		16.00	15.84	99.0 ± 0.32	15.88	99.3 ± 0.25	15.85	99.1 ± 0.28
	75	4.00	3.96	99.0 ± 0.28	3.97	99.3 ± 0.32	3.95	98.8 ± 0.36
		16.00	15.86	99.1 ± 0.30	15.88	99.3 ± 0.28	15.86	99.1 ± 0.32
	50	6.00	5.93	98.8 ± 0.32	5.94	99.0 ± 0.26	5.94	99.0 ± 0.32
		24.00	23.80	99.2 ± 0.26	23.86	99.4 ± 0.22	23.82	99.3 ± 0.28
Folpet (Phaltan) . .	50	5.00	4.95	99.0 ± 0.28	4.94	98.8 ± 0.28	4.95	99.0 ± 0.32
		18.00	17.84	99.1 ± 0.26	17.90	99.4 ± 0.25	17.84	99.1 ± 0.30

* Mean of ten determinations ± standard deviation.

Formulation analysis

Three captan formulations (two containing 75% active ingredient each and one containing 50% active ingredient) and one folpet formulation (containing 50% active ingredient), all wettable powders, were used. A single large sample of each formulation was weighed, shaken with dimethylformamide and filtered. The residue was washed 2–3 times with dimethylformamide. The filtrate and washings were diluted to a known volume with the same solvent. Aliquots were then placed in titration vessels for the determination. The visual and potentiometric titrations were performed in the same manner as described above for the pure compounds. The results of the determinations are given in Table 3.

Results and Discussion

Verma and co-workers have described the use of potassium trithiocarbonate for the reductimetric determination of thiuram disulphides,[3] thiram[4] (a fungicide formulation based on tetramethylthiuram disulphide) and dixanthogens.[5] The reductimetric property of the reagent depends on its mild oxidation to carbon disulphide and sulphur:

$$K_2CS_3 \longrightarrow 2K^+ + CS_2 + S + 2e$$

Its application to the determination of captan and folpet is reported in this paper. The proposed titrimetric method, in addition to being simple, rapid and accurate, possesses the following advantages:

(i) It permits direct determination at room temperature.
(ii) As the reagent is self-indicating, no additional indicator is required in visual titrations.
(iii) Thiols, chloride ions and oxidation products of potassium trithiocarbonate (carbon disulphide and sulphur) do not cause any interference.
(iv) The determination can be performed with a single aliquot of the sample.
(v) The reagent can be easily prepared and its solution, if stored correctly, shows good stability.
(vi) The inert atmosphere required in most reductimetric titrations is not necessary here.
(vii) In potentiometric titrations, the potentials stabilise immediately on the addition of each aliquot of the reagent and the inflection points are marked by sharp drops in potential.

The proposed method has been applied to the determination of pure samples of captan and folpet. The results given in Tables 1 and 2 show that captan and folpet can be determined in the ranges 3–12 and 2.5–9 mg, respectively, with maximum relative standard deviations of 0.6 and 0.7%, respectively. The method was subsequently applied to some commercial formulations based on captan and folpet in order to determine their active ingredients. The recoveries (Table 3), which are in the range 98.8–99.4% with standard deviations in the range 0.2–0.3%, indicate the high accuracy and reproducibility of the proposed titrimetric method. The results obtained by the hydrolysis method[1] for pure compounds and formulations are also given in the respective tables.

Amounts as small as 3 mg of these agrochemicals in 50 ml of solution can be determined visually by direct titration with potassium trithiocarbonate. The potentiometric titration method can be used to determine down to 1.5 mg of these agrochemicals in the same volume of solution.

The results obtained show that each molecule of captan or folpet reacts with 2 mol of the reagent. The most plausible reaction mechanism [shown here for captan (**I**)] is as follows:

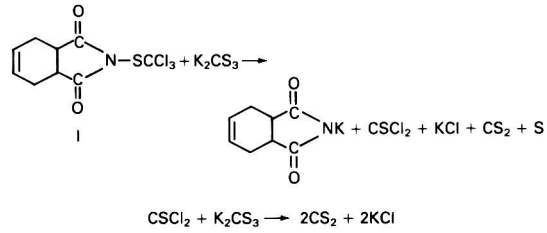

$$CSCl_2 + K_2CS_3 \longrightarrow 2CS_2 + 2KCl$$

Similar reaction mechanisms can be inferred for folpet.

The first reaction is supported by the fact that thiophosgene is indeed the product of the reduction of trichloromethanesulphenyl chloride (**II**),[6,7] and that captan and folpet are imide derivatives of **II**.[8]

$$\underset{\text{II}}{ClSCCl_3} + 2e \longrightarrow CSCl_2 + 2Cl^-$$

The reaction of thiophosgene with potassium trithiocarbonate to form carbon disulphide quantitatively (second reaction) is well known.[9]

The authors thank the Indian Council of Agricultural Research, New Delhi, for financial assistance.

References

1. Ospenson, J. N., Pack, D. E., Kohn, G. K., Burchfield, H. P., and Storrs, E. E., *in* Zweig, G., *Editor*, "Analytical Methods for Pesticides, Plant Growth Regulators and Food Additives," Volume III, Academic Press, New York, 1964, p. 9.
2. Deskin, W. A., *J. Am. Chem. Soc.*, 1958, **80**, 5680.
3. Verma, B. C., Sidhu, H. S., and Sood, R. K., *Talanta*, 1982, **29**, 703.

4. Verma, B. C., Sood, R. K., and Sidhu, H. S., *Indian J. Agric. Sci.*, 1984, **54**, 123.
5. Verma, B. C., Butail, J., and Sood, R. K., *Analyst*, 1982, **107**, 691.
6. Drahowzal, F. A., *in* Kharash, N., *Editor*, "Organic Sulphur Compounds," Volume I, Pergamon Press, New York, 1961, p. 365.
7. Owens, G., and Blaak, G., *Contrib. Boyce Thompson Inst.*, 1960, **20**, 475.
8. Kittleson, A. R., *Science*, 1952, **115**, 84.
9. Gattow, G., and Behrendt, W., *in* Senning, A., *Editor*, "Topics in Sulphur Chemistry," Volume II, Georg Thieme, Stuttgart, 1977, p. 159.

Paper A5/350
Received October 1st, 1985
Accepted November 28th, 1986

Determination of Mercury in Lake Sediments Using a Gold Film Mercury Analyser

Alena Mudroch and Ellie Kokotich
Environmental Contaminants Division, National Water Research Institute, 867 Lakeshore Road, Burlington, Ontario L7R 4A6, Canada

A gold film mercury analyser was used for the determination of mercury in lake sediments. Sediment and soil standards and sediment samples were extracted with a mixture of nitric and hydrochloric acids. Aliquots of the extracts containing between 30 and 50 ng of mercury were used for the determination with the gold film analyser. An absolute deviation of approximately 0.05 μg g^{-1} and an accuracy of ±0.02 μg g^{-1} can be considered typical for the investigated method. The results of the determination of mercury in the sediment standard by the gold film analyser were compatible with the recommended value.

Keywords: *Mercury determination; lake sediments; gold film mercury analyser*

The assessment of the spatial extent of sediment contamination by mercury often requires analyses of many samples. For example, the concentration of mercury was determined in about 270 and 170 sediment samples during the survey of mercury contamination of Lakes Erie and Ontario, respectively.[1,2] The determination of mercury in sediments during extensive surveys is usually carried out by cold-vapour atomic absorption spectrometry. Governmental agencies or other large laboratories are usually equipped with several atomic absorption spectrometers, one of them designated only for mercury analyses. However, small laboratories are often equipped with only one atomic absorption spectrometer. Unless the laboratory specialises in mercury determination, this spectrometer is most likely to be used for the determination of other elements in a graphite furnace or by flame methods. Consequently, any time when mercury is to be determined in some aqueous or solid samples, the spectrometer has to be converted to the cold-vapour technique. Occasionally, the determination of mercury is carried out on a smaller set of sediment samples. In these instances, a reasonably priced, reliable mercury analyser would be an advantage. Recently, a gold film analyser became available for the determination of mercury in water, waste water, urine and blood. The analyser is based on the proportional increase in resistance of a thin gold film in the presence of mercury vapour and is equipped with a microprocessor which controls the operation. Mercury vapour reduced from mercury compounds in analysed solutions is drawn into the analyser by an internal pump. The gold film sensor adsorbs and integrates the mercury with the resulting signal being displayed on a liquid crystal display meter. We tested the suitability of the gold film analyser for the determination of mercury in sediments using certified sediment and soil standards and selected sediment samples from Lake St. Clair, Ontario, Canada. This paper describes the procedure and gives the results obtained.

Experimental

Apparatus

A Model 511 gold film mercury analyser was purchased from Jerome Instrument, Jerome, AZ, USA. The calibration procedure was carried out as recommended by the manufacturer.

Reagents

Hydrochloric and nitric acids. Concentrated acids of analytical-reagent grade (Merck) were used.

Tin(II) chloride solution, 10% *m/V.* Prepared by weighing 3 g of tin(II) chloride ($SnCl_2.2H_2O$, analytical-reagent grade, BDH Chemicals) into a 50-ml stoppered bottle. De-ionised, distilled water (28 ml) was added, followed by 2 ml of concentrated hydrochloric acid. This mixture is a suspension and should be stirred continuously during use, and has to be prepared fresh daily.

De-ionised, distilled water. Distilled water was de-ionised using a mixed-bed resin.

Mercury standard solution. A 1000 mg l^{-1} mercury standard (BDH Chemicals) was used as a stock solution. At the time of analyses of sediment extracts, a calibration graph was prepared using solutions containing 10, 20, 30, 40 and 50 ng of mercury.

Certified sediment and soil standards. The standard sediment WQB-1[3] was obtained from the Quality Assurance Section, National Water Research Institute, Burlington, Ontario. This standard is a Lake Ontario sediment and has a similar geochemical matrix to sediments of Lake St. Clair. The standard soil SO-2 was obtained from the Office of Certified Reference Materials Project, Canada Centre for Mineral and Energy Technology, Ottawa, Ontario. The analyses of many sediments from Lakes Ontario and Erie revealed a similar geochemical and mineralogical composition as the standard soil SO-2.

Procedure

Lake St. Clair sediments

Surface sediments and sediment cores were obtained at 35 sampling stations at Lake St. Clair. All sediment cores were divided into 1-cm sub-samples. The concentration of mercury was determined in all samples; however, we selected results obtained by the analyses of five surface sediment samples randomly chosen from our Lake St. Clair collection. The sediment samples were freeze-dried, sieved through an 841 × 10^{-6} m size sieve to remove shells and organic debris and homogenised by grinding to 100 × 10^{-6} m using an automatic grinder (Siebtechnik, FRG). Certified sediment and soil standards were obtained already pulverised and homogenised. Randlesome and Aston[4] tested different digestion procedures followed by cold-vapour atomic absorption spectrometry for total mercury determination in sediments, and found that the most efficient rapid extraction was with a mixture of concentrated nitric and hydrochloric acids (9 + 1). This procedure is similar to that recommended by Jonasson *et al.*[5] which was used in this work. The standard or sediment samples (0.5–1.0

g) were transferred into a clean (washed with 10% *m/V* nitric acid and rinsed with de-ionised, distilled water), dry 125-ml Erlenmeyer flask. Concentrated nitric acid (20 ml) was added, followed by 1 ml of concentrated hydrochloric acid. The mixture was gently swirled, allowed to stand for 10 min and 40 ml of de-ionised, distilled water were added. The flask was placed in a water-bath (90 °C) and the sample digested for 90 min with occasional mixing. The flask was then removed from the water-bath and allowed to cool to room temperature. The suspension was filtered through a Whatman 40 filter-paper into a 100-ml calibrated flask and diluted to volume with de-ionised, distilled water. A 10-ml aliquot of the extract was pipetted into a 30-ml glass test-tube, concentrated nitric acid (2 ml) was added and the contents of the test-tube were swirled. After 5 min de-ionised, distilled water was added to fill the test-tube completely. After 10 min the solution was transferred into the reaction vessel of the gold film analyser and the vessel was attached to the bubbler. Mercury determination was carried out as recommended in the gold film analyser manual by the injection of 1 ml of tin(II) chloride suspension and switching on the microprocessor. Prior to the next determination, the reaction vessel and the glass bubbler were rinsed several times with de-ionised, distilled water to remove completely any residues of the tin(II) chloride reactant.

Results and Discussion

To determine the precision and accuracy of the method, mercury was determined in ten individual extracts of the standard sediment WQB-1, seven times in one extract from the standard sediment WQB-1 and in ten individual extracts of the standard soil SO-2.

The concentration of mercury recommended for the sediment standard WQB-1 is 1.09 ± 0.15 μg g^{-1}.[3] On analysing ten individual extracts of this standard, we obtained a mercury concentration of 1.05 ± 0.11 μg g^{-1}. By seven repetitions of analyses of one extract of the sediment standard WQB-1, the mercury concentration was found to be 1.11 ± 0.09 μg g^{-1}. The recommended concentration of mercury in soil standard SO-2 is 0.082 μg g^{-1}. By analyses of ten individual extracts of this standard, we obtained 0.093 ± 0.017 μg g^{-1}.

The analytical data and means, standard deviations and coefficients of variation from the determination of mercury concentrations in the top 1 cm of sediments from Lake St. Clair are presented in Table 1. These results indicate a better reproducibility of mercury determination in samples containing a concentration greater than 0.10 μg g^{-1}. The concentration of mercury ranged from 8 to 100 ng in 10-ml aliquots of extracts when 1.0 g of sediment was used. The precision and accuracy of the mercury determination with the gold film analyser depended on the concentration of mercury in the extracts. However, an absolute deviation of approximately 0.05 μg g^{-1} and accuracy of ±0.02 μg g^{-1} can be considered fairly typical. An improved precision was obtained when the concentration of mercury in the analysed aliquots ranged between 30 and 50 ng. On the other hand, a greater spread existed at concentrations less than 10 ng, which was probably due to the sensitivity of the gold film analyser meter response at these concentrations. For future analyses, we concluded that repeated determinations are essential for samples outside the range of optimum mercury concentration with the following changes: (a) use up to 2 g of a sediment with an expected low concentration of mercury (0.020 μg g^{-1}); and (b) modify the volume of the sediment extract according to the calculations from the first analysis. There are two important limits that have to be maintained during the analyses: (a) the ratio of water to acid has to be always 7.5 : 1 in the final solution used in the gold film analyser manufacture to prevent damage to the gold film; and (b) the final sample volume should not exceed 40 ml to fit into the reaction vessel. The advantage of the gold film mercury analyser is the selective adsorption of mercury on gold which eliminates any interferences. Murphy[6] tested a gold film mercury detector for the determination of nanogram amounts of mercury in liquid matrices. He added different chemicals to the analysed samples and found that no interference existed during the determination of mercury by the gold film detector. However, erroneously high values were obtained using cold-vapour atomic absorption spectrometry.

Table 1. Determination of mercury (μg g^{-1}) in sediments from Lake St. Clair

	Sediment No.				
Replicate No.	1	2	3	4	5
1	0.12	0.33	0.38	0.60	0.94
2	0.06	0.23	0.36	0.60	0.90
3	0.11	0.26	0.38	0.56	0.95
4	0.07	0.22	0.45	0.58	0.98
5	0.07	0.24	0.48	0.58	1.01
Mean	0.09	0.26	0.41	0.58	0.97
SD	0.02	0.04	0.05	0.01	0.04
CV, %	22.2	15.4	12.2	1.7	4.1

The apparatus requires a small space (about 1 m^2 of a laboratory bench) and is portable. Consequently, it is suitable for a field laboratory with available facilities for an acid extraction. The procedures for mercury determination in water, including drinking, surface and saline water and municipal and industrial wastes are already described in the analyser manual. The results of our test indicate that the analyser is suitable for the determination of mercury in sediments. However, the operation is completely manual. The present price (1986) of the analyser is about Canadian $9000.

References

1. Thomas, R. L., and Jaquet, J.-M., *J. Fish. Res. Board Can.*, 1976, **33**, 404.
2. Thomas, R. L., *Can. J. Earth Sci.*, 1972, **9**, 636.
3. Cheam, V., and Chau, A. S. Y., *Analyst*, 1984, **109**, 775.
4. Randlesome, J. E., and Aston, S. R., *Environ. Sci. Technol. Lett.*, 1980, **1**, 3.
5. Jonasson, I. R., Lynch, J. J., and Trip, L. J., *Geol. Surv. Can. Pap.*, 1973, No. 73-21.
6. Murphy, P. J., *Anal. Chem.*, 1979, **51**, 1599.

Paper A6/205
Received June 26th, 1986
Accepted December 18th, 1986

BOOK REVIEWS

Characterization of Spilled Oil Samples. Purpose, Sampling Analysis and Interpretation
Edited by J. A. Butt, D. F. Duckworth and S. G. Perry. Pp. x + 95. Wiley for Institute of Petroleum. 1985. Price £17.50. ISBN 0 471 90890 8.

The development of analytical methodologies for the identification of the source of accidental or intentional oil spillages into the marine environment has been the subject of much research since the early 1970s. In 1972 a first review was published by E. R. Adlard in the former *J. Inst. Petrol.* and in 1974, on behalf of the Institute of Petroleum who also published that journal, a technical guide entitled "Marine Pollution by Oil" was edited.

Since then there have been major changes in the whole oil industry, including production and transport patterns, as well as legislative requirements, as a result of the growing concern for the environment. In addition, there have been tremendous advances in the power and capabilities of analytical techniques for oil characterisation, all of these factors making an updated version of that guide necessary. The Editors of the present booklet, published again on behalf of the IP, have intended not only to give advice on the effective use of the analytical techniques for identifying and correcting sources of pollution, but also to provide legislators and enforcers with an overview of analytical capabilities and how these may be used constructively.

To this end the following subject areas are covered: (*i*) administrative aspects; (*ii*) oily pollutants found in the marine environment and their fate; (*iii*) collection, storage and transport of samples; (*iv*) the chemical constitution of petroleum and its application to spill identification; and (v) the analytical approach to spill identification.

The first section outlines what administrators may expect from analysts for management decisions concerning oil spills. Appropriate emphasis is given to the close cooperation that must exist between managers and analysts during the progress of the work. The more guidance that can be given to them, the more effective will be their efforts in tracing sources of pollution. The difficulties in making unequivocal identifications due to the variety and complexity of the samples and the weathering processes involved are underlined in the following sections. Useful indications regarding sample collection and transport are also given. However, in our opinion the procedures detailed for oil recovery from samples are not updated. Distillation units for 2- or 0.5-l flasks are out of use in modern pollution studies.

The last two sections, which constitute more than half of the book, are devoted specifically to the analytical problem. The use of a multi-method approach for oil spill identification is stressed and the key techniques: GC, GC - MS, IR spectroscopy, elemental analysis and luminescence spectroscopy are extensively presented. Although the discussions are obviously focused on oil-type pollutants, others such as vegetable oils are also considered. In this respect, it would have been useful to have included also coal tars, which may be found on beaches and can be characterised by IR spectroscopy.

Bearing in mind the potential and increasing use of GC - MS for oil fingerprinting, the consideration of this technique is most appropriate, but a clearer presentation would have been preferable. The quality of the fragmentograms is very poor, they are difficult to interpret and one figure (6.17) is duplicated in error. The diagnostic ions for isoprenoids are not at *m/z* 71 and 85, but 113 and 183. The explanation of the significance of the n-alkane distributions is somewhat misleading.

The chapter ends with brief coverage of novel or innovative applications of instrumental tehniques for oil spill characterisation (HPLC, ^{13}C NMR, soft ionisation techniques in MS, isotope analysis, etc.). Probably, of all of them only the pattern recognition techniques for data handling will become more widely applied in the near future. The presentation of references in this section in a different form to that used previously is surprising. In addition, some of them cannot be found in the text. References to institutional reports, which are sometimes difficult to obtain, should also have been replaced wherever possible by references to journals of wider circulation.

In conclusion, the book is timely and will be of interest to all those involved in the management of the oil pollution problem but, unfortunately, this wider readership has been catered for at the expense of a more rigorous presentation of some aspects.

J. Albaigés

Advances in Capillary Chromatography
Edited by J. G. Nikelly. *Chromatographic Methods.* Pp. ix + 138. Hüthig. 1986. Price DM56. ISBN 3 7785 1143 2.

This book is a selection of papers that were presented at an American Chemical Society Symposium in 1984. It is intended to cover the field of capillary chromatography but the topic of capillary liquid chromatography is a notable omission.

Advances in capillary GC are reviewed by Jennings with some useful theory that is rather inadequately explained. However, this chapter includes a good review of the relative merits of different column diameters and film thicknesses.

Two chapters deal with capillary supercritical fluid chromatography (one has an emphasis on capillary SFC - MS). Neither chapter succeeds in either giving a clear theoretical background to this emerging technique or persuading the reader that the technique has any great advantage over capillary GC or HPLC. Clearly SFC has a niche for thermally labile compounds, but most of the applications illustrated can be accomplished much better by existing techniques. The application of very rapid pressure programming (to change the solvating power) in capillary SFC is clearly a way of extending its range of application to complex mixture analysis, although the hardware requirements become demanding.

GC - FTIR benefits from a good, clear overview (S. Smith), emphasising optimisation of hardware and the benefits of the interpretative power of carrying out complementary GC - MS and GC - FTIR analyses. H. Widmer discusses some rather obvious criteria for industrial use of capillary GC, but the remainder of this chapter includes some fascinating data on inversion of Kováts retention indices due to subtle changes in film thickness and column temperature—users beware! In a chapter with quantitative GC - MS in the title there is virtually no discussion of the quantitative aspects, but nevertheless some interesting ideas. While tandem MS - MS systems have the ability to reduce analysis times to 30 s, the hardware to deliver the sample to achieve this throughput is yet to be developed. The final chapter discusses an interesting application of stationary phase development technology (Superox-4).

To summarise, my over-all impression is that the book is not very memorable or readable and fails to provide a satisfactory survey of the state of the art. Its low price could make it a useful addition to general libraries for student use but it cannot be strongly recommended for the bookshelf of practising chromatographers.

B. H. Woollen

Coal Science. An Introduction to Chemistry, Technology and Utilization

Rita K. Hessley, John W. Reasoner and John T. Riley. Pp. xii + 269 Wiley-Interscience. 1986. Price £33.75. ISBN 0 471 81225 0.

This book describes in simple terms the formation, structure, methods of analysis and efficient utilisation of American coals. Chapter 1 presents the chemistry and geology involved in coal's formation. Chapter 2 presents the petrology and petrographic characterisation, whilst the structure and organic composition are given in Chapter 3. Chapter 4 describes coal chemistry and reactivity of coal in conversion and utilisation processes, with the final chapter discussing routine testing and analytical classification.

Chapter 1 explains clearly the formation of coal, although a clearer reference to cannel coal should have been incorporated. It was also surprising to see figures first published in 1974 used to depict coal-bearing strata and resources for US coals. Excepting that the authors are American, I still feel that reference to the classical work of Seyler should have been mentioned. This work is regarded by European scientists to be a masterpiece of scientific coal classification. Chapter 2 gives a good understanding of coal petrology but essentially based on the text of Bouska. It addresses the physical and chemical properties of coal and shows how these properties are used to classify and characterise coal. The table used for correlation of Geology and Worldwide Distribution of coal was first published in 1940. The book gives due weight to the UK system of petrographic analysis and the authors detail the changes in petrographic analysis when using coal preparation methods, *e.g.*, vitrain becomes concentrated in coal fines. It is, however, a gross generalisation to state that nearly every element in coal can be determined by atomic absorption spectrometry.

Chapter 3 explains the organic reactivity of coal to pyrolysis, solvent extraction, hydrogenation, alkylation and oxidation. It discusses heteroatoms in coal before moving on to the physical and instrumental analysis of coal. Techniques such as Fourier transform infrared spectroscopy, scanning and transmission electron microscopy and associated X-ray analysis, although mentioned later in the book, are techniques for assessing organic reactivity that have been omitted from this chapter. Chapter 4 explains in detail liquefaction and gasification of coal and the importance of a long-term strategy for efficient coal conversion schemes is emphasised. The processes described are explained clearly with the sensible use of diagrams and illustrations. This chapter was particularly easy to read and understand.

Considering Chapter 5, I feel that any text on coal analysis should stress that empirical tests are used and so only precision is discussed in the standard methods, *e.g.*, ASTM or BSI. The use of modern instrumental methods has shown certain BSI methods to be inaccurate. The section on coal sampling I consider to be too brief and certainly the identification and measurement of systematic error (bias) should have been given. In this section I particularly like the paragraphs on the interpretation and uses of analytical data. The table on typical values of ash composition in bituminous coals is dated 1963 and for the UK coals the figures would need updating. The use of reproducibility and repeatability without explanation may be confusing to the new student.

It is pleasing that the authors mention the possible effect of the formation of the oxides of nitrogen on the determination of carbon content in coal. The discussion of the occurrence of pyrite in coal is too generalised. It is well known in UK coals that pyrite can occur as sub-micrometre particles which form larger spheres (framboids).

The chlorine paragraph is dated as there is evidence to indicate that chlorine in coal (particularly UK) does *not* exist predominantly as alkali metal chlorides. It is a particularly volatile element in coal, being evolved as hydrogen chloride at temperatures as low as 170 °C. The use of video recording cameras for ash fusion measurements is now widely accepted and this should have been included as a routine procedure. The difficulty in obtaining good precision for the analysis of the refractories silica and alumina in coal ash using atomic absorption spectrometry, even with dinitrogen oxide - acetylene flame, is not mentioned.

The references to FTIR for coal analysis are very dated and, considering the success of the technique, this is surprising. I do not like the use of a "secondary reference" because one then needs to find the original reference to identify the source.

The practical limit of SEM - EDXA systems for coal analysis is 3 μm diameter and not 1 μm as stated (this is a literature-quoted figure). Using X-ray fluorescence it is now possible to determine carbon in coal and the high precision of this technique for coal analysis should have been emphasised. The poor precision and accuracy of neutron activation analysis appears to be quickly dismissed and inductively coupled plasma - atomic emission spectrometry is omitted altogether. The use of electrothermal atomisation AAS for trace element determinations in coal should have been mentioned. AAS is just not sensitive enough for the trace element analysis of coal. The solid-sampling AAS references given are also very dated.

The coal classification paragraph is brief and, although outlining the problems, should have discussed a possible universal coal classification system (*cf.*, Seyler). Figures giving comparisons of the coal classification systems might also have been useful.

The authors are right to state that more coal analysis data are needed if new technologies are to be successful and also to stress the importance of grinding coal to produce representative milligram increments for automatic instrumental methods of coal analysis.

Overall the book is very easy to read and ideal for the American undergraduate student of coal science. It is, however, very dated in parts , particularly in the instrumental methods of coal analysis. It does not provide any new information that is not already provided in standard texts.

W. C. Pearce

Food Additives—The Professional and Scientific Approach

Pp. iv + 20. Institute of Food Science and Technology (UK). 1986. ISBN 0 905367 01 4.

This booklet was prepared by the Institute of Food Science and Technology (IFST) Technical and Legislative Committee to help IFST members by providing an objective account of the uses and benefits of food additives and the methods used to evaluate their safety.

The booklet outlines various aspects of food additives, in particular definitions of (and need for) "food additives," the functional properties of the various classes of additives and the assessment procedure for acceptance of food additives in the UK and EEC.

Considering its size, much useful information is given in the booklet and particular guidance is given regarding the responsible use of food additives and the associated responsibilities of food scientists and technologists. The publication of the booklet is to be welcomed by all those concerned with the use of food additives. It has been written at a level appropriate for the use of most IFST members. It would also provide a useful guide to the general public (although possibly supplemented in addition by the Ministry of Agriculture, Fisheries and Food "Food Facts" information sheets).

Roger Wood

Nuclear Magnetic Resonance
Edited by H. F. Linskens and J. F. Jackson. Modern Methods of Plant Analysis, *New Series, Volume* 2. Pp. xii + 196. Springer Verlag. 1986. Price DM139. ISBN 3 540 15910 X; 0 387 15910 X.

This volume is the second in the new series "Modern Methods of Plant Analysis." The eight diverse chapters are written by some of the leading exponents in the field and the Editors believe that this book on the application of NMR to plant cells is the first of its kind.

In the first chapter, by T. J. Simpson, 39 pages are devoted to the principles of stable isotope labelling methods in conjunction with ^{13}C NMR for the study of secondary metabolism in microorganisms and higher plants. The basic requirements are given for potential users and those interested in results. Not only is the carbon skeleton indicated, but also the origin of ^{2}H, ^{15}N and ^{18}O, and it is rightly concluded that ^{13}C NMR has greatly stimulated biosynthetic and metabolic studies. ^{31}P NMR is discussed in the second chapter by J. K. M. Roberts (14 pages) including its role in the determination of the energy status of plant cells. Effectively the concentrations of free ADP and ATP are measured for the quantification of the energy status in plant tissue and to aid the understanding of their energy metabolism. The chapter by C. Abell (25 pages) covers deuterium NMR spectroscopy as a technique for the study of fungal metabolism. Until 1974 mass spectroscopic methods were largely used. Hydrogen distribution is subject to minor chemical changes that do not affect the carbon skeleton, making the combined use of ^{13}C and deuterium labelling a powerful combination. The NMR properties of tritium offer possibilities for the future. ^{1}H NMR studies on DNA structure are discussed by P. Bendel (11 pages). Although detailed and accurate determinations of structural features in nucleic acids rely on X-ray studies of crystals and fibres, the success of NMR lies in its application to aqueous solutions. High-field NMR instruments have contributed to this advance and the methodology, basically involving firstly the analysis of chemical shifts and coupling constants and subsequently the determination of relative proton distances by the use of the NOE approach, is discussed. The NMR determination of intracellular pH is considered by J. K. M. Roberts in the next chapter (18 pages). A comparison with alternative methods is made and the ability of ^{31}P NMR procedures to be used continuously on a single sample during a series of experimental conditions is an advantageous feature.

A general theme emphasised by several contributors is the NMR examination of live samples. This is relevant to the subject matter of the next chapter, "Orientation of chloroplasts in leaves by ^{1}H NMR," contributed by D. C. McCain (20 pages). To be useful in this study, NMR must provide information inaccessible by other techniques.The rapidity of the NMR approach and its ready application to living tissues are advantages. The very practical determination of the rubber content of certain natural species of rubber plant by ^{13}C NMR is discussed in the next chapter (19 pages) by J. Visintainer and R. C. Hirst. The substantially intact sample is examined after size reduction and sample geometric conditions have been fulfilled. The last chapter (18 pages) is concerned with the use of ^{31}P to obtain information on the water content and the membrane state of pollen grains. The use of ^{31}P and ^{13}C NMR techniques is discussed by C. Verhoas and C. Dumar.

A good bibliography is given in each chapter. A short chapter on spectroscopic equipment might have been a useful addition.

Although the applications are highly specialised in some instances, more than half of the chapters are of interest to the general reader needing to be informed of developments in the use of NMR. Almost nothing is included on NMR imaging. At DM139 it seems an expensive book.

J. H. P. Tyman

Atmospheric Chemistry: Fundamentals and Experimental Techniques
Barbara J. Finalyson-Pitts and James N. Pitts,Jr. Pp. xxx + 1098. Wiley–Interscience. 1986. Price £57.45. ISBN 0 471 88227 5.

Practitioners in air monitoring, and also researchers and students of the chemistry of the atmosphere, will greet this book with enthusiasm. From the start one is impressed by the author's method and talent for explanation. The opening chapter gives an overview of the air environment, which provides a firm base for the subsequent detailed discussions of specific topics. It makes fascinating reading as the authors take one through such subjects as sulphurous and photochemical smogs, the profile of the earth's atmosphere, global gaseous emissions, the human respiratory system, meteorology, acid deposition and some of the basic chemistry.

Although their narrative style can hardly be maintained at the same pace in the detailed treatments which follow, their writing reflects their obvious fascination with this subject and overcomes the reader's reticence at tackling topics that require some degree of effort. Even their treatment of such mundane affairs as units and conversion of units is so ordered and concise that one takes pleasure from the benefits to be accrued from this ready source of reference.

Each chapter begins with a treatment of the relevant fundamental principles of the subject under discussion and together these serve as an introduction, or else a refresher course, in many aspects of physical and analytical chemistry.

At the heart of the book is the account of the present understanding of the chemical reactions taking place in the atmosphere, and throughout this complete subject the authors maintain their systematic approach. Wherever possible they describe the effect individual species have on other chemicals in the atmosphere, the competing reactions between them and the effects this may have on the concentrations of important pollutants. For example, nitrate radicals can react with alkenes much more rapidly than does ozone, and the production of nitrated organics could account for some of the health hazards of photochemical smogs.

The authors have also brought together such diverse topics as halocarbons in the stratosphere, the rising level of methane, the physical properties of suspended particles, the bioassay of mutagens, monitoring techniques, the source and fate of pollutants, their reaction mechanisms and kinetics and the effects of nitrogen oxide emissions from supersonic transporters. They do this in a unified approach justified by their affirmation that "The chemistry of the atmosphere from pristine natural areas to heavily polluted urban areas is all part of one continuous cycle."

There is also a substantial and up-to-date compilation of much fundamental data including rate constants, the chemical structures of many unusual and complex pollutants, pollutant concentrations, thermodynamic data and a wealth of literature references. For this alone the book is valuable but it can be recommended much more for the approach which the authors bring to their subject and the enthusiasm they engender.

B. I. Brookes

Fluoride Research 1985

Edited by Humio Tsunoda and Ming-Ho Yu. *Studies in Environmental Science, Volume* 27. Pp. xviii + 435. Elsevier. 1986. Price $103.75; Dfl 280. ISBN 0 444 42678 7.

Despite the reactivity of fluoride and its ubiquity in the environment, its importance in biological systems was only established in the first part of this century when it was recognised that dental mottling was related to the fluoride content of drinking water supplies. Recognition of harmful effects on the skeleton in high-fluoride areas, and the hundreds of studies showing the beneficial effects on teeth at optimal concentrations of water-borne fluoride and from fluoride dentrifices, have stimulated the development of analytical methods for water, rocks and tissues to investigate the biological effects and to monitor environmental fluoride from industrial pollution.

Japan has been alerted to the hazards of uncontrolled and unsuspected chemical pollution by the tragic outbreaks of such conditions as Minamata disease and Itai-Itai disease, due to methylmercury and cadmium, respectively. It was fitting, therefore, that the 14th meeting of the International Society for Fluoride Research should be held in Morioka, Japan. This volume contains selected papers from the conference.

The papers are grouped under Analytical Methods; Environmental Studies; Biological Effects; and Effects in Humans. As often is the case with such publications, the subjects are not treated systematically and a number of gaps in the coverage of the subject can be identified. Although several review papers on individual aspects are included, the value of the book will be mainly appreciated by specialists in one or more of the areas covered.

For such specialists the book will prove interesting, if not essential, reading. The analytical section contains clear descriptions of several relatively new developments including molecular absorption spectrometry of AlF, plasma emission spectrometry and new ion-exchange resins. Environmental studies cover ecological aspects of fluoride transport and distribution, and also epidemiological data on dental and skeletal fluorosis and bone fluoride levels.

The biological papers are less satisfactory, being a piecemeal collection covering whole-body, cellular and subcellular aspects, without any unifying thread. Finally, selected aspects of human fluoride metabolism involving bone, kidney, teeth and saliva are considered, mainly from the point of view of highly toxic doses, rather than in relation to therapeutic intakes.

The book is well produced in hardback on high-quality paper from camera-ready copy. In view of the overwhelmingly Japanese authorship, the standard and clarity of the writing are commendable and any infelicities excusable. Libraries will need to purchase this book for reference purposes, but few other than specialists in the analytical and environmental aspects of fluoride will require to have the book on their own bookshelves.

W. M. Edgar

Selective Gas Chromatographic Detectors

M. Dressler. *Journal of Chromatography Library, Volume 36.* Pp. xiv + 319. Elsevier. 1986. ISBN 0 444 42488 1.

Whereas it is often necessary in gas chromatography to detect all the components of a mixture, in many instances a simpler chromatogram, in which only selected analytes are detected, can often be more useful. This can be especially true if it also results in a more sensitive detection of the analyte of interest. This book includes in-depth descriptions of all the routinely used selective detectors and many of the experimental or commercially available systems, some so specific that their use may be restricted to only a small range of samples. As expected, most of the book is devoted to the three most important selective detector types, the thermionic, flame photometric and electron-capture detectors. In common with other monographs in the *Journal of Chromatography Library* series, the result is a comprehensively researched and detailed review of a specific topic in chromatography.

The discussion of thermionic or nitrogen-phosphorus detectors emphasises the diversity of designs and modes of operation. The detectors are divided into those in which there is a discrete flame, the alkaline flame-ionisation detectors (AFID), and the flameless alkali-sensitised detectors. These variations have resulted in a multitude of studies with often confusing conclusions and the review notes the effects of the conditions and designs on the responses.

Despite its usual assignment as a "universal detector," the flame-ionisation detector can also be used as a selective system. A hydrogen atmosphere or doped carrier gas enhances the response from silicon or halogen compounds and other groups. The selectivity of the photoionisation detectors is discussed primarily in comparison with the FID. Detection methods based on light emission form the basis of the flame photometric and chemiluminescence detectors and the less widely used plasma emission spectrometric detector.

The electrical conductivity and coulometric detectors are described in detail and the range of selectivities is described. The operation of the electron-capture detector is explained, although the author notes his difficulty in not repeating Zlatkis and Poole's earlier comprehensive volume in the same series.

Among the less widely known detectors are the ion-mobility detector and ion-selective electrodes, but the author touches only fleetingly on the rapidly expanding topics of GC-IR and GC-MS and coupling GC to atomic absorption spectrometers.

The coverage is generally to 1984, but for the established detectors it is the detailed collection of the many papers on techniques and operation of the detectors that makes this a valuable reference work. The only reservation is that for the average user of a gas chromatograph the coverage is so comprehensive that the simple criteria of selection of a detector for a particular operation may be obscured. This is therefore primarily a reference work for those wishing to gain a deeper understanding of a particular detector.

Roger M. Smith

Radiochemical Methods

William J. Geary. Pp xx + 229. *Analytical Chemistry by Open Learning.* 1986. Price £9.95 (soft cover); £28 (cloth). ISBN 0 471 91118 6 (soft cover); 0 471 91117 8 (cloth).

This book is said to be aimed at senior technicians wishing to expand their knowledge of radiochemistry and gain further qualifications. Although this is a laudable aim, a major criticism of this book is that it deals mainly with matters better covered by other works, such as nuclear physics, health physics and detection of ionising radiations. Radiochemical methods receive scant treatment and their principles are not mentioned, although the principles of isotope dilution and neutron activation analysis are covered. The text gives three examples of determinations, photocopied from journals, which refer to radioimmunoassay of barbiturates, pseudoisotopic dilution to determine rhenium and instrumental neutron activation of arsenic and antimony. Only two of these give brief details of radiochemical separations. Hence I cannot recommend this book to analysts who wish to learn about radiochemistry or radiochemical methods.

This book is nicely produced with a large, legible type face, and there are few misprints. It lacks an index. Some of the figures, *e.g.*, Figs. 1b and 3.2a, could have been better drawn. Both SI and pre-SI units are used, and all are clearly defined apart from rem on p. 102. Specific activity is confused with

molar activity on p. 42 and elsewhere. The author's chatty and verbose style often conceals oversimplification of physical and technical details. The soft-cover edition is reasonably priced at 4p per page.

H. J. M. Bowen

Cost-effective Quality Control: Managing the Quality and Productivity of Analytical Processes
James O. Westgard and Patricia L. Barry. Pp. x + 230. American Association for Clinical Chemistry. 1986. Price $40. ISBN 0 915274 35 3.

This book gives an absorbing and informative description of the basic principles of quality control, and their application to analytical processes. It is based on experience in clinical laboratories, where, because of the generally high throughput of many clinical systems, there are striking similarities between quality control here and in the industrial environment. However, in principle, the procedures described can be readily adapted for use in almost any laboratory; considerable benefit would be gained by application of the statistical control procedures described to many analytical regimes.

I found Chapter 1 particularly interesting. In it the basic principles of quality control and the philosophy behind it are outlined. The principle of working towards "zero defects" and the statement that "inspection is the price of non-conformance" turns the attitude of many current quality control regimes completely on their head. One should not try to inspect quality in, rather, one should change systems to ensure a good-quality product.

Chapter 2 defines the objectives in a clinical laboratory and outlines some statistical principles of quality control in this environment. Chapters 3–5 further detail useful and relevant statistical regimes to control and measure quality. Chapter 6 deals with measurement and prediction of productivity of analytical systems in terms of "yield"; methods of calculation of "yield" are described.

The final chapter gives guidelines for design and implementation of a cost-effective quality control procedure; there is also a useful glossary of largely statistical terms.

I found this a readable and interesting book, which deals with some fairly detailed statistical ideas in a straightforward and practical fashion. It should prove of interest to all analysts who are concerned about improving the quality of their analytical procedures, but particularly to those using high-throughput automated systems.

B. G. Henshaw

Organo-chlorine Solvents. Health Risks to Workers
Commission of the European Communities. Pp. xvi + 254. Royal Society of Chemistry. 1986. Price £50; $90. ISBN 0 85186 078 8.

This small, well laid out book prepared for the Commission of the European Communities by an expert committee deals with the health risks in using the common organochlorine solvents. Material has been gathered together from published reviews and books and in certain instances from the committee's own original work. Because of the size of the European Community and the number of countries involved, the committee has attempted to take into account all the relevant information when considering its recommendation for occupational exposure limits (OELs), which could not have been easy. As there is no scientific basis for Action Levels, the committee considers it prudent that OELs should not exceed 30–50% of the set limits.

The solvents considered are *p*-dichlorobenzene, chloroform, 1,1,1-trichloroethane, 1,2-dichloroethane, trichloroethylene, 1,1,2-trichloroethane, dichloromethane, 1,2-dichloropropane, perchloroethylene and carbon tetrachloride. Each chapter is devoted to a single solvent and consists of 20 subsections. Those relating to storage, handling and use precautions and fire and reaction hazards are useful reminders of how dangerous these solvents can be. The section on first aid, although repetitive, gives vital information that could save lives. The presentation of the physico-chemical properties of each solvent is sometimes rather lengthy and might have been improved by reducing the amount of similar data, *e.g.*, melting- and boiling-points, vapour pressures, etc., and by at least indicating the currently accepted values.

The bulk of each chapter deals with toxicity. After a general introduction, kinetics are discussed, followed by information on human and animal acute, subacute and chronic toxicity in relation to carcinogenicity, mutagenicity and reproductive effects. Numerous references are listed and a wealth of information is given. Finally, each chapter has sections on medical and health surveillance and recommended occupational exposure limits.

The committee makes sensible comments throughout the book where the literature data differ, and it presents original material when suitable published information is lacking. Because there is no index, searching for specific data on a given solvent can be time consuming, but this should not deter potential users. This reference book should be of considerable use to those involved in occupational health and to those employing solvents in the chemical industries and in education.

R. Perry

ERRATUM

Differential-Pulse Cathodic Stripping Voltammetric Investigation of CrO_4^{2-}, MoO_4^{2-}, WO_4^{2-} and VO_3^-

M. Rasul Jan and W. Franklin Smyth

Analyst, 1986, **111**, 1239–1243

Page 1240, left-hand column, lines 20–25: *for* "This increase suggests that there is an outer multi-layer formed by $HgVO_3$ and $Hg(VO_3)_2$ around the mercury drop. The monolayer is strongly bound to the mercury drop and is stripped at more negative potentials. At lower concentrations only one peak is observed for the DPCSV of VO_3^-." *read* "The mercury salts of VO_3^- therefore give rise to multi-layer formation, with the monolayer being stripped at more positive potentials. It is this peak that is observed at lower concentrations of *ca.* 10^{-6} M."

Page 1241, right-hand column, lines 7–8: *for* "in the monolayer state and is partly successful on the multi-layer" *read* "in the multi-layer state and is partly successful on the monolayer."

Page 1241, right-hand column, lines 19–20: *for* "preferring the multi-layer of $HgVO_3$ - $Hg(VO_3)_2$ around the mercury drops to the monolayer." *read* "competing more successfully with the monolayer state of $HgVO_3$ - $Hg(VO_3)_2$ than with the multi-layer state."

Page 1241, right-hand column, line 29: *for* "disrupts the monolayer" *read* "disrupts the multi-layer."

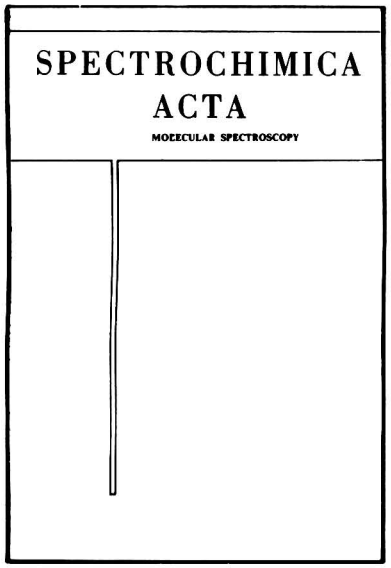

SPECTROCHIMICA ACTA

Part B: Atomic Spectroscopy

Editor-in-Chief: P W J M BOUMANS, *Philips Research Laboratories, Department of Spectrochemistry, PO Box 80.000, 5600 JA Eindhoven, The Netherlands*
Editors: W SLAVIN, *Perkin-Elmer Corporation, USA* and H OECHSNER, *Univerity of Kaiserslautern, Federal Republic of Germany*
Assistant Editor: J A C BROEKAERT, *Institut für Spektrochemie und Angewandte Spektroskopie (ISAS), Federal Republic of Germany*

Spectrochimica Acta, Part B, covers topics from rapidly expanding areas in atomic spectroscopy, mass spectroscopy for inorganic analysis, and surface, interface, thin film and micro analysis. The articles deal with: theory and fundamentals, methodology development, instrumentation, and applications.
Recent years have seen the publication of an ever increasing number and variety of articles contributed by the leading authors in spectroscopy who have understood the impact of *Spectrochimica Acta, Part B,* on the development of atomic spectroscopy and related fields. Therefore the journal is an indispensable source of information for all analytical spectroscopists. Authors can feel assured that the submittance of their manuscripts is followed by fast, thorough and efficient refereeing, substantial editorial advice and rapid publication of the revised text in the journal with the longest tradition in spectroscopy and the unrivalled standard.
Patents Section — The journal contains abstracts and illustrations of recently issued United States Patents and published patent applications filed from over 30 countries under the Patent Co-operation Treaty.

Subscription Information
Published monthly (Volume 42)

Annual subscription (1987)	**DM1245.00**
Two-year rate (1987/88)	**DM2365.50**

A selection of papers
An automated direct sample insertion system for the inductively coupled plasma, W E PETTIT & G HORLICK.
A steady-state approach to evaluation of proposed excitation mechanisms in the analytical ICP, G D RAYSON & G M HIEFTJE.
The determination of trace elements in geochemical exploration samples by ICP-MS, A R DATE & D HUTCHISON.
Interference minimization using second surface atomizer for furnace atomic absorption, T M RETTBERG & J A HOLCOMBE.
Spatial resolution enhancement for linear photodiode array atomic spectrometry, S W McGEORGE & E D SALIN.
Experimental control of the solvent load of ICPs and effects of chloroform plasma load on their analytical performance, F J M J MAESSEN *et al.*
Influence of the generator frequency and the plasma gas inlet area on torch design in ICP-AES, E MICHAUD-POUSSEL & J M MERMET.
An improved interface for ICP-MS, D J DOUGLAS & J B FRENCH.
Scanning electron microscopy studies on surfaces from electrothermal AAS, B WELZ *et al.*
Qualitative and semi-quantitative ICAP-AES analysis using a computer-controlled monochromator, P D P TAYLOR & J DE DONDER.

FREE SAMPLE COPIES AVAILABLE ON REQUEST
Advertising rate card available on request. Back issues and current subscriptions are also available in microform.
The Deutsch Mark prices shown include postage and insurance. For subscription rates in Africa, Asia, Australasia, UK and Eire and the Americas apply to your nearest Pergamon office. Prices are subject to change without notice.

Pergamon Press
Headington Hill Hall, Oxford OX3 0BW, UK
Fairview Park, Elmsford, New York 10523, USA

FIRST FOLD HERE

THE ANALYST READER ENQUIRY SERVICE
For further information about any of the products featured in the advertisements in this issue, write the appropriate number on the postcard, detach and post.

FOLD HERE

THE ANALYST READER ENQUIRY SERVICE

MAY'87

For further information about any of the products featured in the advertisements in this issue, please write the appropriate number in one of the boxes below.
Postage paid if posted in the British Isles but overseas readers must affix a stamp.

PLEASE USE BLOCK CAPITALS LEAVING A SPACE BETWEEN WORDS *Valid 12 months*

1 NAME

2 COMPANY

PLEASE GIVE YOUR BUSINESS ADDRESS IF POSSIBLE. IF NOT, PLEASE TICK HERE ☐

3 STREET

4 TOWN

5 COUNTY
POST CODE

6 COUNTRY

7 DEPARTMENT/
DIVISION

8 YOUR JOB TITLE/
POSITION

9 TELEPHONE NO

OFFICE USE ONLY REC'D PROC'D

FOLD HERE

Postage will be paid by Licensee

Do not affix Postage Stamps if posted in Gt. Britain, Channel Islands, N. Ireland or the Isle of Man

BUSINESS REPLY SERVICE
Licence No. WD 106

Reader Enquiry Service
The Analyst
The Royal Society of Chemistry
Burlington House, Piccadilly
LONDON
W1E 6WF
England

ANALAO 112(5) 557–716 (1987) May 1987

The Analyst

The Analytical Journal of The Royal Society of Chemistry

CONTENTS

continued inside back cover

Typeset and printed by Black Bear Press Limited, Cambridge, England